THE UNIVERSITY OF QUEENSLAND

AUSTRALIA

Physiological Properties of Glycinergic Synapses with Defined Subunit Compositions

Yan Zhang

M.Sc.

A thesis submitted for the degree of Doctor of Philosophy at

The University of Queensland in 2016

Queensland Brain Institute

Abstract

Glycine receptors (GlyRs) mediate fast inhibitory neurotransmission in the spinal cord and brainstem. Four GlyR subunits (α1 – 3, β) have been identified in humans, and their differential anatomical distributions result in a diversity of synaptic isoforms with unique physiological and pharmacological properties. However, despite their importance in controlling neuronal function, little is known about these properties. To address this, we developed an 'artificial' synapse system which allows to control over the synaptic GlyR subunit composition. We induced the formation of recombinant synapses between cultured spinal neurons and HEK293 cells expressing GlyR subunits of interest plus the synapse-promoting molecule, neuroligin-2A. In the heterosynapses thus formed, recombinant α1β and α3β GlyRs mediated fast decaying inhibitory postsynaptic currents (IPSCs) whereas α2β GlyRs mediated slow decaying IPSCs. These results are consistent with the fragmentary information available from native synapses and single channel kinetic studies. As β subunit incorporation is considered essential for localizing GlyRs at the synapse, we were surprised that α1 – 3 homomers supported robust IPSCs with β subunit incorporation accelerating IPSC rise and decay times in α2β and α3β heteromers only. Finally, heterosynapses incorporating $\alpha1^{D80A}\beta$ and $\alpha1^{A52S}\beta$ GlyRs exhibited accelerated IPSC decay rates closely resembling those recorded in native synapses from mutant mice homozygous for these mutations, providing an additional validation of our technique. As our model system successfully recapitulates the effects of known GlyR disease mutations, we employed it to investigate the effects of new GlyR disease mutations.

Hyperekplexia is a human neuromotor disorder caused by mutations that impair glycinergic neurotransmission. We investigated the mechanism by which gain-of-function GlyR mutations cause hyperekplexia. We identified two new gain-of-function mutations (I43F, W170S) and characterised these along with the known gain-of-function mutations (Q226E, V280M, R414H) to identify how they cause hyperekplexia. Using 'artificial' synapses, we show that all mutations prolong the decay of IPSCs and induce spontaneous activation. As these effects may deplete the chloride electrochemical gradient, hyperekplexia could potentially result from reduced glycinergic inhibitory efficacy. However, we consider this unlikely as it should also lead to pain sensitization and a hyperekplexia phenotype that correlates with mutation severity, neither of which is observed in patients. We also rule out small increases in IPSC decay times (as caused by W170S and R414H) as a possible mechanism given that the clinically-important drug, tropisetron, increases glycinergic IPSC decay times without causing motor side effects. A recent study concluded that an elevated intracellular chloride concentration late during development ablates α1β glycinergic synapses but

spares GABAergic synapses. As this mechanism satisfies all our considerations, we propose it is primarily responsible for the gain-of-function hyperekplexia phenotype.

GlyRs containing α2 subunits exert excitatory effects in immature neurons, and thereby modulate neuronal migration and synapse formation. The α2 R350L mutation has been identified in a human patient with autism spectrum disorder (ASD). This mutation was found to slow both the channel closing rate and the IPSC decay time. As mutation of R350 to Ala, Lys or Ile did not affect the IPSC decay time, we propose the Leu mutation specifically affects a molecular interaction responsible for the prolonged IPSC time courses. However, the link between the R350L and ASD remains to be elucidated.

Zn^{2+} is concentrated into presynaptic vesicles at central synapses and is released into the synaptic cleft by nerve terminal stimulation. There is strong evidence that synaptically released Zn^{2+} modulates glutamatergic neurotransmission, although there is debate concerning its peak concentration in the cleft. GlyRs are potentiated by low nanomolar Zn^{2+} and inhibited by micromolar Zn^{2+}. A mutation that ablates Zn^{2+} potentiation of GlyRs results in a hyperekplexia phenotype suggesting that Zn^{2+} physiologically modulates glycinergic neurotransmission. There is, however, little evidence that Zn^{2+} is stored presynaptically at glycinergic terminals and it is possible that the modulation is mediated by tonically bound Zn^{2+}. We sought to estimate the peak Zn^{2+} concentration in the glycinergic synaptic cleft as a means of evaluating whether it is likely to be synaptically released. We generated 'artificial' synapses expressing α1β GlyRs with defined Zn^{2+} sensitivities. By comparing the effect of Zn^{2+} chelation on glycinergic IPSCs with the effects of defined Zn^{2+} plus glycine concentrations applied rapidly to recombinant GlyRs in outside-out patches under simulated synaptic activation conditions, we inferred that synaptic Zn^{2+} rises to at least 1 μM following a single presynaptic stimulation. Moreover, using the fast high-affinity chelator, ZX1, we found no evidence for tonic Zn^{2+} bound constitutively to high affinity GlyR sites. We conclude that diffusible Zn^{2+} reaches 1 μM or higher and is therefore likely to be phasically released at glycinergic synapses.

Taken together, these results provide significant new insights into normal and abnormal glycinergic neurotransmission and the physiological modulatory mechanisms of glycinergic IPSCs.

Declaration by author

This thesis is composed of my original work, and contains no material previously published or written by another person except where due reference has been made in the text. I have clearly stated the contribution by others to jointly-authored works that I have included in my thesis.

I have clearly stated the contribution of others to my thesis as a whole, including statistical assistance, survey design, data analysis, significant technical procedures, professional editorial advice, and any other original research work used or reported in my thesis. The content of my thesis is the result of work I have carried out since the commencement of my research higher degree candidature and does not include a substantial part of work that has been submitted to qualify for the award of any other degree or diploma in any university or other tertiary institution. I have clearly stated which parts of my thesis, if any, have been submitted to qualify for another award.

I acknowledge that an electronic copy of my thesis must be lodged with the University Library and, subject to the policy and procedures of The University of Queensland, the thesis be made available for research and study in accordance with the Copyright Act 1968 unless a period of embargo has been approved by the Dean of the Graduate School.

I acknowledge that copyright of all material contained in my thesis resides with the copyright holder(s) of that material. Where appropriate I have obtained copyright permission from the copyright holder to reproduce material in this thesis.

Publications during candidature

Peer-reviewed papers:

Zhang Y, Keramidas A, Lynch JW. The free zinc concentration in the synaptic cleft of artificial glycinergic synapses reaches > 1 μM. *Frontiers in Molecular Neuroscience*. 2016, 9:88.

Zhang Y, Bode A, Nguyen B, Keramidas A, Lynch JW. Investigating the mechanism by which glycine receptor gain-of-function mutations cause hyperekplexia. *The Journal of Biological Chemistry*. 2016, 291(29):15332-41.

Zhang Y, Dixon CL, Keramidas A, Lynch JW. Functional reconstitution of glycinergic synapses incorporating defined glycine receptor subunit combinations. *Neuropharmacology*. 2015, 89:391–7.

Islam R, **Zhang Y**, Xu L, Sah P, Lynch JW. A chemogenetic receptor that enhances the magnitude and frequency of glycinergic inhibitory postsynaptic currents without inducing a tonic chloride flux. *ACS Chemical Neuroscience.* 2016 (Accepted).

Dixon CL, **Zhang Y**, Lynch JW. Generation of functional inhibitory synapses incorporating defined combinations of GABA(A) or glycine receptor subunits. *Frontiers in Molecular Neuroscience*. 2015, 8:80.

Conference presentations:

Zhang Y, Lynch JW. The TM3-4 loop in the α1 glycine receptor plays a major role in fast inhibitory synaptic transmission. Meeting of the Asian-Pacific Society for Neurochemistry, Kuala Lumpur, Malaysia, 2016. (oral presentation)

Zhang Y, Dixon CL, Keramidas A, Lynch JW. Functional reconstitution of glycinergic synapses incorporating defined glycine receptor subunit combinations. Society for Neuroscience Annual Meeting, Chicago, USA, 2015. (poster presentation)

Zhang Y, Dixon CL, Keramidas A, Lynch JW. Functional reconstitution of glycinergic synapses incorporating defined glycine receptor subunit combinations. International Society for Neurochemistry-Asian Pacific Society Neuroscience Biennial Meeting, Cairns, Australia, 2015. (poster presentation)

Zhang Y, Dixon CL, Keramidas A, Lynch JW. Physiological properties of glycinergic synapse with defined subunit compositions. International Biophysics Congress, Brisbane, Australia, 2014. (poster presentation)

Publications included in this thesis

Zhang Y, Dixon CL, Keramidas A, Lynch JW. Functional reconstitution of glycinergic synapses incorporating defined glycine receptor subunit combinations. *Neuropharmacology*. 2015, 89:391–7 – incorporated as Chapter 2.

Contributor	Statement of contribution
Author Yan Zhang (Candidate)	Experiments (80%) Writing (80%)
Author Christine L. Dixon	Editing (20%)
Author Angelo Keramidas	Experiments (20%) Writing and Editing (20%)
Author Joseph W. Lynch	Editing (60%)

Zhang Y, Bode A, Nguyen B, Keramidas A, Lynch JW. Investigating the mechanism by which glycine receptor gain-of-function mutations cause hyperekplexia. *The Journal of Biological Chemistry*. 2016, 291(29):15332-41. – incorporated as Chapter 3.

Contributor	Statement of contribution
Author Yan Zhang (Candidate)	Experiments (50%) Writing (80%)
Author Anna Bode	Experiments (20%)
Author Bindi Nguyen	Experiments (10%)
Author Angelo Keramidas	Experiments (20%) Writing and Editing (20%)
Author Joseph W. Lynch	Editing (80%)

Zhang Y, Keramidas A, Lynch JW. The free zinc concentration in the synaptic cleft of artificial glycinergic synapses reaches > 1 μM. *Frontiers in Molecular Neuroscience*. 2016, 9:88. – incorporated as Chapter 5.

Contributor	Statement of contribution
Author Yan Zhang (Candidate)	Experiments (80%) Writing (20%)
Author Angelo Keramidas	Experiments (20%) Editing (20%)
Author Joseph W. Lynch	Writing and Editing (80%)

Contributions by others to the thesis

My supervisor Prof. Joseph Lynch advised on the design and interpretation of all the experiments in this thesis. Dr. Christine Dixon advised on the design of the glycinergic 'artificial' synapse experiments described in Chapter 2 and the rapid application experiments described in Chapter 3. Dr. Angelo Keramidas carried out the simulation studies described in Chapter 2, part of rapid application experiments described in Chapter 5, and all the single channel recordings.

Statement of parts of the thesis submitted to qualify for the award of another degree

None.

Acknowledgements

I cannot express enough thanks to my principal supervisor, Prof. Joseph Lynch, for his continued support and encouragement. Without his excellent and valuable guidance, I am not able to complete this thesis. When I look back at my past 4 years of PhD, I am very grateful to have him as my mentor and to be a part of Lynch group, and this has been one of the best experiences of my life.

I owe a special gratitude to Dr. Christine Dixon, who was always willing to help me with my experiments and also my English. I am truly grateful for having her in the lab when I first arrived in Australia and started my PhD here. I also would like to thank Dr. Angelo Keramidas, who is my co-supervisor, for being so kind to help me in my research. Both of them are excellent fellows who I view as role models for my future research career as a postdoc. I also would like to thank Prof. Pankaj Sah, who is my co-supervisor, for providing kind advice and help on my project.

I am also grateful for all the help from Justine Haddrill, our lab manage. With her assistant, every problem in the lab can be solved timely, and every lab trip is full of memorable experiences. I also thank all the Lynch Lab members (Argel, Nela, Ming, Chen, Yang, Robi, Sharifun, Kooi and Atif), also the past members (Han Lu, Qian, Sahil, Anna, Azra, Suzanne and Kristin), for being so kind and generous, which make the lab a warm place to stay. Special thanks to my housemate, Chen, for being a good company in the last year of my PhD.

I also acknowledge the financial support provided by the University of Queensland and Queensland Brain Institute through UQI scholarship. I also would like to thank QBI for providing fantastic facilities and best assistance.

I would like to express my deepest gratitude to my parents for their loving support. They have always encouraged and supported me on this journey. To my loving husband Du, thanks a million for being with me through the good times and the bad times. I won't be this stronger without your love.

Keywords

glycinergic, glycine receptor, inhibitory synapse, IPSC, inhibitory postsynaptic current, hyperekplexia, electrophysiology.

Australian and New Zealand Standard Research Classifications (ANZSRC)

ANZSRC code: 060110, Receptors and Membrane Biology, 60%
ANZSRC code: 111501, Basic Pharmacology, 20%
ANZSRC code: 110903, Central Nervous System, 20%

Fields of Research (FoR) Classification

FoR code: 0601, Biochemistry and Cell Biology, 60%
FoR code: 1115, Pharmacology and Pharmaceutical Sciences, 20%
FoR code: 1109, Neuroscience, 20%

Table of Contents

List of figures and tables

Figures

Tables

List of abbreviations

5-HT_3R	Serotonin 5-hydroxytryptamine type 3 receptor
ASD	Autism spectrum disorder
Ca^{2+}	Calcium ion
Cl^-	Chloride ion
CNS	Central nervous system
ECD	Extracellular domain
EPSC	Excitatory postsynaptic current
$GABA_AR$	γ-amino-butyric acid type A receptor
GFP	Green fluorescent protein
GlyR	Glycine receptor
HEK	Human embryonic kidney
ILD	Intracellular loop domain
IPSC	Inhibitory postsynaptic current
mIPSC	Miniature inhibitory postsynaptic current
nAChR	Nicotinic acetylcholine receptor
NL	Neuroligin
NMDAR	NMDA receptor
PKA	cAMP-dependent protein kinase
PKC	Protein kinase C
pLGIC	Pentameric ligand-gated ion channel
PGE_2	Prostaglandin E_2
SPT	Single particle tracking
TMD	Transmembrane domain
Zn^{2+}	Zinc ion

Chapter 1

Introduction

1 Glycine receptor

1.1 Glycine receptor structure and function

Glycine receptor (GlyR) chloride channels play a critical role in mediating fast inhibitory neurotransmission in the human adult spinal cord, brain stem and retina (Lynch, 2004). They belong to the pentameric ligand-gated ion channels (pLGICs), which also include nicotinic acetylcholine, serotonin 5-hydroxytryptamine type 3 (5-HT_3) and type A γ-amino-butyric acid ($GABA_A$) receptors. GlyRs assemble as homopentamers from α subunits, or heteropentamers from α and β subunits. Heteromeric forms are thought to include three α and two β, or two α and three β (Durisic et al., 2012; Yang et al., 2012). Each transmembrane subunit is composed of an extracellular domain (ECD) harbouring a ligand-binding site, a transmembrane domain (TMD) made of four α-helical TM1-TM4, and a large intracellular loop domain (ILD) connecting the TM3 and TM4 that influences the ion conductance (Carland et al., 2009) and interaction with intracellular proteins (Kim et al., 2006a; Del Pino et al., 2014). Fast quantal (< 1 ms) and high concentration (> 1 mM) release of glycine triggers the opening of channel gate (Legendre, 1998; Beato, 2008), resulting in a flux of anions through the channel pore that causes a rapid hyperpolarization and inhibition of the postsynaptic neurons. The glycinergic inhibition is important in many physiological processes including muscle tone, motor control and sensory processing, and its malfunction has been directly linked to a range of neurological disorders including hyperekplexia, temporal lobe epilepsy, autism, breathing disorders and chronic inflammatory pain.

The structural related proteins provide a framework for the gating mechanism and ligand recognition of GlyRs. Recent reports have revealed the structures of the GlyR in complex with its competitive antagonist strychnine (Du et al., 2015; Huang et al., 2015), also the glycine- and glycine/ivermectin-bound reconstructions (Du et al., 2015) (Fig. 1). These findings enhance current understanding of molecular mechanisms for ligand-dependent gating in GlyRs.

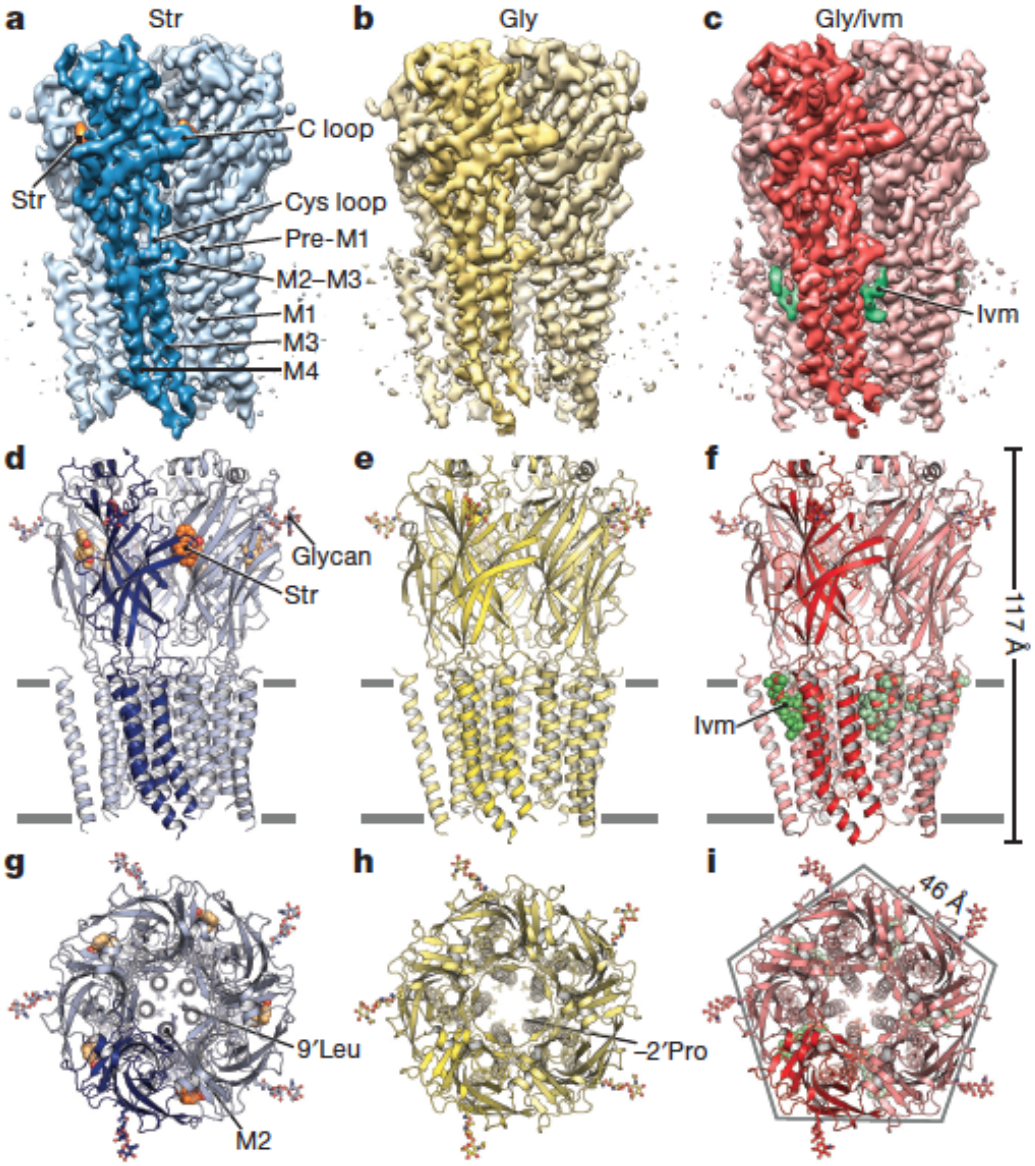

Figure 1: The overall architecture of GlyR. a − c, 3D reconstructions of the strychnine- (blue), glycine- (yellow) and glycine/ivermectin- (red) bound GlyR structures determined by single-particle electron cryo-microscopy, viewed parallel to the plasma membrane. d − f, The cartoon models of a − c. g − i, views from the extracellular side of the membrane (Du et al., 2015)

1.2 Glycine receptor subunit expression

Four isoforms of the α subunit (α1 – α4) and one isoform of β subunit are identified in mammals and share a > 90% amino acid sequence homology with each other. Their gene expression profiles are developmentally and regionally regulated. In the embryonic state, α2 transcripts are abundantly and widely expressed in spinal cord and brainstem (Kuhse et al., 1991). During the developmental period, there is a switch from α2 homomeric GlyRs to α1β heteromeric GlyRs (Lynch, 2009). Nonetheless, reduced densities of α2 mRNA still present in adult hippocampus, cerebral cortex and thalamus (Malosio et al., 1991; Sato et al., 1992; Lynch, 2004). After birth, α1 and α3 expression become more abundant. In situ hybridization studies reveal that α1 are prominently expressed in the

spinal cord, brainstem cerebellar deep nuclei, hypothalamus and colliculi (Malosio et al., 1991; Greferath et al., 1994). α3 subunit expression is relatively lower than α1 subunit at all developmental stages, and restricted to superficial laminae of the dorsal horn and respiratory network of the brainstem (Malosio et al., 1991; Harvey et al., 2004; Manzke et al., 2010). α4 has been described as an embryonic GlyR subunit isoform, which is only expressed in chick spinal cord, lumbosacral sympathetic ganglia and dorsal root ganglia (Harvey et al., 2000), but is presumed to be a pseudo-gene in humans due to a premature stop codon. In contrast, the β subunit gene is transcribed at all developmental stages and cannot form functional receptor alone. β subunit mRNA are widely and abundantly distributed in spinal cord and brain (Grenningloh et al., 1990; Fujita et al., 1991). This pattern of distribution is similar to that of α1 subunit mRNA. β subunit is considered to be indispensable for synaptic clustering by interacting with the receptor-anchoring protein gephrin (Meyer et al., 1995), therefore it is generally assumed that α1β isoform of the GlyR dominates at most "native" adult synapses in the spinal cord and brainstem (Singer et al., 1998).

1.3 Glycine receptor and disease

Alterations in the function of GlyRs have been implicated in many human diseases, such as hyperekplexia, autism, pain, epilepsy, motor neuron disease and breathing disorders.

1.3.1 Hyperekplexia

Loss of glycinergic synaptic signalling has been implicated in a rare hereditary neurological disorder, known as hyperekplexia, or startle disease. Hyperekplexia is characterized by neonatal hypertonia and an exaggerated startle reflex in response to sudden, unexpected stimuli (Bakker et al., 2006). Mutations in the *GLRA1* or *GLRB* genes, which encode the α1 and β GlyR subunits respectively, are the major cause of hyperekplexia (Harvey et al., 2008; Bode and Lynch, 2013, 2014). To date, more than 50 *GLRA* mutations and 18 *GLRB* mutations have been identified in humans (Bode and Lynch, 2014). The vast majority of these mutations are loss-of-function in that they reduce the ability of GlyRs to flux chloride. Recessive hyperekplexia mutations generally result in the loss of α1 or β GlyR protein expression at the cell surface, whereas dominant mutations usually allow strong surface expression but impair channel function via reduced open probability, single channel conductance or glycine sensitivity (Harvey et al., 2008; Bode and Lynch, 2014). In addition, several *GLRA1* gain-of-function hyperekplexia mutations have been detected to evoke spontaneous channel activity, which is paradoxical in that these mutations generated different levels of prolonged postsynaptic glycinergic currents but full hyperekplexia phenotype (Zhang et al., 2016). All genetic forms of hyperekplexia are successfully treated with the benzodiazepine or

clonazepam (Bakker et al., 2006; Thomas et al., 2013), which acts by enhancing GABAergic synaptic transmission.

1.3.2 Autism

Autism spectrum disorders (ASDs) are a group of heterogeneous neurodevelopmental disorders characterized by deficits in social interaction and communication. ASD is thought to result from dysfunctional development of multiple brain areas and to be associated with perturbed excitatory and inhibitory balance. Neuroligins (NLs) are postsynaptic cell-adhesion molecules that are essential for synapse maturation and specification. Mutations in the human NL genes *NLGN3* and *NLGN4* were detected in patients with ASDs (Mackowiak et al., 2014). Using the transgenic mice model, the *NLGN3* mutation was found to affect the balance between inhibition and excitation with an increase of inhibitory neurotransmission (Tabuchi et al., 2007).

GlyRs containing α2 subunits exert excitatory effects in immature neurons, and thereby modulate neuronal migration and synapse formation. Microdeletions and missense mutations in *GLYA*2 gene, encoding the GlyR α2 subunit, have been reported to represent a rare cause of ASDs (Piton et al., 2011; Pilorge et al., 2015). Previous studies have demonstrated that *GLYA2* mutations associated with ASD cause reduced surface GlyR expression and glycine sensitivity, and aberrant plasticity in the prefrontal cortex resulted from altered glycinergic transmission (Pilorge et al., 2015). Further investigation of the precise link between *GLYA2* and neuronal migration abnormalities related to ASDs may provide essential insights into underlying molecular mechanisms.

1.3.3 Pain

Both α1 and α3 GlyR subunits were found to present at glycinergic synapses on pain sensory neurons in the spinal cord superficial laminae (Harvey et al., 2004). GlyR $\alpha3^{-/-}$ mice display a loss of pain sensitization induced by peripheral inflammation without defects in motor coordination (Harvey et al., 2004). Inflammatory mediators (notably prostaglandin E2) induce chronic inflammatory pain by phosphorylating, and inhibiting, α3-containing GlyRs (Ahmadi et al., 2002; Harvey et al., 2004). A reduction of glycinergic inhibition onto superficial dorsal horn neurons leads to an increased transmission of nociceptive input to higher brain region. This mechanism, which provides a paradigm for chronic inflammatory pain sensitisation, implies that compounds that positively modulate α3β GlyRs should be analgesic. Given that α1β GlyRs have broader distribution and potentiating α1β GlyRs causes severe motor disorders and other side effects (Zeilhofer, 2005; Lynch and Callister, 2006), molecules with selectivity for α3β over α1β GlyRs are implicated as new generation treatments for chronic pain.

1.3.4 Temporal lobe epilepsy

In addition to processing of nociceptive signals, α3 GlyRs are also involved in hippocampal pathophysiology of temporal lobe epilepsy (Meier et al., 2005; Eichler et al., 2008; Eichler et al., 2009). It has been demonstrated that post-transcriptional RNA editing produces a new gain-of-function GlyR α3 isoform, GlyR $\alpha3^{P185L}$, resulted from cytidine 554 deamination (C554U) (Meier et al., 2005). The proline to leucine editing of GlyR α3 remarkably enhances sensitivity to glycine and remains open for longer during each synaptic events (Meier et al., 2005; Legendre et al., 2009; Dixon et al., 2015). Additionally, RNA editing of GlyR α2 at the corresponding position (P192L) was found in patients with temporal lobe epilepsy, and also produces receptors with increased agonist affinities (Eichler et al., 2008).

1.3.5 Motor neuron disease

Motor neuron disease or amyotrophic lateral sclerosis (ALS) is an adult onset neurological disease characterized by progressive motor neuron degeneration. A loss of glycinergic innervation of spinal motor neurons is evident in transgenic mouse model of ALS (Chang and Martin, 2009, 2011), suggesting hyperexcitability of motor neurons which results from the insufficient synaptic inhibition could plausibly contribute to the pathogenesis of ALS.

1.3.6 Breathing disorders

Inhibitory interactions between neurons of the brainstem respiratory network enable stable rhythmic breathing. A failure of glycinergic inhibitory transmission has been implicated in impairment of respiratory rhythm (Schmid et al., 1991; Pierrefiche et al., 1998; Busselberg et al., 2001), which may even lead to sudden death (Busselberg et al., 2001; Markstahler et al., 2002; Harvey et al., 2008).

1.4 GlyR pharmacology

1.4.1 Competitive antagonist – strychnine

GlyR channels can be activated by glycine, taurine and β-alanine, and efficiently antagonized by the plant alkaloid strychnine. Strychnine inhibits the function of GlyRs in a competitive manner, with a considerably high affinity (Ki = 16 nM) (Akagi et al., 1991; Brams et al., 2011). Like glycine and other agonist, the binding site for strychnine is located at the extracellular N-terminal domain. The residue Phe-63, Gly-160, Lys-200, Tyr-202 and Phe-207 have been defined the important determinants of strychnine binding, which are closed to agonist binding sites (Vandenberg et al., 1992b; Vandenberg et al., 1992a; Grudzinska et al., 2005; Huang et al., 2015). The core strychnine binding residues are highly conserved across the GlyR subunits but not the other pLGIC members,

which may account for highly selective for GlyRs over any other receptor type. Thus strychnine is commonly used as a unique tool in distinguishing glycinergic from GABAergic inhibition.

1.4.2 Allosteric agonist – ivermectin

Ivermectin, a naturally occurring macrocyclic lactone, potently activates glutamate-gate chloride channel receptor which is present in the neurons and muscle cells of nematodes and some arthropods but is absent in vertebrate (McCavera et al., 2009). Hence, ivermectin commercially used as an antiparasitic agent in both human medicine and veterinary practice (Omura, 2008). Previous study from our laboratory shows that ivermectin acts as a potent agonist of GlyRs that irreversibly activates α1-containing GlyRs, with an EC_{50} of 0.39 μM (Shan et al., 2001). Substitution of the residue Ala-288 and Pro-230 profoundly disrupted GlyR sensitivity to ivermectin, suggesting that the transmembrane regions play a crucial role in influencing allosteric modulation by ivermectin (Lynagh et al., 2011). In addition, ivermectin was found to exert significant allosteric modulation effects on other pLGICs, such as α7 nAChRs and $GABA_A$Rs (Krusek and Zemkova, 1994; Krause et al., 1998).

1.4.3 Allosteric modulators

Zn^{2+} ions allosterically modulate GlyRs in a dose-dependent manner, with low micromolar concentrations of Zn^{2+} potentiate glycine-activated currents and higher concentrations (> 10 μM) of Zn^{2+} inhibit glycine-evoked currents (Bloomenthal et al., 1994; Laube et al., 1995; Miller et al., 2005b; Miller et al., 2005a). The potentiating and inhibiting concentrations are critically determined by the GlyR subunit composition. The major synaptic α1β GlyR isoform is extremely sensitive to Zn^{2+}, whereas other GlyR subtypes display more than 10-fold less sensitive to Zn^{2+} (Miller et al., 2005b; Miller et al., 2005a). Residues involved with the potentiation and inhibition actions of Zn^{2+} appear to be localized distinct regions of the N-terminal domain of the alpha subunit. Sequence alignment and mutagenesis study of α1 and α2 subunits have identified residue Asp-194 in α1 subunit (which corresponds to α2 Glu-201) is a major determinant of the differential sensitivity to Zn^{2+} potentiation (Miller et al., 2005a). However, residue His-107 in α1 subunit contributes significantly to the subtype-selective Zn^{2+} inhibition. Replacing asparagine residue at the homologous position in α2 and α3 subunits with histidine residue markedly increases the potency of Zn^{2+} mediated inhibition (Miller et al., 2005b). Other sites that are important determinants for Zn^{2+} inhibition of GlyR function include His-109, Ser-112 and Ser-133 of the α1 subunit (Harvey et al., 1999; Laube et al., 2000; Nevin et al., 2003). In contrast, residues Asp-80, Glu-192, Asp-194, Thr-151, Trp-170 and His-215 of the α1 subunit are thought to contribute to high-affinity binding sites and are critically for potentiation of GlyR function by low micromolar concentrations of Zn^{2+} (Lynch et al., 1998; Miller et al., 2005a; Zhou et al., 2013). Substitution mutations in the TM1-TM2

and TM2-TM3 domains eliminated Zn^{2+} potentiation of GlyR function, indicating allosteric connection between the Zn^{2+} potentiating site and the glycine binding site, or selective disruption of transduction pathway (Lynch et al., 1998).

Furthermore, a number of different GlyR allosteric modulators have been identified, including cannabinoids, ethanol, anaesthetics, glutamate, neuroactive steroids, tropeines and picrotoxin (Hawthorne and Lynch, 2005; Yevenes and Zeilhofer, 2011). However, these modulator effects are not restricted to certain GlyR subtype but occur in many receptors. Due to lacking of subtype-selective probes, it is therefore almost impossible to dissect out specific GlyR isoform functions in different regions of the mammalian CNS.

2 Glycinergic synapses

2.1 Synaptogenesis and synapse dynamics

2.1.1 Role of GlyR α2 in cortical neuron migration

During the early brain development, migration of newly generated neurons from their site of origin to their target region in a distinct brain area is an important step. Functional α2 homomers have been found in the developing cerebral cortex (Young-Pearse et al., 2006) and can be activated by paracrine release of glycine or taurine (Flint et al., 1998; Qian et al., 2014). Due to low Cl^- extruder expression in immature neurons, intracellular Cl^- concentrations are initially high. Activation of GlyRs can be depolarizing and excitatory in immature neurons, leading to intracellular Ca^{2+} oscillations and Ca^{2+}-dependent synaptogenesis (Kirsch and Betz, 1998; Avila et al., 2013).

Several lines of evidence indicate that α2 subunit-containing GlyRs play a critical function in early development of neocortex. Deletion of *GLYA2* gene in mice results in moderate microcephaly in newborn mice (Avila et al., 2014). Activation of GlyRs promotes tangential migration of cortical interneurons from the medial ganglionic eminence to the cerebral cortex in the developing brain, whereas genetic disruption or pharmacological inhibition of α2 GlyR expression and function impaired the interneuron migration abilities (Avila et al., 2013). After birth, dendrite and spine morphological abnormalities accompanied by the loss of glycinergic signalling were observed in cortical neuron of layer V in *GLYA2* knockout mice, indicating α2 GlyRs also play a critical role in synaptogenesis (Morelli et al., 2016). The importance of GlyR α2 in neuronal migration and cortical network formation is highlighted by the identifying of ASD-related *GLYA2* mutations.

2.1.2 Key regulator of inhibitory synapse formation – gephyrin

Selective clustering of GlyRs at postsynaptic regions of neuronal plasma membrane is indispensible for the formation of functional inhibitory synapses. In the glycinergic postsynapse, gephyrin acts as a bridge between GlyRs and the cytoskeleton (Fig. 2), which can regulate postsynaptic GlyR clustering and lateral diffusion of GlyRs enter and exit synapses (Prior et al., 1992; Charrier et al., 2006). Targeted disruption of the gene encoding gephyrin in mice die within one day after birth and exhibit hypertonic phenotype similar to that of human hyperekplexia (Feng et al., 1998). Loss of GlyRs and most $GABA_AR$ clustering at inhibitory synapses most likely accounts for the early lethality of gephyrin-deficient mice (Grosskreutz et al., 2003). Antisense oligonucleotide treatment against gephyrin resulted in a loss of GlyR clusters in the cultured rat spinal neurons (Feng et al., 1998). Similarly, hippocampal neurons cultured from gephyrin knockout mice lack of GlyR clusters (Levi et al., 2004). These findings suggest that neuronal gephyrin expression is essential for GlyR localization at postsynaptic membrane specializations.

Immunohistochemical analysis has demonstrated that co-localization of GlyRs and gephyrin in a punctate pattern in the mammalian brainstem and spinal cord (Triller et al., 1985; Todd et al., 1996; Baer et al., 2003; Harvey et al., 2004). An 18-amino acid motif within the TM3-TM4 intracellular loop of the GlyR β subunit was found to bind to gephyrin with high affinity (Meyer et al., 1995). Insertion of gephyrin-binding motif derived from GlyR β subunit to the intracellular loop of GlyR α1 subunit significantly enhanced the co-localization of α1 GlyRs and gephyrin in neurons and nonneural cells (Meier et al., 2000; Meier et al., 2001). Incorporation of gephyrin-binding motif to excitatory NMDA receptor (NMDAR) cytoplasmic tail region directed NMDARs to intracellular gephyrin-rich domains in transfected HEK cells (Kins et al., 1999). $GABA_AR$ α6 and δ subunits bearing the gephyrin-binding motifs brought receptors closer to postsynaptic sites (Wu et al., 2012). Thus, gephyrin-binding motif in the TM3-TM4 intracellular loop of GlyR β subunit is sufficient for routing GlyRs to inhibitory postsynaptic sites. In contrast to the GlyR β subunit, there is no evidence for direct interaction of gephyrin to GlyR α subunits.

Heterologous expression of recombinant gephyrin in many cell lines results in intracellular gephyrin aggregation. However, gephyrin clusters were only observed at the selective postsynaptic regions in neurons, suggesting neuron-specific molecular mechanisms exist which ensures gephryin postsynaptic targeting and clustering, like posttranslational modification (Tyagarajan et al., 2011), binding to some neuronal proteins (Kins et al., 2000; Giesemann et al., 2003) and activation of GlyRs (Kirsch and Betz, 1998), etc.

2.1.3 Key regulator of synapse maturation and function – neuroligin

Trans-synaptic interaction between postsynaptic cell adhesion protein neuroligin (NL) and its presynaptic counterpart neurexin is of particular importance for the assembly and function of synaptic specializations (Dean and Dresbach, 2006). Neuroligins are transmenrbrane proteins and bind neurexins via an extracellular esterase-like domain (Fig. 2). Five neuroligin isoforms exist in humans (NL1−3, NL4X and NL4Y), while only four isoforms were found in rodent (NL1−4). NL1 is preferentially distributed in excitatory (glutamatergic) synapses (Song et al., 1999) whereas NL2 and NL4 are exclusively localized to inhibitory (GABAergic/glycinergic) postsynaptic specializaions (Varoqueaux et al., 2004; Hoon et al., 2011). NL3 is present at both excitatory and inhibitory synapses (Budreck and Scheiffele, 2007), but its functional significance is less known. NL2 is known to directly bind gephyrin through a conserved cytoplasmic motif and simultaneously bind to the gephyrin-associated protein, collybistin (Poulopoulos et al., 2009). Similarly, NL4 also interacts with gephyrin and collybistin via intracytoplasmic domain. In contrast, NL1 and NL3 were found to interact with gephyrin without binding to collybistin (Hoon et al., 2011). The significance of the NL2-gephyrin interaction was emphasized by a study showing that knockdown of gephyrin expression in neuronal cultures perturbed synaptic targeting of NL2, with a significant shift of NL2 from inhibition to excitatory synaptic contacts (Levinson et al., 2010).

Expression levels of neuroligins control the number of synapses in neurons. Knockdown of NL1, NL2 and NL3 individually or simultaneously inhibited postsynaptic maturation, as indicated by a substantial reduction in the dendritic spines density on hippocampal neurons (Chih et al., 2005). Further insight into functional evidence for neuroligin was provided by the electrophysiological analysis of *in vivo* synaptic transmission in neuroligin knockout mice. Mice lacking NL1, NL2 and NL3 genes displayed disrupted brainstem respiratory networks, with reduced GABAergic/glycinergic and glutamatergic synaptic transmission (Varoqueaux et al., 2006). Deletion of NL2 in mice resulted in a loss of GABAergic and glycinergic inhibition (Poulopoulos et al., 2009).

Neuroligin along is sufficient to induce the formation of presynaptic terminals. Cocultured NL1 or NL2-expressing nonneuronal cells with neurons induced synaptic vesicle clustering and morphological presynaptic differentiation in contacting axons, which is comparable to the real synapses (Scheiffele et al., 2000).

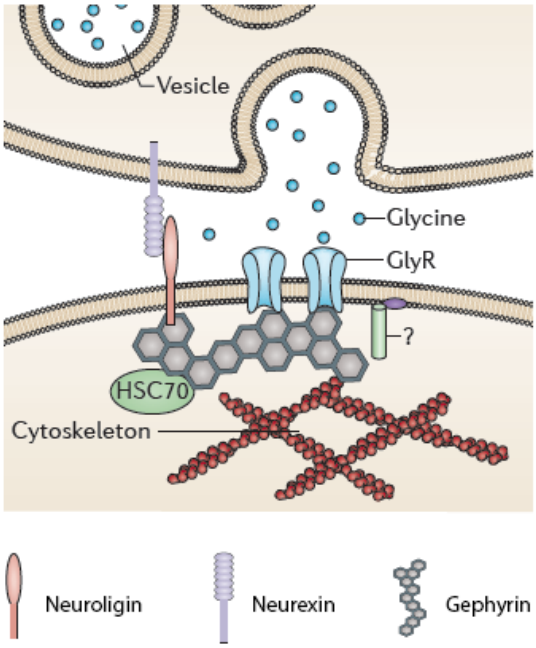

Figure 2: Architecture of essential proteins at glycinergic synapses.

Adapted from (Tyagarajan and Fritschy, 2014).

2.1.4 Regulation of GlyR dynamics at synapses

The postsynaptic components of inhibitory synapses are complex and dynamic structures. Single particle tracking (SPT) techniques is a powerful tool which involves real time monitoring lateral mobility of a small probe attached to a membrane protein of interest in living cells. The detailed analysis of individual molecular trajectories, such as quantifying diffusion properties, identifying behavioral transitions, measuring transition frequency and dwell time at synaptic or non-synaptic locations, advances our understanding of dynamic properties of synaptic receptors in the plasma membrane and their underlying mechanisms related to molecular movements (Alcor et al., 2009).

For GlyRs, the first observation of receptor dynamics at synapses was using single-quantum dot tracking on spinal cord neurons (Dahan et al., 2003). GlyRs have been demonstrated to be more confined at synaptic compartments and exchange between synapses and extrasynapses within minutes. Another study using SPT has revealed that cytoskeleton contributes to rapidly regulate GlyR levels at synapses as pharmacological disruption of cytoskeleton reduced the amount of both GlyR and gephyrin at synapse, associated with an increased GlyR transition between the synaptic and extrasynaptic sites and a decreased GlyR dwell time at synapses (Charrier et al., 2006). In addition, diffusion properties of synaptic GlyRs can be regulated through gephyrin-gephyrin interaction which can stabilize GlyRs at synapses by forming scaffolding clusters (Ehrensperger et al., 2007). Furthermore, some extrasynaptic GlyRs were proposed to diffuse in a gephyrin-bond form (Ehrensperger et al., 2007). To date, the diffusion properties of different GlyR subtypes still remain to be elucidated, with important implications for our understanding of the mechanisms

underlying the heterogeneity in inhibitory post-synaptic currents (IPSCs) kinetics and synaptic plasticity, and of tonic glycine currents, i.e. the dynamics and function of the extrasynaptic pool.

2.2 Glycinergic IPSCs

2.2.1 α1β GlyR -mediated IPSCs

The distribution glycinergic synapses have been implicated in olfactory bulb, cerebellum, hippocampus, hypothalamus, retina and gray matter in spinal cord (van den Pol and Gorcs, 1988; Wassle et al., 2009). The α1β heteromer is the predominant adult synaptic GlyR isoform and mediates the bulk of glycinergic transmission in brainstem, spinal cord and retina (Lynch, 2009). Electrophysiological recordings of glycinergic IPSCs in adult neurons show that α1β GlyR mediates IPSCs characterized by fast IPSC kinetics. In neurons of the rat anteroventral cochlear nucleus, where glycinergic synapses are somatic and thus not subject to dendritic filtering, the mean 10 – 90 % rise time was 0.42 ms and the decay time course was fitted by the sum of two exponentials with time constants of 3.6 and 28.4 ms (Lim et al., 1999). In rat dorsal horn neurons, the mean 10 – 90 % rise times and decay time constants were 0.76 and 10.2 ms, respectively (Takahashi et al., 1992). In rat lumbar motor neurons the values were comparable at 0.79 and 7.1 ms, respectively (Beato, 2008). In adult hypoglossal motor neurons the 10 – 90 % rise times and decay time constants ranged between 0.6 – 1.8 and 4.9 – 7.7 ms, respectively (Singer et al., 1998; Graham et al., 2006; Hirzel et al., 2006).

2.2.2 α2β GlyR -mediated IPSCs

The α2β GlyR predominates at glycinergic synapses in embryonic rat neurons (Lynch, 2009). Functional studies have presented that IPSCs mediated by α2β GlyR have slower decay times. Glycinergic IPSCs in embryonic day 20 rat dorsal horn neurons exhibited a mean 10 – 90 % rise time of 0.91 ms and a mean decay time constant of 27 ms (Takahashi et al., 1992), with comparable values observed in embryonic zebrafish Mauthner neurons (Ali et al., 2000), perinatal rat hypoglossal neurons (Singer et al., 1998) and adult rat wide-field amacrine cells (Veruki et al., 2007) which are unusual for adult neurons in that they selectively express α2β GlyRs (Wassle et al., 2009).

2.2.3 α3β GlyR -mediated IPSCs

The α3β GlyR is generally sparsely expressed *in vivo*, although it is co-located with α1β GlyRs in glycinergic synapses on neurons in the superficial laminae of the spinal cord dorsal horn (Harvey et al., 2004). Although α3β-mediated IPSCs have yet to be recorded in isolation in native synapses, their kinetic properties appear indistinguishable from those of α1β GlyRs (Harvey et al., 2004).

2.2.4 Modulation of glycinergic IPSCs

GlyRs are targets for phosphorylation by cAMP-dependent protein kinase (PKA) and protein kinase (PKC) (Vaello et al., 1994). Heterologous expression experiments indicate that a PKA-dependent phosphorylation occurs in the intracellular loop of α3 GlyRs which induces current inhibition (Han et al., 2013). This finding fits nicely to observations that inhibition of PKA led to a diminution of prostaglandin E_2 (PGE_2)-mediated depression of glycinergic neurotransmission in spinal dorsal horn (Ahmadi et al., 2002; Harvey et al., 2004). Despite the role of PKC in suppress of glycine receptor function has been studied extensively in Xenopus oocytes and neurons (Nishizaki and Ikeuchi, 1995; Schonrock and Bormann, 1995), (Uchiyama et al., 1994; Vaello et al., 1994), no functional evidence has demonstrated the direct effects of phosphorylation of GlyRs by PKC on glycinergic transmission. In contrast, it has been reported that phosphorylation of intracellular loop of GlyR β subunit by PKC influences the GlyR-gephyrin interaction, resulting in an enhanced GlyRs diffusion and a reduced GlyR number at inhibitory synapses (Specht et al., 2011), but the functional consequences still need to be determined.

Clinically relevant concentrations (< 100 mM) of ethanol have shown a potentiation in glycinergic activity with increases in the frequency and decay rates of miniature IPSC (mIPSC) in spinal neurons, brainstem motoneurons, and neurons in the ventral tegmental area (Eggers et al., 2000; Ye et al., 2001; Sebe et al., 2003; Mariqueo et al., 2014). Neurons primarily expressing mature α1-containing synapses are more sensitive to ethanol than neonate neurons expressing primarily α2-containing GlyRs (Eggers et al., 2000). The enhanced mIPSC frequency is due to presynaptically effect whereas the increased decay rate is due to ethanol modulation effects of GlyR function (Eggers and Berger, 2004; Mariqueo et al., 2014).

In addition, inflammatory cytokine interleukin-1β has been implicated in the potentiation of glycinergic synaptic currents from dorsal horn neurons (Chirila et al., 2014). GlyRs are also found in the presynaptic nerve terminals. Exogenous application of glycine (3 μM) resulted in an increased frequency of glycinergic IPSCs in rat spinal sacral dorsal commissural nucleus neurons while their amplitudes and decay times were unaffected (Jeong et al., 2003). This indicates that glycine could also acts presynaptically to modulate glycine release.

2.3 Heterosynapses

The subunit composition of native GlyRs varies both developmentally and regionally (Baer et al., 2009). The heterogeneity of subunit composition underlies the heterogeneity in GlyR-mediated IPSC kinetics. Each GlyR isoform has unique properties that contribute to modulate neuronal

activity and behavior, and disruptions to these properties can result in human diseases. For example, hereditary mutations of GlyR α and β subunits cause human hyperekplexia by affecting subcellular location and intrinsic properties of receptors, finally leading to the reduced glycinergic transmission (Bode and Lynch, 2014). Due to the multitude of other isoforms present at the same synapse and the difficulty in pharmacologically or genetically isolating the receptor isoform of interest, only limited information is available for understand the role of specific GlyR isoform in the human health and disease.

Although GlyRs are not currently pharmacological targets for clinically important agents, molecules that selectively enhance α3-containing GlyRs are considered promising as new generation treatments for chronic pain (Zeilhofer, 2005; Lynch and Callister, 2006). Because α1- and α3-containing GlyRs are both expressed in inhibitory synapses on spinal pain sensory neuron, with α3 possibly as the minor partner (Graham et al., 2011), any pharmacological effect of α3-specific drugs may be diluted by the presence of other isoforms. Moreover, drugs that act non-specifically at the GlyRs in the CNS may cause undesirable motor disorders and other side effects. By developing strategies that specifically target IPSCs mediated by defined GlyR isoforms, it is possible to evaluate drug efficacy and selectivity under realistic synaptic activation conditions.

Co-culture synapses were first described more than fifteen years ago to investigate molecular mechanisms underlying synaptogenesis (Scheiffele et al., 2000). Neuroligins-expressing nonneuronal cells stimulate the formation of presynaptic structure in contacting axons of co-cultured neurons (Scheiffele et al., 2000; Kim et al., 2006b). Accordingly, neurexin-expressing nonneuronal cells induce postsynaptic differentiation in contacting dendrites of co-cultured neurons (Graf et al., 2004). In addition, other synaptic cell adhesion molecules including postsynaptic netrin-G ligand-2 (Kim et al., 2006b), SynCAM (Biederer et al., 2002; Sara et al., 2005) were found to be able to trigger formation of excitatory synapses by using co-culture methods. Co-culture of human HEK293 cells co-expressing SynCAM and GluR2 with hippocampal neurons exhibited postsynaptic glutamatergic transmission similar to those of neurons (Biederer et al., 2002). Excitatory postsynaptic currents (EPSCs) were also obtained in HEK293 cells transfected with neuroligins together with NMDA or AMPA receptors in a co-culture with cerebella granule cells (Fu et al., 2003). Later, expressing NL2 with $GABA_A$Rs (Dong et al., 2007), or $GABA_A$Rs along (Fuchs et al., 2013) in the HEK293 cell lines successfully reconstituted functional GABAergic synapses by co-culturing with medium spiny neurons, hippocampal neurons or hypothalamic neurons. Recent studies have used cortical neuron-HEK cell heterosynapse to investigate synaptic targeting properties of different $GABA_A$R subunits (Wu et al., 2012; Dixon et al., 2014) with

GABAerigc IPSCs recorded from the 'artificial' synapse agree very well with those recorded from neurons, and to identify the structural determinant of $GABA_A$Rs in synaptic contact formation (Brown et al., 2016). The 'artificial' synapse can be easily extended to investigate the impact of disease-related neuroligin mutations on GABAergic synaptogenesis (Chubykin et al., 2005; Sun et al., 2011).

Viewed together, the 'artificial' synapse offers a best tool for investigation into the kinetic properties of IPSCs mediated by defined GlyR isoforms and the effects of drugs on IPSCs mediated by selective GlyR isoforms. Furthermore, it is also possible to examine the effects of posttranslational modifications (e.g., phosphorylation) and hereditary disease mutations on the formation and function of glycinergic synapses, and molecular mechanisms regulating the synaptogenesis and synaptic clustering.

3 Zinc: role in synaptic transmission

3.1 Zinc modulation of glutamatergic synapses

The free ionic form of zinc (Zn^{2+}) plays a dynamic role in many biological processes including synaptic transmission (Sensi et al., 2009). At many glutamatergic synapses in the central nervous system (CNS), it is well known that Zn^{2+} is concentrated into presynaptic vesicles (Frederickson, 1989) and is released into the synaptic cleft by nerve terminal stimulation (Assaf and Chung, 1984; Howell et al., 1984). The estimation of how Zn^{2+} concentration increase during synaptic activation is spanning four orders of magnitude from 10 nM (Kay, 2003) to > 100 μM (Vogt et al., 2000). The lower estimate stems from studies that concluded that Zn^{2+} is not released in a phasic manner at all, but rather becomes 'externalized' following exocytosis and then binds tightly to presynaptic proteins forming a 'veneer' (Kay, 2003; Kay and Toth, 2006, 2008).

The NMDARs incorporating GluN2A subunits that populate most glutamatergic synapses are unique in that they inhibited by Zn^{2+} at low nanomolar concentrations (Paoletti et al., 1997). Mutation in the gene encoding GluN2A subunit led to impaired GluN2A-Zn^{2+} interaction in children with idiopathic focal epilepsy (Lemke et al., 2013), revealing an essential role of high-affinity Zn^{2+} inhibition in human health. Previous experiments demonstrate that at hippocampal mossy fiber synapses, the presence of endogenous Zn^{2+} tonically occupies the high-affinity binding site of NMDARs, and synaptically released Zn^{2+} during neuronal activity occupies the lower-affinity binding site of NMDARs, resulting in the depression of NMDAR response (Vogt et al., 2000). However, this concept has been challenged by recent electrophysiological observations

under normal extracellular condition (Vergnano et al., 2014). Vergnano *et al* found a lack of the high-affinity, voltage-independent inhibition at MF-CA synapses, which are the mainly Zn^{2+}-enriched synapses within the brain, whereas fast repetitive stimulation unveiled Zn^{2+}-mediated inhibition of EPSCs (Vergnano et al., 2014). This indicates that ambient Zn^{2+} levels at resting conditions are insufficient to populate the high-affinity GluN2A Zn^{2+} binding sites, and a short burst of synaptic stimulation is required for Zn^{2+} modulation of NMDAR-mediated EPSCs. In contrast, another investigation using a high-affinity Zn^{2+} chelator at the same synapses concluded that synaptic release of Zn^{2+} in response to a single action potential is capable of modulating NMDAR-mediated activity (Pan et al., 2011). In addition, ambient Zn^{2+} levels were proposed to be lower at synaptic site but higher at extrasynaptic site, thus extrasynaptic NMDARs activated by glutamate spillover can be subjected to tonic Zn^{2+}-mediated inhibitory modulation (Anderson et al., 2015).

Kainate and AMPA receptors are other abundant types of glutamate receptors involving in synaptic transmission. By using zinc chelator, endogenous Zn^{2+} was found to selectively inhibit kainate but not AMPA receptors at mossy fiber synapses (Mott et al., 2008).

3.2 Zinc modulation of GABAergic synapses

Zn^{2+} also have potent inhibition effects on $GABA_AR$ (Westbrook and Mayer, 1987). The sensitivities to Zn^{2+} are considerably different among the $GABA_AR$ subtypes (Draguhn et al., 1990; Smart et al., 1991). For example, $GABA_ARs$ containing the γ subunits are far less sensitive to low concentrations of Zn^{2+} (Draguhn et al., 1990; Smart et al., 1991), and Zn^{2+} inhibition was found greater in $GABA_ARs$ containing α2 and α3 subunits than those containing α1 subunits (White and Gurley, 1995). Ruiz *et al* first demonstrate that GABA and Zn^{2+} can be co-localized in the same mossy fiber varicosities and endogenous Zn^{2+} can inhibit GABAergic response in CA3 pyramidal neurons in guinea pig hippocampal slices (Ruiz et al., 2004). In this study, Ruiz *et al* also suggest extracellular Zn^{2+} associated with mossy fibers inhibit $GABA_AR$ in a tonic fashion, with little dynamic modulation of inhibition by synaptically released Zn^{2+} with physiological patterns of stimuli. Furthermore, it is demonstrated that endogenous Zn^{2+} not only depresses monosynaptic GABAergic synaptic transmission though direct binding to $GABA_ARs$, but also inhibits di-synaptic GABAergic signalling by regulating the excitability of presynaptic interneurons (Grauert et al., 2014).

3.3 Zinc in the glycinergic synaptic cleft

GlyRs have been identified as one of the potential synaptic targets for zinc effects on inhibitory transmission. As discussed above, the positive or negative modulatory effects of Zn^{2+} on GlyRs

depends on its concentration. The major synaptic α1β GlyR isoform is extremely sensitive to Zn^{2+}, with low (10 – 1000 nM) Zn^{2+} concentrations potentiating EC_{50} glycine-gated currents and higher Zn^{2+} concentrations (3 – 300 μM) eliciting a dose-dependent inhibition (Bloomenthal et al., 1994; Laube et al., 1995; Miller et al., 2005b; Miller et al., 2005a). In experiments with membrane-impermeant Zn^{2+} buffers and chelators, it has been shown that glycinergic IPSCs are positively modulated by tonic Zn^{2+} (Suwa et al., 2001; Hirzel et al., 2006; Perez-Rosello et al., 2015). The knock-in mice carrying a point mutation ($\alpha1^{D80A}$) that selectively ablated the sensitivity of α1 GlyRs to Zn^{2+} potentiation displayed a severe motor phenotype with symptoms resemble those observed in human hypereplexia (Hirzel et al., 2006). Electrophysiological recordings from the brainstem hypoglossal neurons detected a reduced amplitude and a accelerated decay time of glycinergic IPSCs in knock-in mice, consistent with a loss of Zn^{2+} potentiation. Since no changes were observed in glycine sensitivity, GlyR expression levels, synaptic localization, and glycinergic IPSC kinetics when neurons predominately expressed α2 instead of α1 subunits, it was concluded that the hyperekplexia-type phenotype in $\alpha1^{D80A}$ GlyR knock-in mice is due to the impaired Zn^{2+} potentiation (Hirzel et al., 2006). As to the action of synaptic Zn^{2+}, a tonic and/or a phasic manner for Zn^{2+}-mediated potentiation of glycinergic IPSCs has been proposed by Kay *et al* (Kay et al., 2006).

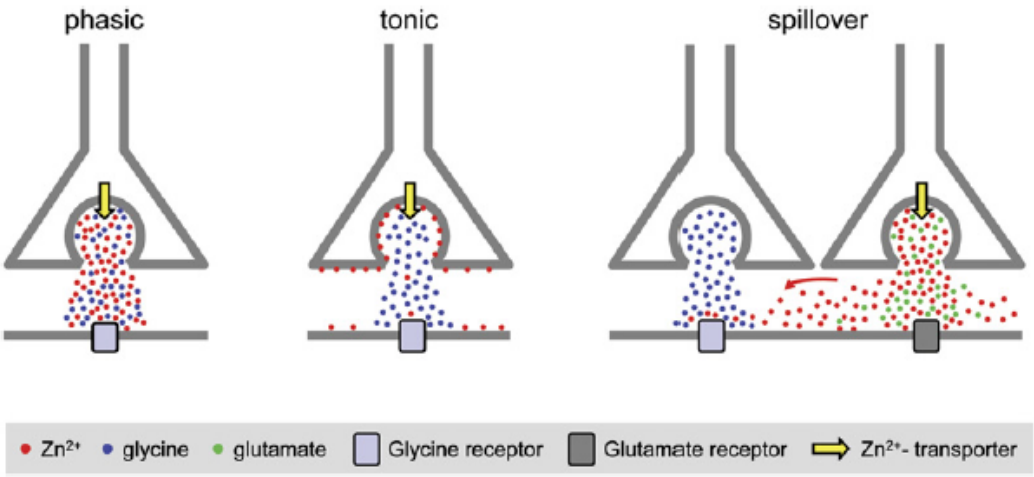

Figure 3: The proposed mechanisms for Zn^{2+}-mediated modulation of glycinergic transmission. In the phasic model, Zn^{2+} is co-released with other neurotransmitter into glycinergic synaptic cleft upon exocytosis, and rapidly pumped back into cells. However, in the tonic model, only a few Zn^{2+} could be released into the extracellular space, and most Zn^{2+} would tonically bind to proteins on the pre- and postsynaptic membranes, forming a veneer layer of Zn^{2+}. Alternatively, spillover of Zn^{2+} from the vicinity of synapses (e.g. glutamatergic synapses) could be another source (Kay et al., 2006).

Despite a co-localization of Zn^{2+} and glycine has been reported at presynaptic terminals in the spinal cord of the lamprey (Birinyi et al., 2001), there is currently no direct evidence for the co-

localization of Zn^{2+}, glycine and vesicular Zn^{2+} transporter (ZnT3) at glycinergic presynaptic terminals in the mammalian brainstem or spinal cord. Thus, the origin of Zn^{2+} in glycinergic synapses remains enigmatic. A recent study reported that tonic Zn^{2+}-mediated potentiation of glycinergic neurotransmission decreased spontaneous firing in mice auditory brainstem nucleus, and the increase in spontaneous firing frequency by removal of Zn^{2+} in ZnT3 knock-out mice was comparable to the increase observed in wild-type mice (Perez-Rosello et al., 2015). The authors proposed that Zn^{2+}-mediated modulation of neuronal excitability probably in the areas that are not closed to the sites of synaptically released Zn^{2+}.

At physiological concentrations, Zn^{2+} can also modulate a variety of ion channel in CNS, including voltage-gated calcium channels, voltage-gated potassium channels, acid-sensing ion channels, P2X receptors, $5HT_3R$ and nAChRs, etc (Marger et al., 2014). As Zn^{2+} can have very different (sometimes opposite) effects on the function of potential targets depending on the concentrations, quantitative estimation of zinc concentration in the synaptic cleft will help us to understand both the synaptic targets and action of synaptically released Zn^{2+}.

Aims of the thesis

The overall aim of this thesis was to establish glycinergic 'artificial' synapse system which can provide some aspects of normal and abnormal glycinergic neurotransmission in health and disease.

Aim 1: Establish the methods for reliably generating recombinant glycinergic synapses that incorporate defined GlyR isoforms of interest.

Aim 2: Investigate the mechanism by which gain-of-function *GLRA1* mutations cause hyperekplexia by using 'artificial' synapse.

Aim 3: Investigate the effects of α2 GlyR autism mutations on glycinergic synaptic function.

Aim 4: Estimate the free zinc concentration in the glycinergic synaptic cleft following a single presynaptic stimulation.

REFERENCES:

Ahmadi S, Lippross S, Neuhuber WL, Zeilhofer HU (2002) PGE(2) selectively blocks inhibitory glycinergic neurotransmission onto rat superficial dorsal horn neurons. Nat Neurosci 5:34-40.

Akagi H, Hirai K, Hishinuma F (1991) Functional properties of strychnine-sensitive glycine receptors expressed in Xenopus oocytes injected with a single mRNA. Neurosci Res 11:28-40.

Alcor D, Gouzer G, Triller A (2009) Single-particle tracking methods for the study of membrane receptors dynamics. Eur J Neurosci 30:987-997.

Ali DW, Drapeau P, Legendre P (2000) Development of spontaneous glycinergic currents in the Mauthner neuron of the zebrafish embryo. J Neurophysiol 84:1726-1736.

Anderson CT, Radford RJ, Zastrow ML, Zhang DY, Apfel UP, Lippard SJ, Tzounopoulos T (2015) Modulation of extrasynaptic NMDA receptors by synaptic and tonic zinc. Proc Natl Acad Sci U S A 112:E2705-2714.

Assaf SY, Chung SH (1984) Release of endogenous Zn2+ from brain tissue during activity. Nature 308:734-736.

Avila A, Vidal PM, Dear TN, Harvey RJ, Rigo JM, Nguyen L (2013) Glycine receptor alpha2 subunit activation promotes cortical interneuron migration. Cell Rep 4:738-750.

Avila A, Vidal PM, Tielens S, Morelli G, Laguesse S, Harvey RJ, Rigo JM, Nguyen L (2014) Glycine receptors control the generation of projection neurons in the developing cerebral cortex. Cell Death Differ 21:1696-1708.

Baer K, Waldvogel HJ, Faull RL, Rees MI (2009) Localization of glycine receptors in the human forebrain, brainstem, and cervical spinal cord: an immunohistochemical review. Front Mol Neurosci 2:25.

Baer K, Waldvogel HJ, During MJ, Snell RG, Faull RLM, Rees MI (2003) Association of gephyrin and glycine receptors in the human brainstem and spinal cord: An immuniphistochemical analysis. Neuroscience 122:773-784.

Bakker MJ, van Dijk JG, van den Maagdenberg AM, Tijssen MA (2006) Startle syndromes. Lancet Neurol 5:513-524.

Beato M (2008) The time course of transmitter at glycinergic synapses onto motoneurons. Journal of Neuroscience 28:7412-7425.

Biederer T, Sara Y, Mozhayeva M, Atasoy D, Liu XR, Kavalali ET, Sudhof TC (2002) SynCAM, a synaptic adhesion molecule that drives synapse assembly. Science 297:1525-1531.

Birinyi A, Parker D, Antal M, Shupliakov O (2001) Zinc co-localizes with GABA and glycine in synapses in the lamprey spinal cord. J Comp Neurol 433:208-221.

Bloomenthal AB, Goldwater E, Pritchett DB, Harrison NL (1994) Biphasic modulation of the strychnine-sensitive glycine receptor by Zn2+. Mol Pharmacol 46:1156-1159.

Bode A, Lynch JW (2013) Analysis of Hyperekplexia Mutations Identifies Transmembrane Domain Rearrangements That Mediate Glycine Receptor Activation. Journal of Biological Chemistry 288:33760-33771.

Bode A, Lynch JW (2014) The impact of human hyperekplexia mutations on glycine receptor structure and function. Mol Brain 7:2.

Brams M, Pandya A, Kuzmin D, van Elk R, Krijnen L, Yakel JL, Tsetlin V, Smit AB, Ulens C (2011) A structural and mutagenic blueprint for molecular recognition of strychnine and d-tubocurarine by different cys-loop receptors. PLoS Biol 9:e1001034.

Brown LE, Nicholson MW, Arama JE, Mercer A, Thomson AM, Jovanovic JN (2016) gamma-aminobutyric acid type A (GABAA) receptor subunits play a direct structural role in synaptic contact formation via their N-terminal extracellular domains. J Biol Chem.

Budreck EC, Scheiffele P (2007) Neuroligin-3 is a neuronal adhesion protein at GABAergic and glutamatergic synapses. European Journal of Neuroscience 26:1738-1748.

Busselberg D, Bischoff AM, Becker K, Becker CM, Richter DW (2001) The respiratory rhythm in mutant oscillator mice. Neurosci Lett 316:99-102.
Carland JE, Cooper MA, Sugiharto S, Jeong HJ, Lewis TM, Barry PH, Peters JA, Lambert JJ, Moorhouse AJ (2009) Characterization of the effects of charged residues in the intracellular loop on ion permeation in alpha1 glycine receptor channels. J Biol Chem 284:2023-2030.
Chang Q, Martin LJ (2009) Glycinergic innervation of motoneurons is deficient in amyotrophic lateral sclerosis mice: a quantitative confocal analysis. Am J Pathol 174:574-585.
Chang Q, Martin LJ (2011) Glycine receptor channels in spinal motoneurons are abnormal in a transgenic mouse model of amyotrophic lateral sclerosis. J Neurosci 31:2815-2827.
Charrier C, Ehrensperger MV, Dahan M, Levi S, Triller A (2006) Cytoskeleton regulation of glycine receptor number at synapses and diffusion in the plasma membrane. Journal of Neuroscience 26:8502-8511.
Chih B, Engelman H, Scheiffele P (2005) Control of excitatory and inhibitory synapse formation by neuroligins. Science 307:1324-1328.
Chirila AM, Brown TE, Bishop RA, Bellono NW, Pucci FG, Kauer JA (2014) Long-term potentiation of glycinergic synapses triggered by interleukin 1beta. Proc Natl Acad Sci U S A 111:8263-8268.
Chubykin AA, Liu X, Comoletti D, Tsigelny I, Taylor P, Sudhof TC (2005) Dissection of synapse induction by neuroligins: effect of a neuroligin mutation associated with autism. J Biol Chem 280:22365-22374.
Dahan M, Levi S, Luccardini C, Rostaing P, Riveau B, Triller A (2003) Diffusion dynamics of glycine receptors revealed by single-quantum dot tracking. Science 302:442-445.
Dean C, Dresbach T (2006) Neuroligins and neurexins: linking cell adhesion, synapse formation and cognitive function. Trends Neurosci 29:21-29.
Del Pino I, Koch D, Schemm R, Qualmann B, Betz H, Paarmann I (2014) Proteomic analysis of glycine receptor beta subunit (GlyRbeta)-interacting proteins: evidence for syndapin I regulating synaptic glycine receptors. J Biol Chem 289:11396-11409.
Dixon C, Sah P, Lynch JW, Keramidas A (2014) GABAA receptor alpha and gamma subunits shape synaptic currents via different mechanisms. J Biol Chem 289:5399-5411.
Dixon CL, Zhang Y, Lynch JW (2015) Generation of Functional Inhibitory Synapses Incorporating Defined Combinations of GABA(A) or Glycine Receptor Subunits. Front Mol Neurosci 8:80.
Dong N, Qi J, Chen G (2007) Molecular reconstitution of functional GABAergic synapses with expression of neuroligin-2 and GABAA receptors. Mol Cell Neurosci 35:14-23.
Draguhn A, Verdorn TA, Ewert M, Seeburg PH, Sakmann B (1990) Functional and Molecular Distinction between Recombinant Rat Gaba-a Receptor Subtypes by Zn-2+. Neuron 5:781-788.
Du J, Lu W, Wu S, Cheng Y, Gouaux E (2015) Glycine receptor mechanism elucidated by electron cryo-microscopy. Nature 526:224-229.
Durisic N, Godin AG, Wever CM, Heyes CD, Lakadamyali M, Dent JA (2012) Stoichiometry of the Human Glycine Receptor Revealed by Direct Subunit Counting. Journal of Neuroscience 32:12915-12920.
Eggers ED, Berger AJ (2004) Mechanisms for the modulation of native glycine receptor channels by ethanol. J Neurophysiol 91:2685-2695.
Eggers ED, O'Brien JA, Berger AJ (2000) Developmental changes in the modulation of synaptic glycine receptors by ethanol. J Neurophysiol 84:2409-2416.
Ehrensperger MV, Hanus C, Vannier C, Triller A, Dahan M (2007) Multiple association states between glycine receptors and gephyrin identified by SPT analysis. Biophysical Journal 92:3706-3718.
Eichler SA, Kirischuk S, Juttner R, Schaefermeier PK, Legendre P, Lehmann TN, Gloveli T, Grantyn R, Meier JC (2008) Glycinergic tonic inhibition of hippocampal neurons with

depolarizing GABAergic transmission elicits histopathological signs of temporal lobe epilepsy. J Cell Mol Med 12:2848-2866.
Eichler SA, Forstera B, Smolinsky B, Juttner R, Lehmann TN, Fahling M, Schwarz G, Legendre P, Meier JC (2009) Splice-specific roles of glycine receptor alpha3 in the hippocampus. Eur J Neurosci 30:1077-1091.
Feng GP, Tintrup H, Kirsch J, Nichol MC, Kuhse J, Betz H, Sanes JR (1998) Dual requirement for gephyrin in glycine receptor clustering and molybdoenzyme activity. Science 282:1321-1324.
Flint AC, Liu X, Kriegstein AR (1998) Nonsynaptic glycine receptor activation during early neocortical development. Neuron 20:43-53.
Frederickson CJ (1989) Neurobiology of zinc and zinc-containing neurons. Int Rev Neurobiol 31:145-238.
Fu Z, Washbourne P, Ortinski P, Vicini S (2003) Functional excitatory synapses in HEK293 cells expressing neuroligin and glutamate receptors. J Neurophysiol 90:3950-3957.
Fuchs C, Abitbol K, Burden JJ, Mercer A, Brown L, Iball J, Anne Stephenson F, Thomson AM, Jovanovic JN (2013) GABA(A) receptors can initiate the formation of functional inhibitory GABAergic synapses. Eur J Neurosci 38:3146-3158.
Fujita M, Sato K, Sato M, Inoue T, Kozuka T, Tohyama M (1991) Regional distribution of the cells expressing glycine receptor beta subunit mRNA in the rat brain. Brain Res 560:23-37.
Giesemann T, Schwarz G, Nawrotzki R, Berhorster K, Rothkegel M, Schluter K, Schrader N, Schindelin H, Mendel RR, Kirsch J, Jockusch BM (2003) Complex formation between the postsynaptic scaffolding protein gephyrin, profilin, and mena: A possible link of the microfilament system. Journal of Neuroscience 23:8330-8339.
Graf ER, Zhang X, Jin SX, Linhoff MW, Craig AM (2004) Neurexins induce differentiation of GABA and glutamate postsynaptic specializations via neuroligins. Cell 119:1013-1026.
Graham BA, Tadros MA, Schofield PR, Callister RJ (2011) Probing glycine receptor stoichiometry in superficial dorsal horn neurones using the spasmodic mouse. J Physiol-London 589:2459-2474.
Graham BA, Schofield PR, Sah P, Margrie TW, Callister RJ (2006) Distinct physiological mechanisms underlie altered glycinergic synaptic transmission in the murine mutants spastic, spasmodic, and oscillator. J Neurosci 26:4880-4890.
Grauert A, Engel D, Ruiz AJ (2014) Endogenous zinc depresses GABAergic transmission via T-type Ca(2+) channels and broadens the time window for integration of glutamatergic inputs in dentate granule cells. J Physiol 592:67-86.
Greferath U, Brandstatter JH, Wassle H, Kirsch J, Kuhse J, Grunert U (1994) Differential expression of glycine receptor subunits in the retina of the rat: a study using immunohistochemistry and in situ hybridization. Vis Neurosci 11:721-729.
Grenningloh G, Pribilla I, Prior P, Multhaup G, Beyreuther K, Taleb O, Betz H (1990) Cloning and expression of the 58 kd beta subunit of the inhibitory glycine receptor. Neuron 4:963-970.
Grosskreutz Y, Betz H, Kneussel M (2003) Rescue of molybdenum cofactor biosynthesis in gephyrin-deficient mice by a Cnx1 transgene. Biochem Bioph Res Co 301:450-455.
Grudzinska J, Schemm R, Haeger S, Nicke A, Schmalzing G, Betz H, Laube B (2005) The beta subunit determines the ligand binding properties of synaptic glycine receptors. Neuron 45:727-739.
Han L, Talwar S, Wang Q, Shan Q, Lynch JW (2013) Phosphorylation of alpha3 glycine receptors induces a conformational change in the glycine-binding site. ACS Chem Neurosci 4:1361-1370.
Harvey RJ, Topf M, Harvey K, Rees MI (2008) The genetics of hyperekplexia: more than startle! Trends Genet 24:439-447.
Harvey RJ, Thomas P, James CH, Wilderspin A, Smart TG (1999) Identification of an inhibitory Zn2+ binding site on the human glycine receptor alpha1 subunit. J Physiol 520 Pt 1:53-64.

Harvey RJ, Schmieden V, Von Holst A, Laube B, Rohrer H, Betz H (2000) Glycine receptors containing the alpha4 subunit in the embryonic sympathetic nervous system, spinal cord and male genital ridge. Eur J Neurosci 12:994-1001.

Harvey RJ, Depner UB, Wassle H, Ahmadi S, Heindl C, Reinold H, Smart TG, Harvey K, Schutz B, Abo-Salem OM, Zimmer A, Poisbeau P, Welzl H, Wolfer DP, Betz H, Zeilhofer HU, Muller U (2004) GlyR alpha3: an essential target for spinal PGE2-mediated inflammatory pain sensitization. Science 304:884-887.

Hawthorne R, Lynch JW (2005) A picrotoxin-specific conformational change in the glycine receptor M2-M3 loop. J Biol Chem 280:35836-35843.

Hirzel K, Muller U, Latal AT, Hulsmann S, Grudzinska J, Seeliger MW, Betz H, Laube B (2006) Hyperekplexia phenotype of glycine receptor alpha1 subunit mutant mice identifies Zn(2+) as an essential endogenous modulator of glycinergic neurotransmission. Neuron 52:679-690.

Hoon M, Soykan T, Falkenburger B, Hammer M, Patrizi A, Schmidt KF, Sassoe-Pognetto M, Lowel S, Moser T, Taschenberger H, Brose N, Varoqueaux F (2011) Neuroligin-4 is localized to glycinergic postsynapses and regulates inhibition in the retina. P Natl Acad Sci USA 108:3053-3058.

Howell GA, Welch MG, Frederickson CJ (1984) Stimulation-induced uptake and release of zinc in hippocampal slices. Nature 308:736-738.

Huang X, Chen H, Michelsen K, Schneider S, Shaffer PL (2015) Crystal structure of human glycine receptor-alpha3 bound to antagonist strychnine. Nature 526:277-280.

Jeong HJ, Jang IS, Moorhouse AJ, Akaike N (2003) Activation of presynaptic glycine receptors facilitates glycine release from presynaptic terminals synapsing onto rat spinal sacral dorsal commissural nucleus neurons. J Physiol 550:373-383.

Kay AR (2003) Evidence for chelatable zinc in the extracellular space of the hippocampus, but little evidence for synaptic release of Zn. J Neurosci 23:6847-6855.

Kay AR, Toth K (2006) Influence of location of a fluorescent zinc probe in brain slices on its response to synaptic activation. J Neurophysiol 95:1949-1956.

Kay AR, Toth K (2008) Is Zinc a Neuromodulator? Science Signaling 1.

Kay AR, Neyton J, Paoletti P (2006) A startling role for synaptic zinc. Neuron 52:572-574.

Kim EY, Schrader N, Smolinsky B, Bedet C, Vannier C, Schwarz G, Schindelin H (2006a) Deciphering the structural framework of glycine receptor anchoring by gephyrin. EMBO J 25:1385-1395.

Kim S, Burette A, Chung HS, Kwon SK, Woo J, Lee HW, Kim K, Kim H, Weinberg RJ, Kim E (2006b) NGL family PSD-95-interacting adhesion molecules regulate excitatory synapse formation. Nat Neurosci 9:1294-1301.

Kins S, Betz H, Kirsch J (2000) Collybistin, a newly identified brain-specific GEF, induces submembrane clustering of gephyrin. Nature Neuroscience 3:22-29.

Kins S, Kuhse J, Laube B, Betz H, Kirsch J (1999) Incorporation of a gephyrin-binding motif targets NMDA receptors to gephyrin-rich domains in HEK 293 cells. Eur J Neurosci 11:740-744.

Kirsch J, Betz H (1998) Glycine-receptor activation is required for receptor clustering in spinal neurons. Nature 392:717-720.

Krause RM, Buisson B, Bertrand S, Corringer PJ, Galzi JL, Changeux JP, Bertrand D (1998) Ivermectin: a positive allosteric effector of the alpha7 neuronal nicotinic acetylcholine receptor. Mol Pharmacol 53:283-294.

Krusek J, Zemkova H (1994) Effect of ivermectin on gamma-aminobutyric acid-induced chloride currents in mouse hippocampal embryonic neurones. Eur J Pharmacol 259:121-128.

Kuhse J, Kuryatov A, Maulet Y, Malosio ML, Schmieden V, Betz H (1991) Alternative splicing generates two isoforms of the alpha 2 subunit of the inhibitory glycine receptor. FEBS Lett 283:73-77.

Laube B, Kuhse J, Betz H (2000) Kinetic and mutational analysis of Zn2+ modulation of recombinant human inhibitory glycine receptors. J Physiol 522 Pt 2:215-230.
Laube B, Kuhse J, Rundstrom N, Kirsch J, Schmieden V, Betz H (1995) Modulation by zinc ions of native rat and recombinant human inhibitory glycine receptors. J Physiol 483 (Pt 3):613-619.
Legendre P (1998) A reluctant gating mode of glycine receptor channels determines the time course of inhibitory miniature synaptic events in zebrafish hindbrain neurons. Journal of Neuroscience 18:2856-2870.
Legendre P, Forstera B, Juttner R, Meier JC (2009) Glycine Receptors Caught between Genome and Proteome - Functional Implications of RNA Editing and Splicing. Front Mol Neurosci 2:23.
Lemke JR et al. (2013) Mutations in GRIN2A cause idiopathic focal epilepsy with rolandic spikes. Nat Genet 45:1067-1072.
Levi S, Logan SM, Tovar KR, Craig AM (2004) Gephyrin is critical for glycine receptor clustering but not for the formation of functional GABAergic synapses in hippocampal neurons. Journal of Neuroscience 24:207-217.
Levinson JN, Li R, Kang R, Moukhles H, El-Husseini A, Bamji SX (2010) Postsynaptic scaffolding molecules modulate the localization of neuroligins. Neuroscience 165:782-793.
Lim R, Alvarez FJ, Walmsley B (1999) Quantal size is correlated with receptor cluster area at glycinergic synapses in the rat brainstem. J Physiol 516 (Pt 2):505-512.
Lynagh T, Webb TI, Dixon CL, Cromer BA, Lynch JW (2011) Molecular Determinants of Ivermectin Sensitivity at the Glycine Receptor Chloride Channel. Journal of Biological Chemistry 286:43913-43924.
Lynch JW (2004) Molecular structure and function of the glycine receptor chloride channel. Physiological Reviews 84:1051-1095.
Lynch JW (2009) Native glycine receptor subtypes and their physiological roles. Neuropharmacology 56:303-309.
Lynch JW, Callister RJ (2006) Glycine receptors: a new therapeutic target in pain pathways. Curr Opin Investig Drugs 7:48-53.
Lynch JW, Jacques P, Pierce KD, Schofield PR (1998) Zinc potentiation of the glycine receptor chloride channel is mediated by allosteric pathways. Journal of Neurochemistry 71:2159-2168.
Mackowiak M, Mordalska P, Wedzony K (2014) Neuroligins, synapse balance and neuropsychiatric disorders. Pharmacol Rep 66:830-835.
Malosio ML, Marqueze-Pouey B, Kuhse J, Betz H (1991) Widespread expression of glycine receptor subunit mRNAs in the adult and developing rat brain. EMBO J 10:2401-2409.
Manzke T, Niebert M, Koch UR, Caley A, Vogelgesang S, Hulsmann S, Ponimaskin E, Muller U, Smart TG, Harvey RJ, Richter DW (2010) Serotonin receptor 1A-modulated phosphorylation of glycine receptor alpha3 controls breathing in mice. J Clin Invest 120:4118-4128.
Marger L, Schubert CR, Bertrand D (2014) Zinc: an underappreciated modulatory factor of brain function. Biochem Pharmacol 91:426-435.
Mariqueo TA, Agurto A, Munoz B, San Martin L, Coronado C, Fernandez-Perez EJ, Murath P, Sanchez A, Homanics GE, Aguayo LG (2014) Effects of ethanol on glycinergic synaptic currents in mouse spinal cord neurons. J Neurophysiol 111:1940-1948.
Markstahler U, Kremer E, Kimmina S, Becker K, Richter DW (2002) Effects of functional knock-out of alpha 1 glycine-receptors on breathing movements in oscillator mice. Respir Physiol Neurobiol 130:33-42.
McCavera S, Rogers AT, Yates DM, Woods DJ, Wolstenholme AJ (2009) An ivermectin-sensitive glutamate-gated chloride channel from the parasitic nematode Haemonchus contortus. Mol Pharmacol 75:1347-1355.

Meier J, Meunier-Durmort C, Forest C, Triller A, Vannier C (2000) Formation of glycine receptor clusters and their accumulation at synapses. J Cell Sci 113 (Pt 15):2783-2795.
Meier J, Vannier C, Serge A, Triller A, Choquet D (2001) Fast and reversible trapping of surface glycine receptors by gephyrin. Nat Neurosci 4:253-260.
Meier JC, Henneberger C, Melnick I, Racca C, Harvey RJ, Heinemann U, Schmieden V, Grantyn R (2005) RNA editing produces glycine receptor alpha3(P185L), resulting in high agonist potency. Nat Neurosci 8:736-744.
Meyer G, Kirsch J, Betz H, Langosch D (1995) Identification of a Gephyrin Binding Motif on the Glycine Receptor-Beta Subunit. Neuron 15:563-572.
Miller PS, Da Silva HMA, Smart TG (2005a) Molecular basis for zinc potentiation at strychnine-sensitive glycine receptors. Journal of Biological Chemistry 280:37877-37884.
Miller PS, Beato M, Harvey RJ, Smart TG (2005b) Molecular determinants of glycine receptor alphabeta subunit sensitivities to Zn2+-mediated inhibition. J Physiol 566:657-670.
Morelli G, Avila A, Ravanidis S, Aourz N, Neve RL, Smolders I, Harvey RJ, Rigo JM, Nguyen L, Brone B (2016) Cerebral Cortical Circuitry Formation Requires Functional Glycine Receptors. Cereb Cortex.
Mott DD, Benveniste M, Dingledine RJ (2008) pH-dependent inhibition of kainate receptors by zinc. J Neurosci 28:1659-1671.
Nevin ST, Cromer BA, Haddrill JL, Morton CJ, Parker MW, Lynch JW (2003) Insights into the structural basis for zinc inhibition of the glycine receptor. Journal of Biological Chemistry 278:28985-28992.
Nishizaki T, Ikeuchi Y (1995) Activation of endogenous protein kinase C enhances currents through alpha 1 and alpha 2 glycine receptor channels. Brain Res 687:214-216.
Omura S (2008) Ivermectin: 25 years and still going strong. Int J Antimicrob Agents 31:91-98.
Pan E, Zhang XA, Huang Z, Krezel A, Zhao M, Tinberg CE, Lippard SJ, McNamara JO (2011) Vesicular zinc promotes presynaptic and inhibits postsynaptic long-term potentiation of mossy fiber-CA3 synapse. Neuron 71:1116-1126.
Paoletti P, Ascher P, Neyton J (1997) High-affinity zinc inhibition of NMDA NR1-NR2A receptors. J Neurosci 17:5711-5725.
Perez-Rosello T, Anderson CT, Ling C, Lippard SJ, Tzounopoulos T (2015) Tonic zinc inhibits spontaneous firing in dorsal cochlear nucleus principal neurons by enhancing glycinergic neurotransmission. Neurobiol Dis 81:14-19.
Pierrefiche O, Schwarzacher SW, Bischoff AM, Richter DW (1998) Blockade of synaptic inhibition within the pre-Botzinger complex in the cat suppresses respiratory rhythm generation in vivo. J Physiol 509 (Pt 1):245-254.
Pilorge M et al. (2015) Genetic and functional analyses demonstrate a role for abnormal glycinergic signaling in autism. Mol Psychiatry.
Piton A et al. (2011) Systematic resequencing of X-chromosome synaptic genes in autism spectrum disorder and schizophrenia. Mol Psychiatry 16:867-880.
Poulopoulos A, Aramuni G, Meyer G, Soykan T, Hoon M, Papadopoulos T, Zhang M, Paarmann I, Fuchs C, Harvey K, Jedlicka P, Schwarzacher SW, Betz H, Harvey RJ, Brose N, Zhang W, Varoqueaux F (2009) Neuroligin 2 drives postsynaptic assembly at perisomatic inhibitory synapses through gephyrin and collybistin. Neuron 63:628-642.
Prior P, Schmitt B, Grenningloh G, Pribilla I, Multhaup G, Beyreuther K, Maulet Y, Werner P, Langosch D, Kirsch J, Betz H (1992) Primary Structure and Alternative Splice Variants of Gephyrin, a Putative Glycine Receptor Tubulin Linker Protein. Neuron 8:1161-1170.
Qian T, Chen R, Nakamura M, Furukawa T, Kumada T, Akita T, Kilb W, Luhmann HJ, Nakahara D, Fukuda A (2014) Activity-dependent endogenous taurine release facilitates excitatory neurotransmission in the neocortical marginal zone of neonatal rats. Front Cell Neurosci 8:33.
Ruiz A, Walker MC, Fabian-Fine R, Kullmann DM (2004) Endogenous zinc inhibits GABA(A) receptors in a hippocampal pathway. J Neurophysiol 91:1091-1096.

Sara Y, Biederer T, Atasoy D, Chubykin A, Mozhayeva MG, Sudhof TC, Kavalali ET (2005) Selective capability of SynCAM and neuroligin for functional synapse assembly. J Neurosci 25:260-270.

Sato K, Kiyama H, Tohyama M (1992) Regional distribution of cells expressing glycine receptor alpha 2 subunit mRNA in the rat brain. Brain Res 590:95-108.

Scheiffele P, Fan J, Choih J, Fetter R, Serafini T (2000) Neuroligin expressed in nonneuronal cells triggers presynaptic development in contacting axons. Cell 101:657-669.

Schmid K, Bohmer G, Gebauer K (1991) Glycine receptor-mediated fast synaptic inhibition in the brainstem respiratory system. Respir Physiol 84:351-361.

Schonrock B, Bormann J (1995) Modulation of hippocampal glycine receptor channels by protein kinase C. Neuroreport 6:301-304.

Sebe JY, Eggers ED, Berger AJ (2003) Differential effects of ethanol on GABA(A) and glycine receptor-mediated synaptic currents in brain stem motoneurons. J Neurophysiol 90:870-875.

Sensi SL, Paoletti P, Bush AI, Sekler I (2009) Zinc in the physiology and pathology of the CNS. Nat Rev Neurosci 10:780-791.

Shan Q, Haddrill JL, Lynch JW (2001) Ivermectin, an unconventional agonist of the glycine receptor chloride channel. J Biol Chem 276:12556-12564.

Singer JH, Talley EM, Bayliss DA, Berger AJ (1998) Development of glycinergic synaptic transmission to rat brain stem motoneurons. J Neurophysiol 80:2608-2620.

Smart TG, Moss SJ, Xie X, Huganir RL (1991) GABAA receptors are differentially sensitive to zinc: dependence on subunit composition. Br J Pharmacol 103:1837-1839.

Song JY, Ichtchenko K, Sudhof TC, Brose N (1999) Neuroligin 1 is a postsynaptic cell-adhesion molecule of excitatory synapses. Proc Natl Acad Sci U S A 96:1100-1105.

Specht CG, Grunewald N, Pascual O, Rostgaard N, Schwarz G, Triller A (2011) Regulation of glycine receptor diffusion properties and gephyrin interactions by protein kinase C. EMBO J 30:3842-3853.

Sun C, Cheng MC, Qin R, Liao DL, Chen TT, Koong FJ, Chen G, Chen CH (2011) Identification and functional characterization of rare mutations of the neuroligin-2 gene (NLGN2) associated with schizophrenia. Hum Mol Genet 20:3042-3051.

Suwa H, Saint-Amant L, Triller A, Drapeau P, Legendre P (2001) High-affinity zinc potentiation of inhibitory postsynaptic glycinergic currents in the zebrafish hindbrain. J Neurophysiol 85:912-925.

Tabuchi K, Blundell J, Etherton MR, Hammer RE, Liu X, Powell CM, Sudhof TC (2007) A neuroligin-3 mutation implicated in autism increases inhibitory synaptic transmission in mice. Science 318:71-76.

Takahashi T, Momiyama A, Hirai K, Hishinuma F, Akagi H (1992) Functional correlation of fetal and adult forms of glycine receptors with developmental changes in inhibitory synaptic receptor channels. Neuron 9:1155-1161.

Thomas RH, Chung SK, Wood SE, Cushion TD, Drew CJ, Hammond CL, Vanbellinghen JF, Mullins JG, Rees MI (2013) Genotype-phenotype correlations in hyperekplexia: apnoeas, learning difficulties and speech delay. Brain 136:3085-3095.

Todd AJ, Watt C, Spike RC, Sieghart W (1996) Colocalization of GABA, glycine, and their receptors at synapses in the rat spinal cord. Journal of Neuroscience 16:974-982.

Triller A, Cluzeaud F, Pfeiffer F, Betz H, Korn H (1985) Distribution of Glycine Receptors at Central Synapses - an Immunoelectron Microscopy Study. Journal of Cell Biology 101:683-688.

Tyagarajan SK, Fritschy JM (2014) Gephyrin: a master regulator of neuronal function? Nat Rev Neurosci 15:141-156.

Tyagarajan SK, Ghosh H, Yevenes GE, Nikonenko I, Ebeling C, Schwerdel C, Sidler C, Zeilhofer HU, Gerrits B, Muller D, Fritschy JM (2011) Regulation of GABAergic synapse formation and plasticity by GSK3 beta-dependent phosphorylation of gephyrin. P Natl Acad Sci USA 108:379-384.

Uchiyama M, Hirai K, Hishinuma F, Akagi H (1994) Down-regulation of glycine receptor channels by protein kinase C in Xenopus oocytes injected with synthetic RNA. Brain Res Mol Brain Res 24:295-300.
Vaello ML, Ruiz-Gomez A, Lerma J, Mayor F, Jr. (1994) Modulation of inhibitory glycine receptors by phosphorylation by protein kinase C and cAMP-dependent protein kinase. J Biol Chem 269:2002-2008.
van den Pol AN, Gorcs T (1988) Glycine and glycine receptor immunoreactivity in brain and spinal cord. J Neurosci 8:472-492.
Vandenberg RJ, Handford CA, Schofield PR (1992a) Distinct agonist- and antagonist-binding sites on the glycine receptor. Neuron 9:491-496.
Vandenberg RJ, French CR, Barry PH, Shine J, Schofield PR (1992b) Antagonism of ligand-gated ion channel receptors: two domains of the glycine receptor alpha subunit form the strychnine-binding site. Proc Natl Acad Sci U S A 89:1765-1769.
Varoqueaux F, Jamain S, Brose N (2004) Neuroligin 2 is exclusively localized to inhibitory synapses. European Journal of Cell Biology 83:449-456.
Varoqueaux F, Aramuni G, Rawson RL, Mohrmann R, Missler M, Gottmann K, Zhang W, Sudhof TC, Brose N (2006) Neuroligins determine synapse maturation and function. Neuron 51:741-754.
Vergnano AM, Rebola N, Savtchenko LP, Pinheiro PS, Casado M, Kieffer BL, Rusakov DA, Mulle C, Paoletti P (2014) Zinc dynamics and action at excitatory synapses. Neuron 82:1101-1114.
Veruki ML, Gill SB, Hartveit E (2007) Spontaneous IPSCs and glycine receptors with slow kinetics in wide-field amacrine cells in the mature rat retina. J Physiol 581:203-219.
Vogt K, Mellor J, Tong G, Nicoll R (2000) The actions of synaptically released zinc at hippocampal mossy fiber synapses. Neuron 26:187-196.
Wassle H, Heinze L, Ivanova E, Majumdar S, Weiss J, Harvey RJ, Haverkamp S (2009) Glycinergic transmission in the Mammalian retina. Front Mol Neurosci 2:6.
Westbrook GL, Mayer ML (1987) Micromolar concentrations of Zn2+ antagonize NMDA and GABA responses of hippocampal neurons. Nature 328:640-643.
White G, Gurley DA (1995) Alpha subunits influence Zn block of gamma 2 containing GABAA receptor currents. Neuroreport 6:461-464.
Wu X, Wu Z, Ning G, Guo Y, Ali R, Macdonald RL, De Blas AL, Luscher B, Chen G (2012) gamma-Aminobutyric Acid Type A (GABA(A)) Receptor alpha Subunits Play a Direct Role in Synaptic Versus Extrasynaptic Targeting. Journal of Biological Chemistry 287:27417-27430.
Yang Z, Taran E, Webb TI, Lynch JW (2012) Stoichiometry and subunit arrangement of alpha1beta glycine receptors as determined by atomic force microscopy. Biochemistry 51:5229-5231.
Ye JH, Tao L, Ren J, Schaefer R, Krnjevic K, Liu PL, Schiller DA, McArdle JJ (2001) Ethanol potentiation of glycine-induced responses in dissociated neurons of rat ventral tegmental area. J Pharmacol Exp Ther 296:77-83.
Yevenes GE, Zeilhofer HU (2011) Allosteric modulation of glycine receptors. Br J Pharmacol 164:224-236.
Young-Pearse TL, Ivic L, Kriegstein AR, Cepko CL (2006) Characterization of mice with targeted deletion of glycine receptor alpha 2. Mol Cell Biol 26:5728-5734.
Zeilhofer HU (2005) The glycinergic control of spinal pain processing. Cell Mol Life Sci 62:2027-2035.
Zhang Y, Bode A, Nguyen B, Keramidas A, Lynch JW (2016) Investigating the Mechanism by which Gain-of-Function Mutations to the alpha1 Glycine Receptor cause Hyperekplexia. J Biol Chem.
Zhou N, Wang CH, Zhang S, Wu DC (2013) The GLRA1 missense mutation W170S associates lack of Zn2+ potentiation with human hyperekplexia. J Neurosci 33:17675-17681.

Chapter 2

Functional reconstitution of glycinergic synapses incorporating defined glycine receptor subunit combinations

Functional reconstitution of glycinergic synapses incorporating defined glycine receptor subunit combinations

Yan Zhang[1], Christine L. Dixon[1], Angelo Keramidas[1], Joseph W. Lynch[1,2]*.

[1]Queensland Brain Institute and [2]School of Biomedical Sciences, University of Queensland, Brisbane QLD Australia 4072

Running title: Reconstitution of glycinergic synapses

*To whom correspondence should be addressed: Queensland Brain Institute, Building 79, University of Queensland, St Lucia, QLD 4072, Australia. Phone: +61 7 33466375, Fax: +61 7 33466301, E-mail: j.lynch@uq.edu.au

Abbreviations

GlyR, glycine receptor
IPSC, inhibitory postsynaptic current
NL2, neuroligin-2
NL2A, neuroligin-2A

Highlights

- We present a method for generating recombinant glycinergic synapses
- Inhibitory postsynaptic currents resemble those of native glycinergic synapses
- The method will be useful for validating the effects of GlyR isoform-specific drugs
- It will also be useful for evaluating the effects of GlyR disease mutations

Abstract

Glycine receptor (GlyR) chloride channels mediate fast inhibitory neurotransmission in the spinal cord and brainstem. Four GlyR subunits (α1 – 3, β) have been identified in humans, and their differential anatomical distributions result in a diversity of synaptic isoforms with unique physiological and pharmacological properties. To improve our understanding of these properties, we induced the formation of recombinant synapses between cultured spinal neurons and HEK293 cells expressing GlyR subunits of interest plus the synapse-promoting molecule, neuroligin-2A. In the heterosynapses thus formed, recombinant α1β and α3β GlyRs mediated fast decaying inhibitory postsynaptic currents (IPSCs) whereas α2β GlyRs mediated slow decaying IPSCs. These results are consistent with the fragmentary information available from native synapses and single channel kinetic studies. As β subunit incorporation is considered essential for localizing GlyRs at the synapse, we were surprized that α1 – 3 homomers supported robust IPSCs with β subunit incorporation accelerating IPSC rise and decay times in α2β and α3β heteromers only. Finally, heterosynapses incorporating $\alpha1^{D80A}\beta$ and $\alpha1^{A52S}\beta$ GlyRs exhibited accelerated IPSC decay rates closely resembling those recorded in native synapses from mutant mice homozygous for these mutations, providing an additional validation of our technique. Glycinergic heterosynapses should prove useful for evaluating the effects of drugs, hereditary disease mutations or other interventions on defined GlyR subunit combinations under realistic synaptic activation conditions.

Keywords

inhibitory neurotransmission, synaptogenesis, neuroligin, human, synaptic kinetics, patch-clamp

Chemical compounds studied in this article

Lindane (PubChem CID: 727), tricine (PubChem CID: 79784), strychnine (PubChem CID: 441071)

Introduction

Glycine receptor (GlyR) chloride channels mediate fast inhibitory neurotransmission in the brainstem and spinal cord, and disruptions to their function underlie a range of disorders including chronic inflammatory pain (Lynch and Callister, 2006; Zeilhofer, 2005), hyperekplexia (Bode and Lynch, 2014), tinnitus (Wang et al., 2009), temporal lobe epilepsy (Eichler et al., 2008) and neuropsychiatric disorders (Winkelmann et al., 2014). GlyRs are pentameric ligand-gated ion channels comprizing either homomeric assemblies of α subunits or heteromeric assemblies of α and β subunits in either 2α:3β or 3α:2β stoichiometries (Durisic et al., 2012; Grudzinska et al., 2005; Yang et al., 2012). The β subunit is considered essential for clustering GlyRs at synapses due to its direct interaction with the cytoplasmic clustering protein, gephyrin (Fritschy et al., 2008; Kneussel and Loebrich, 2007; Meyer et al., 1995). In humans, four GlyR subunits (α1 – 3 and β) have been identified and their distribution varies both developmentally and regionally (Baer et al., 2009). This underlies a heterogeneity in inhibitory postsynaptic current (IPSC) kinetics and synaptic plasticity mechanisms that provide appropriately nuanced influences on network behavior in the central nervous system.

Because it is often not possible to ascertain which GlyR subunits are present in a particular synapse, our understanding of the synaptic properties of different GlyR isoforms is incomplete. For example, although α3 immunoreactivity suggests it is strongly expressed in synapses on spinal nociceptive neurons (Harvey et al., 2004), there is doubt as to whether α3β GlyRs contribute significantly to the function of these synapses (Graham et al., 2011).

A related issue is that it is difficult to validate the effects of drugs on defined GlyR isoforms under synaptic activation conditions. For example, compounds that potentiate α3-containing GlyRs but do not affect other GlyRs are considered potential leads for analgesic development (Lynch and Callister, 2006; Zeilhofer, 2005). Because α1- and α3-containing GlyRs are both expressed in inhibitory synapses on spinal pain sensory neuron, with α3 possibly as the minor partner (Graham et al., 2011), any pharmacological effect of α3-specific drugs may be diluted by the presence of other isoforms.

It has proved routinely possible to reconstitute GABAergic synapses between cultured GABAergic neurons (that provide the presynaptic terminals) and HEK293 cells that express the desired GABA-A subunits plus neuroligin 2 (NL2) (Dixon et al., 2014; Dong et al., 2007; Fuchs et al., 2013; Wu et al., 2012). We refer to these as ‘heterosynapses’. Postsynaptic NL2 is key to generating such synapses due to its ability to promote synapse formation by binding to trans-synaptic neurexins (Lise and El-Husseini, 2006). Because NL2 is also important for glycinergic synapse maturation (Poulopoulos et al., 2009), we reasoned that it should be feasible to induce glycinergic heterosynapse formation between cultured spinal glycinergic neurons and HEK293 cells

expressing NL2 plus the GlyR subunits of interest. In the present study, we show that this is indeed feasible and we employ this approach to characterize heterosynaptic IPSCs mediated by a variety of wild type and mutant GlyR subunit combinations.

Materials and methods

Cell culture and molecular biology

Plasmid DNAs encoding the human α1 (pCIS), human α2 (pCIS), rat α3 (pcDNA3.1) and human β (pcDNA3.1) GlyR subunits were transfected into HEK293 cells via calcium phosphate-DNA coprecipitation. We transfected α cDNA with β cDNA at different ratios from 1:1 to 1:100. Homomeric GlyRs were produced by transfecting α subunit only. In addition, the mouse NL2A splice variant (pNice) and rat gephyrin (pCIS) were co-transfected along with GlyR subunits, which facilitated the formation of heterosynapses. eGFP, which acted as expression marker was also transfected. The total amount of the final cDNA mixture per 35-mm petri dish was kept at 1 – 2 μg. Site-directed mutagenesis was performed using the QuikChange mutagenesis kit, and the successful incorporation of mutation was confirmed by DNA sequencing.

Primary cultures of spinal cord neurons were prepared as previously described (Hoch et al., 1989; Levi et al., 1998) from embryonic day 15 rat pups. Cells were plated at a density of ~80000 cells per 18 mm poly-D-lysine coated coverslip in DMEM medium with 10% fetal bovine serum. After 24 hours, the plating medium was changed to Neurobasal medium supplemented with 2% B27 and 1% glutamax, and a second feed after one week replaced half of this medium. Neurons were grown for 1 – 4 weeks *in vitro* and the heterosynaptic co-cultures were prepared by directly introducing transfected HEK293 cells onto the primary neuronal cultures 1 – 3 days prior to recordings.

Electrophysiology

Whole-cell recordings were performed under voltage-clamp mode using a HEKA EPC10 amplifier (HEKA Electronics, Lambrecht, Germany) and Patchmaster software (HEKA), at room temperature. Series resistance was routinely compensated to 60% of maximum and was monitored throughout the recording. Both spontaneous and action potential-evoked glycinergic IPSCs in HEK cells were recorded at a holding potential −60 mV and signals were filtered at 4 kHz and sampled at 10 kHz. Patch pipettes (4 − 8 MΩ resistance), made from borosilicate glass (GC150F-7.5, Harvard apparatus), were filled with an intracellular solution containing the following (in mM): 145 CsCl, 2 $CaCl_2$, 2 $MgCl_2$, 10 HEPES, 10 EGTA and 2 MgATP, adjusted to pH 7.4 with NaOH. Cells were

continuously perfused with extracellular solution comprizing (in mM): 140 NaCl, 5 KCl, 2 $CaCl_2$, 1 $MgCl_2$, 10 HEPES, and 10 D-glucose, adjusted to pH 7.4 with NaOH.

In the pharmacological studies, lindane, strychnine or tricine (all from Sigma-Aldrich) were applied by bath perfusion. After waiting 2 min for drug effects to stabilize, we compared at least 3 min of spontaneous activity before and after drug application.

Analysis

Analyses of IPSC amplitude, 10 − 90% rise time, and decay time constant (single-exponential) were performed using Axograph X (Axograph Scientific). Only cells with a stable series resistance of < 25 MΩ throughout the recording period were included in the analysis. Single peak IPSCs with amplitudes of at least three times above the background noise were detected using a semiautomated sliding template. Each detected event was visually inspected and only well-separated IPSCs with no inflections in the rizing or decay phases were included. The kinetics of IPSCs were determined by averaging the selected currents. These averages from multiple recording days were then pooled to obtain group data. Statistical analysis and plotting were performed with Prism 5 (GraphPad Software). All data are presented as mean ± SEM. One-way and two-way ANOVA were employed for multiple comparisons. Drug group comparisons were made using paired Student's *t*-tests. For all tests, the number of asterisks corresponds to level of significance: $*p < 0.05$, $**p < 0.01$, $***p < 0.001$ and $****p < 0.0001$.

Results

Establishing the conditions for reliable β subunit expression in heterosynapses

As synaptic GlyRs are considered to comprise heteromers of α and β subunits (Lynch, 2009), it is important to verify that αβ heteromeric GlyRs are predominantly expressed in our system. This is a particular concern given that a recent single channel study reported difficulty in reliably expressing heteromers of α3 and β subunits (Marabelli et al., 2013). As a negative control for β subunit incorporation, we first tested whether α1, α2 or α3 subunits could form synaptic-like currents in the absence of the β subunit. These experiments involved transfecting HEK293 cells with the relevant α subunit plus NL2A and gephyrin. Sample recordings of IPSCs from HEK293 cells expressing these constructs suggest markedly different decay kinetics for α1, α2 and α3 GlyRs (Fig. 1A). Next, we transfected α and β cDNAs at different ratios (ranging from 1:1 to 1:100) to identify the conditions required to achieve a high level of heteromeric receptor expression (Fig. 1B, C). In Fig. 1B, each data point represents the average of all IPSCs recorded from a single cell. Examples of IPSCs recorded from cells expressing the indicated heteromeric GlyRs are shown in

Fig. 1C. To pharmacologically verify β subunit incorporation into recombinant GlyRs, we applied 30 µM lindane which completely inhibits homomeric GlyRs but does not affect α1β heteromeric GlyRs (Islam and Lynch, 2012). As expected, lindane completely inhibited IPSCs in cells expressing homomeric GlyRs but had no significant effect on those expressing heteromeric GlyRs (Fig. 1C, D). We also confirmed that heterosynaptic IPSCs mediated by all subunit combinations were completely inhibited by 10 µM strychnine (e.g., Fig. 1D), a potent but nonspecific GlyR antagonist (Legendre, 2001; Lynch, 2004).

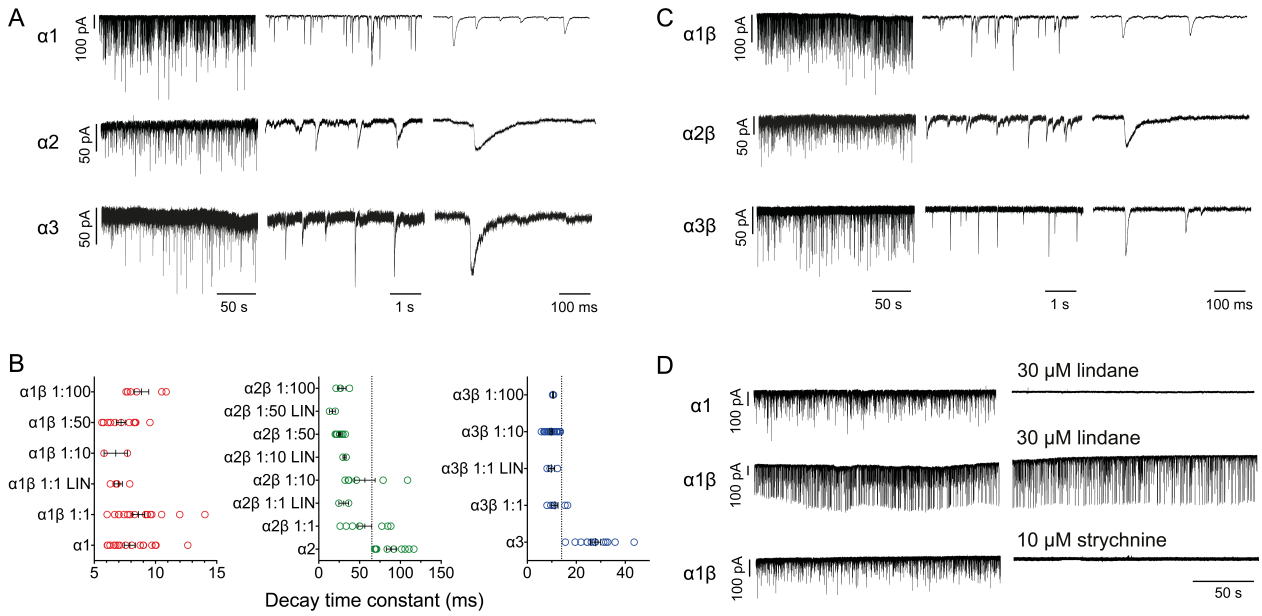

Figure 1. Homomeric and heteromeric GlyR-mediated IPSCs in heterosynapses. **A**. Representative recordings of glycinergic IPSCs in HEK293 cells expressing the indicated homomeric GlyRs at three different temporal resolutions. **B**. Distribution of decay time constants for IPSCs recorded with the indicated transfection ratios, showing the effects of incorporation of β subunit on IPSC decay times. Data were obtained in the absence and presence of extracellular lindane (LIN, 30 µM). Each data point represents the mean of all events recorded in a single cell. **C**. Representative glycinergic IPSCs recorded from HEK293 cells expressing the indicated heteromeric GlyRs. α and β GlyR cDNA were transfected at different ratios (1α:50β for α1β and α2β, 1α:10β for α3β) to minimize contamination by homomeric α receptors. **D**. Sample recordings illustrating the effect of lindane and strychnine on HEK293 cells expressing the indicated subunits. A transfection ratio of 1α:50β was used to generate α1β GlyRs. Mean results for lindane are shown in panel B.

With increasing β subunit expression, we observed a trend toward faster IPSC decay time constants in α2 and α3-containing cells, but not in α1-containing cells (Fig. 1B). When α2 and β cDNAs were cotransfected at 1:1 and 1:10 ratios, decay time constants were broadly distributed, suggesting that the heterosynapses contained a mixed population of α2 homomeric and α2β heteromeric GlyRs. Lindane selectively eliminated the slower events, demonstrating that they were indeed mediated by homomeric α2 GlyRs (Fig. 2B). Lindane had no effect at α2:β transfection

ratios of 1:50 and 1:100, suggesting that a reasonably pure population of heteromeric GlyRs had been attained. Co-expression with the β subunit also reduced decay time constants in HEK293 cells expressing the α3 subunit (Fig. 1A – C). However, the impact of increasing the proportion of β cDNA on mean decay time constants was less variable. With an α3:β transfection ratio of 1:10, all heterosynapses appeared to exclusively express α3β GlyRs (Fig. 1B). Thus, the optimal transfection ratios for generating heteromeric IPSCs were 1:50 for α2:β and 1:10 for α3:β (Fig. 1C). These ratios were used throughout the remainder of this study.

We could not distinguish α1 from α1β GlyR-mediated IPSCs according to their decay kinetics (Fig. 1A – C). For the remainder of this study we employed a 1:50 transfection ratio for α1:β, consistent with previous studies that verified the incidence of heteromer formation by monitoring single channel conductance (Burzomato et al., 2004; Pitt et al., 2008).

Kinetic properties of glycinergic heterosynapses

We characterized the mean amplitudes, 10 – 90 % rise times and decay time constants of IPSCs mediated by recombinant α1, α2, α3, α1β, α2β and α3β GlyRs (Fig. 2). Intriguingly, heterosynapses incorporating α1β and α3β GlyRs exhibited similar IPSC characteristics (Fig. 2A), with mean amplitudes of 58.6 ± 6.4 pA and 53.7 ± 10.1 pA ($p > 0.05$), mean 10 – 90 % rise times of 1.6 ± 0.1 ms and 2.0 ± 0.1 ms ($p > 0.05$) and mean decay time constants of 7.2 ± 0.4 ms and 9.7 ± 0.5 ms ($p > 0.05$), respectively. Conversely, α2β GlyR-mediated heterosynapses exhibited IPSCs with dramatically slower decay time constants (25.7 ± 1.5 ms) than those mediated by α1β or α3β GlyRs (Fig. 2A, right panel). As noted above, α1 is the only subunit that supports identical homomeric and heteromeric IPSC kinetics. In contrast, decay time constants measured from α2 and α3 homomeric heterosynapses were considerably longer than their heteromeric counterparts (Fig. 2A). A two-way ANOVA indicated that both α and β subunits had high significantly effects on current decay time constants ($p < 0.0001$).

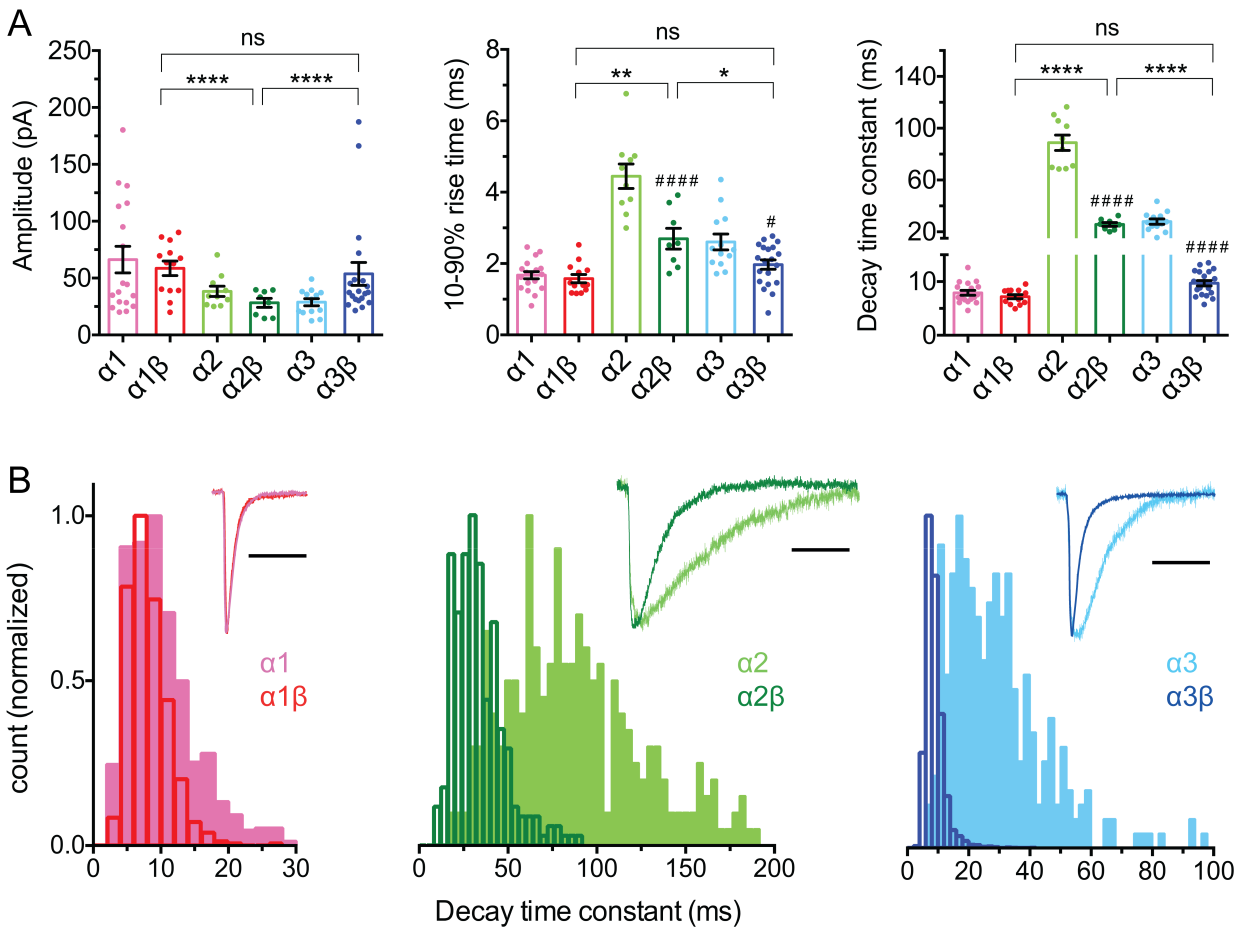

Figure 2. Comparison of the kinetics of heteromeric and homomeric GlyR-mediated IPSCs. **A.** Mean values for the amplitude, 10 – 90% rise time and decay time constant of IPSCs recorded from homomeric and heteromeric GlyRs (transfection ratios- 1α:50β for α1β and α2β, 1α:10β for α3β). Each data point represents the mean of all events recorded in a single cell. **B.** Distribution histograms of IPSC decay time constants plotted against normalized number of events (n = 6 cells for each subtype). Inset shows homomer and heteromer averages for comparison (n > 30 events for homomers; n > 150 events for heteromers), normalized to peak amplitude. Scale bar, 50 ms. *$p < 0.05$, **$p < 0.01$, ****$p < 0.0001$; #$p < 0.05$, ####$p < 0.0001$ relative to corresponding homomers. ns, not significant.

The event distribution histograms (Fig. 2B), which pooled the decay time constants of all individual events in six cells selected at random expressing the indicated homomeric and heteromeric GlyRs, confirms that the β subunit had little effect on the distribution of events in α1 GlyR-containing heterosynapses. In contrast, incorporation of the β subunit into α2 and α3-containing GlyRs shifted the distribution in the decay time constants to much lower values (Fig. 2B). Finally, we found that 10 – 90 % rise times and decay time constants were not significantly correlated for any of the six GlyR isoforms (all linear correlation coefficients < 0.33). Together these results suggest that events mediated by each individual isoform cannot be segregated into different categories (e.g., synaptic *vs*. peri-synaptic).

In summary, the kinetics of α1β and α3β GlyR-mediated IPSCs were similar to each other but faster than α2β GlyR-mediated IPSCs. In addition, the β subunit enhanced the decay rate of IPSCs mediated by α2- and α3-containing GlyRs only.

Comparison of heterosynaptic and native synapses incorporating mutant α1 subunits

Low (10 – 300 nM) zinc concentrations rapidly potentiate α1 GlyRs whereas higher concentrations (3 – 300 μM) elicit a dose-dependent, slowly-developing inhibition (Bloomenthal et al., 1994). Zinc exerts broadly similar effects at all GlyR subtypes (Miller et al., 2005a) and the molecular determinants of both potentiation and inhibition are spatially distinct and have been well characterized (Grudzinska et al., 2008; Harvey et al., 1999; Laube et al., 1995; Laube et al., 2000; Lynch et al., 1998; Miller et al., 2005a; Miller et al., 2005b; Nevin et al., 2003). Zinc is released from presynaptic glycinergic terminals upon nerve stimulation (Birinyi et al., 2001) and modulates glycinergic synaptic transmission *in vivo* by binding to and potentiating GlyRs. Given that the glycine concentration in the native synaptic cleft is saturating (Beato, 2008), the physiological effect of zinc is to prolong IPSC duration. The $\alpha1^{D80A}$ mutation is one of several mutations known to selectively eliminate zinc potentiation (Hirzel et al., 2006; Lynch et al., 1998). Consistent with this, a genetically modified mouse harbouring the homozygous $\alpha1^{D80A}$ mutation exhibited rapidly decaying glycinegic IPSCs in adult hypoglossal motor neurons that predominantly express α1β GlyRs (Hirzel et al., 2006).

We performed two experiments to evaluate whether endogenous zinc prolongs the duration of IPSCs in α1β GlyR-mediated heterosynapses. The first involved applying a 10 mM concentration of the zinc chelator, tricine. Fig. 3A displays sample recordings before and after tricine application, with the respective averaged, normalized IPSCs shown in Fig. 3B. As summarized in Fig. 3C, 10 mM tricine significantly reduced the decay time constant (from 7.6 ± 0.7 to 6.2 ± 0.8 ms; $p < 0.01$, paired *t* test; n = 6 cells), but had no effect on current amplitude (from 40.0 ± 6.3 to 37.1 ± 7.4 pA; $p > 0.05$, paired *t* test; n = 6 cells).

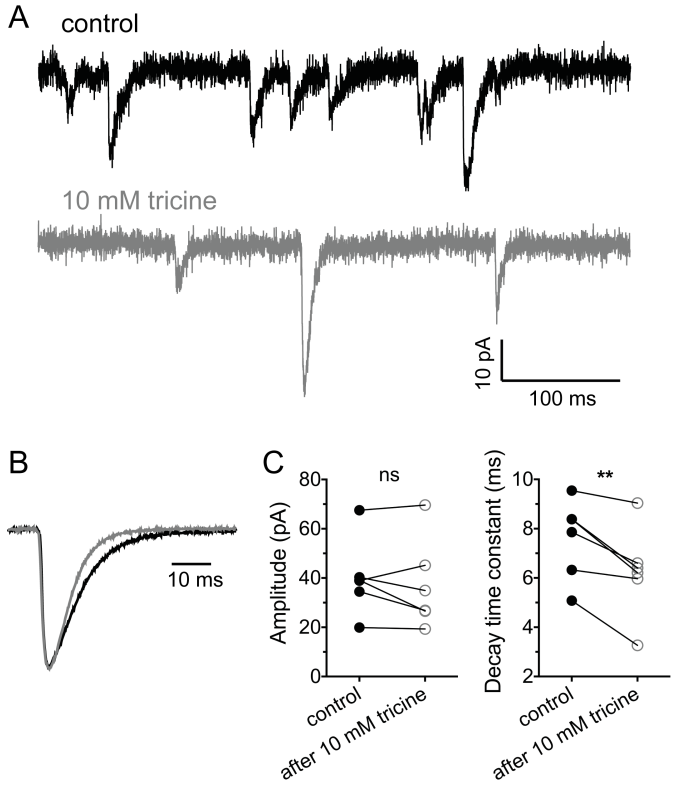

Figure 3. Tricine shortens IPSC duration. **A**. Representative traces recorded from an α1β GlyR-expressing cell before (black trace) and after 10 mM tricine (grey trace). **B**. Superimposed averaged traces of IPSCs (n > 200 events) recorded before (black trace) and after tricine treatment (grey trace), normalized to peak amplitude. **C**. Mean IPSC amplitude and decay time constants in α1β GlyR-expressing cells before (filled black symbols) and after tricine treatment (unfilled grey symbols, n = 6). ns, not significant.

We next compared the IPSCs recorded *in vitro* from homozygous $\alpha1^{D80A}$ mice with those from heterosynapses incorporating recombinant $\alpha1^{D80A}\beta$ GlyRs. Sample recordings from α1β and $\alpha1^{D80A}\beta$ GlyRs are shown in Fig. 4A, with the respective averaged, normalized IPSCs shown in Fig. 4B. We observed no significant difference in amplitude but a dramatic reduction in decay time constants (α1β, 7.2 ± 0.4 ms *vs.* $\alpha1^{D80A}\beta$, 3.1 ± 0.3 ms; $p < 0.0001$; Fig. 4B, C). These results correspond remarkably well with those observed in native glycinergic IPSCs from $\alpha1^{D80A}$ mice (see Fig. 7E and F in (Hirzel et al., 2006)), implying similar zinc concentrations in the respective synaptic clefts.

The $\alpha1^{A52S}$ mutation occurs naturally in the *Spasmodic* mouse where it reduces GlyR sensitivity to glycine, thereby accelerating IPSC deactivation and causing a hyperekplexia phenotype (Plested et al., 2007; Ryan et al., 1994). Consistent with this, IPSCs recorded from hypoglossal motor neurons and spinal dorsal horn neurons of homozygous adult *Spasmodic* mice exhibit reduced amplitudes and accelerated decay rates (Graham et al., 2006; Graham et al., 2011). To assess whether the glycine concentration in the synaptic cleft of our heterosynapses is comparable with that found in native synapses, we investigated the effect of the A52S mutation. Figure. 4A shows examples of IPSCs recorded from heterosynapses containing $\alpha1^{A52S}\beta$ GlyRs. As summarized in Fig. 4B and C, the mutation resulted in significant reductions in both IPSC amplitude (α1β, 58.6 ± 6.4 pA *vs.* $\alpha1^{A52S}\beta$, 33.8 ± 4.3 pA; $p < 0.05$) and decay time constants (α1β, 7.2 ± 0.4 ms *vs.* $\alpha1^{A52S}\beta$, 3.6 ± 0.4 ms; $p < 0.0001$). As these changes closely mirror those of glycinergic IPSCs recorded *in vitro* from homozygous *Spasmodic* mice (Graham et al., 2006;

Graham et al., 2011) they imply that a molecular perturbation affecting GlyR agonist sensitivity exerts similar effects in native synapses and heterosynapses.

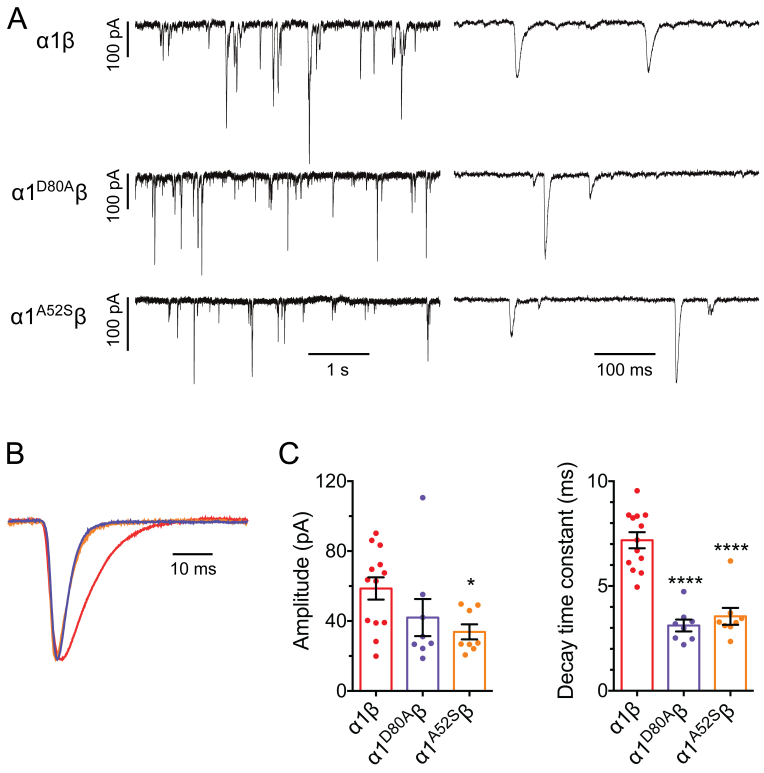

Figure 4. Effects of the D80A and A52S α1 subunit mutations on IPSCs mediated by α1β GlyRs **A**. Representative glycinergic IPSCs recorded from HEK cells expressing α1β, $\alpha1^{A52S}\beta$ and $\alpha1^{D80A}\beta$ GlyRs. **B**. Superimposed averaged glycinergic IPSCs (n > 150 events) mediated by α1β (red), $\alpha1^{A52S}\beta$ (orange) and $\alpha1^{D80A}\beta$ (purple) GlyRs, normalized to peak amplitude. **C**. Averaged amplitude and decay time constants of α1β (n = 13), $\alpha1^{A52S}\beta$ (n = 8) and $\alpha1^{D80A}\beta$ (n = 8) receptor-mediated IPSCs.

Comparison of heterosynaptic IPSC kinetics with the intrinsic kinetic properties of their component GlyRs

Table 1 provides a summary of the mean 10 – 90 % rise times and decay time constants for IPSCs mediated by all six wild type GlyR isoforms. Knowledge of the intrinsic activation and deactivation time courses of the GlyRs populating these heterosynapses would enable us to infer whether IPSC kinetics are determined by the intrinsic channel properties or by extrinsic factors such as the neurotransmitter concentration and time course. Intrinsic channel kinetic properties can be quantitated by single channel kinetic analysis. To date, this analysis has been employed to derive activation mechanisms for recombinant α1, α2 and α3 homomeric and α1β heteromeric GlyRs (Beato et al., 2004; Burzomato et al., 2004; Krashia et al., 2011; Marabelli et al., 2013). Figure 5 presents examples of simulated IPSCs reconstituted using the optimal activation mechanism that was derived in each of these four studies. The relevant parameters from these simulations are also included in Table 1. For α1, α1β and α2 GlyRs, the IPSC decay rate and the intrinsic channel closing rate are in reasonable accord, but for α3 GlyRs the IPSC decay rate is 3-fold slower than predicted by the intrinsic closing rate. In contrast, the rise times of heterosynaptic IPSCs are all much slower than the intrinsic channel activation rates, suggesting delayed activation by neurotransmitter in the synaptic cleft.

Table 1: GlyR kinetic properties

		α1β	α2β	α3β	α1	α2	α3
10-90% Rise time (ms)	Heterosynapses	1.6 ± 0.1 (n = 13)	2.7 ± 0.3 (8)	1.9 ± 0.1 (20)	1.7 ± 0.1 (18)	4.4 ± 0.3 (13)	2.6 ± 0.2 (10)
	Simulation	0.1	na	na	0.1	0.2	0.2
Deactivation time constant (ms)	Heterosynapses	7.2 ± 0.4	25.7 ± 1.5	9.7 ± 0.5	7.9 ± 0.5	88.8 ± 6.0	27.9 ± 2.0
	Simulation	10	na	na	11	163	6.3

Number of cells in parentheses

na, not available

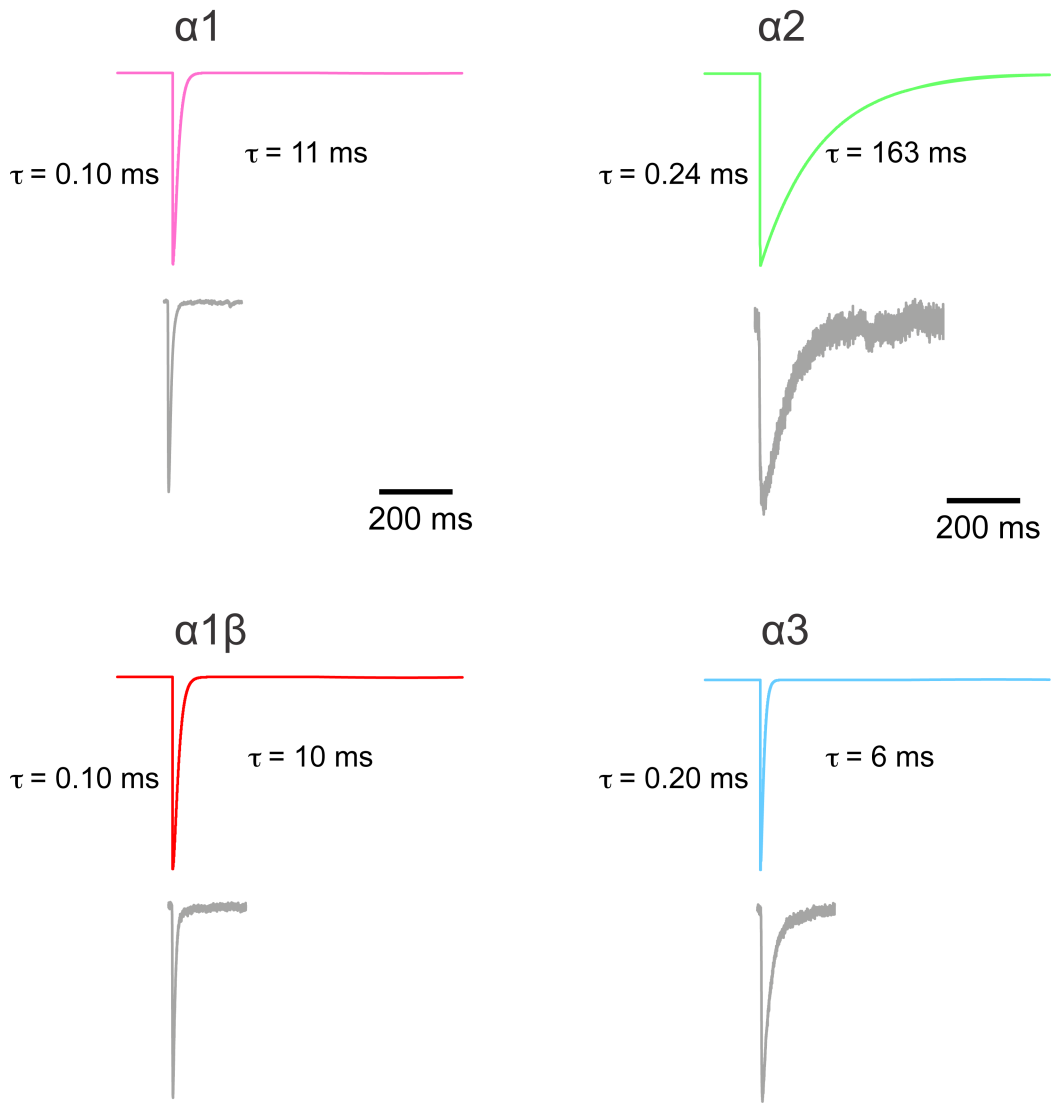

Figure 5. Ensemble current simulations based on intrinsic receptor activation properties. Simulated ensemble currents (shown as colored traces) for homomeric α1, α2, α3, and heteromeric α1β receptors were generated using functional activation mechanisms derived from single channel analysis. Accompanying the traces are the activation times (10 – 90%) and deactivation time constants from either a single, or weighted sum of two exponential fits. The simulations were generated in QuB (Nicolai and Sachs, 2013) for 1000 receptors in response to a 1 ms application of agonist using 'flip' mechanisms. The mechanisms and rate constants employed in these simulations were obtained as follows: α1

homomeric GlyRs – scheme 5 from (Burzomato et al., 2004); α2 homomeric GlyRs – scheme 2 from (Krashia et al., 2011); α3 homomeric GlyRs – scheme 3 from (Marabelli et al., 2013); α1β heteromeric GlyRs – scheme 5 of (Burzomato et al., 2004). Corresponding mean recorded IPSCs, reproduced from Fig. 2B, are included for comparison.

Discussion

Here we present a simple, robust method for inducing synapse formation between native glycinergic presynaptic terminals and HEK293 cells that recombinantly express the GlyR subunits of interest. This system was developed to provide a tractable means of evaluating the effects of drugs, hereditary disease mutations or other interventions on defined GlyR subunit combinations under realistic synaptic activation conditions. In the present study we sought to validate this method by comparing the influence of different GlyR subunits, both wild type and mutant, with information obtained by others in native glycinergic synapses.

The α1β heteromer is the predominant adult synaptic GlyR isoform (Lynch, 2009). Allowing for variations in rise and decay times due to variations in dendritic filtering and intracellular chloride concentrations (Pitt et al., 2008), electrophysiological recordings of native glycinergic IPSCs in acute spinal cord or brain stem slices exhibit similar rise and decay times as observed in our heterosynapses. For example, in neurons of the rat anteroventral cochlear nucleus, where glycinergic synapses are somatic and thus not subject to dendritic filtering, the mean 10 – 90 % rise time was 0.42 ms and the decay time course was fitted by the sum of two exponentials with time constants of 3.6 and 28.4 ms (Lim et al., 1999). In rat dorsal horn neurons, the mean 10 – 90 % rise times and decay time constants were 0.76 and 10.2 ms, respectively (Takahashi et al., 1992). In rat lumbar motor neurons the values were comparable at 0.79 and 7.1 ms, respectively (Beato, 2008). In adult hypoglossal motor neurons the 10 – 90 % rise times and decay time constants ranged between 0.6 – 1.8 and 4.9 – 7.7 ms, respectively (Graham et al., 2006; Hirzel et al., 2006; Muller et al., 2006; Singer et al., 1998). The α1β GlyR isoform is likely to predominate at all these synapses (Lynch, 2009). The mean decay time constant for α1β GlyRs measured in our heterosynapses (7.2 ms) fits well with these data, although our 10 – 90 % rise time (1.6 ms) is slower by a factor of two.

A striking finding was that α1- and α1β-mediated IPSCs exhibit identical kinetic profiles (Fig. 2). Since the IPSC decay time constants correspond well with the intrinsic channel deactivation time constants (Fig. 5, Table 1), we infer that both α1 and α1β GlyRs are activated by transmitter pulses briefer than their respective intrinsic channel closing rates. This implies that α1 GlyRs can mediate synaptic transmission as efficiently as α1β GlyRs. This is a surprising result given that the β subunit is considered essential for synaptic clustering via its specific interaction with gephyrin (Fritschy et al., 2008; Kneussel and Loebrich, 2007; Meyer et al., 1995). However,

immunolabeling studies have found that GlyR α1 and α2 subunits can form small cell surface clusters independently of gephyrin (Meier et al., 2000) and an electrophysiological study has found evidence for IPSCs mediated by α1 homomeric GlyRs in embryonic zebrafish neurons (Legendre, 1997).

The α2β GlyR predominates at glycinergic synapses in embryonic rat neurons (Lynch, 2009). Glycinergic IPSCs in embryonic day 20 rat dorsal horn neurons exhibited a mean 10 – 90 % rise time of 0.91 ms and a mean decay time constant of 27 ms (Takahashi et al., 1992), with comparable values observed in embryonic zebrafish Mauthner neurons (Ali et al., 2000), perinatal rat hypoglossal neurons (Singer et al., 1998) and adult rat wide-field amacrine cells (Veruki et al., 2007) which are unusual for adult neurons in that they selectively express α2β GlyRs (Wassle et al., 2009). The mean decay time constant recorded in the present study (26 ms) fits well with these data although our 10 – 90 % rise time (2.4 ms) is dramatically slower. The intrinsic deactivation properties of recombinant α2β GlyRs have yet to be investigated.

The mean decay time constant of homomeric α2 GlyR-mediated IPSCs was very slow (~89 ms) but consistent with the intrinsic closing rate of these receptors (Fig. 5). Given this close correspondence, we infer that their respective channel closing rates governs the decay rates of recombinant α2 and α2β-mediated IPSCs.

The α3β GlyR is generally sparsely expressed *in vivo*, although it is co-located with α1β GlyRs in glycinergic synapses on neurons in the superficial laminae of the spinal cord dorsal horn (Harvey et al., 2004). Although α3β-mediated IPSCs have yet to be recorded in isolation in native synapses, their kinetic properties appear indistinguishable from those of α1β GlyRs (Harvey et al., 2004). This fits well with the results of the present study (Fig. 2).

The rise and decay times of homomeric α3 GlyR-mediated IPSCs were significantly slower than those of α3β GlyRs (Fig. 2). Importantly, the homomeric decay time constants were also significantly slower than predicted by the intrinsic channel closing rate (Fig. 4). This suggests that the kinetic properties of α3-mediated IPSCs are governed by slow agonist access and removal. The fact that the rise times of α3β-mediated IPSCs are dramatically faster could indicate an impact on receptor gating, or could imply they are located closer to synaptic release sites, which would be consistent with the role of the β subunit in gephyrin-dependent clustering.

Chelation of synaptic zinc by tricine reduced the IPSC decay time constant from 7.6 ± 0.7 to 6.2 ± 0.8 ms, consistent with a reduction in zinc potentiation. However, the D80A mutation, accelerated the decay rate by a much greater margin (7.2 ± 0.4 to 3.1 ± 0.3 ms). There are several possible reasons for this discrepancy. First, 10 mM tricine may not have completely chelated synaptic zinc. Second, the D80A mutation may have had a secondary accelerating effect on the intrinsic channel deactivation rate. Third, the complete elimination of zinc potentiation by the

D80A mutation may have uncovered a high potency zinc inhibitory effect that may have contributed to the enhanced decay rate.

To summarise the main points, the decay rates of IPSCs mediated by α1β, α2β and α3β GlyRs in our heterosynapses are in close accord with those observed in native synapses comprizing the same subunits. These results, along with the close correspondence in the effects of the A52S and D80A mutations between native and heterosynapses, provide an important validation of our technique. However, IPSC rise times in our heterosynapses were relatively slow, implying either a greater distance between presynaptic release sites and postsynaptic GlyRs or a reduced neurotransmitter diffusion rate in the cleft (Nielsen et al., 2004). Our results also suggest that the decay rates of IPSCs mediated by α1 and α2 homomeric GlyRs are governed by the intrinsic channel closing rate, whereas those mediated by α3 homomeric GlyRs are governed by the slow rate of agonist access and removal. A possible explanation could be that α1, α1β and α3β GlyRs are clustered (or at least localized relatively close) to synaptic release sites and α3 GlyRs are either unclustered or located further away from release sites. Finally, α2-containing GlyRs deactivate so slowly that it is difficult to infer their location although their slow rise times imply they are located a substantial distance from presynaptic terminals.

Specific GlyR isoforms are emerging as therapeutic targets for a range of disorders. For example, drugs that selectively potentiate α3-containing GlyRs are candidate lead compounds for chronic inflammatory pain (Lynch and Callister, 2006; Xiong et al., 2012; Zeilhofer, 2005). One of our motivations for developing the glycinergic heterosynaptic system was to validate the efficacy of α3 GlyR-specific drugs under synaptic activation conditions. It is difficult to do this in native synapses due to the co-localisation of α1β and α3β GlyRs in individual synapses on nociceptive neurons (Harvey et al., 2004), the similarity in their kinetic and pharmacological properties (Lynch, 2009) and the apparent low abundance of α3β versus α1β expression (Graham et al., 2011). The heterosynapse system not only avoids these problems but offers the opportunity of investigating GlyR clustering mechanisms, and the effects of posttranslational modifications (e.g., phosphorylation) and hereditary disease (e.g., hyperekplexia) mutations on the formation and function glycinergic synapses.

Acknowledgements

This study was funded by the Australian Research Council and the National Health and Medical Research Council.

References

Ali, D.W., Drapeau, P., Legendre, P., 2000. Development of spontaneous glycinergic currents in the Mauthner neuron of the zebrafish embryo. J Neurophysiol. 84**,** 1726-36.

Baer, K., et al., 2009. Localization of glycine receptors in the human forebrain, brainstem, and cervical spinal cord: an immunohistochemical review. Front Mol Neurosci. 2**,** 25.

Beato, M., et al., 2004. The activation mechanism of alpha1 homomeric glycine receptors. J Neurosci. 24**,** 895-906.

Beato, M., 2008. The time course of transmitter at glycinergic synapses onto motoneurons. J Neurosci. 28**,** 7412-25.

Birinyi, A., et al., 2001. Zinc co-localizes with GABA and glycine in synapses in the lamprey spinal cord. J Comp Neurol. 433**,** 208-21.

Bloomenthal, A.B., et al., 1994. Biphasic modulation of the strychnine-sensitive glycine receptor by Zn2+. Mol Pharmacol. 46**,** 1156-9.

Bode, A., Lynch, J.W., 2014. The impact of human hyperekplexia mutations on glycine receptor structure and function. Mol Brain. 7**,** 2.

Burzomato, V., et al., 2004. Single-channel behavior of heteromeric alpha1beta glycine receptors: an attempt to detect a conformational change before the channel opens. J Neurosci. 24**,** 10924-40.

Dixon, C., et al., 2014. GABAA receptor alpha and gamma subunits shape synaptic currents via different mechanisms. J Biol Chem. 289**,** 5399-411.

Dong, N., Qi, J., Chen, G., 2007. Molecular reconstitution of functional GABAergic synapses with expression of neuroligin-2 and GABAA receptors. Mol Cell Neurosci. 35**,** 14-23.

Durisic, N., et al., 2012. Stoichiometry of the human glycine receptor revealed by direct subunit counting. J Neurosci. 32**,** 12915-20.

Eichler, S.A., et al., 2008. Glycinergic tonic inhibition of hippocampal neurons with depolarizing GABAergic transmission elicits histopathological signs of temporal lobe epilepsy. J Cell Mol Med. 12**,** 2848-66.

Fritschy, J.M., Harvey, R.J., Schwarz, G., 2008. Gephyrin: where do we stand, where do we go? Trends Neurosci. 31**,** 257-64.

Fuchs, C., et al., 2013. GABA(A) receptors can initiate the formation of functional inhibitory GABAergic synapses. Eur J Neurosci. 38**,** 3146-58.

Graham, B.A., et al., 2006. Distinct physiological mechanisms underlie altered glycinergic synaptic transmission in the murine mutants spastic, spasmodic, and oscillator. J Neurosci. 26**,** 4880-90.

Graham, B.A., et al., 2011. Probing glycine receptor stoichiometry in superficial dorsal horn neurones using the spasmodic mouse. Journal of Physiology-London. 589**,** 2459-2474.

Grudzinska, J., et al., 2005. The beta subunit determines the ligand binding properties of synaptic glycine receptors. Neuron. 45**,** 727-39.

Grudzinska, J., et al., 2008. Mutations within the agonist-binding site convert the homomeric alpha1 glycine receptor into a Zn2+-activated chloride channel. Channels (Austin). 2**,** 13-8.

Harvey, R.J., et al., 1999. Identification of an inhibitory Zn2+ binding site on the human glycine receptor alpha1 subunit. J Physiol. 520 Pt 1**,** 53-64.

Harvey, R.J., et al., 2004. GlyR alpha3: an essential target for spinal PGE2-mediated inflammatory pain sensitization. Science. 304**,** 884-7.

Hirzel, K., et al., 2006. Hyperekplexia phenotype of glycine receptor alpha1 subunit mutant mice identifies Zn(2+) as an essential endogenous modulator of glycinergic neurotransmission. Neuron. 52**,** 679-90.

Hoch, W., Betz, H., Becker, C.M., 1989. Primary cultures of mouse spinal cord express the neonatal isoform of the inhibitory glycine receptor. Neuron. 3**,** 339-48.

Islam, R., Lynch, J.W., 2012. Mechanism of action of the insecticides, lindane and fipronil, on glycine receptor chloride channels. Br J Pharmacol. 165**,** 2707-20.

Kneussel, M., Loebrich, S., 2007. Trafficking and synaptic anchoring of ionotropic inhibitory neurotransmitter receptors. Biol Cell. 99**,** 297-309.
Krashia, P., et al., 2011. The long activations of alpha 2 glycine channels can be described by a mechanism with reaction intermediates ("flip"). Journal of General Physiology. 137**,** 197-216.
Laube, B., et al., 1995. Modulation by zinc ions of native rat and recombinant human inhibitory glycine receptors. J Physiol. 483 (Pt 3)**,** 613-9.
Laube, B., Kuhse, J., Betz, H., 2000. Kinetic and mutational analysis of Zn2+ modulation of recombinant human inhibitory glycine receptors. J Physiol. 522 Pt 2**,** 215-30.
Legendre, P., 1997. Pharmacological evidence for two types of postsynaptic glycinergic receptors on the Mauthner cell of 52-h-old zebrafish larvae. J Neurophysiol. 77**,** 2400-15.
Legendre, P., 2001. The glycinergic inhibitory synapse. Cell Mol Life Sci. 58**,** 760-93.
Levi, S., Vannier, C., Triller, A., 1998. Strychnine-sensitive stabilization of postsynaptic glycine receptor clusters. J Cell Sci. 111 (Pt 3)**,** 335-45.
Lim, R., Alvarez, F.J., Walmsley, B., 1999. Quantal size is correlated with receptor cluster area at glycinergic synapses in the rat brainstem. J Physiol. 516 (Pt 2)**,** 505-12.
Lise, M.F., El-Husseini, A., 2006. The neuroligin and neurexin families: from structure to function at the synapse. Cell Mol Life Sci. 63**,** 1833-49.
Lynch, J.W., et al., 1998. Zinc potentiation of the glycine receptor chloride channel is mediated by allosteric pathways. J Neurochem. 71**,** 2159-68.
Lynch, J.W., 2004. Molecular structure and function of the glycine receptor chloride channel. Physiol Rev. 84**,** 1051-95.
Lynch, J.W., Callister, R.J., 2006. Glycine receptors: a new therapeutic target in pain pathways. Curr Opin Investig Drugs. 7**,** 48-53.
Lynch, J.W., 2009. Native glycine receptor subtypes and their physiological roles. Neuropharmacology. 56**,** 303-9.
Marabelli, A., et al., 2013. The kinetic properties of the alpha3 rat glycine receptor make it suitable for mediating fast synaptic inhibition. J Physiol. 591**,** 3289-308.
Meier, J., et al., 2000. Formation of glycine receptor clusters and their accumulation at synapses. J Cell Sci. 113 (Pt 15)**,** 2783-95.
Meyer, G., et al., 1995. Identification of a gephyrin binding motif on the glycine receptor beta subunit. Neuron. 15**,** 563-72.
Miller, P.S., et al., 2005a. Molecular determinants of glycine receptor alphabeta subunit sensitivities to Zn2+-mediated inhibition. J Physiol. 566**,** 657-70.
Miller, P.S., Da Silva, H.M., Smart, T.G., 2005b. Molecular basis for zinc potentiation at strychnine-sensitive glycine receptors. J Biol Chem. 280**,** 37877-84.
Muller, E., et al., 2006. Developmental dissociation of presynaptic inhibitory neurotransmitter and postsynaptic receptor clustering in the hypoglossal nucleus. Mol Cell Neurosci. 32**,** 254-73.
Nevin, S.T., et al., 2003. Insights into the structural basis for zinc inhibition of the glycine receptor. J Biol Chem. 278**,** 28985-92.
Nicolai, C., Sachs, F., 2013. Solving ion channel kinetics with the QuB software. Biophys Rev Lett. 8**,** 1-21.
Nielsen, T.A., DiGregorio, D.A., Silver, R.A., 2004. Modulation of glutamate mobility reveals the mechanism underlying slow-rising AMPAR EPSCs and the diffusion coefficient in the synaptic cleft. Neuron. 42**,** 757-71.
Pitt, S.J., Sivilotti, L.G., Beato, M., 2008. High intracellular chloride slows the decay of glycinergic currents. J Neurosci. 28**,** 11454-67.
Plested, A.J., et al., 2007. Single-channel study of the spasmodic mutation alpha1A52S in recombinant rat glycine receptors. J Physiol. 581**,** 51-73.
Poulopoulos, A., et al., 2009. Neuroligin 2 drives postsynaptic assembly at perisomatic inhibitory synapses through gephyrin and collybistin. Neuron. 63**,** 628-42.

Ryan, S.G., et al., 1994. A missense mutation in the gene encoding the alpha 1 subunit of the inhibitory glycine receptor in the spasmodic mouse. Nat Genet. 7**,** 131-5.
Singer, J.H., et al., 1998. Development of glycinergic synaptic transmission to rat brain stem motoneurons. J Neurophysiol. 80**,** 2608-20.
Takahashi, T., et al., 1992. Functional correlation of fetal and adult forms of glycine receptors with developmental changes in inhibitory synaptic receptor channels. Neuron. 9**,** 1155-61.
Veruki, M.L., Gill, S.B., Hartveit, E., 2007. Spontaneous IPSCs and glycine receptors with slow kinetics in wide-field amacrine cells in the mature rat retina. J Physiol. 581**,** 203-19.
Wang, H., et al., 2009. Plasticity at glycinergic synapses in dorsal cochlear nucleus of rats with behavioral evidence of tinnitus. Neuroscience. 164**,** 747-59.
Wassle, H., et al., 2009. Glycinergic transmission in the Mammalian retina. Front Mol Neurosci. 2**,** 6.
Winkelmann, A., et al., 2014. Changes in neural network homeostasis trigger neuropsychiatric symptoms. J Clin Invest. 124**,** 696-711.
Wu, X., et al., 2012. gamma-Aminobutyric acid type A (GABAA) receptor alpha subunits play a direct role in synaptic versus extrasynaptic targeting. J Biol Chem. 287**,** 27417-30.
Xiong, W., et al., 2012. Cannabinoids suppress inflammatory and neuropathic pain by targeting alpha3 glycine receptors. J Exp Med. 209**,** 1121-34.
Yang, Z., et al., 2012. Stoichiometry and subunit arrangement of alpha1beta glycine receptors as determined by atomic force microscopy. Biochemistry. 51**,** 5229-31.
Zeilhofer, H.U., 2005. The glycinergic control of spinal pain processing. Cell Mol Life Sci. 62**,** 2027-35.

Chapter 3

Investigating the mechanism by which gain-of-function mutations to the α1 glycine receptor cause hyperekplexia

Investigating the mechanism by which gain-of-function mutations to the α1 glycine receptor cause hyperekplexia

Yan Zhang[1], Anna Bode[1], Bindi Nguyen[1], Angelo Keramidas[1] and Joseph W. Lynch[1,2]

[1]Queensland Brain Institute and [2]School of Biomedical Sciences, University of Queensland, Brisbane, QLD Australia 4072

Running title: *Gain-of-function glycine receptor mutants and hyperekplexia*

To whom correspondence should be addressed: Prof. Joseph Lynch, Queensland Brain Institute, Building 79, University of Queensland, St Lucia, QLD 4072, Australia. Phone: +61 7 33466375, Fax: +61 7 33466301, E- mail: j.lynch@uq.edu.au

Keywords: glycinergic; glycine receptor; inhibitory neurotransmission; startle disease; tropisetron

---

ABSTRACT

Hyperekplexia is a rare human neuromotor disorder caused by mutations that impair the efficacy of glycinergic inhibitory neurotransmission. Loss-of-function mutations in the *GLRA1* or *GLRB* genes, which encode the α1 and β glycine receptor (GlyR) subunits, are the major cause. Paradoxically, gain-of-function *GLRA1* mutations also cause hyperekplexia, although the mechanism is unknown. Here we identify two new gain-of-function mutations (I43F, W170S) and characterize these along with known gain-of-function mutations (Q226E, V280M, R414H) to identify how they cause hyperekplexia. Using artificial synapses, we show that all mutations prolong the decay of inhibitory postsynaptic currents (IPSCs) and induce spontaneous GlyR activation. As these effects may deplete the chloride electrochemical gradient, hyperekplexia could potentially result from reduced glycinergic inhibitory efficacy. However, we consider this unlikely as the depleted chloride gradient should also lead to pain sensitization and to a hyperekplexia phenotype that correlates with mutation severity, neither of which is observed in patients with *GLRA1* hyperekplexia mutations. We also rule out small increases in IPSC decay times (as caused by W170S and R414H) as a possible mechanism given that the clinically important drug, tropisetron, significantly increases glycinergic IPSC decay times without causing motor side effects. A recent study on cultured spinal neurons concluded that an elevated intracellular chloride concentration late during development ablates α1β glycinergic synapses but spares GABAergic synapses. As this mechanism satisfies all our considerations, we propose it is primarily responsible for the hyperekplexia phenotype.

Glycine receptor (GlyR) chloride channels mediate fast inhibitory neurotransmission in the spinal cord, brainstem and retina, and are thus essential for controlling motor and sensory function (1-3). Like other members of the pentameric ligand-gated ion channel family, GlyRs are assembled from five subunits arranged around a central water-filled pore. Each GlyR subunit is composed of an N-terminal extracellular domain, a transmembrane domain containing four α-helical domains (termed M1−M4) and a long intracellular domain linking M3 and M4. Synaptic GlyRs are formed as heteromers of α1-3 and β subunit isoforms with a stoichiometry of 2α:3β or 3α:2β (4,5). The dominant native synaptic isoform is the α1β heteromer, with the β subunit responsible for anchoring GlyRs at postsynaptic densities by directly binding to the cytoplasmic clustering protein, gephyrin (6-8).

Human hereditary hyperekplexia, or startle disease, is a rare neurological disorder characterized by neonatal hypertonia and an exaggerated startle reflex in response to sudden, unexpected stimuli (9). It is most commonly caused by mutations that reduce the efficacy of glycinergic synaptic signalling. Mutations in the *GLRA1* or *GLRB* genes, which encode the α1 and β GlyR subunits respectively, are the major cause of hyperekplexia (9-12). The vast majority of these mutations are loss-of-function in that they reduce the ability of GlyRs to flux chloride. Recessive hyperekplexia mutations generally result in the loss of α1 or β GlyR protein expression at the cell surface, whereas dominant mutations usually allow strong surface expression but impair channel function via reduced open probability, single channel conductance or glycine sensitivity (11,13). Despite recessive mutations often resulting in the complete loss of α1 subunit expression (14) and dominant negative mutations often involving only moderate disruption to α1 subunit function, there is no evidence for 'major' or 'minor' forms of hyperekplexia and no evidence for a correlation between inheritance mode and phenotype (12). Thus, it appears that as long as the deleterious effect of a *GLRA1* mutation exceeds a certain threshold, a common hyperekplexia phenotype will result. All genetic forms of hyperekplexia are successfully treated with the benzodiazepine, clonazepam (9,12). This works by potentiating GABA type-A receptor ($GABA_AR$) chloride channels to compensate for the loss of glycinergic inhibition (15).

Hyperekplexia can also be caused by gain-of-function *GLRA1* mutations (16,17). To date four such mutations have been identified (Y128C, Q226E, V280M and R414H). All of these result in spontaneous channel activation, whereas Y128C and V280M also significantly enhance glycine sensitivity (16,17). While characterizing a range of other *GLRA1* hyperekplexia mutations, we discovered that spontaneous activity is also induced by the recently characterized W170S mutation (18,19) and by the as yet uncharacterized I43F mutation (20). From the clinical descriptions, it is evident that the hyperekplexia phenotype induced by gain-of-function mutations is no different to

that caused by loss-of-function mutations and clonazepam remains an effective treatment (16,18,20).

In this study we sought to provide insight into the mechanism by which gain-of-function mutations cause hyperekplexia. We have recently developed an 'artificial' synapse system that allows control over the subunit composition of GlyRs in glycinergic synapses (21). We inserted heteromeric α1β GlyRs incorporating each mutation in turn to evaluate the properties of the inhibitory postsynaptic currents (IPSCs) mediated by each mutant isoform. We then evaluated whether the hyperekplexia phenotype is likely to result from the change in IPSC properties or from the spontaneous channel activity.

EXPERIMENTAL PROCEDURES

Cell culture and molecular biology - The human GlyR α1 (pCIS) and β (pCIS) plasmid DNAs were combined in a ratio of 1α:50β (artificial synapse and macropatch recordings) or 1α:100β (single channel recordings) and transfected into HEK293 cells via calcium phosphate-DNA co-precipitation. This resulted in the expression of α1β heteromeric GlyRs (21). For artificial synapse experiments, mouse neuroligin-2A (pNice) and rat gephyrin (pCIS) were co-transfected along with GlyR plasmids to facilitate the formation of artificial synapses. Empty pEGFP plasmid was also transfected as an expression marker. Mutagenesis was performed using the QuikChange mutagenesis kit, and the successful incorporation of mutations was confirmed by DNA sequencing.

Artificial synapse formation - E15 timed-pregnant rats were euthanized via CO_2 inhalation in accordance with procedures approved by the University of Queensland Animal Ethics Committee. Primary cultures of embryonic spinal cord neurons were prepared as previously described (21,22). Cells were plated at a density of ~80,000 cells per 18 mm poly-D-lysine coated coverslip in DMEM medium with 10% fetal bovine serum. After 24 h, the plating medium was changed to Neurobasal medium supplemented with 2% B27 and 1% glutamax, and a second feed after one week replaced half of this medium. Neurons were grown for 1 − 4 weeks *in vitro* and the heterosynaptic co-cultures were prepared by directly introducing transfected HEK293 cells onto the primary neuronal cultures 1 − 3 days prior to recordings.

Electrophysiology - Whole-cell recordings were performed in voltage-clamp mode using a HEKA EPC10 amplifier (HEKA Electronics, Lambrecht, Germany) and Patchmaster software (HEKA), at room temperature. Cells were continuously perfused with extracellular solution comprizing (in mM): 140 NaCl, 5 KCl, 2 $CaCl_2$, 1 $MgCl_2$, 10 HEPES, and 10 D-glucose, adjusted to pH 7.4 with NaOH. Patch pipettes (1 − 3 MΩ resistance), made from borosilicate glass (GC150F-7.5, Harvard apparatus), were filled with an intracellular solution containing the

following (in mM): 145 CsCl, 2 $CaCl_2$, 2 $MgCl_2$, 10 HEPES, 10 EGTA and 2 MgATP, adjusted to pH 7.4 with NaOH. Glycine-gated currents were recorded at a holding potential of −40 mV, digitized at 2.9 kHz and filtered at 10 kHz. For IPSC recordings, the patch pipette resistance was adjusted to 4 − 6 MΩ and filled with the same internal solution. Series resistance was routinely compensated to 60% of maximum and was monitored throughout the recording. Spontaneous glycinergic IPSCs in HEK293 cells were recorded at a holding potential −60 mV and signals were filtered at 4 kHz and sampled at 10 kHz. As these IPSCs were completely abolished by 1 μM tetrodotoxin (not shown), we infer they were induced by spontaneous action potentials.

Single-channel currents were recorded from outside-out excised patches at a clamped potential of −70 mV. Glass electrodes were pulled from borosilicate glass (G150F-3; Warner Instruments), coated with a silicone elastomer (Sylgard-184; Dow Corning) and heat-polished to a final tip resistance of 8 – 15 MΩ when filled with an intracellular solution containing (in mM) 145 CsCl, 2 $MgCl_2$, 2 $CaCl_2$, 10 HEPES, and 5 EGTA, pH 7.4. Excised patches were directly perfused with extracellular solution by placing them in front of one barrel of a double-barreled glass tube. Single channel currents were either recorded while the patch was exposed to extracellular solution (without added glycine) or elicited by exposing the patch continuously to glycine (100 μM) containing solution. Experiments were recorded using an Axopatch 200B amplifier (Molecular Devices), filtered at 5 kHz and digitized at 20 kHz using Clampex (pClamp 10, Molecular Devices) via a Digidata 1440A digitizer. The currents were filtered off-line at 3 kHz for making figures.

In the pharmacological studies, tropisetron (Sigma-Aldrich) was applied by bath perfusion. After waiting 2 min for drug effects to stabilize, we compared at least 3 min of spontaneous activity before, during and after drug application.

Macropatch recordings were performed in the excised outside-out patch clamp configuration. Patch pipettes were fired-polished to a resistance of approximately 10 MΩ and filled with the same internal solution. Macroscopic currents in outside-out patches pulled from transfected HEK293 cells were activated by brief (<1ms) exposure to agonists using a piezo-electric translator (Siskiyou). We regularly calibrated the speed of the solution exchange system by rapidly switching the solution perfusing an open patch pipette between standard extracellular solution and an extracellular solution that had been diluted by 50% with distilled water. By monitoring the resulting pipette current, we were able to ensure that the solution perfusing the macropatch was completely exchanged within 200 μs (23). Recordings were performed using a Multiclamp 700B amplifer and pClamp9 software (Molecular Devices), filtered at 4 kHz and sampled at 10 kHz.

Analysis - Analyses of IPSC amplitudes, 10 − 90% rise times, and weighted decay time constants were performed using Axograph (Axograph Scientific). Only cells with a stable series resistance of <25 MΩ throughout the recording period were included in the analysis. Single peak IPSCs with

amplitudes of at least three times above the background noise were detected using a semi-automated sliding template. Each detected event was visually inspected and only well-separated IPSCs with no inflections in the rising or decay phases were included. To calculate macroscopic current decay time constants, averaged macroscopic traces were fitted with double-exponential functions in Axograph X, and a weighted time constant was calculated from individual time constants (τ1, τ2) and their relative amplitude (A1, A2) as followings: $\tau_{weighted}$ = (τ1×A1+τ2×A2)/(A1+A2). The averaged data from individual cells were then pooled to obtain group data. Statistical analysis, and plotting were performed with Prism 5 (GraphPad Software). The fitting of single Gaussian functions to IPSC amplitude and decay time constant distributions was also performed using Prism 5. All data are presented as mean ± SEM. Student's *t*-tests or one-way ANOVAs, as appropriate, were employed for comparisons. For all tests, the number of asterisks corresponds to level of significance: **p* < 0.05, ***p* < 0.01, ****p* < 0.001 and *****p* < 0.0001.

Single channel recordings were analysed with pClamp 10 (Clampfit) or QuB software. Segments of single channel activity separated by long periods of baseline were idealized into noise-free open and shut events using a temporal resolution of 70 μs. Single channel activations were separated using a shut period ranging between 6 – 30 ms.

RESULTS

Properties of GlyRs measured by whole cell recording – The locations of the mutations investigated in this study are shown in Fig. 1. The glycine EC_{50} and I_{max} values for GlyRs incorporating the Y128C, W170S, Q226E, V280M and R414H mutations have previously been characterized by whole cell recording (16,17,19). The Y128C mutation was found to induce a sufficiently large spontaneous leak current as to degrade HEK293 cell viability (17) and thus we did not study it further. The V280M mutation significantly reduced both the glycine EC_{50} and the I_{max} values, although the W170S, Q226E and R414H mutations had little effect of these parameters (16,19). The Q226E, V280M and R414H mutations have previously been shown to induce spontaneous single channel activity (16,24). In this study we filled in the gaps by quantifying the glycine EC_{50} and I_{max} values of $\alpha1^{I43F}\beta$ GlyRs by whole cell recording. We also employed outside-out patch clamp recording to characterize the properties of spontaneous single channel events mediated by $\alpha1^{I43F}\beta$ and $\alpha1^{W170S}\beta$ GlyRs.

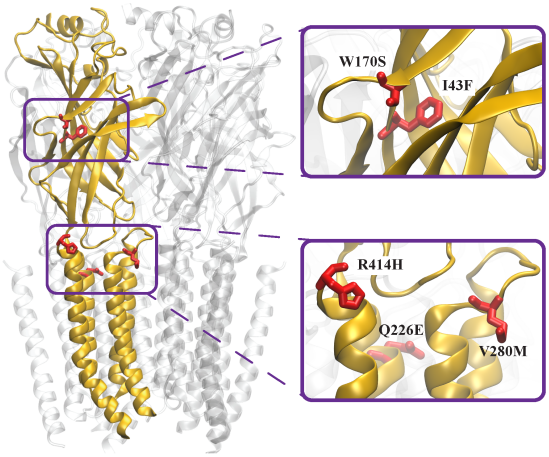

Figure 1. Model of the α1 GlyR viewed from within the membrane. The model is based on the cryoEM structure of zebrafish α1 GlyR in the glycine-bound conformation (PDB access code: 3JAE) (40). One subunit is depicted in gold with gain-of-function hyperekplexia mutations (red) shown in stick form.

Examples of whole cell currents activated by increasing glycine concentrations at α1β and $\alpha1^{I43F}\beta$ GlyRs are shown in Fig. 2A. Averaged glycine dose-response relationships for α1, $\alpha1^{I43F}$, α1β and $\alpha1^{I43F}\beta$ GlyRs shown in Fig. 2B, with mean parameters presented in Table 1. In both homomeric and heteromeric GlyRs, the I43F mutation resulted in a drastically increased sensitivity to glycine.

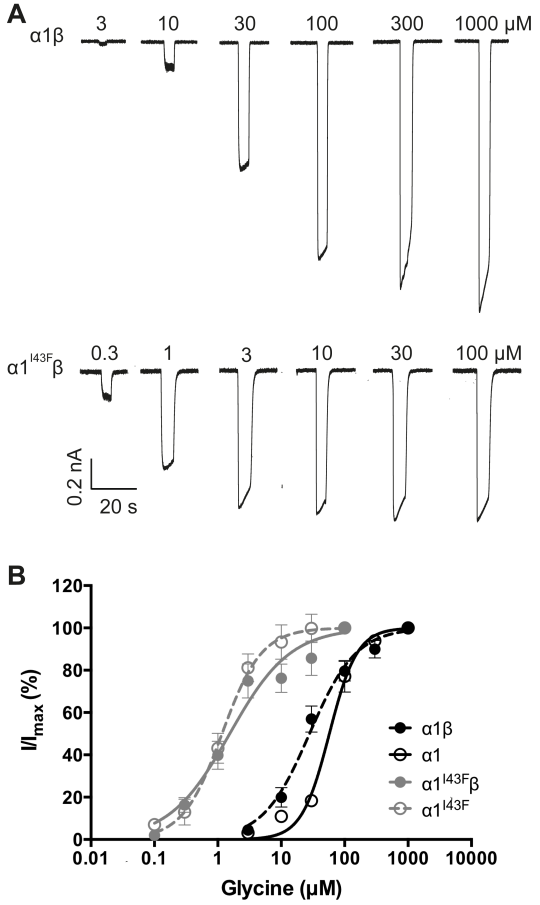

Figure. 2. Effect of the α1 subunit I43F mutation examined by whole cell patch clamp recording. Recordings were performed at −60 mV. **A**. Sample whole cell recordings for heteromeric α1β and $\alpha1^{I43F}\beta$ GlyRs in the presence of indicated glycine concentrations. **B**. Averaged whole cell glycine dose-response curves for α1, α1β, $\alpha1^{I43F}$ and $\alpha1^{I43F}\beta$ GlyRs. Mean parameters of best fit are provided in Table 1.

Table 1. Effect of the I43F mutation on GlyR functional properties

	α1β	α1	$\alpha1^{I43F}\beta$	$\alpha1^{I43F}$
EC_{50} (μM)	29.5 ± 3.7	52.8 ± 8.3	2.8 ± 1.3***	1.3 ± 0.3****
Hill slope	1.4 ± 0.3	2.0 ± 0.4	1.2 ± 0.2	1.8 ± 0.7
I_{max} (nA)	1.1 ± 0.2	1.2 ± 0.1	1.0 ± 0.2	0.7 ± 0.2
n	6	6	9	6

***$p < 0.001$ and ****$p < 0.0001$ relative to the corresponding homo- or heteromeric wild type GlyR via unpaired *t* test.

Spontaneous channel activity in $\alpha1^{W170S}\beta$ and $\alpha1^{I43F}\beta$ GlyRs - To investigate the presence of spontaneous activity, 100 μM picrotoxin alone was applied to whole cells expressing either the $\alpha1^{W170S}\beta$ GlyR (Fig. 3A) or the $\alpha1^{I43F}\beta$ GlyR (Fig. 3B). We observed small but consistent upward current deflections in the presence of picrotoxin, which was particularly prominent for the $\alpha1^{I43F}\beta$ GlyR. To quantify the level of spontaneous activity in both receptors we carried out single channel measurements in excised outside out patches.

In the absence of applied glycine, the $\alpha1^{W170S}\beta$ GlyR exhibited brief spontaneous openings of 1.4 ms mean duration, the majority of which were simple open-shut events (Fig. 3C). We determined the frequency of these openings by dividing their occurrence over time by an estimate of the number of channels contained in each recorded patch (between 3-6 channels). This yielded an open frequency of 0.2 Hz per channel. Wild-type α1β GlyRs under the similar recording conditions exhibit negligible spontaneous activity (10,24-26).

In the presence of 100 μM glycine, single channel currents mediated by $\alpha1^{W170S}\beta$ GlyRs occurred in clusters of tightly spaced open-shut transitions (Fig. 3D). The mean duration of the clusters was 621 ± 69 ms (n = 3), which is only 1.2-fold longer than wild type α1β GlyRs (~ 500 ms at saturating glycine (24)). The mean single channel amplitude measured at −70 mV was 3.31 ± 0.06 pA (n = 4), yielding a conductance of 41.6 ± 0.7 pS. This is similar to that of 45.9 ± 1.4 pS for wild type receptors (24) and suggests that the $\alpha1^{W170S}$ mutation has no appreciable effect on conductance.

Similar experiments were carried out using the $\alpha1^{I43F}\beta$ GlyR. This receptor also exhibited spontaneous openings, but their mean duration was 11.2 ms, which is 8-fold greater than that of the $\alpha1^{W170S}\beta$ GlyR. Moreover, the activity consisted of brief, single open-shut bursts in addition to a significant number of more complex bursts, where the receptor oscillated between open and shut configurations multiple times before terminating (Fig. 3E). The calculated spontaneous open frequency of this receptor, from patches containing 1-5 channels, was 0.5 Hz. This receptor exhibited a greater level of spontaneous activity than the $\alpha1^{W170S}\beta$ GlyR, with longer, more complex bursts and a 2.5-fold higher frequency of occurrence.

A 100 μM concentration of glycine elicited long clusters of activity that had a mean duration of 1030 ± 73 ms (n =3), similar to those of the $\alpha1^{Q226E}\beta$ GlyR (24). The single channel mean amplitude the $\alpha1^{I43F}\beta$ GlyR was 3.64 ± 0.05 pA (n = 3), producing a conductance at −70 mV of 45.7 ± 0.7 pS. This value is also close to that of wild type α1β GlyRs, suggesting that this mutation also has little effect on channel conductance.

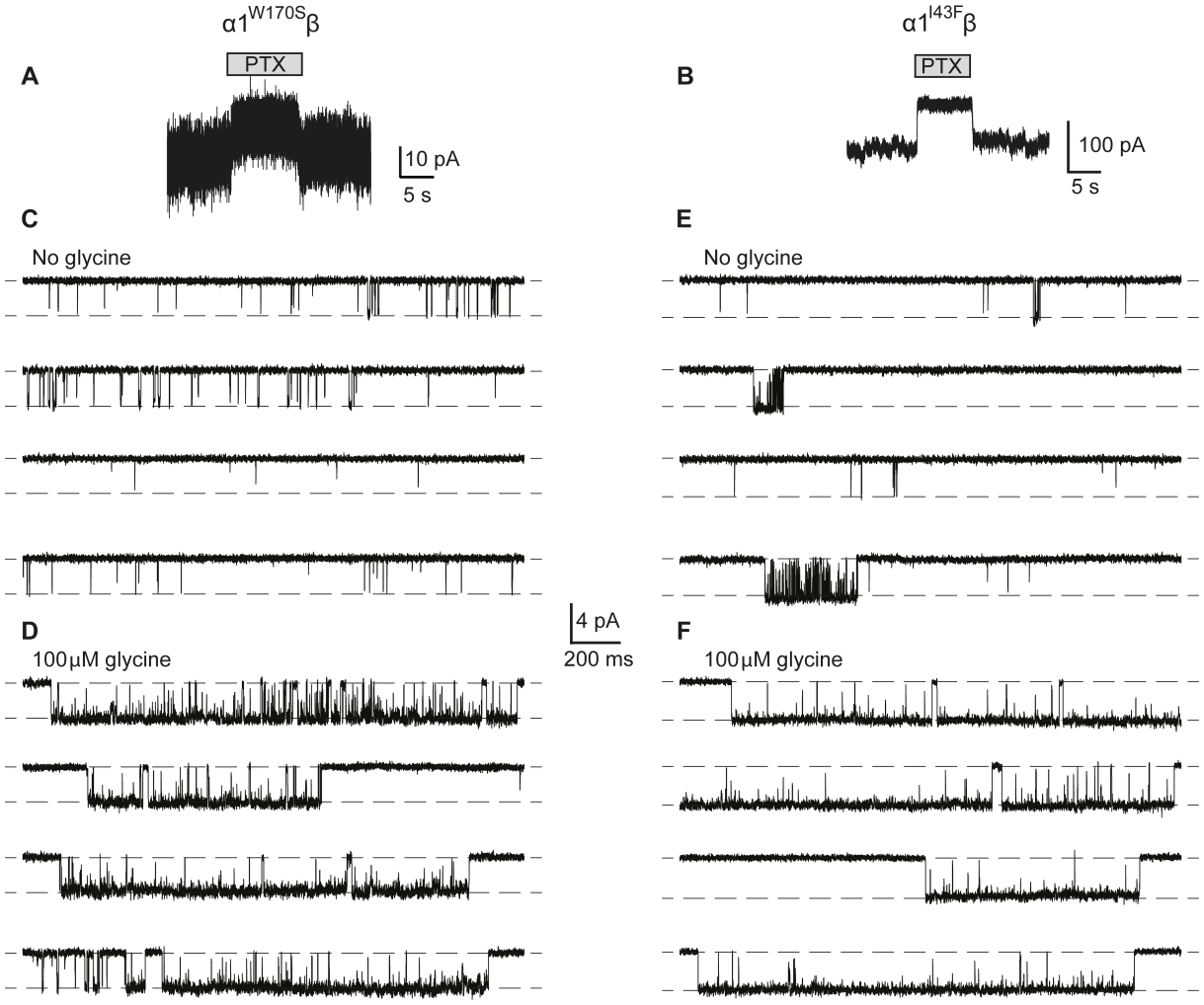

Figure 3. Spontaneous activity in $\alpha1^{W170S}\beta$ and $\alpha1^{I43F}\beta$ GlyRs. Whole-cell steady-state currents showing the effect of 100 μM picrotoxin (PTX) on $\alpha1^{W170S}\beta$ **(A)** and $\alpha1^{I43F}\beta$ **(B)** GlyRs. Paired single channel recordings of the $\alpha1^{W170S}\beta$ GlyR in the absence of applied glycine **(C)** and in the presence of 100 μM glycine **(D)**. The patch contained an estimate of 6 channels. Paired single channel recordings of the $\alpha1^{I43F}\beta$ GlyR in the absence of applied glycine **(E)** and in the presence of 100 μM glycine **(F)**. The patch contained an estimate of 4 channels.

Hyperekplexia mutations prolong the duration of IPSCs - Next we characterized the mean amplitudes, 10−90% rise times and decay time constants of spontaneous IPSCs mediated by recombinant α1β, $\alpha1^{I43F}\beta$, $\alpha1^{W170S}\beta$, $\alpha1^{Q226E}\beta$, $\alpha1^{V280M}\beta$ and $\alpha1^{R414H}\beta$ GlyRs (Fig. 4). Sample recordings from artificial synapses incorporating each isoform are shown at three progressively increasing temporal resolutions in Fig. 4A with a globally averaged, normalized IPSC shown for each isoform in Fig. 4B. The averaged IPSC amplitudes, 10−90% rise times and decay time constants for each isoform are presented in Fig. 4C and Table 2. Relative to α1β GlyRs, IPSCs mediated by $\alpha1^{I43F}\beta$ and $\alpha1^{V280M}\beta$ GlyRs exhibited significantly larger amplitudes, whereas those mediated by $\alpha1^{W170S}\beta$, $\alpha1^{Q226E}\beta$ and $\alpha1^{R414H}\beta$ GlyRs exhibited no significant change (Fig. 4C). All five mutations resulted in either modest (W170S and R414H) or dramatic (I43F, Q226E and V280M) increases in the mean IPSC decay time constant (Fig. 4C). The $\alpha1^{I43F}\beta$ and $\alpha1^{V280M}\beta$

GlyRs also exhibited significantly slower rise times relative to the α1β GlyR (Fig. 4C). As illustrated in Fig. 5, the IPSC amplitudes and decay time constants were monotonically distributed for all isoforms, suggesting a single postsynaptic GlyR population in each case. It is likely that the prolonged IPSC rise and decay times in the mutant GlyRs is due either to altered intrinsic channel gating or to altered geometric factors within the synapse (e.g., synaptic cleft width, GlyR clustering propensity) that may slow access of neurotransmitter to the receptors. Our next experiments sought to distinguish between these possibilities by comparing the IPSC rise and decay rates with the intrinsic channel opening and closing rates for each mutant GlyR.

Table 2. Comparison of 10-90 % rise times and decay time constants of IPSCs and macropatch currents mediated by the indicated wild type and mutant GlyRs.

		α1β	$\alpha1^{R414H}\beta$	$\alpha1^{W170S}\beta$	$\alpha1^{Q226E}\beta$	$\alpha1^{I43F}\beta$	$\alpha1^{V280M}\beta$
10-90% rise time (ms)	IPSCs	1.6 ± 0.1 (n=17)	1.2 ± 0.1 (7)	2.6 ± 0.3 (12)	2.7 ± 0.4 (5)	5.1 ± 0.6^{****} (13)	7.0 ± 0.9^{****} (10)
	macropatch currents	0.8 ± 0.1 (11)	0.9 ± 0.2 (8)	1.2 ± 0.2 (6)	0.8 ± 0.1 (11)	0.7 ± 0.1 (7)	0.5 ± 0.1 (9)
deactivation time constant (ms)	IPSCs	7.2 ± 0.5	10.9 ± 0.8	18.7 ± 1.5	$102 \pm 5^{***}$	96 ± 12^{****}	181 ± 31^{****}
	macropatch currents	26.2 ± 3.4	32.4 ± 4.1	30.4 ± 3.1	221 ± 23^{****}	311 ± 46^{****}	$139 \pm 21^{***}$

*$p < 0.05$, **$p < 0.01$, ***$p < 0.001$ and ****$p < 0.0001$ relative to the wild type α1β GlyR via one-way ANOVA followed by Bonferroni's post-hoc correction.

For IPSCs, the n values refer to the total number of cells from which data were collected. For each cell, parameters were analyzed from a single IPSC waveform that was digitally averaged from >50 individual events.

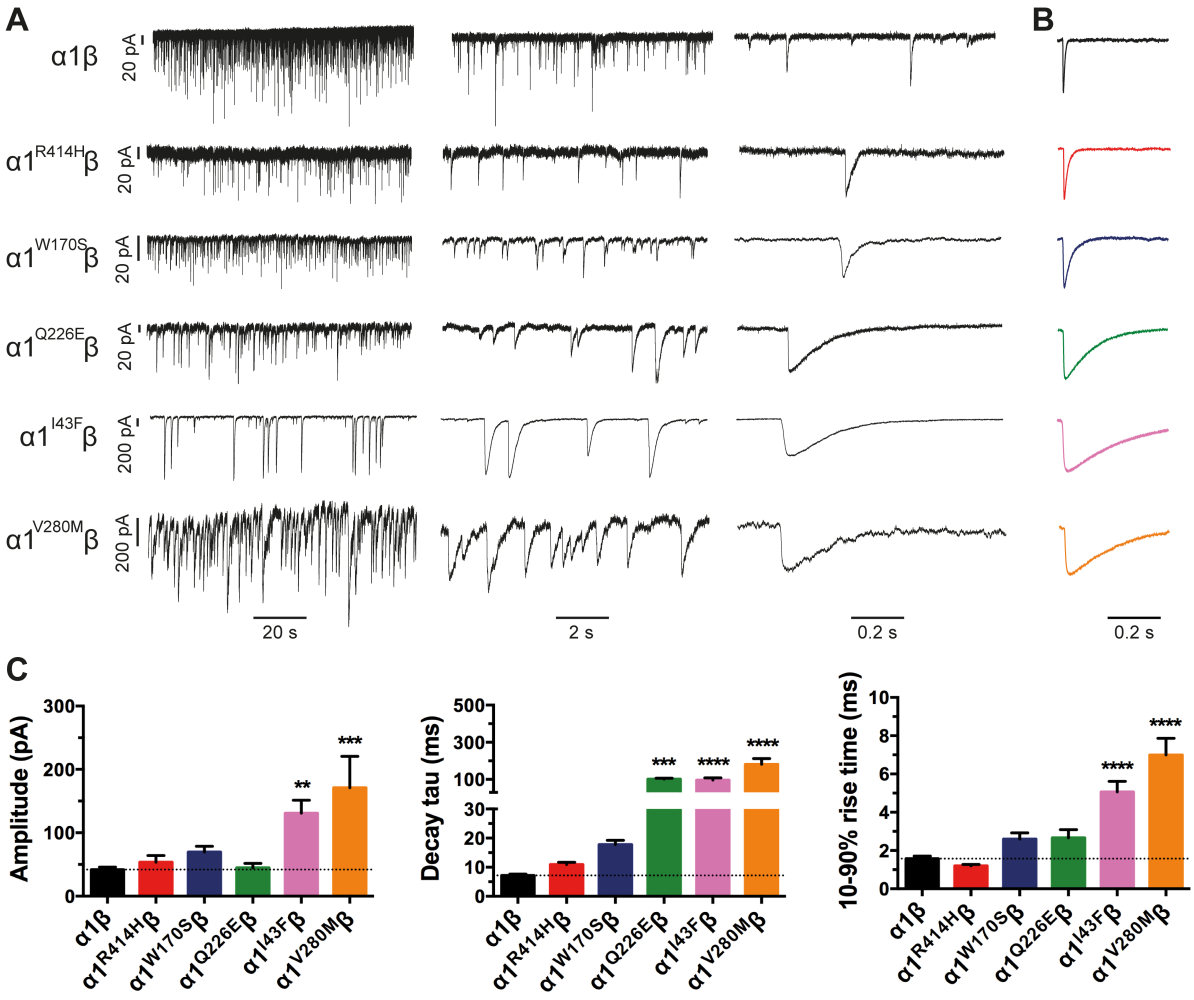

Figure 4. Properties of spontaneous IPSCs mediated by wild type and mutant GlyRs in artificial synapses. Recordings were performed at −60 mV. **A**. Representative recordings of glycinergic IPSCs in HEK293 cells expressing the indicated heteromeric GlyRs at three different temporal resolutions. **B**. Averaged, normalized IPSCs each averaged from >50 events from the corresponding cell in **A**. **C.** Comparison of mean IPSC amplitude, decay time constant and 10-90% rise time for the indicated GlyRs. Statistical significance was determined via one-way ANOVA followed by Bonferroni's post-hoc correction with significance represented by $^{**}p < 0.01$, $^{***}p < 0.001$ and $^{****}p < 0.0001$ relative to α1β GlyRs.

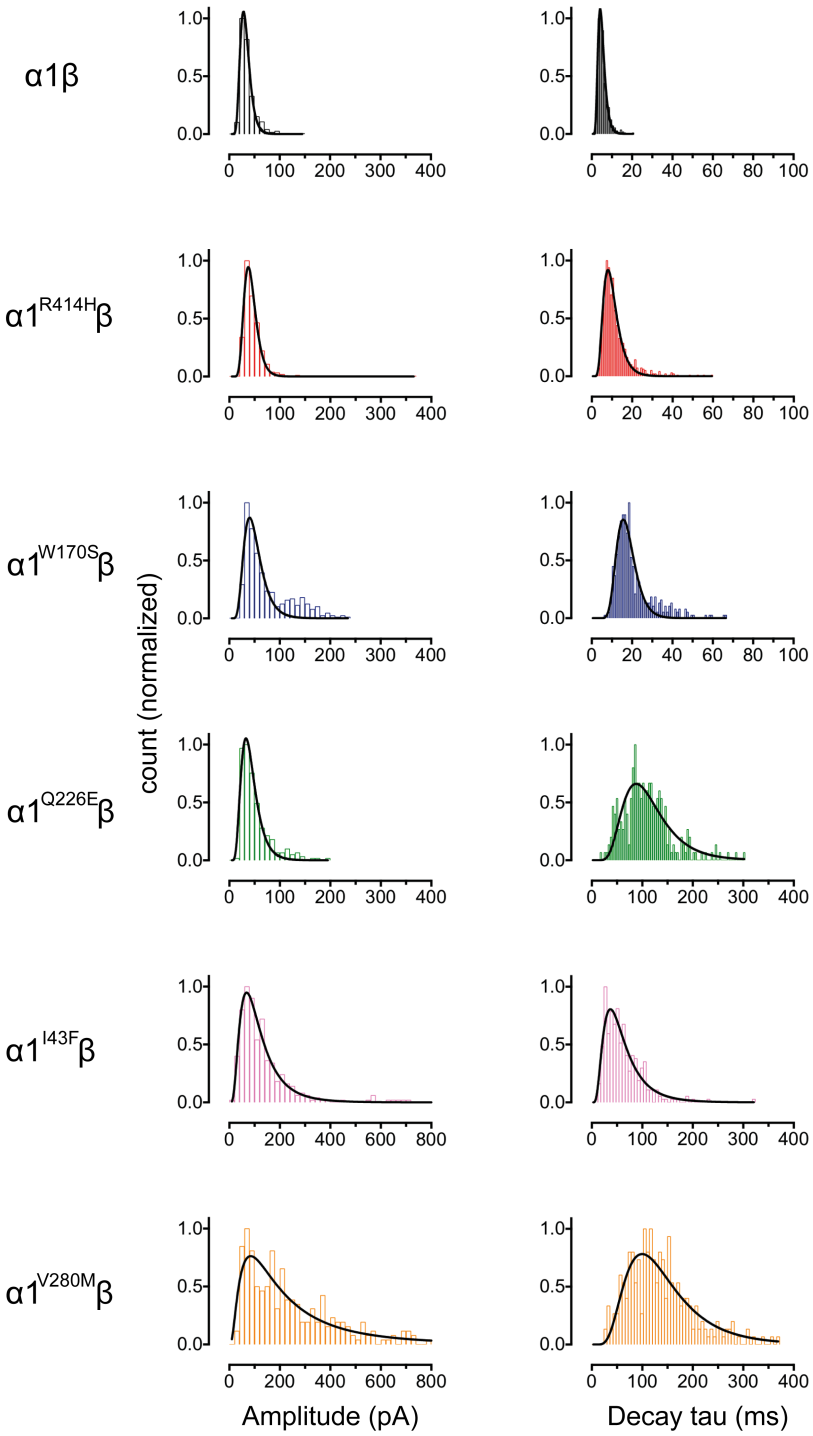

Figure 5. Distribution histograms for the peak amplitude and decay time constants of IPSCs recorded from wild type and mutant GlyRs (n = 6 cells for each subtype). Curves represent single Gaussian functions of best fit to the data.

Characterization of intrinsic channel closing rates - The peak synaptic glycine concentration has been estimated to reach 1 – 3 mM in embryonic zebrafish neurons (27) and 2.2 – 3.5 mM in adult rat spinal neurons (25). Glycine is removed from the cleft with a time constant of 0.6 – 0.9 ms (25). Considering these parameters, we simulated synaptic activation conditions by rapidly applying 1 mM glycine for a period of ~1 ms to outside-out macropatches expressing each receptor. We regularly calibrated the speed of the solution exchange system by rapidly switching the solution

perfusing an open patch pipette between standard extracellular solution and an extracellular solution that had been diluted by 50% with distilled water. By monitoring the resulting pipette current, we were able to ensure that the solution perfusing the macropatch was completely exchanged within 200 μs (23). Under these conditions, the α1β GlyR activated robustly with a mean 10-90% rise time of 0.8 ± 0.1 ms and mean decay time constant of 26.2 ± 3.4 ms (Fig. 6, Table 2). This rise time was conserved for all five mutant GlyRs, which is surprising given that the mean IPSC rise times for the mutant GlyRs were all significantly slower than the wild type α1β GlyR value (Table 2). We also observed a systematic discrepancy between the IPSC decay time constants and the macropatch current deactivation time constants for the wild type and mutant GlyRs (Fig. 6, Table 2). With the exception of the $\alpha1^{V280M}\beta$ GlyR, the intrinsic channel deactivation time constants were a factor of 1.7 – 3.6 slower than the IPSC decay time constants. The discrepancies between the macropatch and synaptic rise and decay times are presumably caused by factors specific to the synapse. One possibility is that synaptic GlyRs are clustered by a binding interaction with a protein that alters their gating properties. It is also possible that we have made an incorrect assumption about the temporal profile and/or peak glycine concentration in the synaptic cleft. However, given the strong correlation between IPSC decay time constants and macropatch deactivation time constants in the $\alpha1^{I43F}\beta$, $\alpha1^{Q226E}\beta$ and $\alpha1^{V280M}\beta$ GlyRs, we infer that the dramatic slowing in their IPSC decay rates is dominated by changes in their intrinsic channel gating properties. Indeed, we have characterised the molecular basis of these gating changes in the $\alpha1^{Q226E}\beta$ and $\alpha1^{V280M}\beta$ GlyRs (10,24).

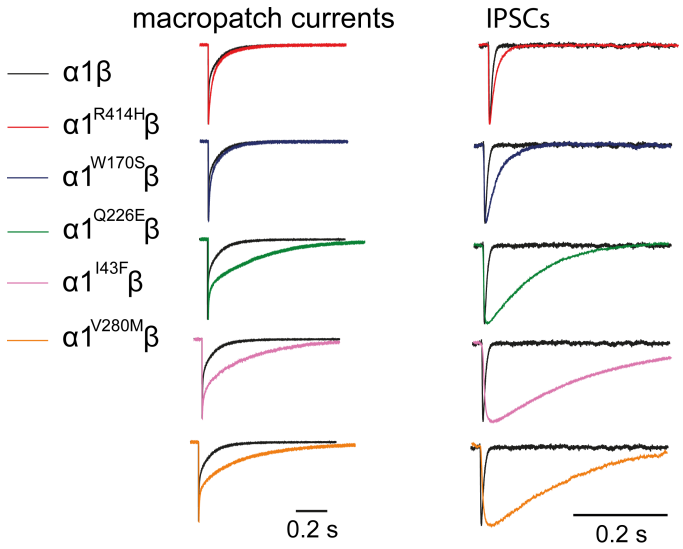

Figure 6. Comparison of the IPSC decay rate with the corresponding intrinsic receptor deactivation rate. Averaged macropatch currents recorded from outside-out patches containing the indicated GlyR. The currents were activated by brief (~1 ms) exposure to saturating (1 mM) glycine. Recordings were performed at −60 mV. Corresponding averaged IPSCs (right panel, black traces), reproduced from Fig. 3B, are included for comparison.

Tropisetron significantly increased α1β GlyR-mediated IPSC decay time constant - The R414H mutation results in a full hyperekplexia phenotype (16) despite causing a relatively small increase in IPSC decay time constant (from 7.2 to 11.4 ms). Can a small increase in the IPSC decay time

constant alone result in a motor impairment? We addressed this question by investigating the effects 1 nM tropisetron on IPSCs mediated by α1β GlyRs.

Tropisetron, a 5-hydroxytryptamine type-3 receptor (5-HT_3R) antagonist, is clinically important for the treatment of postoperative and chemotherapy induced emesis and, importantly, it causes no motor side effects (28). As tropisetron inhibits the $5HT_3R$ with an IC_{50} near 1 nM (29,30), we assume this concentration is clinically relevant. This concentration is also known to potentiate recombinant α1β GlyRs activated by a low (e.g., EC_{20}) glycine concentration (4,31), although its effect on glycinergic IPSCs has never been reported. Sample recordings of α1β GlyR-mediated IPSCs in the absence and presence of 1 nM tropisetron are shown in Fig. 7A. The globally averaged and normalised IPSCs suggest that 1 nM tropisetron exerted a prolonging effect on IPSC decay times (Fig. 7B). The averaged data presented in Fig. 7C reveal that 1 nM tropisetron had no significant effect on IPSC amplitude or 10 – 90 % rise times, although it significantly increased the decay time constant from 5.8 ± 0.3 to 7.6 ± 0.4 ms ($p < 0.05$, paired t test; n = 6 cells). The percentage increase (32 %) in the IPSC decay time constant in 1 nM tropisetron was modestly lower than that caused by either the R414H or W170S mutations (59% and 56%, respectively).

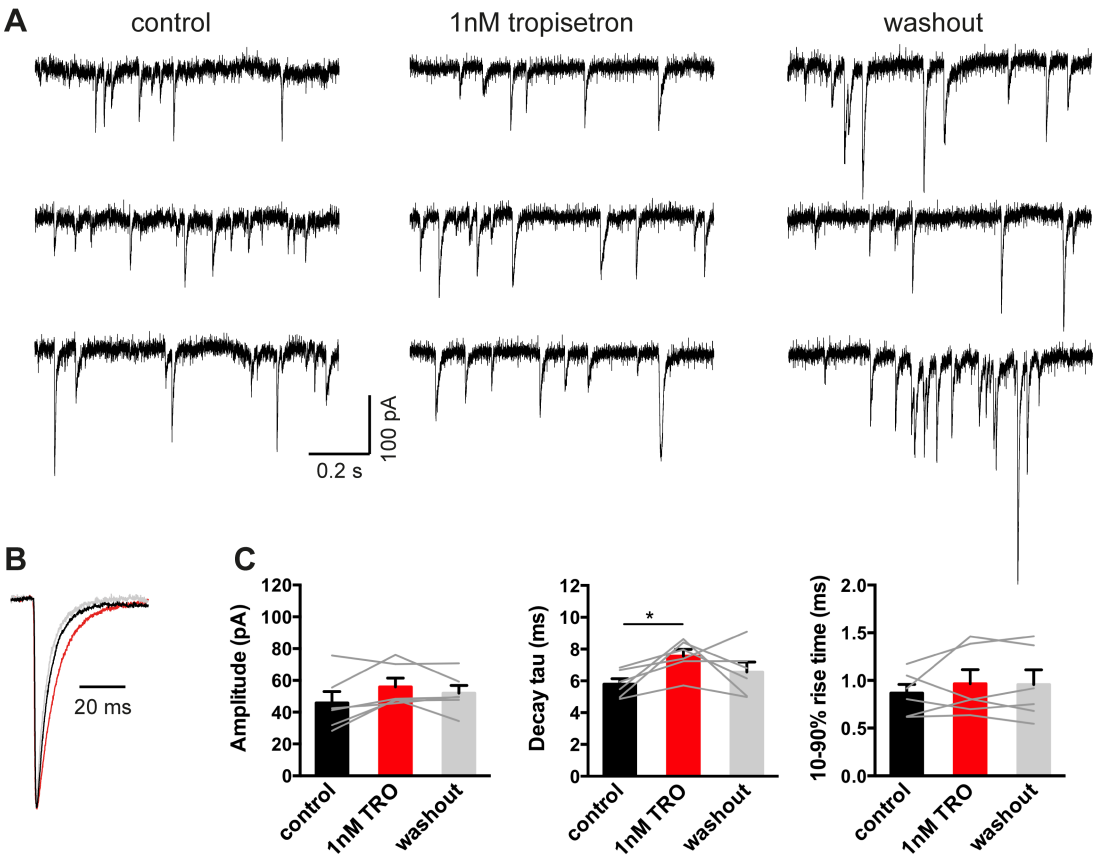

Figure 7. A clinically relevant concentration of tropisetron prolongs the IPSC duration. **A**. Representative IPSC recordings from an α1β GlyR-expressing cell before, during and after the application of 1 nM tropisetron. Recordings were performed at −60 mV. **B**. Superimposed averaged traces of IPSCs (n > 200 events) recorded in control (black trace), 1 nM tropisetron exposure (red trace), and 5 min after the tropisetron washout (grey trace). Currents have been

normalised. C. The decay time constant of IPSCs mediated by α1β GlyRs was significantly prolonged by 1 nM tropisetron whereas the amplitude and 10-90% rise times were unchanged. *$p < 0.05$ relative to drug-free control.

DISCUSSION

Validation of the artificial synapse technique - We have previously validated our artificial synapse system by showing that the decay rates of IPSCs mediated by α1β, α2β and α3β GlyRs in artificial synapses are similar to those mediated by the same isoforms in native neuronal synapses (21). We have also compared the effects of α1 GlyR subunit mutations in artificial and native synapses. The α1 GlyR subunit loss-of-function D80A and A52S mutations have previously been shown to cause hyperekplexia-like phenotypes in mice (32,33). Artificial synapses incorporating recombinant $\alpha1^{D80A}\beta$ and $\alpha1^{A52S}\beta$ mutant GlyRs exhibited accelerated IPSC decay rates that were quantitatively similar to those recorded in native synapses in mutant mice homozygous for the same mutations (21). The main trends in our artificial synapse data are also supported by the fast agonist application experiments (Fig. 6). Thus, the possible existence of ultrastructural or protein expression differences between native and artificial synapses are unlikely to seriously affect the IPSC decay rates as reported here.

Summary of results - We have identified two new *GLRA1* gain-of-function hyperekplexia mutations, I43F and W170S. The I43F mutation resulted in prolonged bursts of spontaneous channel activity (Fig. 3E) similar to that previously demonstrated for the Q226E mutation (24). These bursts most likely underlie the observed slow IPSC decay rates. Indeed, synaptic currents mediated by other ligand-gated ion channels have also been shown to deactivate as a function of the durations of single channel burst activity (23,34-37). Conversely, the short-lived spontaneous bursts induced by $\alpha1^{W170S}\beta$ and $\alpha1^{R414H}\beta$ GlyRs most likely underlie their faster IPSC decay rates, compared to those mediated by $\alpha1^{I43F}\beta$ and $\alpha1^{Q226E}\beta$ GlyRs.

The original electrophysiological characterisation of the $\alpha1^{W170S}\beta$ GlyR showed that zinc potentiation was abolished (19). Physiological levels of zinc potentiate GlyRs (38,39), and the loss of zinc potentiation via the $\alpha1^{D80A}$ mutation accelerated the IPSC decay rate and thus caused hyperekplexia in a knock-in mouse model (32). Thus, it was reasonable to hypothesise that the W170S-mediated hyperekplexia phenotype was due to a diminished capacity of IPSCs to transfer chloride ions (19). However, in the present study we found that the decay time constant of IPSCs mediated by $\alpha1^{W170S}\beta$ GlyRs was actually longer than that of α1β GlyRs (Fig. 4C). Thus, the loss of zinc potentiation does not explain the hyperekplexia phenotype.

It seems surprising that the R414H mutation also resulted in a full hyperekplexia phenotype, especially given its autosomal dominant inheritance mode (16). This mutation resulted in a modest level of spontaneous channel activity (16) and a modestly prolonged IPSC duration (Fig. 4C),

similar to that induced by W170S. Due to its inheritance mode, the magnitudes of these effects in heterozygote patients may be further reduced by the equivalent levels of expression of mutant and wild type α1 subunits.

Molecular mechanisms of the mutations -Q226 lies at the top of the M1 domain (Fig. 1). As the channel opens, Q226 moves closer to R271 at the top of M2 (40). We have previously demonstrated that channel activation is facilitated by an energetic interaction between these residues (10,24). This interaction is strengthened by the Q226E mutation, resulting in the longer active periods that underlie the gain-of-function startle phenotype (10,24). V280 is located in the M2-M3 loop (Fig. 1) where it is closely apposed to I225 at the top of M1. We previously concluded that the bulky V280M substitution exerts a steric repulsion against I225, thereby tilting the M2 outwards to facilitate spontaneous channel opening (10,24). I49 and W170 lie in close proximity in the inner and outer β-sheets, respectively, of the extracellular domain (Fig. 1). It is possible that mutations to either of these residues disrupt the relative orientations of the β-sheets and this could lead to allosteric defects including aberrant receptor activation. The molecular mechanism of R414H, which lies at the extracellular C-terminus of M4 (Fig. 1), remains elusive.

Proposed mechanism of hyperekplexia by gain-of-function GLRA1 mutants - Synaptic inhibition in adult spinal motor neurons is mediated exclusively by glycine (41,42) or by a combination of glycine and GABA (43,44). The chloride concentration in adult neurons is normally very low, and as a result small increases in the chloride influx rate can have a significant effect on the strength, or even polarity, of glycinergic signalling (45). If a tonic increase in intracellular chloride concentration in otherwise healthy adult spinal motor neurons causes hyperekplexia, then the I43F, Q226E or V280M mutations should cause a more severe phenotype than the W170S or R414H mutations, due to the large disparity in their rates of spontaneous and glycine-mediated chloride influx (45). Furthermore, if spontaneous GlyR activity results in increased chloride accumulation in spinal motor neurons then it should do likewise in spinal dorsal horn nociceptive neurons that also receive glycinergic inputs (46), and this should result in chronic pain (45). As neither chronic pain nor a correlation between *GLRA1* mutation severity and startle phenotype have ever been reported in hyperekplexia patients (12), we consider it unlikely that hyperekplexia is predominantly due to an elevated chloride concentration in adult motor neurons.

Another possibility is that the mutation-induced increase in IPSC decay time constant directly elicits hyperekplexia, perhaps by a presynaptic effect on an excitatory or inhibitory input onto motor neurons. We demonstrate that a clinically relevant (1 nM) concentration of tropisetron significantly prolongs the decay time constant of α1β-mediated IPSCs (Fig. 7). This is notable because tropisetron has never been reported to cause hyperekplexia or other motor side effects (28,47). As the tropisetron-induced increase in IPSC decay time constant almost reaches the levels

induced by the W170S and R414H mutations, it is unlikely that the modest slowing in the IPSC decay rate induced by these mutations could cause hyperekplexia.

Prenatally in the rat, the α2 subunit is the predominant GlyR isoform. However, a developmental switch occurs during the first three postnatal weeks, whereby most of the α2 subunits are replaced by α1 (3). Simultaneously, the intracellular chloride concentration is reduced due to chloride extrusion by the KCC2 and KCC3 chloride-potassium co-transporters to the point where it supports efficient synaptic inhibition (48). A recent study that inhibited KCC2 function in cultured spinal neurons during this period found that the elevated chloride concentration reduced the number and size of α1 GlyR dendritic clusters without affecting neighbouring α2 GlyR clusters (49). Concomitantly, glycinergic miniature IPSCs were reduced in amplitude and frequency although GABAergic IPSCs were not affected. This mechanism, which is thought to be active during the final maturation stage of spinal motor neurons (49), provides a mechanism for explaining how gain-of-function hyperekplexia mutations can cause a single common hyperekplexia phenotype without necessarily requiring an elevated chloride concentration in adult neurons.

Relevance of findings to pain drug development - Glycinergic synapses on pain sensory neurons in the spinal cord superficial laminae are unique in that they incorporate both α1 and α3 GlyR subunits (50). Inflammatory mediators (notably prostaglandin E2) induce chronic inflammatory pain by phosphorylating, and inhibiting, α3-containing GlyRs (50,51). This reduces the magnitude of IPSCs in spinal pain sensory neurons, which in turn 'disinhibits' them and thereby increases the rate of transmission of pain impulses to the brain. This mechanism, which provides a paradigm for chronic inflammatory pain sensitisation, implies that drugs that selectively potentiate (i.e., restore) α3β GlyR-mediated IPSCs should be analgesic. It is generally assumed that such drugs should avoid potentiating α1β GlyRs due to their broader distribution and the consequent risk of motor and other side effects (46,52). However, developing drugs specific for α3-containing GlyRs has proved difficult (53), due largely to the high amino acid sequence identity of α1 and α3 subunits, particularly in the known ligand binding sites. Our demonstration that a clinically relevant tropisetron concentration potentiates α1β GlyR-mediated IPSCs without causing motor or other side effects suggests the policy of avoiding α1 potentiation during analgesic drug development may be overemphasized.

Conclusion - Given that hyperekplexia is normally associated with a loss of glycinergic inhibitory tone, it seems paradoxical that an increase in glycinergic tone elicits an identical phenotype. We demonstrate here that all known *GLRA1* gain-of-function hyperekplexia mutations act similarly to induce spontaneous GlyR activity and slow the decay rate of glycinergic IPSCs. We argue that mutations with modest IPSC prolonging effects (W170S, R414H) are unlikely to cause

hyperekplexia by simply slowing the IPSC decay rate. We also argue that intracellular chloride accumulation in otherwise healthy adult neurons is unlikely to be solely responsible, although it may contribute to the phenotype. It has been shown that an elevated intracellular chloride concentration late in development selectively ablates α1β GlyR-containing synapses on spinal neurons. We consider this provides a plausible mechanism for gain-of-function *GLRA1* hyperekplexia mutations because the loss of synapses would result in a single common hyperekplexia phenotype without requiring significant chloride accumulation in adult neurons.

Acknowledgements: This project was supported by research grants from the Australian Research Council (DP150102428) and the National Health and Medical Research Council (1058542, 1080976).

Conflict of interest: The authors declare that they have no conflict of interest.

Author contributions: J.L. conceived the project. Y.Z., A.B., B.N. and A.K. performed experiments and analysed data. Y.Z. and J.L. wrote the manuscript. All authors reviewed the content of the manuscript.

REFERENCES

1. Dutertre, S., Becker, C. M., and Betz, H. (2012) Inhibitory glycine receptors: an update. *J Biol Chem* **287**, 40216-40223
2. Legendre, P. (2001) The glycinergic inhibitory synapse. *Cell Mol Life Sci* **58**, 760-793
3. Lynch, J. W. (2004) Molecular structure and function of the glycine receptor chloride channel. *Physiol Rev* **84**, 1051-1095
4. Yang, Z., Ney, A., Cromer, B. A., Ng, H. L., Parker, M. W., and Lynch, J. W. (2007) Tropisetron modulation of the glycine receptor: femtomolar potentiation and a molecular determinant of inhibition. *J Neurochem* **100**, 758-769
5. Durisic, N., Godin, A. G., Wever, C. M., Heyes, C. D., Lakadamyali, M., and Dent, J. A. (2012) Stoichiometry of the human glycine receptor revealed by direct subunit counting. *J Neurosci* **32**, 12915-12920
6. Choii, G., and Ko, J. (2015) Gephyrin: a central GABAergic synapse organizer. *Exp Mol Med* **47**, e158
7. Meyer, G., Kirsch, J., Betz, H., and Langosch, D. (1995) Identification of a gephyrin binding motif on the glycine receptor beta subunit. *Neuron* **15**, 563-572
8. Tyagarajan, S. K., and Fritschy, J. M. (2014) Gephyrin: a master regulator of neuronal function? *Nat Rev Neurosci* **15**, 141-156
9. Bakker, M. J., van Dijk, J. G., van den Maagdenberg, A. M., and Tijssen, M. A. (2006) Startle syndromes. *Lancet Neurol* **5**, 513-524
10. Bode, A., and Lynch, J. W. (2013) Analysis of hyperekplexia mutations identifies transmembrane domain rearrangements that mediate glycine receptor activation. *J Biol Chem* **288**, 33760-33771
11. Harvey, R. J., Topf, M., Harvey, K., and Rees, M. I. (2008) The genetics of hyperekplexia: more than startle! *Trends Genet* **24**, 439-447

12. Thomas, R. H., Chung, S. K., Wood, S. E., Cushion, T. D., Drew, C. J., Hammond, C. L., Vanbellinghen, J. F., Mullins, J. G., and Rees, M. I. (2013) Genotype-phenotype correlations in hyperekplexia: apnoeas, learning difficulties and speech delay. *Brain* **136**, 3085-3095
13. Bode, A., and Lynch, J. W. (2014) The impact of human hyperekplexia mutations on glycine receptor structure and function. *Mol Brain* **7**, 2
14. Brune, W., Weber, R. G., Saul, B., von Knebel Doeberitz, M., Grond-Ginsbach, C., Kellerman, K., Meinck, H. M., and Becker, C. M. (1996) A GLRA1 null mutation in recessive hyperekplexia challenges the functional role of glycine receptors. *Am J Hum Genet* **58**, 989-997
15. Schaefer, N., Vogel, N., and Villmann, C. (2012) Glycine receptor mutants of the mouse: what are possible routes of inhibitory compensation? *Front Mol Neurosci* **5**, 98
16. Bode, A., Wood, S. E., Mullins, J. G., Keramidas, A., Cushion, T. D., Thomas, R. H., Pickrell, W. O., Drew, C. J., Masri, A., Jones, E. A., Vassallo, G., Born, A. P., Alehan, F., Aharoni, S., Bannasch, G., Bartsch, M., Kara, B., Krause, A., Karam, E. G., Matta, S., Jain, V., Mandel, H., Freilinger, M., Graham, G. E., Hobson, E., Chatfield, S., Vincent-Delorme, C., Rahme, J. E., Afawi, Z., Berkovic, S. F., Howell, O. W., Vanbellinghen, J. F., Rees, M. I., Chung, S. K., and Lynch, J. W. (2013) New hyperekplexia mutations provide insight into glycine receptor assembly, trafficking, and activation mechanisms. *J Biol Chem* **288**, 33745-33759
17. Chung, S. K., Vanbellinghen, J. F., Mullins, J. G., Robinson, A., Hantke, J., Hammond, C. L., Gilbert, D. F., Freilinger, M., Ryan, M., Kruer, M. C., Masri, A., Gurses, C., Ferrie, C., Harvey, K., Shiang, R., Christodoulou, J., Andermann, F., Andermann, E., Thomas, R. H., Harvey, R. J., Lynch, J. W., and Rees, M. I. (2010) Pathophysiological mechanisms of dominant and recessive GLRA1 mutations in hyperekplexia. *J Neurosci* **30**, 9612-9620
18. Al-Futaisi, A. M., Al-Kindi, M. N., Al-Mawali, A. M., Koul, R. L., Al-Adawi, S., and Al-Yahyaee, S. A. (2012) Novel mutation of GLRA1 in Omani families with hyperekplexia and mild mental retardation. *Pediatr Neurol* **46**, 89-93
19. Zhou, N., Wang, C. H., Zhang, S., and Wu, D. C. (2013) The GLRA1 missense mutation W170S associates lack of Zn2+ potentiation with human hyperekplexia. *J Neurosci* **33**, 17675-17681
20. Horvath, E., Farkas, K., Herczegfalvi, A., Nagy, N., and Szell, M. (2014) Identification of a novel missense GLRA1 gene mutation in hyperekplexia: a case report. *J Med Case Rep* **8**, 233
21. Zhang, Y., Dixon, C. L., Keramidas, A., and Lynch, J. W. (2015) Functional reconstitution of glycinergic synapses incorporating defined glycine receptor subunit combinations. *Neuropharmacology* **89**, 391-397
22. Dixon, C. L., Zhang, Y., and Lynch, J. W. (2015) Generation of Functional Inhibitory Synapses Incorporating Defined Combinations of GABA(A) or Glycine Receptor Subunits. *Front Mol Neurosci* **8**, 80
23. Dixon, C., Sah, P., Lynch, J. W., and Keramidas, A. (2014) GABAA receptor alpha- and gamma- subunits shape synaptic currents via different mechanisms. *J Biol Chem* **289**, 5399-5411
24. Scott, S., Lynch, J. W., and Keramidas, A. (2015) Correlating structural and energetic changes in glycine receptor activation. *J Biol Chem* **290**, 5621-5634
25. Beato, M. (2008) The time course of transmitter at glycinergic synapses onto motoneurons. *J Neurosci* **28**, 7412-7425
26. Lewis, T. M., Sivilotti, L. G., Colquhoun, D., Gardiner, R. M., Schoepfer, R., and Rees, M. (1998) Properties of human glycine receptors containing the hyperekplexia mutation alpha1(K276E), expressed in Xenopus oocytes. *J Physiol* **507**, 25-40

27. Legendre, P. (1998) A reluctant gating mode of glycine receptor channels determines the time course of inhibitory miniature synaptic events in zebrafish hindbrain neurons. *J Neurosci* **18**, 2856-2870
28. Haus, U., Spath, M., and Farber, L. (2004) Spectrum of use and tolerability of 5-HT3 receptor antagonists. *Scand J Rheumatol* **33**, 12-18
29. Lankiewicz, S., Lobitz, N., Wetzel, C. H., Rupprecht, R., Gisselmann, G., and Hatt, H. (1998) Molecular cloning, functional expression, and pharmacological characterization of 5-hydroxytryptamine3 receptor cDNA and its splice variants from guinea pig. *Mol Pharmacol* **53**, 202-212
30. Miyake, A., Mochizuki, S., Takemoto, Y., and Akuzawa, S. (1995) Molecular cloning of human 5-hydroxytryptamine3 receptor: heterogeneity in distribution and function among species. *Mol Pharmacol* **48**, 407-416
31. Supplisson, S., and Chesnoy-Marchais, D. (2000) Glycine receptor beta subunits play a critical role in potentiation of glycine responses by ICS-205,930. *Mol Pharmacol* **58**, 763-770
32. Hirzel, K., Muller, U., Latal, A. T., Hulsmann, S., Grudzinska, J., Seeliger, M. W., Betz, H., and Laube, B. (2006) Hyperekplexia phenotype of glycine receptor alpha1 subunit mutant mice identifies Zn(2+) as an essential endogenous modulator of glycinergic neurotransmission. *Neuron* **52**, 679-690
33. Graham, B. A., Schofield, P. R., Sah, P., Margrie, T. W., and Callister, R. J. (2006) Distinct physiological mechanisms underlie altered glycinergic synaptic transmission in the murine mutants spastic, spasmodic, and oscillator. *J Neurosci* **26**, 4880-4890
34. Dixon, C. L., Harrison, N. L., Lynch, J. W., and Keramidas, A. (2015) Zolpidem and eszopiclone prime alpha1beta2gamma2 GABAA receptors for longer duration of activity. *Br J Pharmacol* **172**, 3522-3536
35. Elenes, S., Ni, Y., Cymes, G. D., and Grosman, C. (2006) Desensitization contributes to the synaptic response of gain-of-function mutants of the muscle nicotinic receptor. *J Gen Physiol* **128**, 615-627
36. Sine, S. M., and Engel, A. G. (2006) Recent advances in Cys-loop receptor structure and function. *Nature* **440**, 448-455
37. Wyllie, D. J., Behe, P., and Colquhoun, D. (1998) Single-channel activations and concentration jumps: comparison of recombinant NR1a/NR2A and NR1a/NR2D NMDA receptors. *J Physiol* **510**, 1-18
38. Laube, B., Kuhse, J., Rundstrom, N., Kirsch, J., Schmieden, V., and Betz, H. (1995) Modulation by zinc ions of native rat and recombinant human inhibitory glycine receptors. *J Physiol* **483**, 613-619
39. Miller, P. S., Da Silva, H. M. A., and Smart, T. G. (2005) Molecular basis for zinc potentiation at strychnine-sensitive glycine receptors. *J Biol Chem* **280**, 37877-37884
40. Du, J., Lu, W., Wu, S., Cheng, Y., and Gouaux, E. (2015) Glycine receptor mechanism elucidated by electron cryo-microscopy. *Nature* **526**, 224-229
41. Bhumbra, G. S., Moore, N. J., Moroni, M., and Beato, M. (2012) Co-Release of GABA Does Not Occur at Glycinergic Synapses onto Lumbar Motoneurons in Juvenile Mice. *Front Cell Neurosci* **6**, 8
42. Jiang, J., and Alstermark, B. (2015) Not GABA but glycine mediates segmental, propriospinal, and bulbospinal postsynaptic inhibition in adult mouse spinal forelimb motor neurons. *J Neurosci* **35**, 1991-1998
43. Gao, B. X., Stricker, C., and Ziskind-Conhaim, L. (2001) Transition from GABAergic to glycinergic synaptic transmission in newly formed spinal networks. *J Neurophysiol* **86**, 492-502
44. Martin, L. J., and Chang, Q. (2012) Inhibitory synaptic regulation of motoneurons: a new target of disease mechanisms in amyotrophic lateral sclerosis. *Mol Neurobiol* **45**, 30-42

45. De Koninck, Y. (2007) Altered chloride homeostasis in neurological disorders: a new target. *Curr Opin Pharmacol* **7**, 93-99
46. Zeilhofer, H. U. (2005) The glycinergic control of spinal pain processing. *Cell Mol Life Sci* **62**, 2027-2035
47. Carlisle, J. B., and Stevenson, C. A. (2006) Drugs for preventing postoperative nausea and vomiting. *Cochrane Database Syst Rev*, CD004125
48. Blaesse, P., Airaksinen, M. S., Rivera, C., and Kaila, K. (2009) Cation-chloride cotransporters and neuronal function. *Neuron* **61**, 820-838
49. Schwale, C., Schumacher, S., Bruehl, C., Titz, S., Schlicksupp, A., Kokocinska, M., Kirsch, J., Draguhn, A., and Kuhse, J. (2016) KCC2 knockdown impairs glycinergic synapse maturation in cultured spinal cord neurons. *Histochem Cell Biol* **145**, 637-646
50. Harvey, R. J., Depner, U. B., Wassle, H., Ahmadi, S., Heindl, C., Reinold, H., Smart, T. G., Harvey, K., Schutz, B., Abo-Salem, O. M., Zimmer, A., Poisbeau, P., Welzl, H., Wolfer, D. P., Betz, H., Zeilhofer, H. U., and Muller, U. (2004) GlyR alpha3: an essential target for spinal PGE2-mediated inflammatory pain sensitization. *Science* **304**, 884-887
51. Ahmadi, S., Lippross, S., Neuhuber, W. L., and Zeilhofer, H. U. (2002) PGE(2) selectively blocks inhibitory glycinergic neurotransmission onto rat superficial dorsal horn neurons. *Nat Neurosci* **5**, 34-40
52. Lynch, J. W., and Callister, R. J. (2006) Glycine receptors: a new therapeutic target in pain pathways. *Curr Opin Investig Drugs* **7**, 48-53
53. Balansa, W., Islam, R., Fontaine, F., Piggott, A. M., Zhang, H., Xiao, X., Webb, T. I., Gilbert, D. F., Lynch, J. W., and Capon, R. J. (2013) Sesterterpene glycinyl-lactams: a new class of glycine receptor modulator from Australian marine sponges of the genus Psammocinia. *Org Biomol Chem* **11**, 4695-4701

Chapter 4

Effects of alpha2 GlyR autism mutations on glycinergic synaptic function

Effects of alpha2 GlyR autism mutations on glycinergic synaptic function

Abstract

Autism spectrum disorder (ASD), characterized by deficits in social interaction and communication, is thought to result from dysfunctional development of neural circuits and is associated with perturbed excitatory-inhibitory balance. Glycine receptors (GlyRs) are postsynaptic ligand-gated ion channel receptors mediating fast inhibitory neurotransmission in the mature brain. The α2 GlyR is the dominant isoform expressed in neurons during neurodevelopment. As the activity of α2 GlyRs in immature neurons is essential for neuronal migration and synapse formation, they play an important role in neurodevelopment. Defects in the *GLYA2* gene, which encode the α2 GlyR subunit, have been identified in human patients with ASD. Using artificial synapse and macroscopic current recording techniques, we found that the newly identified ASD-causing mutation, R350L, in the TM3-TM4 intracellular loop, altered postsynaptic performance by significantly increasing IPSC rise and decay times. Interestingly, R350L also exhibited reduced glycine sensitivity. To test the role of the arginine in normal GlyR function, we replaced R350 with alanine (reduced side-chain), lysine (retains the positive charge of arginine) or isoleucine (an analogous residue of leucine) residues. Replacement of alanine, lysine and isoleucine at this domain yielded IPSCs with similar kinetic properties to those of wild-type GlyRs.

1. Introduction

Autism spectrum disorders (ASDs) are a group of heterogeneous neurodevelopmental disorders centered on three core deficits: communication impairment, social impairment and restricted interests often accompanied by repetitive behaviours (Geschwind, 2009). Typically, ASD symptoms are manifested in early childhood and persist through adulthood. Abnormalities in the genes encoding glutamatergic receptors (Tarabeux et al., 2011; Uzunova et al., 2014) and GABA-A receptors (Bundey et al., 1994; Schroer et al., 1998; Hogart et al., 2007), or cell-adhesion molecules such as neurexin (Kim et al., 2008; Gauthier et al., 2011; Bena et al., 2013) and neuroligins (Jamain et al., 2003; Laumonnier et al., 2004; Yan et al., 2005) have been reported in ASD patients, suggesting a proportion of ASDs are synaptopathies.

The glycine receptor (GlyR) is a member of pentameric ligand-gated ion channel (pLGIC) family that mediates inhibitory signalling by conducting chloride ion flux in response to the binding of glycine. The superfamily also includes the nicotinic acetylcholine receptor (nAChR), 5-hydroxytryptamine type-3 receptor (5-HT_3R) and γ-aminobutyric acid type-A receptor ($GABA_A$R), each of which is comprised of five subunits surrounding a central ion-conducting pore. Each

subunit shares a common topology contains three domains, N-terminal extracellular domain (ECD) that harbours the ligand-binding site, four transmembrane domains (TM1-TM4) and a large intracellular loop domain (ILD) connecting TM3 and TM4. The intracellular TM3 - TM4 loop of the GlyR harbours phosphorylation sites (Han et al., 2013), and plays an important role in channel gating (Breitinger et al., 2009), conductance (Carland et al., 2009), modulation (Burgos et al., 2015), intracellular sorting (Melzer et al., 2010) and interactions with intracellular proteins (Kim et al., 2006; Del Pino et al., 2014). Three functional isoforms of the α subunit and one isoform of β subunit are found in humans (Lynch, 2009). Pentameric GlyRs can be formed as homomers consist of α subunits only, or as heteromers comprising α and β subunits in the form of 3α:2β or 2α:3β (Grudzinska et al., 2005; Durisic et al., 2012; Yang et al., 2012). The β subunit is important for synaptic localization as it interacts directly with gephyrin, an intracellular protein essential for clustering GlyRs at synapses (Sola et al., 2004; Maric et al., 2014). The maturation of glycinergic synapses is associated with changes in the composition and functional properties of GlyRs. During early CNS development, the α2 subunit is broadly expressed throughout the brain, well before the formation of synaptic contacts. Glycine acts as an excitatory depolarising transmitter due to an inverted chloride gradient in immature neurons (Flint et al., 1998). After birth, GlyR α2 expression is gradually decreased accompanied by markedly increased α1 and α3 expression (Akagi et al., 1991; Malosio et al., 1991; Watanabe and Akagi, 1995). The glycinergic synaptic currents decay rates were observed to be much faster after a progressive replacement of α2 by α1 and α3 subunits (Takahashi et al., 1992), thereby allowing efficient synaptic transmission.

Dysfunction of glycinergic signaling has been implicated in neurological disorders known as hyperekplexia (Bode and Lynch, 2014). Recently, microdeletions and missense mutations in *GLYA2* gene, encoding the GlyR α2 subunit, have been reported to represent a rare cause of ASDs (Piton et al., 2011; Pilorge et al., 2015). To date, three missense mutations (N136S, R153Q and R350L) have been identified. Previous studies have characterized the functional defects of N136S and R153S mutations through whole-cell patch-clamp analysis (Pilorge et al., 2015). The marked reduction in the glycine sensitivity caused by N136S and R153Q mutations would prevent them from responding appropriately to the physiological levels of glycine, thereby reducing the efficacy of glycinergic inhibitory neurotransmission. The Arg-350 to Leu-350 (R350L) substitution, which alters a conserved residue located near the C-terminal end of TM3 in the ILD (Fig. 1A), has yet to be functionally characterised. The aim of this this study is to examine the molecular mechanism by which R350L mutation contributes to ASD pathogenesis.

2. Materials and method

2.1. Cell culture and molecular biology

The human GlyR α2 (pCIS) and β (pCIS) plasmid DNAs were combined in a 1α:50β ratio (for artificial synapse and macropatch recordings) and transfected into HEK293 cells via calcium phosphate-DNA co-precipitation. This resulted in a high level of expression of α2β heteromeric GlyRs (Zhang et al., 2015). For artificial synapse experiments, the mouse NL2A splice variant (pNice), rat gephyrin (pCIS) were co-transfected along with GlyR plasmids to facilitate the formation of artificial synapses. Empty pEGFP plasmid was also transfected as an expression marker. Mutagenesis was performed using the QuikChange mutagenesis kit, and the successful incorporation of mutations was confirmed by DNA sequencing.

2.2. Artificial synapse formation

Primary cultures of spinal cord neurons were prepared as previously described (Dixon et al., 2015; Zhang et al., 2015). E15 timed-pregnant rats were euthanized via CO_2 inhalation in accordance with procedures approved by the University of Queensland Animal Ethics Committee. Cells were plated at a density of ~80,000 cells per 18 mm poly-D-lysine coated coverslip in DMEM medium with 10% fetal bovine serum. After 24 h, the plating medium was changed to Neurobasal medium supplemented with 2% B27 and 1% glutamax, and a second feed after one week replaced half of this medium. Neurons were grown for 1 − 4 weeks *in vitro* and the heterosynaptic co-cultures were prepared by directly introducing transfected HEK293 cells onto the primary neuronal cultures 1 − 3 days prior to recordings.

2.3. Electrophysiology

Whole-cell recordings were performed on transfected HEK293 cells under voltage-clamp mode using a HEKA EPC10 amplifier (HEKA Electronics, Lambrecht, Germany) and Patchmaster software (HEKA), at room temperature. Cells were placed in an external solution comprising (in mM): 140 NaCl, 5 KCl, 2 $CaCl_2$, 1 $MgCl_2$, 10 HEPES, and 10 D-glucose, adjusted to pH 7.4 with NaOH. Patch pipettes (1−3 MΩ resistance), were pulled from borosilicate glass (GC150F-7.5, Harvard apparatus), and filled with an intracellular solution containing the following (in mM): 145 CsCl, 2 $CaCl_2$, 2 $MgCl_2$, 10 HEPES, 10 EGTA and 2 MgATP, adjusted to pH 7.4 with NaOH. Glycine-gated currents were recorded at a holding potential of −40 mV, digitized at 2.9 kHz and filtered at 10 kHz. For IPSC recordings, patch pipettes resistance were adjusted to 4 − 6 MΩ and filled with the same internal solution. Series resistance was routinely compensated to 60% of maximum and was monitored throughout the recording. Both spontaneous and action potential-evoked glycinergic IPSCs in HEK cells were recorded at a holding potential −60 mV and signals

were digitally sampled at 10 kHz and filtered at 4 kHz. As these IPSCs were completely abolished by 1 μM tetrodotoxin (not shown), we infer they were induced by spontaneous action potentials.

Macropatch recordings were performed in the excised outside-out patch clamp configuration. Patch pipettes were fired-polished to a resistance of approximately 10 MΩ and filled with the same internal solution. Macroscopic currents in outside-out patches pulled from transfected HEK293 cells were activated by brief (<1ms) exposure to agonists using a piezo-electric translator (Siskiyou). We regularly calibrated the speed of the solution exchange system by rapidly switching the solution perfusing an open patch pipette between standard extracellular solution and an extracellular solution that had been diluted by 50% with distilled water. By monitoring the resulting pipette current, we were able to ensure that the solution perfusing the macropatch was completely exchanged within 200 μs (Dixon et al., 2014). Recordings were performed using a Multiclamp 700B amplifer and pClamp9 software (Molecular Devices), filtered at 4 kHz and sampled at 10 kHz.

2.4. Analysis

Analyses of IPSC amplitudes, 10 − 90% rise times, and weighted decay time constants were performed using Axograph (Axograph Scientific). Only cells with a stable series resistance of < 25 MΩ throughout the recording period were included in the analysis. Single peak IPSCs with amplitudes of at least three times above the background noise were detected using a semi-automated sliding template. Each detected event was visually inspected and only well-separated IPSCs with no inflections in the rising or decay phases were included. To calculate macroscopic current decay time constants, averaged macroscopic traces were fitted with double-exponential functions in Axograph X, and a weighted time constant was calculated from individual time constants (τ1, τ2) and their relative amplitude (A1, A2) as followings: $\tau_{weighted} = (\tau1\times A1+\tau2\times A2)/(A1+A2)$. The averaged data from individual cells were then pooled to obtain group data. Statistical analysis, and plotting were performed with Prism 5 (GraphPad Software). All data are presented as mean ± SEM. Student's unpaired t-tests or one-way ANOVAs, as appropriate, were employed for comparisons. For all tests, the number of asterisks corresponds to level of significance: *$p < 0.05$, **$p < 0.01$, ***$p < 0.001$ and ****$p < 0.0001$.

3. Results

Effects of the ASD-causing $\alpha2^{R350L}$ mutation on channel properties

The R350 is highly conserved among GlyR subunits (Fig. 1A). To determine the functional effects of ASD-causing $\alpha2^{R350L}$ mutation, we first analyzed the efficacy of glycine in activating

recombinant homomeric $\alpha2^{R350L}$ GlyRs and heteromeric $\alpha2^{R350L}\beta$ receptors. Fig. 1B illustrates whole-cell currents recorded in response to increasing concentrations of glycine in HEK293 cells expressing wild-type or mutated α2 receptors. The glycine dose-response curve of the homomeric and heteromeric $\alpha2^{R350L}$-containing receptors was modestly right-shifted relative to that of the corresponding wild-type GlyR (Fig. 1C) with mean parameters of best fit to the concentration-response curves presented in Fig. 1D. In both homomeric and heteromeric GlyRs, the R350L mutation resulted in an apparent decrease in glycine sensitivity. This suggests that the R350L mutation in M3-M4 loop may induce a global conformational change that propagates to the glycine-binding site.

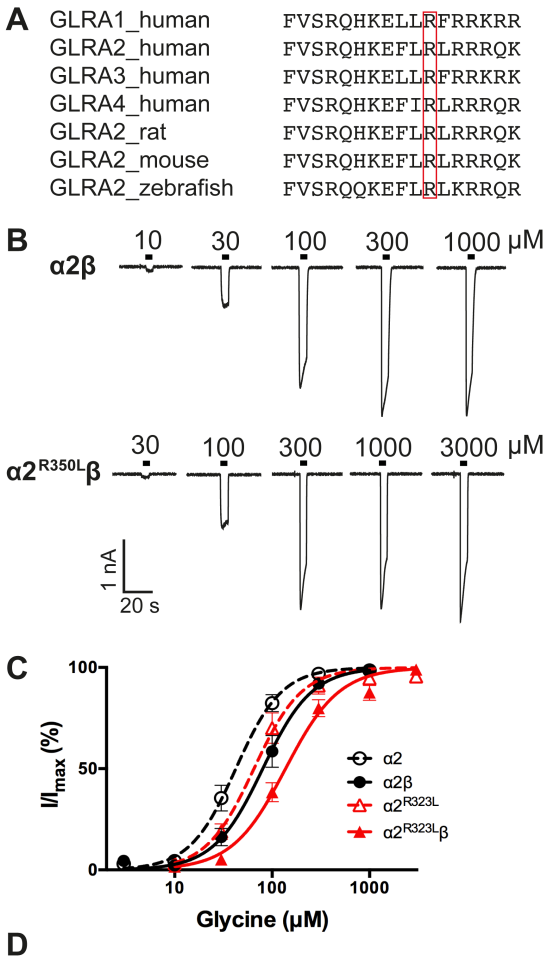

Fig. 1. Effect of the α2 subunit R350L mutation examined by whole cell patch clamp recording. **A**. Alignments of various GlyR α2 subunit amino acid sequences. The conserved arginine residue at position 350 in human GlyR α2 subunit is boxed in red. **B.** Sample whole cell recordings for heteromeric α2β and $\alpha2^{R350L}\beta$ GlyRs in the presence of indicated glycine concentrations. **C.** Averaged whole cell glycine dose-response curves for α2, α2β, $\alpha2^{R350L}$ and $\alpha2^{R350L}\beta$ GlyRs. **D.** Summary of dose-response analysis data. $*p < 0.05$ relative to the corresponding homo- or heteromeric wild type GlyR via unpaired t test.

D

	α2β	α2	$\alpha2^{R350L}\beta$	$\alpha2^{R350L}$
EC_{50} (μM)	90.3 ± 14.6	46.6 ± 6.7	143.0 ± 12.9*	67.9 ± 13.4
Hill slope	2.1 ± 0.1	2.2 ± 0.1	2.0 ± 0.3	2.1 ± 0.2
I_{max} (nA)	2.1 ± 0.3	1.6 ± 0.2	1.7 ± 0.2	1.5 ± 0.4
n	11	12	13	9

Effects of the ASD-causing $\alpha2^{R350L}$ mutation on intrinsic channel gating

The peak glycine concentrations in the synaptic cleft are thought to reach 1 − 3 mM in embryonic zebrafish neurons (Legendre, 1998) and 2.2 − 3.5 mM in adult rat spinal neurons (Beato, 2008).

The clearance of the glycine away from the cleft was estimated on a 0.6 − 0.9 ms time scale (Beato, 2008). Based on these parameters, we examined intrinsic channel properties by rapidly applying saturating glycine (3 mM) for a period of ~1 ms to excised outside-out HEK cell patches expressing the wild-type and $\alpha2^{R323L}\beta$ receptors. Sample macroscopic currents are shown in Fig. 2A. The time course of desensitisation was fitted by a double exponential function with a mean time constant value of 61.8 ± 7.9 ms (n = 15) for wild-type and a mean time constant value of 88.0 ± 9.3 ms (n = 17) for $\alpha2^{R323L}\beta$ (Fig. 2B). The deactivation time constant in the $\alpha2^{R323L}\beta$ receptors was ~1.5-fold slower compared to wild-type receptors ($p < 0.05$), but the rise time did not differ from the wild-type receptors (α2β, 1.3 ± 0.1 ms; $\alpha2^{R323L}\beta$, 1.4 ± 0.2 ms; $p > 0.05$), indicating that the R350L mutation in M3-M4 loop altered intrinsic channel properties by significantly slowing channel closing rate.

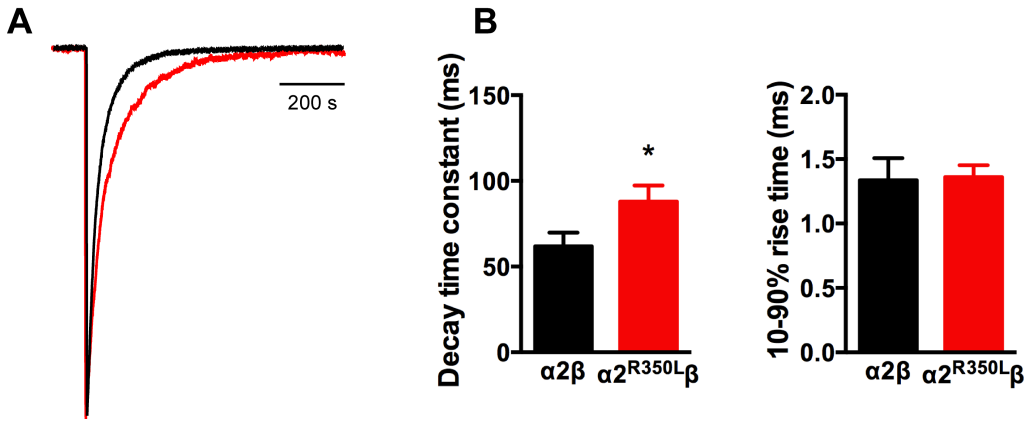

Fig. 2. Glycine-evoked $\alpha2^{R350L}\beta$ currents had slower intrinsic kinetic properties, compared to wild-type currents. **A.** Averaged macropatch currents recorded from outside-out patches containing the α2β (black trace) and $\alpha2^{R350L}\beta$ (red trace) GlyRs. The currents were activated by brief (~1 ms) exposure to saturating (3 mM) glycine. To allow comparison the kinetic properties, the currents were normalized to the same peak amplitude. **B.** Comparison of mean macropatch currents decay time constant and 10-90% rise time. *$p < 0.05$ relative to α2β GlyRs via unpaired t test.

Effects of the ASD-causing $\alpha2^{R350L}$ mutation on glycinergic IPSC kinetics

To test whether the impairment of GlyR channel function altered glycinergic transmission, we used an 'artificial' synapse system that allows control over the subunit composition of GlyRs in glycinergic synapses (Zhang et al., 2015). We inserted wild-type and mutant α2β GlyRs in turn into these synapses to evaluate the properties of the IPSCs mediated by $\alpha2^{R323L}\beta$ receptors. Sample IPSC recordings from artificial synapses incorporating wild-type and $\alpha2^{R323L}\beta$ isoforms are shown at two different temporal resolutions in Fig. 3A with a globally averaged normalised averaged normalised IPSC presented in in colour on the right. Mean IPSC amplitudes, decay time constants and rise times are shown in Fig. 3B. The averaged IPSC amplitudes, 10 – 90% rise times and decay time constants for wild-type and mutant receptors are presented in Fig. 3C. We observed that IPSCs

mediated by α2^{R323L}β receptors display 2-fold slower rise and decay time than those mediated by wild-type GlyRs (10-90% rise time: α2β, 2.6 ± 0.3 ms, n = 7; α2^{R323L}β, 4.9 ± 0.8 ms, n = 6, p < 0.01; decay time: α2β, 27.0 ± 1.5 ms; α2^{R323L}β, 60.8 ± 4.9 ms, p < 0.0001), while the mean IPSC amplitude did not differ significantly (α2β, 32.8 ± 2.5 pA; α2^{R323L}β, 34.0 ± 11.9 pA; p >0.05). As the change in IPSC decay rates corresponds well with the fast application data presented in Fig. 2, we infer that the slower decay of IPSCs is dominated by the slowed intrinsic channel deactivation rates.

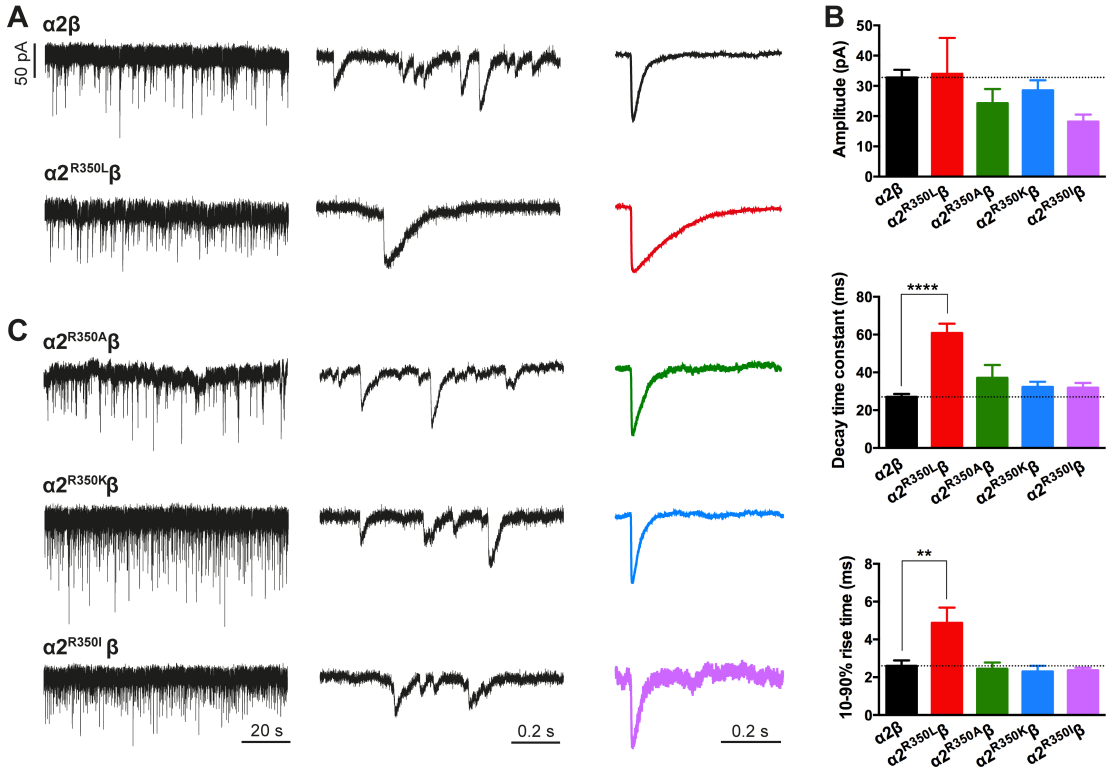

Fig. 3. Leucine substitution at Arg-350 position is indeed responsible for the prolonged IPSCs. **A**. Representative recordings of glycinergic IPSCs in HEK293 cells expressing the α2β and α2^{R350L}β GlyRs at different temporal resolutions. Averaged, normalized IPSCs each averaged from > 50 events from the corresponding cell are shown in the right panel (color traces). **B.** Comparison of mean IPSC amplitude, decay time constant and 10 − 90% rise time for the indicated GlyRs. **C**. Representative recordings of glycinergic IPSCs in HEK293 cells expressing the α2^{R350A}β, α2^{R350K}β and α2^{R350I}β GlyRs at different temporal resolutions. Recordings were performed at −60 mV. Statistical significance was determined via one-way ANOVA followed by Bonferroni's post-hoc correction with significance represented by **p < 0.01 and ****p < 0.0001 relative to α2β GlyRs.

The side chain of leucine dominates the time-course of glycinergic IPSCs

The TM3-TM4 inctracellular loop is the region of lowest amino acid sequence identity among different pLGIC subunits, but the Arg-350 residue is highly conserved in all α-subunits of the human GlyRs and *GLRA2* across a wide range of vertebrates (Fig. 1A). The disturbance of glycinergic transmission is caused by the substitution of a positively charged arginine residue for an

uncharged leucine residue. We next sought to investigate whether the side chain charge or the steric characteristics of the residue contributes directly to the normal function or dysfunction of glycinergic signaling. The arginine residue was first mutated to alanine (R350A), whose side chain only contains a methyl group and is absent of both bulk and charge. We also investigated the lysine substitution, which retains the arginine's positive charge but has a slightly reduced volume, and isoleucine, which retains the hydrophobicity of leucine. We then characterized the effects each mutation on the kinetics of IPSCs. Fig. 3C shows sample recordings from artificial synapses incorporating three mutated constructs, and averaged normalised IPSCs are presented in the right panel. Interestingly, the R350A, R350K and R350I mutations all produce IPSCs that have kinetics similar to those of the wild-type receptors (Table 1). This suggests that loss of either the bulky side chain or the positive charge at position 350 are not responsible for the effects of the R350L mutation on IPSC time course.

Table 1. Comparison of 10 – 90 % rise times and decay time constants of IPSCs and macropatch currents mediated by the indicated wild type and mutant GlyRs.

		$\alpha2\beta$	$\alpha2^{R350L}\beta$	$\alpha2^{R350A}\beta$	$\alpha2^{R350K}\beta$	$\alpha2^{R350I}\beta$
10-90% rise time (ms)	IPSCs	2.6 ± 0.3 (n = 7)	4.9 ± 0.8** (6)	2.5 ± 0.3 (4)	2.3 ± 0.3 (7)	2.4 ± 0.1 (5)
	macropatch currents	1.3 ± 0.2 (15)	1.4 ± 0.1 (17)			
deactivation time constant (ms)	IPSCs	27.0 ± 1.5	60.8 ± 4.9****	37.1 ± 6.8	32.3 ± 2.8	32.0 ± 2.5
	macropatch currents	61.8 ± 7.9	88.0 ± 9.3*			

*$p < 0.05$, **$p < 0.01$ and ****$p < 0.0001$ relative to the wild type α1β GlyR, unpaired *t*-test for comparisons between two groups and one-way ANOVA followed by Bonferroni's post-hoc correction for multiple comparisons. For IPSCs, the n values refer to the total number of cells from which data were collected. For each cell, parameters were analyzed from a single IPSC waveform that was digitally averaged from > 50 individual events.

4. Discussion

In this study we have characterized a new ASD-causing mutation R350L located in the ILD of GlyR α2 subunit, and used a combination of rapid glycine application and artificial synapse recordings to investigate the intrinsic channel kinetic and IPSC kinetic properties of $\alpha2^{R350L}\beta$ GlyRs. We have shown that the R350L mutation reduced the glycine sensitivity, but led to dramatic decreases in channel closing rate and IPSC decay rate. These findings provide new evidence that

intracellular regions of the GlyRs also contribute to determining agonist action, channel conductance, intrinsic channel gating and IPSC kinetics.

In contrast to the extracellular and membrane spanning domains, the TM3-TM4 loop of intracellular domain has lowest conservation in amino acid sequence and length across either the wide range of pLGIC family members or different subunits of the same receptors. Residues in the TM3-TM4 loop domain have been shown to contribute to the ion permeation pathway in some closely related pLGIC family members. Modifications of ILD length of human recombinant α3 GlyRs resulted in drastic changes in current responses while surface protein expression levels were unaltered (Breitinger et al., 2009). Truncation of ILD in $GABA_AR$ α1 subunits maintained their functionality, but remarkably altered both channel conductance and agonist apparent affinity (O'Toole and Jenkins, 2011), suggesting the ILD plays an important role in receptor activation. However, replacement of $5HT_3R$, GABAρ1R or α1 GlyR subunit sequence with a shorter TM3-TM4 linker displayed channel properties similar to those of wild-type channel (Jansen et al., 2008; Moroni et al., 2011; Papke and Grosman, 2014), implying that the functional significance of ILD may depend on the pLGIC member. The effects of mutations to the ILD on single channel conductance have been examined in GlyRs. Mutation of eight positively charged residues within the α1 GlyR ILD to negatively charged residues simultaneously gave rise to a non-functional channel. Inverting the charge at the Arg-377, Lys-378, Lys-385 and Lys-386 position had the greatest reduction in the channel conductance (Carland et al., 2009). An earlier study reported that disruptions to membrane insertion and transport from endoplasmic reticulum occurred when a cluster of positively charged residues in GlyR α1 ILD, ^{316}RFRRKRR (Arg-316 in α1 subunit corresponding to Arg-350 in α2 subunit) was neutralized causing an aberrantly folded TM3-TM4 loop (Sadtler et al., 2003).

Substitution of Arg-350, which is conserved in all α-subunits of the human GlyRs and in GlyR subunits across species, to leucine in *GLRA2* dramatically slowed down the IPSC time course. This provided a strong rationale to investigate its functional importance. We chose to assess the relative significance of the side-chains from the arginine and leucine residues by mutating arginine to alanine, lysine and isoleucine, and measuring the direct effects on heterosynaptic IPSCs. Substitution of positively charged arginine for the neutralized and smaller amino acid alanine (R350A) exhibits wild-type IPSC kinetics, suggests that the positive charge or steric properties of the residue at position 350 of α2 GlyR are not major determinants of synaptic current kinetics. Positive charge substitutions at Arg-350 (R350K) likewise preserved wild-type IPSC characteristics. α-amino groups are not critical to achieve longer IPSC duration, as suggested by the

functional equivalence of leucine residue at this position (R350I). This indicates that electrostatic properties of Arg-350 have no significant impact on glycinergic IPSCs. Altogether, our findings demonstrated that both charges and structural modifications at Arg-350 position are not the critical elements responsible for prolonged IPSCs. We suggest that the R350L may either specifically generate or disrupt an interaction with some cytoplasmic factor essential for normal GlyR function.

Variations in *GLRA1* and *GLRB* genes have been associated with hyperekplexia, which is a rare neurological disorder characterized by neonatal hypertonia and an exaggerated startle reflex in response to sudden, unexpected stimuli (Bode and Lynch, 2014). Hyperekplexia is generally considered to be associated with a loss of glycinergic inhibitory tone. Both *GLRA1* loss- and gain-of-function hyperekplexia mutations have been identified in patients with identical phenotypes. For *GLRA2* linked with autism, some examples of microdeletion such as $GLRA2^{\Delta ex8-9}$ that results in loss of transmembrane domains TM3 and TM4, and missense mutations such as N136S and R153Q have been reported (Pilorge et al., 2015). The previous reports show that deleted and mutated channels have loss-of-function defects with disrupted surface expression or dramatically decreased agonist sensitivity (Pilorge et al., 2015). We observed that R350L increased the IPSC time course, whereas no significant effect on the amplitude of IPSCs was observed. These findings suggested R350L mutation is a gain-of-function mutation.

During embryogenesis, α2 GlyRs are functionally expressed in the cerebral cortex (Young-Pearse et al., 2006) where they were suggested to play a critical function in early development of neocortex. Deletion of *GLYA2* gene in mice results in moderate microcephaly in newborn mice (Avila et al., 2014). Moreover, activation of GlyRs promotes tangential migration of cortical interneurons from the medial ganglionic eminence to the cerebral cortex in the developing brain, whereas genetic disruption or pharmacological inhibition of α2 GlyR expression and function impaired the interneuron migration abilities (Avila et al., 2013). After birth, dendrite and spine morphological abnormalities accompanied by the loss of glycinergic signaling were observed in cortical neuron of layer V in *GLYA2* knockout mice, supporting the idea that α2 GlyRs also play an important role in synaptogenesis (Morelli et al., 2016). It is not surprising that mutations affecting *GLYA2* gene, which contribute to the generation and migration of cerebral cortical neurons, may cause severe brain malfunctions leading to the symptoms observed in individuals with ASDs.

Here, we show that R350L mutation identified from ASD patients have major defects in glycinergic inhibitory synaptic transmission arising from altered intrinsic channel gating. Future work to further

investigate the link between R350L mutation and autism could involve studying the morphological and functional changes in cortical neurons.

References

Akagi H, Hirai K, Hishinuma F (1991) Cloning of a glycine receptor subtype expressed in rat brain and spinal cord during a specific period of neuronal development. FEBS letters 281:160-166.

Avila A, Vidal PM, Dear TN, Harvey RJ, Rigo JM, Nguyen L (2013) Glycine receptor alpha2 subunit activation promotes cortical interneuron migration. Cell reports 4:738-750.

Avila A, Vidal PM, Tielens S, Morelli G, Laguesse S, Harvey RJ, Rigo JM, Nguyen L (2014) Glycine receptors control the generation of projection neurons in the developing cerebral cortex. Cell Death Differ 21:1696-1708.

Beato M (2008) The time course of transmitter at glycinergic synapses onto motoneurons. Journal of Neuroscience 28:7412-7425.

Bena F et al. (2013) Molecular and clinical characterization of 25 individuals with exonic deletions of NRXN1 and comprehensive review of the literature. Am J Med Genet B Neuropsychiatr Genet 162B:388-403.

Bode A, Lynch JW (2014) The impact of human hyperekplexia mutations on glycine receptor structure and function. Molecular brain 7:2.

Breitinger HG, Villmann C, Melzer N, Rennert J, Breitinger U, Schwarzinger S, Becker CM (2009) Novel regulatory site within the TM3-4 loop of human recombinant alpha3 glycine receptors determines channel gating and domain structure. The Journal of biological chemistry 284:28624-28633.

Bundey S, Hardy C, Vickers S, Kilpatrick MW, Corbett JA (1994) Duplication of the 15q11-13 region in a patient with autism, epilepsy and ataxia. Dev Med Child Neurol 36:736-742.

Burgos CF, Castro PA, Mariqueo T, Bunster M, Guzman L, Aguayo LG (2015) Evidence for alpha-helices in the large intracellular domain mediating modulation of the alpha1-glycine receptor by ethanol and Gbetagamma. J Pharmacol Exp Ther 352:148-155.

Carland JE, Cooper MA, Sugiharto S, Jeong HJ, Lewis TM, Barry PH, Peters JA, Lambert JJ, Moorhouse AJ (2009) Characterization of the effects of charged residues in the intracellular loop on ion permeation in alpha1 glycine receptor channels. The Journal of biological chemistry 284:2023-2030.

Del Pino I, Koch D, Schemm R, Qualmann B, Betz H, Paarmann I (2014) Proteomic analysis of glycine receptor beta subunit (GlyRbeta)-interacting proteins: evidence for syndapin I regulating synaptic glycine receptors. The Journal of biological chemistry 289:11396-11409.

Dixon C, Sah P, Lynch JW, Keramidas A (2014) GABAA receptor alpha and gamma subunits shape synaptic currents via different mechanisms. The Journal of biological chemistry 289:5399-5411.

Dixon CL, Zhang Y, Lynch JW (2015) Generation of Functional Inhibitory Synapses Incorporating Defined Combinations of GABA(A) or Glycine Receptor Subunits. Frontiers in molecular neuroscience 8:80.

Durisic N, Godin AG, Wever CM, Heyes CD, Lakadamyali M, Dent JA (2012) Stoichiometry of the human glycine receptor revealed by direct subunit counting. The Journal of neuroscience : the official journal of the Society for Neuroscience 32:12915-12920.

Flint AC, Liu X, Kriegstein AR (1998) Nonsynaptic glycine receptor activation during early neocortical development. Neuron 20:43-53.

Gauthier J et al. (2011) Truncating mutations in NRXN2 and NRXN1 in autism spectrum disorders and schizophrenia. Hum Genet 130:563-573.

Geschwind DH (2009) Advances in autism. Annu Rev Med 60:367-380.
Grudzinska J, Schemm R, Haeger S, Nicke A, Schmalzing G, Betz H, Laube B (2005) The beta subunit determines the ligand binding properties of synaptic glycine receptors. Neuron 45:727-739.
Han L, Talwar S, Wang Q, Shan Q, Lynch JW (2013) Phosphorylation of alpha3 glycine receptors induces a conformational change in the glycine-binding site. ACS chemical neuroscience 4:1361-1370.
Hogart A, Nagarajan RP, Patzel KA, Yasui DH, Lasalle JM (2007) 15q11-13 GABAA receptor genes are normally biallelically expressed in brain yet are subject to epigenetic dysregulation in autism-spectrum disorders. Human molecular genetics 16:691-703.
Jamain S, Quach H, Betancur C, Rastam M, Colineaux C, Gillberg IC, Soderstrom H, Giros B, Leboyer M, Gillberg C, Bourgeron T, Paris Autism Research International Sibpair S (2003) Mutations of the X-linked genes encoding neuroligins NLGN3 and NLGN4 are associated with autism. Nat Genet 34:27-29.
Jansen M, Bali M, Akabas MH (2008) Modular design of Cys-loop ligand-gated ion channels: functional 5-HT3 and GABA rho1 receptors lacking the large cytoplasmic M3M4 loop. J Gen Physiol 131:137-146.
Kim EY, Schrader N, Smolinsky B, Bedet C, Vannier C, Schwarz G, Schindelin H (2006) Deciphering the structural framework of glycine receptor anchoring by gephyrin. The EMBO journal 25:1385-1395.
Kim HG et al. (2008) Disruption of neurexin 1 associated with autism spectrum disorder. American journal of human genetics 82:199-207.
Laumonnier F, Bonnet-Brilhault F, Gomot M, Blanc R, David A, Moizard MP, Raynaud M, Ronce N, Lemonnier E, Calvas P, Laudier B, Chelly J, Fryns JP, Ropers HH, Hamel BC, Andres C, Barthelemy C, Moraine C, Briault S (2004) X-linked mental retardation and autism are associated with a mutation in the NLGN4 gene, a member of the neuroligin family. American journal of human genetics 74:552-557.
Legendre P (1998) A reluctant gating mode of glycine receptor channels determines the time course of inhibitory miniature synaptic events in zebrafish hindbrain neurons. The Journal of neuroscience : the official journal of the Society for Neuroscience 18:2856-2870.
Lynch JW (2009) Native glycine receptor subtypes and their physiological roles. Neuropharmacology 56:303-309.
Malosio ML, Marqueze-Pouey B, Kuhse J, Betz H (1991) Widespread expression of glycine receptor subunit mRNAs in the adult and developing rat brain. The EMBO journal 10:2401-2409.
Maric HM, Kasaragod VB, Hausrat TJ, Kneussel M, Tretter V, Stromgaard K, Schindelin H (2014) Molecular basis of the alternative recruitment of GABA(A) versus glycine receptors through gephyrin. Nature communications 5:5767.
Melzer N, Villmann C, Becker K, Harvey K, Harvey RJ, Vogel N, Kluck CJ, Kneussel M, Becker CM (2010) Multifunctional basic motif in the glycine receptor intracellular domain induces subunit-specific sorting. The Journal of biological chemistry 285:3730-3739.
Morelli G, Avila A, Ravanidis S, Aourz N, Neve RL, Smolders I, Harvey RJ, Rigo JM, Nguyen L, Brone B (2016) Cerebral Cortical Circuitry Formation Requires Functional Glycine Receptors. Cerebral cortex.
Moroni M, Biro I, Giugliano M, Vijayan R, Biggin PC, Beato M, Sivilotti LG (2011) Chloride ions in the pore of glycine and GABA channels shape the time course and voltage dependence of agonist currents. The Journal of neuroscience : the official journal of the Society for Neuroscience 31:14095-14106.
O'Toole KK, Jenkins A (2011) Discrete M3-M4 intracellular loop subdomains control specific aspects of gamma-aminobutyric acid type A receptor function. The Journal of biological chemistry 286:37990-37999.

Papke D, Grosman C (2014) The role of intracellular linkers in gating and desensitization of human pentameric ligand-gated ion channels. The Journal of neuroscience : the official journal of the Society for Neuroscience 34:7238-7252.
Pilorge M et al. (2015) Genetic and functional analyses demonstrate a role for abnormal glycinergic signaling in autism. Molecular psychiatry.
Piton A et al. (2011) Systematic resequencing of X-chromosome synaptic genes in autism spectrum disorder and schizophrenia. Molecular psychiatry 16:867-880.
Sadtler S, Laube B, Lashub A, Nicke A, Betz H, Schmalzing G (2003) A basic cluster determines topology of the cytoplasmic M3-M4 loop of the glycine receptor alpha1 subunit. The Journal of biological chemistry 278:16782-16790.
Schroer RJ, Phelan MC, Michaelis RC, Crawford EC, Skinner SA, Cuccaro M, Simensen RJ, Bishop J, Skinner C, Fender D, Stevenson RE (1998) Autism and maternally derived aberrations of chromosome 15q. Am J Med Genet 76:327-336.
Sola M, Bavro VN, Timmins J, Franz T, Ricard-Blum S, Schoehn G, Ruigrok RW, Paarmann I, Saiyed T, O'Sullivan GA, Schmitt B, Betz H, Weissenhorn W (2004) Structural basis of dynamic glycine receptor clustering by gephyrin. The EMBO journal 23:2510-2519.
Takahashi T, Momiyama A, Hirai K, Hishinuma F, Akagi H (1992) Functional correlation of fetal and adult forms of glycine receptors with developmental changes in inhibitory synaptic receptor channels. Neuron 9:1155-1161.
Tarabeux J et al. (2011) Rare mutations in N-methyl-D-aspartate glutamate receptors in autism spectrum disorders and schizophrenia. Translational psychiatry 1:e55.
Uzunova G, Hollander E, Shepherd J (2014) The role of ionotropic glutamate receptors in childhood neurodevelopmental disorders: autism spectrum disorders and fragile x syndrome. Current neuropharmacology 12:71-98.
Watanabe E, Akagi H (1995) Distribution patterns of mRNAs encoding glycine receptor channels in the developing rat spinal cord. Neurosci Res 23:377-382.
Yan J, Oliveira G, Coutinho A, Yang C, Feng J, Katz C, Sram J, Bockholt A, Jones IR, Craddock N, Cook EH, Jr., Vicente A, Sommer SS (2005) Analysis of the neuroligin 3 and 4 genes in autism and other neuropsychiatric patients. Molecular psychiatry 10:329-332.
Yang Z, Taran E, Webb TI, Lynch JW (2012) Stoichiometry and subunit arrangement of alpha1beta glycine receptors as determined by atomic force microscopy. Biochemistry 51:5229-5231.
Young-Pearse TL, Ivic L, Kriegstein AR, Cepko CL (2006) Characterization of mice with targeted deletion of glycine receptor alpha 2. Mol Cell Biol 26:5728-5734.
Zhang Y, Dixon CL, Keramidas A, Lynch JW (2015) Functional reconstitution of glycinergic synapses incorporating defined glycine receptor subunit combinations. Neuropharmacology 89:391-397.

Chapter 5

Estimating the free zinc concentration in the glycinergic synaptic cleft

The free zinc concentration in the synaptic cleft of artificial glycinergic synapses reaches > 1 μM

Yan Zhang[1], Angelo Keramidas[1] and Joseph W. Lynch[1,2*]

[1] Queensland Brain Institute, The University of Queensland, Brisbane, QLD 4072, Australia

[2] School of Biomedical Sciences, The University of Queensland, Brisbane, QLD 4072, Australia

Correspondence to: Professor Joseph Lynch, Queensland Brain Institute, University of Queensland, Brisbane, QLD 4072, Australia. Phone: +617 33466375, Email: j.lynch@uq.edu.au

Running title: Zinc in the glycinergic synaptic cleft

Keywords: glycine receptor, chloride channel, zinc chelator, inhibitory synapse, tricine, ZX1

Abstract: Zn^{2+} is concentrated into presynaptic vesicles at many central synapses and is released into the synaptic cleft by nerve terminal stimulation. There is strong evidence that synaptically released Zn^{2+} modulates glutamatergic neurotransmission, although there is debate concerning the peak concentration it reaches in the synaptic cleft. Glycine receptors (GlyRs), which mediate inhibitory neurotransmission in the spinal cord and brainstem, are potentiated by low nanomolar Zn^{2+} and inhibited by micromolar Zn^{2+}. Mutations that ablate Zn^{2+} potentiation of GlyRs result in hyperekplexia phenotypes suggesting that Zn^{2+} physiologically modulates glycinergic neurotransmission. There is, however, little evidence that Zn^{2+} is stored presynaptically at glycinergic terminals and an alternate possibility is that GlyRs are modulated by constitutively bound Zn^{2+}. We sought to estimate the peak Zn^{2+} concentration in the glycinergic synaptic cleft as a means of evaluating whether it is likely to be synaptically released. We employed 'artificial' synapses because they permit the insertion of engineered α1β GlyRs with defined Zn^{2+} sensitivities into synapses. By comparing the effect of Zn^{2+} chelation on glycinergic IPSCs with the effects of defined Zn^{2+} and glycine concentrations applied rapidly to the same recombinant GlyRs in outside-out patches under simulated synaptic activation conditions, we inferred that synaptic Zn^{2+} rises to at least 1 μM following a single presynaptic stimulation. Moreover, using the fast high-affinity chelator, ZX1, we found no evidence for tonic Zn^{2+} bound constitutively to high affinity GlyR binding sites. We conclude that diffusible Zn^{2+} reaches 1 μM or higher and is therefore likely to be phasically released in artificial glycinergic synapses.

INTRODUCTION

The free ionic form of zinc (Zn^{2+}) is present in the extracellular CNS solution at low nM concentrations (Frederickson et al., 2006). We define this as 'tonic' Zn^{2+}. It is also concentrated into presynaptic vesicles at many brain glutamatergic synapses (Frederickson, 1989) and is released into the synaptic cleft by nerve terminal stimulation (Assaf and Chung, 1984; Howell et al., 1984). The GluN2A-containing NMDA receptor (NMDAR) cation channels that populate these synapses are inhibited by Zn^{2+} at low nM concentrations (Paoletti et al., 1997). Recent studies have found evidence for the transient modulation of synaptic NMDARs by phasically released Zn^{2+} (Vergnano et al., 2014; Anderson et al., 2015) and for the constitutive modulation of extrasynaptic NMDARs by tonic Zn^{2+} (Anderson et al., 2015). A major unresolved question concerns the concentration to which Zn^{2+} rises during synaptic activation, with estimates spanning four orders of magnitude from 10 nM (Kay, 2003) to > 100 μM (Vogt et al., 2000). It is important to resolve this because many neuronal membrane proteins are modulated by Zn^{2+} at high concentrations (Marger et al., 2014), and a knowledge of the peak Zn^{2+} concentration would permit the identification of potential physiological targets of synaptically-released Zn^{2+}.

It is also unclear whether tonic or synaptically-released Zn^{2+} modulates neurotransmission at other synapses. Glycine receptor (GlyR) chloride channels, which mediate inhibitory neurotransmission in the spinal cord and brainstem (Lynch, 2004), are a likely candidate for Zn^{2+} modulation for several reasons. First, the major synaptic α1β GlyR isoform is extremely sensitive to Zn^{2+}, with low (10 – 1000 nM) Zn^{2+} concentrations potentiating EC_{50} glycine-gated currents and higher Zn^{2+} concentrations (3 – 300 μM) eliciting a dose-dependent inhibition (Bloomenthal et al., 1994; Laube et al., 1995; Miller et al., 2005a; Miller et al., 2005b). Second, selectively ablating the sensitivity of α1 GlyRs to Zn^{2+} potentiation led to impaired glycinergic inhibition and a hyperekplexia-type phenotype in $\alpha1^{D80A}$ GlyR knock-in mice (Hirzel et al., 2006). Third, by eliminating free Zn^{2+} from the synaptic cleft via Zn^{2+} buffers and chelators, it has been shown that glycinergic inhibitory postsynaptic currents (IPSCs) are positively modulated by either tonic or synaptically-released Zn^{2+} (Suwa et al., 2001; Hirzel et al., 2006; Perez-Rosello et al., 2015). Fourth, there is strong evidence for the co-localization of Zn^{2+} and glycine at presynaptic terminals in the spinal cord of the lamprey (Birinyi et al., 2001) although the evidence for their co-localization at glycinergic presynaptic terminals in the mammalian spinal cord is less clear cut (Wang et al., 2001). However, to date there has been no investigation into the possibility that Zn^{2+} may be phasically released at glycinergic synapses.

Since glycine reaches a saturating concentration in the cleft during synaptic stimulation (Legendre, 1998; Beato, 2008), potentiating concentrations of Zn^{2+} cannot further increase the IPSC magnitude, and as a result Zn^{2+} potentiation is manifest as a slowing in the IPSC decay rate (Suwa et al., 2001; Laube, 2002; Hirzel et al., 2006; Eto et al., 2007). However, miniature IPSCs, which are mediated by the stochastic release of single glycine vesicles and thus involve sub-saturating glycine concentrations, are increased in magnitude by potentiating concentrations of Zn^{2+} (Suwa et al., 2001; Hirzel et al., 2006; Perez-Rosello et al., 2015).

We have recently developed an 'artificial' synapse system whereby glycinergic synapses are induced to form between presynaptic terminals of cultured spinal glycinergic interneurons and HEK293 cells expressing recombinant heteromeric GlyRs (Dixon et al., 2015; Zhang et al., 2015). This system has two main advantages over neuronal synapses. First, it allows control over the subunit composition of postsynaptic GlyRs. Second, the electrotonically compact shape of HEK293 cells avoids problems associated with dendritic filtering, allowing IPSC waveforms to be resolved with high fidelity. In the present study, we engineered the Zn^{2+} sensitivities of the recombinant GlyRs so that they could act as reporters of synaptic Zn^{2+} over different concentration ranges. By comparing the effect of Zn^{2+} chelation on IPSCs with the effects of buffered Zn^{2+} plus glycine concentrations applied rapidly to the same recombinant GlyRs to simulate synaptic activation, we sought to provide an estimate of the concentration to which Zn^{2+} rises in response to a single presynaptic stimulation. We also sought to determine whether Zn^{2+} inhibition is physiologically relevant.

MATERIALS AND METHODS

Molecular biology and HEK293 cell transfection

We employed plasmid DNAs encoding the human α1 (pCIS), rat α3L (pcDNA3.1) and human β (pcDNA3.1) GlyR subunits, plus mouse neuroligin 2A (pNice) and rat gephyrin P1 (pCIS). Empty pEGFP plasmid was also transfected as an expression marker. Site-directed mutagenesis was performed using the QuikChange mutagenesis kit (Agilent Technologies) according to manufacturers' instructions and the successful incorporation of mutations was confirmed by DNA sequencing. The plasmid DNAs were transfected into HEK293 cells via a calcium phosphate-DNA co-precipitation protocol. When expressing α1β GlyRs, we transfected the following DNA quantities into each 35 mm culture dish of HEK293 cells: 0.03 μg α1 GlyR, 1.5 μg β GlyR, 0.2 μg neuroligin 2A, 0.2 μg gephyrin, 0.1 μg EGFP. When expressing α3β GlyRs, we transfected the following DNA quantities into each 35 mm culture dish: 0.15 μg α3L GlyR, 1.5 μg β GlyR, 0.2 μg neuroligin 2A, 0.2 μg

gephyrin, 0.1 μg EGFP. We have previously validated that these transfection conditions result in a high level of expression of heteromeric α1β and α3β GlyRs, respectively (Zhang et al., 2015).

Artificial synapse formation

Details of this method have recently been published (Dixon et al., 2015; Zhang et al., 2015). Briefly, E15 timed-pregnant rats were euthanized via CO_2 inhalation in accordance with procedures approved by the University of Queensland Animal Ethics Committee (approval number: QBI/203/13/ARC). Embryos were surgically removed and placed into ice cold Ca^{2+}-Mg^{2+}-free Hank's Balanced Salt Solution under sterile conditions. The spinal cords were then dissected out and pinned at the wider proximal end while meninges were carefully detached. The dissected neurons were then triturated, centrifuged and resuspended in Dulbecco's Modified Eagles Medium supplemented with 10 % fetal bovine serum. The cells were then counted and between 40,000 - 80,000 neurons were plated onto each 12 mm poly-D-lysine-coated coverslip in 4-well plates. Neuronal cultures were always maintained in a 5 % CO_2 incubator at 37 ^{o}C. After incubation for 24 h the entire Dulbecco's Modified Eagles Medium supplemented plus 10 % fetal bovine serum medium was replaced with Neurobasal medium including 2 % B27 and 1 % GlutaMAX supplements. A second (and final) feed 1 wk later replaced half of this medium. Neurons were used in co-culture experiments 1 – 4 wk later. Heterosynaptic co-cultures were prepared by directly introducing transfected HEK293 cells onto the primary neuronal cultures 1 − 3 d prior to electrophysiological recording.

Electrophysiology

All experiments were performed at 20 – 22 ^{o}C at a holding potential of −60 mV. Whole-cell recordings were obtained with a HEKA EPC10 amplifier (HEKA Electronics, Lambrecht, Gremany) and Patchmaster software (HEKA), with currents filtered at 4 kHz and sampled at 10 kHz. Series resistance was compensated to 60% and monitored throughout the recording. Patch pipettes (4 - 8 MΩ) made from thick-walled borosilicate glass (GC150F-7.5, Harvard Apparatus) were filled with an internal solution comprising (in mM): 145 CsCl, 2 $CaCl_2$, 2 $MgCl_2$, 10 HEPES, 10 EGTA and 2 MgATP, pH 7.4 with NaOH. Cells were perfused with extracellular solution comprising (in mM): 140 NaCl, 5 KCl, 2 $CaCl_2$, 1 $MgCl_2$, 10 HEPES, and 10 D-glucose, pH 7.4 with NaOH.

For outside-out recordings, pipettes were fired-polished to a resistance of ~10 MΩ and filled with the same internal solution. Macroscopic currents in outside-out patches pulled from transfected HEK293 cells were activated by brief (< 1 ms) exposure to agonists using a piezoelectric translator (Siskiyou). Currents were recorded using a Multiclamp 700B amplifer and pClamp9 software (Molecular Devices), filtered at 4 kHz and sampled at 10 kHz.

In accordance with standard practice in the field, solutions containing buffered concentrations of free Zn^{2+} were made by adding 10, 100, 500 and 1000 μM free Zn^{2+} to the standard extracellular solution + 10 mM tricine (Sigma-Aldrich) to produce buffered Zn^{2+} concentrations of 0.1, 1, 5 and 10 μM, respectively (Paoletti et al., 1997; Low et al., 2000; Miller et al., 2005b; Vergnano et al., 2014). The added Zn^{2+} concentration was aliquoted from a 10 mM aqueous $ZnCl_2$ stock solution on the day of the experiment. ZX1 (Strem Chemicals) was dissolved as a 100 mM stock in water and added to the control solution on the day of the experiment.

Data Analysis

Analyses of IPSC amplitudes, 10−90% rise times and decay time constants were performed using Axograph X (Axograph Scientific). Single peak IPSCs with amplitudes of at least three times the background noise were detected using a semi-automated sliding template. Events were visually inspected and only well-separated IPSCs with no inflections in the rising or decay phases were included. Current decay phases were fitted with double-exponential functions and a weighted time constant was calculated from individual time constants (τ1, τ2) and their relative amplitudes (A1, A2) as follows: $\tau_{weighted} = (\tau1 \times A1 + \tau2 \times A2)/(A1+A2)$. Statistical comparisons were performed using non-parametric tests in Prism 6 (GraphPad Software Inc.). For multiple comparisons we used the Friedman test or the Wilcoxon matched-pairs signed rank test and for single comparisons we used the Mann-Whitney U test. In all tests we took $p < 0.05$ to be statistically significant.

RESULTS

Zn^{2+}-sensitivity of IPSCs mediated by α1β, $\alpha1^{H107N}\beta$ and $\alpha1^{W170S}\beta$ GlyRs

The α1β GlyR is the main synaptic isoform (Lynch, 2009). Zn^{2+} potentiates EC_{50} glycine-gated currents in recombinant α1β GlyRs with an EC_{50} near 40 nM (Miller et al., 2005b) and inhibits with an IC_{50} near 13 μM (Miller et al., 2005a). We also investigated the $\alpha1^{H107N}\beta$ and the $\alpha1^{W170S}\beta$ GlyRs. The H107N mutation eliminates Zn^{2+} inhibition and increases the Zn^{2+} potentiation EC_{50} to 0.8 μM (Miller et al., 2005b). We reasoned that this receptor should respond only to high nanomolar or micromolar concentrations of Zn^{2+}. The W170S mutation, which occurs naturally in a sporadic case of human hyperekplexia (Al-Futaisi et al., 2012), eliminates Zn^{2+} potentiation but leaves Zn^{2+} inhibition intact with an IC_{50} near 5 μM (Zhou et al., 2013). We employed this mutant as both a negative control for the potentiating effect of Zn^{2+} and to determine whether Zn^{2+} inhibition (when isolated from potentiation) is capable of affecting IPSC parameters.

In order to precisely control the extracellular Zn^{2+} concentration, we buffered it with 10 mM tricine as described in Materials and Methods. We also applied 10 mM tricine with no added Zn^{2+} to buffer the free Zn^{2+} concentration to virtually zero, although as recently demonstrated, this may not remove tonic Zn^{2+} that is bound strongly to low nanomolar affinity Zn^{2+} binding sites (Anderson et al., 2015). Thus, our starting hypothesis is that 10 mM tricine ablates freely diffusing Zn^{2+} but not constitutively bound Zn^{2+}.

Sample recordings of spontaneous IPSCs from HEK293 cells expressing each of these constructs are shown in Figure 1A. As IPSCs were almost entirely abolished by 1 μM tetrodotoxin (not shown), we infer they were induced by spontaneous action potentials. The remaining miniature IPSCS were too small to analyse. Figure 1A (left) shows sample recordings of spontaneous IPSCs recorded from single cells expressing either the α1β GlyR (top), the $\alpha1^{H107N}\beta$ GlyR (middle) or the $\alpha1^{W170S}\beta$ GlyR (bottom). The left panels show control recordings in tricine-free extracellular solution, the centre panels show the effect of 10 mM tricine and the right panels show the effect of adding 5 μM free Zn^{2+}. Individual IPSCs from the recordings in A were normalised and digitally averaged to produce the global mean IPSC waveforms as displayed in Figure 1B. The mean IPSC amplitudes, decay time constants and 10 – 90 % rise times for each construct recorded in tricine-free extracellular solution are presented in Figure 1C. We found that IPSCs mediated by $\alpha1^{W170S}\beta$ GlyRs exhibited significantly larger amplitudes, longer decay time constants and slower rise times relative to those mediated by α1β GlyRs. This indicates that the W170S mutation affects intrinsic receptor gating or synaptic clustering properties in addition to ablating Zn^{2+} potentiation.

Figure 1D-F summarises the effects of adding either 10 mM tricine alone or 5 μM free Zn^{2+} to IPSCs mediated by the three constructs. We observed no effect 10 mM tricine on the IPSC amplitude mediated by any construct (Figure 1D). However, the removal of free Zn^{2+} significantly accelerated the decay rate of α1β GlyRs (Figure 1E) indicating that the free Zn^{2+} concentration is high enough to positively modulate these receptors. In contrast, 10 mM tricine had no effect on the IPSC decay rate mediated by $\alpha1^{W170S}\beta$ GlyRs. This not only provides a control for the GlyR-specificity of the Zn^{2+} potentiating effect, but also indicates that the low affinity inhibitory effect of Zn^{2+} does not appreciably affect IPSC parameters. All these findings are reinforced by the converse experiment whereby increasing free Zn^{2+} to 5 μM significantly slowed the decay rate in α1β GlyRs and $\alpha1^{H107N}\beta$ GlyRs but had no effect on $\alpha1^{W170S}\beta$ GlyRs (Figure 1E). The removal free Zn^{2+} also accelerated the rise times of IPSCs mediated by α1β GlyRs only (Figure 1F).

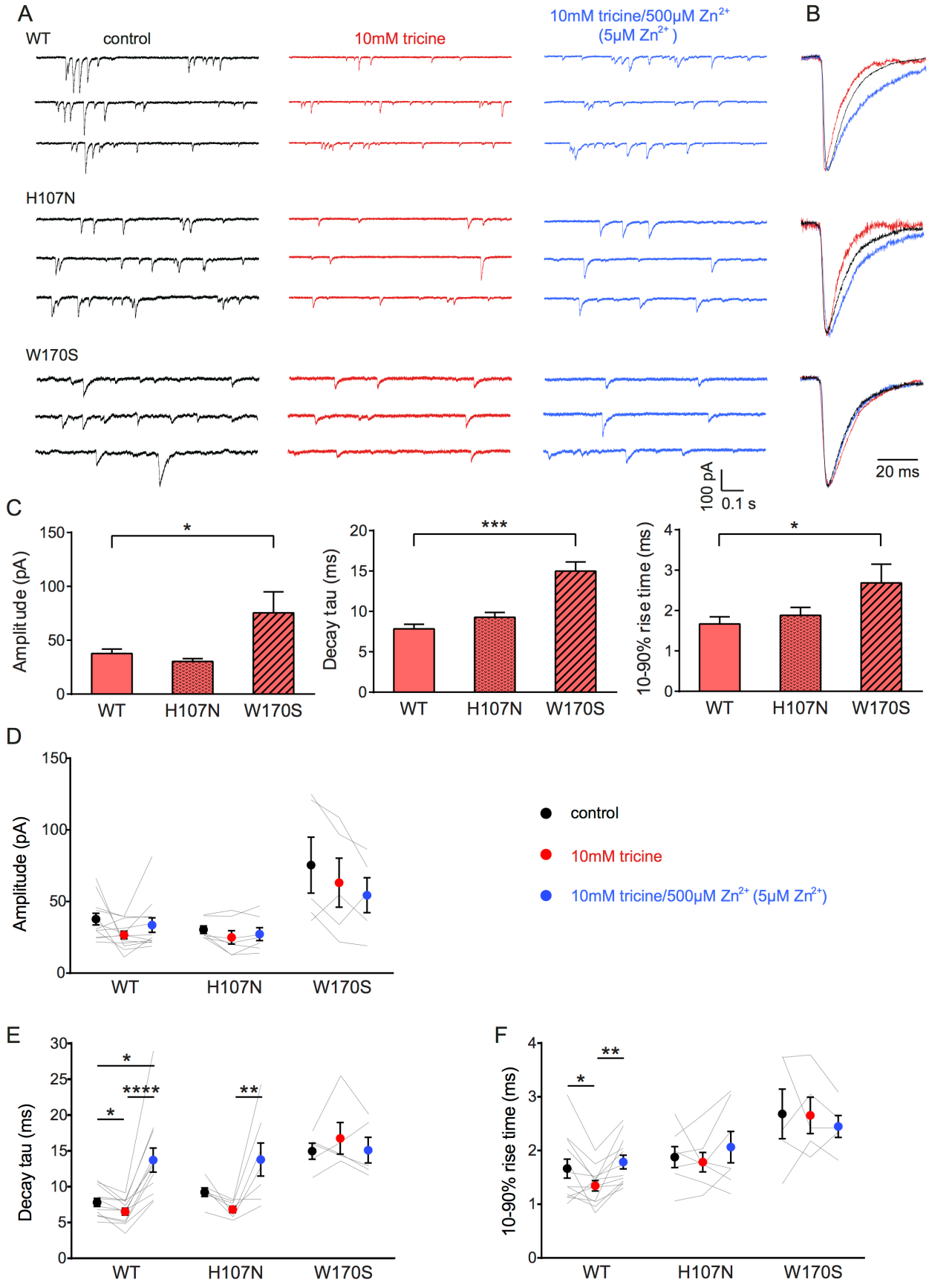

Figure 1. Effects of synaptic Zn^{2+} on spontaneous IPSCs mediated by α1β, $\alpha1^{H107N}\beta$ and $\alpha1^{W170S}\beta$ GlyRs. **(A)** Representative recordings of IPSCs mediated by the indicated constructs are shown in the presence of tricine-free solution

(black traces), 10 mM added tricine (red traces) and 10 mM added tricine + 500 μM added Zn^{2+} (= 5 μM free Zn^{2+}: blue traces). **(B)** Superimposed, digitally averaged, normalized IPSCs from the corresponding cell in **(A)**. The total number of events included in each averaged IPSC was as follows: α1β GlyR (control: 86; 10mM added tricine: 63; 10 mM added tricine + 500 μM added Zn^{2+}: 92), $\alpha1^{H107N}\beta$ GlyR (control: 72; 10mM added tricine: 56; 10 mM added tricine + 500 μM added Zn^{2+}: 89), $\alpha1^{W170S}\beta$ GlyR (control: 53; 10mM added tricine: 61; 10 mM added tricine + 500 μM added Zn^{2+}: 68). **(C)** Comparison of mean IPSC amplitude, decay time constant and 10 – 90 % rise time for the three constructs in tricine-free solution. Statistical significance was determined by Mann-Whitney U test. The distributions in WT and W170S values differed significantly for amplitude (U = 11, $*p < 0.05$), decay time constant (U = 0, $***p < 0.001$) and 10 – 90 % rise time (U = 10, $*p < 0.05$). **(D)** Comparison of the effects of the indicated solutions on IPSC amplitude, decay time constant and 10 – 90 % rise time for the three constructs. Comparisons between the constructs are not shown. Statistical significance was determined by Friedman test with significance represented by $*p < 0.05$, $**p < 0.01$, $***p < 0.001$, $****p < 0.0001$. Relative to their values in 10 mM tricine, the decay time constants for α1β and $\alpha1^{H107N}\beta$ GlyRs increased by 74 ± 13 % and 50 ± 24 %, respectively, in standard extracellular solution and by 109 ± 15 % and 101 ± 28 %, respectively, in 5 μM free Zn^{2+}. In panels **(C)** and **(D)**, we analyzed 12 cells expressing α1β GlyRs, 7 cells expressing $\alpha1^{H107N}\beta$ GlyRs and 5 cells expressing $\alpha1^{W170S}\beta$ GlyRs.

Zn^{2+}-sensitivity of IPSCs mediated by α3β GlyRs

In an attempt to generalize our findings, we investigated the Zn^{2+}-sensitivity of the other major adult synaptic GlyR isoform, the α3β, which mediates synaptic inhibition onto nociceptive neurons in superficial laminae of the adult spinal cord dorsal horn (Zeilhofer et al., 2012). Despite their importance in pain signal processing mechanisms and their relevance as novel therapeutic targets for inflammatory pain (Lynch, 2009; Zeilhofer et al., 2012), the Zn^{2+} sensitivity of α3β GlyRs has never been investigated. We thus repeated the experiment of Figure 1A on spontaneous IPSCs mediated by α3β GlyRs. Examples of normalized, averaged IPSCs recorded from one cell exposed sequentially to standard extracellular solution containing no tricine, 10 mM tricine or 10 mM tricine plus 5 μM free Zn^{2+} are shown in Figure 2A, with averaged results summarized in Figure 2B – D. According to the non-parametric Friedman test, these data reveal that the removal of free Zn^{2+} by 10 mM tricine had no significant effect on any IPSC parameter. However, as all data distributions in Figure 2B satisfied the D'Agostino-Pearson omnibus test for normality (using $p < 0.05$ as cutoff), we performed a repeated measures one-way ANOVA on decay time constants of the control versus 10 mM tricine and 10 mM tricine plus 5 μM free Zn^{2+} experimental conditions. As 10 mM tricine significantly accelerated the IPSC decay rate according to this test ($p < 0.05$, n = 8), we conclude that the endogenous levels of Zn^{2+} in artificial synapses significantly prolong the decay time constant of α3β GlyR-mediated IPSCs.

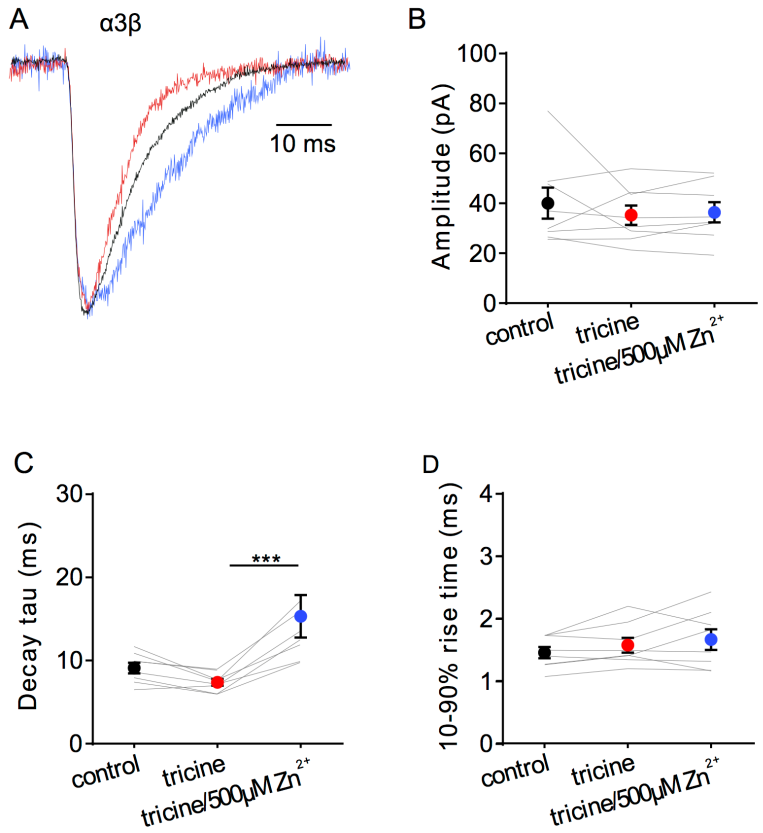

Figure 2. Effects of synaptic Zn^{2+} on IPSCs mediated by α3β GlyRs. **(A)** Superimposed averaged, normalized IPSCs each averaged from > 50 events from the same cell. Recordings were made in the presence of tricine-free solution (black trace; averaged from 52 events), 10 mM added tricine (red trace; averaged from 55 events) and 10 mM added tricine + 500 µM added Zn^{2+} (= 5 µM free Zn^{2+}: blue trace; averaged from 83 events). **(B – D)** Comparison of the effects of the indicated solutions on IPSC amplitude, decay time constant and 10 – 90 % rise time for α3β-mediated IPSCs. All results were averaged from 8 cells. Statistical significance was determined by Friedman test with significance represented by ***$p < 0.001$.

Calibrating the Zn^{2+}-sensitivity of α1β, α1^{H107N}β and α1^{W170S}β GlyRs under simulated synaptic activation conditions

The α1β GlyR Zn^{2+} EC_{50} and IC_{50} values cited above were obtained under steady-state applications of Zn^{2+} and EC_{50} glycine (Miller et al., 2005a; Miller et al., 2005b). As these conditions do not apply to the synapse, we calibrated the Zn^{2+} sensitivity of the GlyR constructs using fast solution exchange to mimic synaptic activation conditions. The glycine concentration in the synaptic cleft has been estimated to reach a peak of 1 – 3 mM in embryonic zebrafish hindbrain neurons (Legendre, 1998) and 2.2 – 3.5 mM in adult rat spinal motor neurons (Beato, 2008). Glycine is cleared from the cleft with a time constant of 0.6 – 0.9 ms (Beato, 2008). Considering these parameters, we simulated synaptic activation conditions by applying 1 mM glycine with or without free Zn^{2+} for 0.5 – 1 ms to outside-out macropatches expressing the GlyR isoform of interest. To calibrate and optimize the solution application system, we rapidly switched the solution perfusing an open patch pipette between standard extracellular solution and an extracellular solution that had been diluted by 50 % with distilled water. Figure 3A shows an example of an open pipette response, indicating the typical solution exposure profile. We performed this control regularly to ensure that the solution switching rate remained constant within and between experiments.

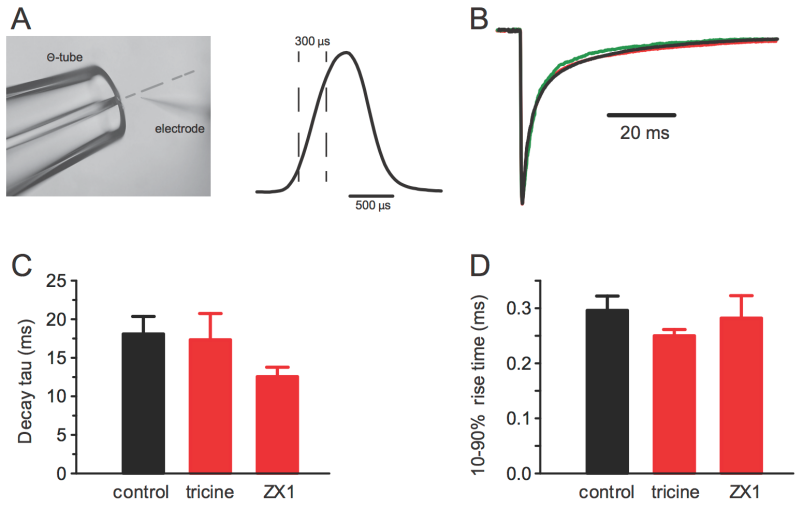

Figure 3. Control experiments employing rapid solution exchange over macropatches expressing α1β GlyRs. **(A)** (*Left*) Image of the double-barrelled θ-tube used to perform the rapid solution exchange experiments on macropatches. The image also shows an open recording pipette and the position of the solution interface (broken line). (*Right*) Open pipette response obtained by switching the solution over the electrode tip from the standard extracellular solution to one diluted to 10% with water. The rise and decay times are approximately 300 µs. **(B)** Overlayed macropatch recordings (averages of 6 – 20 sweeps) of control (black, 1 mM glycine) and co-application of 1 mM glycine with either 10 mM tricine (red) or 100 µM ZX1 (green). **(C)** Summary bar plots of the weighted decay time constant for control and the two Zn^{2+} chelators. **(D)** Summary bar plots of the rise times for control and the two Zn^{2+} chelators. Mann Whitney U test revealed no significant differences in the distributions of either the decay or rise times, $p > 0.05$ for both, n = 3 – 8 macropatches for each condition.

Contaminating Zn^{2+} released into solution from plastic and glass laboratory ware is thought to reach concentrations as high as 100 nM (Kay, 2004), which is high enough to modulate steady-state GlyR currents activated by low glycine concentrations (Miller et al., 2005b; Cornelison and Mihic, 2014). We determined whether Zn^{2+} contamination might have contributed to the results of Figures 1 and 2 via two sets of control experiments. The first involved switching rapidly between a control (putatively Zn^{2+}-contaminated) solution and a Zn^{2+}-chelating solution. In this experiment the control and test solutions both comprised our standard extracellular solution plus 1 mM glycine, although the test solution also contained either 10 mM tricine or 100 µM ZX1 (Perez-Rosello et al., 2015). A sample recording from a single macropatch containing α1β GlyRs suggests the chelators had little effect on decay rate (Figure 3B) and the averaged result confirms the lack of a significant effect on either the decay or rise times (Figure 3C, D). It is evident, however, that ZX1 showed a tendency to decrease the decay time constant that may become significant with a larger number of observations. If so, this effect could be due to either (1) a direct allosteric inhibitory effect on the GlyR or (2) the removal of tonically-bound Zn^{2+} from the GlyR. The second possibility will be investigated below.

In a second control experiment, we initially exposed macropatches to a buffered 100 nM Zn^{2+} solution and switched this rapidly to either a control (putatively Zn^{2+}-contaminated) solution (n = 10 macropatches) or to a Zn^{2+}-chelating solution (i.e., control + 10 mM tricine, n = 3 macropatches). Again, no significant differences in rise times or decay rates were observed in either experiment ($p >$

0.05 by Mann-Whitney U test). Together, these results strongly suggest that contaminating Zn^{2+} in our extracellular solution had no significant effect on IPSC rise or decay rates.

To mimic synaptic activation, we employed standard extracellular solution without added tricine as the control solution to replicate the conditions employed in Figures 1 and 2. Test solutions had the same composition except that we added 1 mM glycine either alone or together with 10 mM tricine and 100 nM, 1 μM or 10 μM free Zn^{2+}. Examples of current responses to the sequential application of each of these four solutions to α1β, $\alpha1^{H107N}\beta$ and $\alpha1^{W170S}\beta$ GlyRs are shown in Figure 4A, with averaged weighted deactivation time constants shown in Figure 4B. The averaged individual time constants (τ1, τ2) and their relative amplitudes (A1, A2) for each experimental condition are presented in Table 1. For the α1β GlyR, we observed no change in the deactivation rate or 10 – 90 % rise time at 100 nM Zn^{2+}. We observed a statistically significant slowing in the deactivation rate at 1 μM and a dramatic slowing in deactivation rate at 10 μM free Zn^{2+}. We also observed a statistically significant slowing in the deactivation rate at 10 μM free Zn^{2+}at the $\alpha1^{H107N}\beta$ GlyR. At 10 μM Zn^{2+}, the percentage increase in the macropatch current deactivation time constant at both receptors (α1β: 76 ± 41 %; $\alpha1^{H107N}\beta$: 76 ± 19 %) was comparable to the magnitude of the IPSC decay time constant increase from 10 mM tricine-containing to standard extracellular solution (α1β: 74±13 %, $\alpha1^{H107N}\beta$: 50 ± 24 %). In contrast, at the $\alpha1^{W170S}\beta$ GlyR we observed no change in IPSC magnitude, decay rate or rise time at free Zn^{2+} concentrations up to 10 μM (Figure 4A – C). Together, these results suggest that the free synaptic Zn^{2+} concentration reaches a concentration of at least 1 μM following a single synaptic stimulation. The lack of an inhibitory effect of 10 μM Zn^{2+} on $\alpha1^{W170S}\beta$ GlyRs is most likely due to the slow onset of Zn^{2+} inhibition and the brief exposure time to Zn^{2+} in our experiments.

We next considered the possibility that the magnitude of the Zn^{2+} effect may depend on the synaptic glycine concentration. We therefore repeated the experiment of Figure 4A at α1β GlyRs using 3 mM glycine, in line with the maximum predicted synaptic glycine concentration (Legendre, 1998; Beato, 2008). Sample recordings reveal that 10 μM Zn^{2+} exerts a diminished prolonging effect on deactivation rate of currents activated by brief applications of 3 mM glycine (Figure 4C). This trend is supported by the averaged data shown in Figure 4D. Thus, if the concentration of glycine in the synaptic cleft is 3 mM or higher, our results imply that Zn^{2+} must rise to concentrations greater than 10 μM during synaptic transmission to account for the effect of 10 mM tricine on the IPSC decay rate.

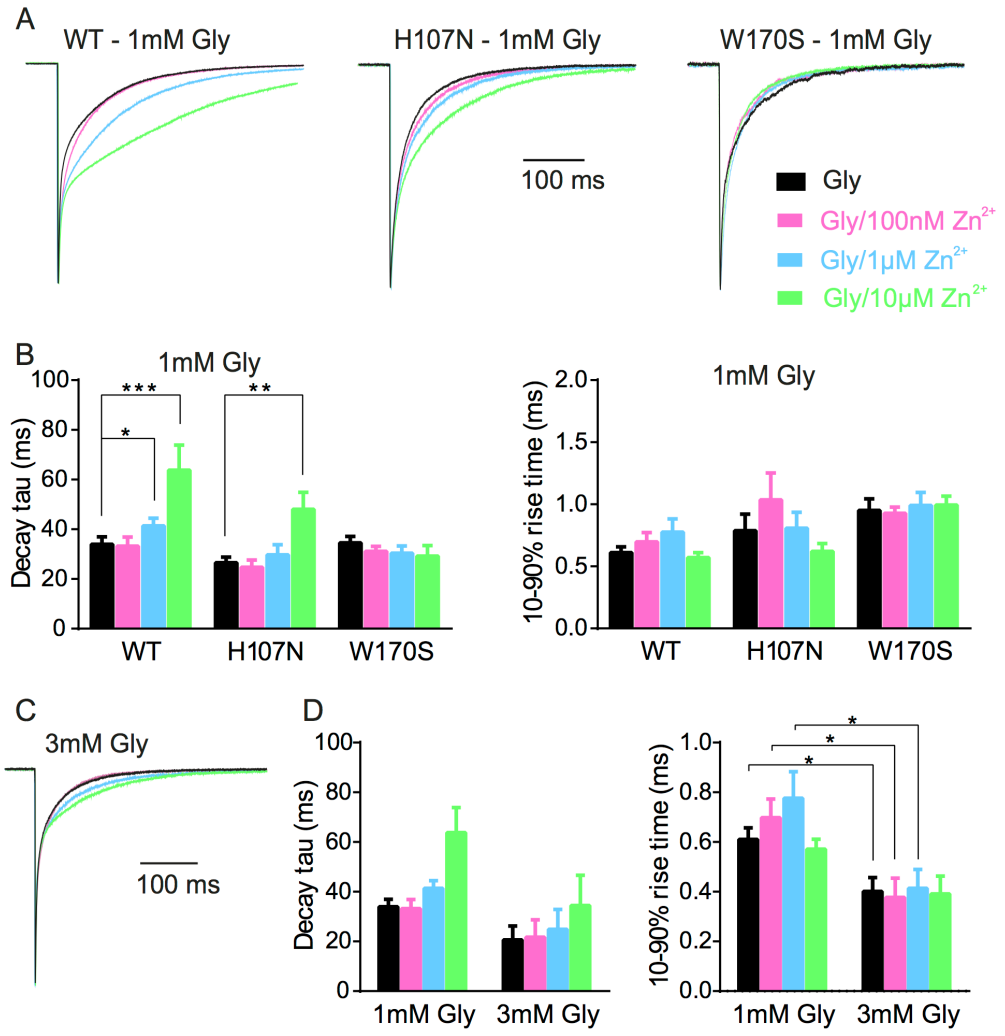

Figure 4. Calibration of the Zn^{2+}-sensitivity of α1β, $\alpha1^{H107N}\beta$ and $\alpha1^{W170S}\beta$ GlyRs under simulated synaptic activation conditions. **(A)** Representative macropatch currents mediated by indicated constructs upon switching from control extracellular solution to one containing 1 mM glycine plus 10 mM tricine plus the indicated concentration of free Zn^{2+}. Traces were averaged from >10 sweeps each and normalized. **(B)** Mean values for weighted decay time constants and 10 – 90 % rise times for the three constructs. See Supplementary Table 1 for a full breakdown of n values, mean τ1 and τ2 values and their relative proportions. Statistical significance was determined by Mann-Whitney U test. The distributions in WT (glycine only) and WT (glycine + 1 μM Zn^{2+}) values differed significantly for decay time constant (U = 63, $*p <$ 0.05, n1 = 17 macropatches, n2 = 13 macropatches). The distributions in WT (glycine only) and WT (glycine + 10 μM Zn^{2+}) values also differed significantly for decay time constant (U = 20, $***p < 0.001$, n1 = 17 macropatches, n2 = 10 macropatches). The distributions in H107N (glycine only) and H107N (glycine + 10 μM Zn^{2+}) values also differed significantly for decay time constant (U = 16, $**p < 0.01$, n1 = 13 macropatches, n2 = 8 macropatches). **(C)** Representative macropatch currents mediated by α1β GlyRs upon switching from control extracellular solution to one containing 3 mM glycine plus 10 mM tricine plus the indicated free Zn^{2+} concentration. Traces were averaged from >10 sweeps each and normalized. **(D)** Mean values for weighted decay time constant and 10 – 90 % rise time for two glycine concentrations. Statistical significance was determined by Mann-Whitney U test. The distributions in the 1 and 3 mM glycine 10 – 90 % rise time values differed significantly for Zn^{2+} concentrations of 0, 100 nM and 1 μM (U = 9 – 15, $*p < 0.05$, n1 = 10 – 17 macropatches, n2 = 5 macropatches).

Effect of a fast, high-affinity Zn^{2+} chelator on IPSC parameters

ZX1 is a fast, high affinity Zn^{2+} chelator (Radford and Lippard, 2013). When applied at a concentration of 100 μM, it has been shown to efficiently remove tonic Zn^{2+} bound constitutively to NMDARs (Anderson et al., 2015). Given that GlyRs and NMDARs both have high affinity Zn^{2+} sites with similar nanomolar affinities, it is reasonable to hypothesize that ZX1 should have the same effect on GlyRs. Indeed, a recent study has suggested that ZX1 does remove tonic Zn^{2+} bound to synaptic GlyRs (Perez-Rosello et al., 2015). We investigated the effects of 100 μM ZX1 on IPSCs mediated by α1β GlyRs both as a control for possible nonspecific (e.g., pharmacological) effects of tricine and to investigate the possibility that tonic Zn^{2+} might be bound tightly to synaptic GlyRs. Figure 5A shows examples of normalized, averaged IPSCs recorded from one cell before, during and after exposure to 100 μM ZX1. Results averaged from nine cells recorded under identical conditions reveal that 100 μM ZX1 had no significant effect on IPSC amplitude (Figure 5B) or 10 – 90 % rise time (Figure 5C) although it significantly reduced the IPSC decay time constant (Figure 5D). However, there was no significant difference in the magnitude of the effect of 10 mM tricine and 100 μM ZX1 on the IPSC decay time constant (Figure 5E – G). Moreover, in five cells where we quantitated the effects of 10 mM tricine and 100 μM ZX1 sequentially in the same cell, we found the ZX1 exerted no significant additional effect on the IPSC decay time constant (not shown). Thus, if tonic Zn^{2+} is bound with high affinity to synaptic α1β GlyRs in our artificial synapses, then its removal has no functional consequence. We thus infer that the effect of tricine and ZX1 on glycinergic IPSCs is mediated by freely diffusing Zn^{2+}.

In a final experiment, we quantitated the recovery time course of IPSC decay time constant following ZX1 washout (Figure 5H). In this experiment we digitally averaged all events within each 30 s interval during the recovery phase and fitted a single decay time constant to the averaged data. Results were averaged from five cells. As seen in Figure 5H, complete recovery from ZX1 application required around 1 min, although the decay time constant eventually stabilized at a value that was significantly higher than the initial control IPSC decay time constant (Figure 5D, H). This suggests that the concentration of free synaptic Zn^{2+} is not depleted over time under our experimental conditions.

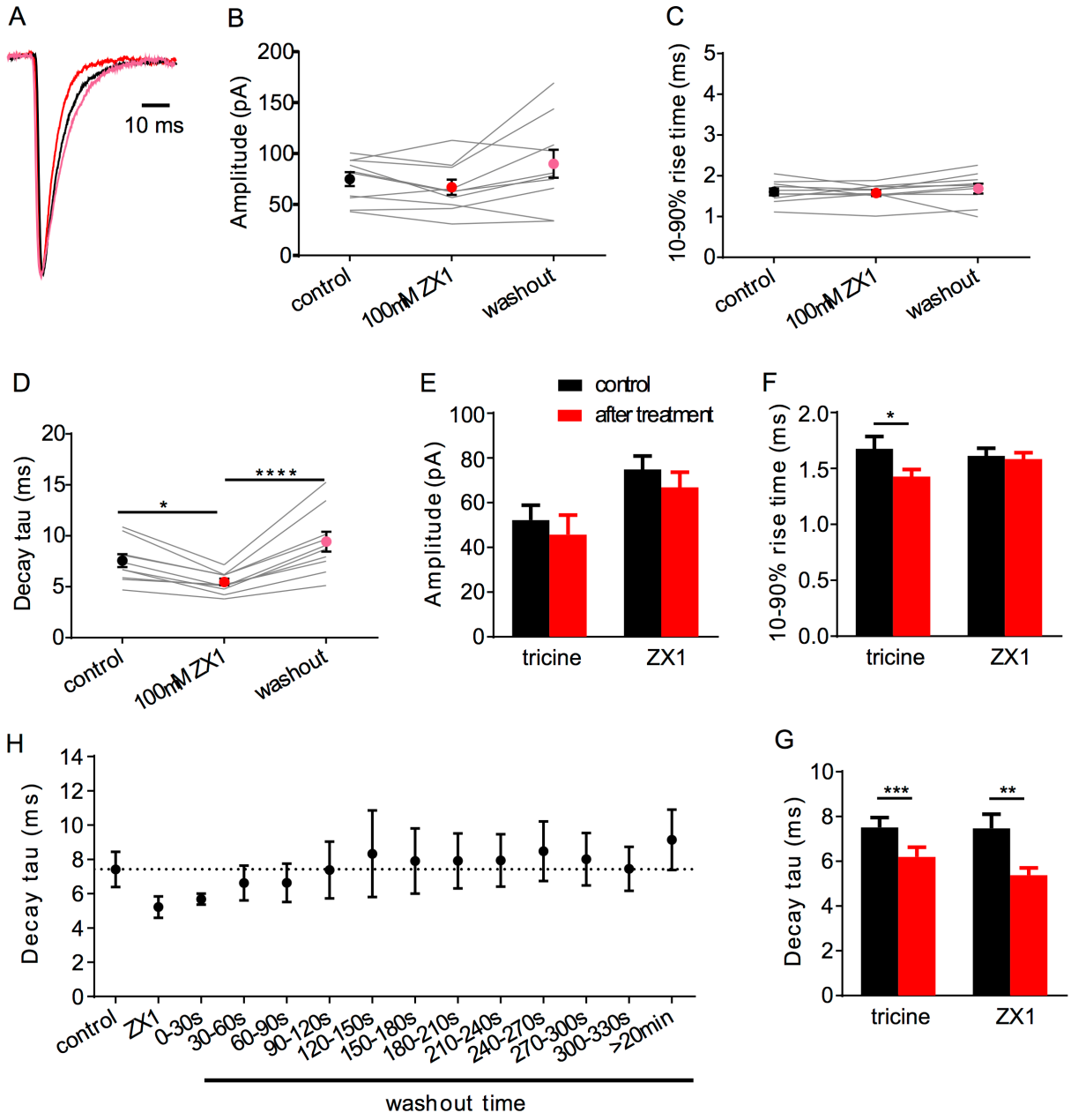

Figure 5. Effects of 100 μM ZX1 on IPSCs mediated by α1β GlyRs. **(A)** Superimposed averaged, normalized IPSCs each averaged from > 50 events from the same cell. Recordings were made in the presence of control solution (black trace; averaged from 79 events), after addition of 100 μM ZX1 (red trace; averaged from 61 events) and after 5 min washout (pink trace; averaged from 52 events). **(B – D)** Effects of 100 μM ZX1 on IPSC amplitude, decay time constant and 10 – 90 % rise time for α1β-mediated IPSCs. All results were averaged from 10 cells. Statistical significance in **D** was determined by Friedman test with significance represented by $*p < 0.05$, and $****p < 0.0001$. **(E - G)** Comparison of the effects of 10 mM tricine and 100 μM ZX1 on IPSC amplitude, decay time constant and 10 – 90 % rise time for α1β-mediated IPSCs. There was no significant difference in the decay time constants in either condition. Statistical significance in **G** was determined by two-tailed Wilcoxon matched-pairs signed rank test, with significance represented by $**p < 0.01$ and $***p < 0.001$. **(H)** Time course of washout of the ZX1 effect on decay time constant. ZX1 was applied for 3 min. All data points were averaged from five cells.

DISCUSSION

The main advantage of our artificial synapse system is that it allows control over the GlyR subunit composition. However, a potential limitation is that artificial synapses may not faithfully replicate real synapses, especially in terms of synaptic cleft geometry or the location and density of Zn^{2+} and glycine transporters. Although such factors could affect Zn^{2+} and glycine concentrations in the synaptic cleft, we think they are unlikely to seriously compromise our conclusions for several reasons. First, IPSCs from artificial synapses containing α1β and α2β GlyRs exhibit decay times that are remarkably similar to those from native neuronal synapses expressing the same isoforms (Zhang et al., 2015). Second, the decay time constants of IPSCs recorded *in vitro* from homozygous $\alpha1^{D80A}$ knock-in mice (where Zn^{2+} potentiation is abolished) or from homozygous *Spasmodic* $\alpha1^{A52S}$ mice (where glycine sensitivity is reduced 10-fold) were quantitatively similar to those recorded from artificial synapses incorporating the same mutant subunits (Graham et al., 2006; Hirzel et al., 2006; Zhang et al., 2015). These results suggest a reasonably close correspondence in the concentration profiles of Zn^{2+} and glycine between artificial and real glycinergic synapses. Turning to the present study, tricine-mediated buffering of extracellular Zn^{2+} significantly accelerated the decay rate of IPSCs mediated by α1β and $\alpha1^{H107N}\beta$ GlyRs. However, no change in IPSC amplitude was observed. Together these results imply that the Zn^{2+} concentration in the synaptic cleft is high enough to modulate IPSCs, and that the glycine concentration is saturating. These observations fit well with previous studies on neuronal glycinergic synapses. For example, a study that investigated glycinergic IPSCs in zebrafish neurons found that 10 mM tricine reduced IPSC duration to a similar extent as observed here (Suwa et al., 2001). In addition, studies by Legendre (1998) and Beato (2008) found that the synaptic glycine concentration reaches > 1 mM, which is saturating at α1β GlyRs.

By comparing the effects of 10 mM tricine on IPSCs to the effects of co-applied glycine plus free Zn^{2+} to macropatches, we infer that the free synaptic Zn^{2+} rises to at least 1 μM following a single action potential. The dramatic slowing in the IPSC decay rate that we observed in the presence of 5 μM free added Zn^{2+} (Figure 1E) is probably due to the total (tonic plus synaptically-released) free Zn^{2+} rising to ≥ 6 μM. In addition, the absence of any effect of Zn^{2+} at concentrations up to 10 μM in the $\alpha1^{W170S}\beta$ GlyR suggests that the well-characterized inhibitory effect of Zn^{2+} (Laube et al., 1995; Nevin et al., 2003; Miller et al., 2005a) is not physiologically relevant, at least at low synaptic stimulation rates. Finally, given the similarity in the effects of 10 mM tricine and 100 μM ZX1 on the IPSC decay rate (Figure 5G), we find no evidence for tonic Zn^{2+} binding tightly to high affinity sites on the GlyR (Perez-Rosello et al., 2015).

It is yet to be demonstrated that Zn^{2+} is co-released with glycine in a phasic manner. However, in the absence of a phasic release mechanism it is difficult to explain how a ≥ 1 μM Zn^{2+} concentration could be maintained in the cleft for periods typically exceeding 20 min (Figure 5H) when the bulk extracellular (tonic) concentration is presumably in the low nM range (Frederickson et al., 2006).

A similar type of analysis of synaptic Zn^{2+} concentration was recently performed on glutamatergic synapses (Vergnano et al., 2014). GluN2A-containing NMDARs exhibit both high affinity Zn^{2+} inhibition in the 10 – 20 nM range and low affinity inhibition in the 10 – 50 μM range (Paoletti et al., 1997). Vergnano *et al* compared the effect of 10 mM tricine on GluN2A-mediated synaptic currents from control mice to those from knock-in mice that overexpressed a mutant GluN2A deficient in high affinity Zn^{2+} binding (Vergnano et al., 2014). They found no effect of tricine on single action potential-mediated excitatory postsynaptic currents (EPSCs) in either case, although fast repetitive stimulation unveiled Zn^{2+}-mediated inhibition of EPSCs in control animals only. From this they concluded that synaptic Zn^{2+} does not rise high enough to bind to the low affinity sites. It is noteworthy that α1β GlyRs and GluN2A-containing NMDARs have similar high affinities to Zn^{2+}. Given that a single action potential releases sufficient Zn^{2+} to modulate glycinergic IPSCs but not NMDAR-mediated EPSCs, we infer that Zn^{2+} rises to significantly higher concentrations in the glycinergic synaptic cleft. Indeed, high affinity chelation of Zn^{2+} by 100 μM ZX1 to remove tonic Zn^{2+} bound to NMDARs is needed to detect an effect of Zn^{2+} released by a single action potential (Anderson et al., 2015). This implies that the Zn^{2+} concentration increase in the glutamatergic synaptic cleft response to a single action potential is in the low nM range.

GlyRs are also potentiated by La^{3+}, Pb^{2+} and Co^{2+} and inhibited by Cu^{2+} and Ni^{2+} (Lynch, 2004). As tricine is a low affinity chelator with poor specificity among heavy metals (Ferreira et al., 2015), it is possible that its effect of GlyRs may be due to the chelation of other metal contaminants in the recording solution. Since tricine inhibits glycinergic currents, we infer that any metal contaminant must be a GlyR potentiator. However, the three known potentiators (La^{3+}, Pb^{2+} and Co^{2+}) are unlikely to be present as contaminants in our recording solutions at concentrations high enough (100 μM) to positively modulate GlyRs. Thus, it is highly likely that the effects of tricine on α1β GlyR-mediated IPSCs is mediated by Zn^{2+}.

Human hyperekplexia, or startle disease, is most commonly caused by hereditary mutations in α1 or β GlyR subunits that disrupt glycinergic neurotransmission (Bode and Lynch, 2014). Most startle mutations result in the complete or partial loss of glycinergic inhibitory function (Chung et al., 2010; Bode et al., 2013; Bode and Lynch, 2014). Given that the human $\alpha1^{W170S}$ startle mutation abolished Zn^{2+} potentiation, it was originally concluded that the startle phenotype was due to a diminished IPSC magnitude or duration (Zhou et al., 2013). In support of this, a startle phenotype had previously been

demonstrated in a knock-in mouse overexpressing a mutant $\alpha1^{D80A}$ GlyR subunit in which Zn^{2+} potentiation had been eliminated (Hirzel et al., 2006). Our fast application experiments demonstrate that the inherent deactivation rates of $\alpha1\beta$ and $\alpha1^{W170S}\beta$ GlyRs in the absence of Zn^{2+} are similar (Figure 4B), implying that the loss of Zn^{2+} potentiation in $\alpha1^{W170S}\beta$ GlyRs may indeed lead to a net diminished current carrying capacity. However, in artificial synapses we found that both the mean amplitude and decay rate of IPSCs mediated by $\alpha1^{W170S}\beta$ GlyRs were comparable to those of $\alpha1\beta$ GlyRs that had been maximally positively modulated by Zn^{2+} (Figure 1C, E). This effect could either be due to altered gating properties or differential clustering at the synapse. We have recently shown that the $\alpha1^{W170S}\beta$ GlyR also exhibits spontaneous activation (Zhang et al., 2016) and suggested that, like other gain-of-function startle disease mutations, W170S may cause startle disease via a developmental defect that prevents the maturation of $\alpha1\beta$ GlyR synapses (Zhang et al., 2016).

CONCLUSION

In conclusion, we infer that the free Zn^{2+} concentration in the artificial glycinergic synaptic cleft reaches at least 1 μM following a single presynaptic stimulation. As this concentration at least an order of magnitude higher than the tonic Zn^{2+} concentration, we assume that diffusible Zn^{2+} is somehow concentrated in the synaptic cleft. The most likely explanation is that Zn^{2+} is phasically released from presynaptic terminals. It is noteworthy that this peak concentration is significantly higher than that reached under similar conditions in the glutamatergic synaptic cleft. We also found no evidence for tonic Zn^{2+} binding to high affinity GlyR sites. Similarly, we found no evidence for Zn^{2+} inhibition in response to a single action potential in synapses where GlyR Zn^{2+} potentiation had been eliminated. These results provide new insights into the physiological modulatory mechanisms of glycinergic IPSCs.

Supplementary information: Supplementary Table 1.

Acknowledgements: This research was supported by the Australian Research Council (DP130101702 and DP150102428) and the National Health and Medical Research Council (APP1058542). We thank Profs Jochen Meier and Robert Harvey for kindly providing cDNAs encoding the rat α3L GlyR and rat gephyrin P1, respectively. The authors have no conflict of interest to declare.

Author contributions: J.W.L. conceived the project; Y.Z. and A.K. performed experiments and analysed the data; and Y.Z, A.K. and J.W.L. wrote the manuscript.

Competing financial interests: The authors declare no competing financial interests.

Supplementary Table 1. Summary of the fast and slow deactivation time constants, and their relative amplitudes, measured in response to the rapid application of 1 mM glycine to macropatches expressing the indicated GlyR isoforms.

GlyR	parameter	1 mM Gly	+100 nM Zn^{2+}	+1 μM Zn^{2+}	+10 μM Zn^{2+}
α1β	τ1 (ms)	12.0 ± 1.6 (17)	11.6 ± 1.4 (13)	12.6 ± 1.4 (13)	11.0 ± 1.2 (10)
	A1 (%)	69.0 ± 3.2 (17)	67.6 ± 3.6 (13)	61.6 ± 3.1 (13)	58.0 ± 5.5 (10)
	τ2 (ms)	87.3 ± 8.3 (17)	80.3 ± 9.5 (13)	87.8 ±5.2 (13)	133.8 ± 13.4**(10)
	A2 (%)	31.0 ± 3.2 (17)	32.4 ± 3.6 (13)	38.4 ± 3.1 (13)	42.0 ± 5.5 (10)
$\alpha1^{H107N}\beta$	τ1 (ms)	10.1 ± 1.6 (13)	11.0 ± 2.1 (10)	10.7 ± 1.2 (10)	10.1 ± 1.5 (8)
	A1 (%)	74.4 ± 4.0 (13)	75.1 ± 5.0 (10)	70.0 ± 5.5 (10)	62.5 ± 5.8 (8)
	τ2 (ms)	67.3 ± 9.2 (13)	71.4 ± 16.9 (10)	64.7 ± 6.3 (10)	94.0 ± 11.3 (8)
	A2 (%)	25.6 ± 4.0 (13)	24.9 ± 5.0 (10)	30.0 ± 5.5 (10)	37.5 ± 5.8 (8)
$\alpha1^{W170S}\beta$	τ1 (ms)	14.1 ± 2.0 (14)	13.7 ± 2.3 (10)	13.1 ± 1.7 (10)	12.9 ± 2.0 (9)
	A1 (%)	61.4 ± 6.0 (14)	64.8 ± 6.1 (10)	58.5 ± 5.7 (10)	68.5 ± 6.7 (9)
	τ2 (ms)	61.2 ± 5.3 (14)	62.0 ± 4.9 (10)	53.0 ± 3.0 (10)	59.1 ± 7.4 (9)
	A2 (%)	38.6 ± 6.0 (14)	35.2 ± 6.1 (10)	41.5 ± 5.7 (10)	31.2 ± 6.7 (9)

Parameters: τ1 – fast decay time constant; A1 – relative amplitude of τ1; τ2 – slow decay time constant; A2 – relative amplitude of τ2.

n values for each experiment are given in brackets.

**$p < 0.01$ by nonparametric Mann-Whitney U test.

REFERENCES

Al-Futaisi, A. M., Al-Kindi, M. N., Al-Mawali, A. M., Koul, R. L., Al-Adawi, S., and Al-Yahyaee, S. A. (2012). Novel mutation of GLRA1 in Omani families with hyperekplexia and mild mental retardation. *Pediatr Neurol* 46, 89-93.

Anderson, C. T., Radford, R. J., Zastrow, M. L., Zhang, D. Y., Apfel, U. P., Lippard, S. J., and Tzounopoulos, T. (2015). Modulation of extrasynaptic NMDA receptors by synaptic and tonic zinc. *Proc Natl Acad Sci USA* 112, E2705-14.

Assaf, S. Y., and Chung, S. H. (1984). Release of endogenous Zn2+ from brain tissue during activity. *Nature* 308, 734-6.

Beato, M. (2008). The time course of transmitter at glycinergic synapses onto motoneurons. *J Neurosci* 28, 7412-25.

Birinyi, A., Parker, D., Antal, M., and Shupliakov, O. (2001). Zinc co-localizes with GABA and glycine in synapses in the lamprey spinal cord. *J Comp Neurol* 433, 208-21.

Bloomenthal, A. B., Goldwater, E., Pritchett, D. B., and Harrison, N. L. (1994). Biphasic modulation of the strychnine-sensitive glycine receptor by Zn2+. *Mol Pharmacol* 46, 1156-9.

Bode, A., and Lynch, J. W. (2014). The impact of human hyperekplexia mutations on glycine receptor structure and function. *Mol Brain* 7, 2.

Bode, A., Wood, S. E., Mullins, J. G., Keramidas, A., Cushion, T. D., Thomas, R. H., Pickrell, W. O., Drew, C. J., Masri, A., Jones, E. A., Vassallo, G., Born, A. P., Alehan, F., Aharoni, S., Bannasch, G., Bartsch, M., Kara, B., Krause, A., Karam, E. G., Matta, S., Jain, V., Mandel,

H., Freilinger, M., Graham, G. E., Hobson, E., Chatfield, S., Vincent-Delorme, C., Rahme, J. E., Afawi, Z., Berkovic, S. F., Howell, O. W., Vanbellinghen, J. F., Rees, M. I., Chung, S. K., and Lynch, J. W. (2013). New hyperekplexia mutations provide insight into glycine receptor assembly, trafficking, and activation mechanisms. *J Biol Chem* 288, 33745-59.

Chung, S. K., Vanbellinghen, J. F., Mullins, J. G., Robinson, A., Hantke, J., Hammond, C. L., Gilbert, D. F., Freilinger, M., Ryan, M., Kruer, M. C., Masri, A., Gurses, C., Ferrie, C., Harvey, K., Shiang, R., Christodoulou, J., Andermann, F., Andermann, E., Thomas, R. H., Harvey, R. J., Lynch, J. W., and Rees, M. I. (2010). Pathophysiological mechanisms of dominant and recessive GLRA1 mutations in hyperekplexia. *J Neurosci* 30, 9612-20.

Cornelison, G. L., and Mihic, S. J. (2014). Contaminating levels of zinc found in commonly-used labware and buffers affect glycine receptor currents. *Brain Res Bull* 100, 1-5.

Dixon, C. L., Zhang, Y., and Lynch, J. W. (2015). Generation of functional inhibitory synapses incorporating defined combinations of GABA(A) or glycine receptor subunits. *Front. Mol. Neurosci.* In press.

Eto, K., Arimura, Y., Nabekura, J., Noda, M., and Ishibashi, H. (2007). The effect of zinc on glycinergic inhibitory postsynaptic currents in rat spinal dorsal horn neurons. *Brain Res* 1161, 11-20.

Ferreira, C. M., Pinto, I. S., Soares, E. V., and Soares, H. M. (2015). (Un)suitability of the use of pH buffers in biological, biochemical and environmental studies and their interaction with metal ions – a review. *Royal Society of Chemistry Advances* 5, 30989-31003.

Frederickson, C. J. (1989). Neurobiology of zinc and zinc-containing neurons. *Int Rev Neurobiol* 31, 145-238.

Frederickson, C. J., Giblin, L. J., Krezel, A., McAdoo, D. J., Mueller, R. N., Zeng, Y., Balaji, R. V., Masalha, R., Thompson, R. B., Fierke, C. A., Sarvey, J. M., de Valdenebro, M., Prough, D. S., and Zornow, M. H. (2006). Concentrations of extracellular free zinc (pZn)e in the central nervous system during simple anesthetization, ischemia and reperfusion. *Exp Neurol* 198, 285-93.

Graham, B. A., Schofield, P. R., Sah, P., Margrie, T. W., and Callister, R. J. (2006). Distinct physiological mechanisms underlie altered glycinergic synaptic transmission in the murine mutants spastic, spasmodic, and oscillator. *J Neurosci* 26, 4880-90.

Hirzel, K., Muller, U., Latal, A. T., Hulsmann, S., Grudzinska, J., Seeliger, M. W., Betz, H., and Laube, B. (2006). Hyperekplexia phenotype of glycine receptor alpha1 subunit mutant mice identifies Zn(2+) as an essential endogenous modulator of glycinergic neurotransmission. *Neuron* 52, 679-90.

Howell, G. A., Welch, M. G., and Frederickson, C. J. (1984). Stimulation-induced uptake and release of zinc in hippocampal slices. *Nature* 308, 736-8.

Kay, A. R. (2003). Evidence for chelatable zinc in the extracellular space of the hippocampus, but little evidence for synaptic release of Zn. *J Neurosci* 23, 6847-55.

Kay, A. R. (2004). Detecting and minimizing zinc contamination in physiological solutions. *BMC Physiol* 4, 4.

Laube, B. (2002). Potentiation of inhibitory glycinergic neurotransmission by Zn2+: a synergistic interplay between presynaptic P2X2 and postsynaptic glycine receptors. *Eur J Neurosci* 16, 1025-36.

Laube, B., Kuhse, J., Rundstrom, N., Kirsch, J., Schmieden, V., and Betz, H. (1995). Modulation by zinc ions of native rat and recombinant human inhibitory glycine receptors. *J Physiol* 483, 613-9.

Legendre, P. (1998). A reluctant gating mode of glycine receptor channels determines the time course of inhibitory miniature synaptic events in zebrafish hindbrain neurons. *J Neurosci* 18, 2856-70.

Low, C. M., Zheng, F., Lyuboslavsky, P., and Traynelis, S. F. (2000). Molecular determinants of coordinated proton and zinc inhibition of N-methyl-D-aspartate NR1/NR2A receptors. *Proc Natl Acad Sci USA* 97, 11062-7.

Lynch, J. W. (2004). Molecular structure and function of the glycine receptor chloride channel. *Physiol Rev* 84, 1051-95.
Lynch, J. W. (2009). Native glycine receptor subtypes and their physiological roles. *Neuropharmacology* 56, 303-9.
Marger, L., Schubert, C. R., and Bertrand, D. (2014). Zinc: an underappreciated modulatory factor of brain function. *Biochem Pharmacol* 91, 426-35.
Miller, P. S., Beato, M., Harvey, R. J., and Smart, T. G. (2005a). Molecular determinants of glycine receptor alphabeta subunit sensitivities to Zn2+-mediated inhibition. *J Physiol* 566, 657-70.
Miller, P. S., Da Silva, H. M., and Smart, T. G. (2005b). Molecular basis for zinc potentiation at strychnine-sensitive glycine receptors. *J Biol Chem* 280, 37877-84.
Nevin, S. T., Cromer, B. A., Haddrill, J. L., Morton, C. J., Parker, M. W., and Lynch, J. W. (2003). Insights into the structural basis for zinc inhibition of the glycine receptor. *J Biol Chem* 278, 28985-92.
Paoletti, P., Ascher, P., and Neyton, J. (1997). High-affinity zinc inhibition of NMDA NR1-NR2A receptors. *J Neurosci* 17, 5711-25.
Perez-Rosello, T., Anderson, C. T., Ling, C., Lippard, S. J., and Tzounopoulos, T. (2015). Tonic zinc inhibits spontaneous firing in dorsal cochlear nucleus principal neurons by enhancing glycinergic neurotransmission. *Neurobiol Dis* 81, 14-9.
Radford, R. J., and Lippard, S. J. (2013). Chelators for investigating zinc metalloneurochemistry. *Curr Opin Chem Biol* 17, 129-36.
Renganathan, M., and Bose, S. (1990). Inhibition of photosystem II activity by Cu(++) ion. Choice of buffer and reagent is critical. *Photosynth Res* 23, 95-9.
Suwa, H., Saint-Amant, L., Triller, A., Drapeau, P., and Legendre, P. (2001). High-affinity zinc potentiation of inhibitory postsynaptic glycinergic currents in the zebrafish hindbrain. *J Neurophysiol* 85, 912-25.
Vergnano, A. M., Rebola, N., Savtchenko, L. P., Pinheiro, P. S., Casado, M., Kieffer, B. L., Rusakov, D. A., Mulle, C., and Paoletti, P. (2014). Zinc dynamics and action at excitatory synapses. *Neuron* 82, 1101-14.
Vogt, K., Mellor, J., Tong, G., and Nicoll, R. (2000). The actions of synaptically released zinc at hippocampal mossy fiber synapses. *Neuron* 26, 187-96.
Wang, Z., Li, J. Y., Dahlstrom, A., and Danscher, G. (2001). Zinc-enriched GABAergic terminals in mouse spinal cord. *Brain Res* 921, 165-72.
Zeilhofer, H. U., Wildner, H., and Yevenes, G. E. (2012). Fast synaptic inhibition in spinal sensory processing and pain control. *Physiol Rev* 92, 193-235.
Zhang, Y., Bode, A., Nguyen, B., Keramidas, A., and Lynch, J. W. (2016). Investigating the mechanism by which gain-of-function mutations to the alpha1 glycine receptor cause hyperekplexia. *J Biol Chem* 291, 15332-41.
Zhang, Y., Dixon, C. L., Keramidas, A., and Lynch, J. W. (2015). Functional reconstitution of glycinergic synapses incorporating defined glycine receptor subunit combinations. *Neuropharmacology* 89, 391-7.
Zhou, N., Wang, C. H., Zhang, S., and Wu, D. C. (2013). The GLRA1 missense mutation W170S associates lack of Zn2+ potentiation with human hyperekplexia. *J Neurosci* 33, 17675-81.

Chapter 6

General discussion

Chapter 6: General Discussion

The overall aim of my PhD project was to develop and validate a protocol for efficiently generating functional glycinergic 'artificial' synapses incorporating defined glycine receptor subunit combinations. Secondary aims were to use this assay to investigate the effects of startle disease and autism mutations on glycinergic IPSCs and to probe the Zn^{2+} concentration in the glycinergic synaptic cleft. Here, I will summarise the major findings as presented in each chapter and propose some future directions on the basis of current research.

1. The 'artificial' synapse is a reliable means of generating functional recombinant glycinergic synapses that selectively incorporate the GlyR isoform of interest.

The main advantage of the artificial synapse preparation is that it allows control over the subunit composition of postsynaptic GlyRs. It is critical to establish that the spontaneous IPSCs generated from the artificial synapses exhibit similar characteristics to those mediated by native synapses incorporating the same subunits. Glycinergic IPSCs recorded from artificial synapses containing α1β and α2β GlyRs exhibit decay times that correspond remarkably closely to those from native neuronal synapses expressing the same isoforms. Additionally, the accelerated IPSC decay rates recorded from homozygous $\alpha1^{D80A}$ knock-in mice or from homozygous *spasmodic* $\alpha1^{A52S}$ mice closely resemble those recorded from artificial synapses incorporating the same mutant subunits (Graham et al., 2006; Hirzel et al., 2006). These results provide an important validation of our technique. However, potential limitations of the 'artificial' synapse approach include the possibility of different geometries of the synaptic microenvironment, or the possible lack of essential transporters or clustering proteins in the postsynaptic cells, which may be reflected in slower glycinergic IPSC rise times in artificial synapses. Thus, it would be of interest to use electron microscopy to measure the width of the synaptic cleft and compare the synaptic morphology of artificial synapses with that of native neuronal synapses. This has been achieved with GABAergic artificial synapses where it was shown that the presynaptic terminals were similar to native GABAergic synapses in that they exhibited close apposition between pre- and postsynaptic membranes, together with a high density of presynaptic membrane-bound vesicles and mitochondria (Fuchs et al., 2013). It would be of interest to employ this approach on artificial glycinergic synapses.

An additional means of comparing artificial with real synapses would be to employ high resolution imaging. Superresolution photoactivation localization microscopy (sptPALM) measurements on live cells could be employed to monitor the diffusion rate of individual GlyRs in both the synaptic

and extrasynaptic compartments in neurons and in HEK cells containing artificial synapses (Manley et al., 2010). By comparing the relative abilities of the respective synapses to restrain GlyR movement, it would be possible to determine whether the synaptic clustering mechanisms are similar in strength between the two systems. PALM imaging on fixed neurons or HEK cells could also be used to compare both synaptic cluster sizes and the densities of GlyRs within individual synaptic clusters. Finally, it would be useful to probe the relative expression levels and functional roles of specific proteins that might contribute to synaptogenesis and synaptic clustering mechanisms in artificial and native synapses. Together, this information would greatly enhance our ability to determine the extent to which glycinergic 'artificial' synapses recapitulate their native neuronal counterparts.

2. α1- and α1β-mediated IPSCs exhibit identical kinetic profiles.

Incorporation of the β subunit into α2 and α3-containing GlyRs accelerates IPSC rise and decay times. This result is consistent with the notion that β subunit is essential for clustering GlyRs at the postsynaptic sites via directly binding to gephyrin (Fritschy et al., 2008). In contrast, incorporation of the β subunit into α1 containing GlyRs does not alter the kinetic properties, implying that GlyR α1 can be localized to postsynaptic sites by a gephyrin-dependent or a gephyrin-independent mechanism. Single particle tracking studies have shown that the GlyR α1 diffused much faster and was less confined in both Hela cell and neuron membrane compared to that of GlyR α1 containing the gephyrin-binding motifs (Ehrensperger et al., 2007). Therefore, if gephyrin is the sole means of clustering GlyRs at synapses, the diffusion and clustering properties of α1 and α1β GlyRs should be different. We hypothesize that α1 homomer-mediated fast IPSCs is independent of the regulation of mobility and clustering by gephyrin. If this is the case, disruption of gephyrin clusters by either gephyrin shRNAs or gene knockout should lead to a specific disruption of the function of the α1β GlyR-mediated synapses but not of α1 GlyR-mediated synapses. Furthermore, search for proteins interacting with GlyR α1 subunit would provide additional details concerning the mechanisms of efficient synaptic transmission mediated by α1 GlyRs.

Chimeras of GlyR α1 and α3 subunits have been used in our laboratory to identify the structural determinants of their efficacy differences (Chen et al., 2009), and the structural domains influencing conformational variations in the glycine-binding site (Han et al., 2013). The predicted intrinsic channel closing rates from the simulation were relatively fast for both α1 and α3 GlyRs. However, in artificial synapses, the time course of α3 GlyR-mediated IPSCs was considerably longer than α1 GlyR-mediated IPSCs, yet the basis for difference in kinetics remains unknown. Chimera

approaches using GlyR α1 and α3 subunits provide a plausible way to investigate the structural basis of their different IPSC characteristics.

3. α1β- and α3β-mediated IPSCs exhibit similar IPSC characteristics.

The glycine sensitivity differs between the α1 and α3 GlyRs, with the EC_{50} for glycine being 10-fold higher in α3-containing GlyRs (~300 μM) than in α1-containing GlyRs (~30 μM). As the glycine EC_{50} for α3β GlyRs is comparable with that of the $\alpha1^{A52S}\beta$ mutant GlyR, we expected to observe faster decay rates in α3β-mediated IPSCs compared to the α1β-mediated IPSCs. However, we observed remarkably similar IPSC rise and decay rates in α1β and α3β-mediated heterosynapses. Although α3β-mediated IPSCs have yet to be recorded in isolation in native synapses, their kinetic properties appear indistinguishable from those of α1β GlyRs (Harvey et al., 2004). This fits well with the results from our artificial synapses. However, the mechanisms by which α1 and α3 GlyRs with drastically different glycine sensitivities are capable of generating IPSCs with identical kinetic properties still need to be determined.

4. Gain-of-function *GLRA1* mutations prolong the decay of IPSCs.

Hyperekplexia, or startle disease, is most commonly caused by hereditary *GLRA1* and *GLRB* mutations that reduce the efficacy of glycinergic transmission. Previous studies have identified several *GLRA1* mutations that result in spontaneous channel activation, suggesting gain-of-function *GLRA1* mutations can also cause hyperekplexia. In my study, we identified two new *GLRA1* gain-of-function hyperekplexia mutations (I43F and W170S) and characterized these along with known gain-of-function mutations (Q226E, V280M and R414H). Using artificial synapses, all gain-of-function mutations exhibit prolonged decay of glycinergic IPSCs. The longer and more complex spontaneous bursts induced by $\alpha1^{I43F}\beta$, $\alpha1^{Q226E}\beta$ and $\alpha1^{V280M}\beta$ most likely underlie the observed drastically slow IPSC decay rates. Conversely, the short-lived spontaneous bursts induced by $\alpha1^{W170S}\beta$ and $\alpha1^{R414H}\beta$ most likely underlie their faster IPSC decay rates, compared to those mediated by other gain-of-function mutations.

As to how *GLRA1* gain-of-function mutations cause hyperekplexia, we proposed several possible mechanisms. First, we considered the spontaneous Cl^- current may deplete the Cl^- gradient in adult neurons leading to reduced efficacy of glycinergic inhibition. However, we consider this unlikely as it should also lead to pain sensitization and a hyperekplexia phenotype that correlates with mutation severity, neither of which is observed in patients with gain-of-function mutations. Second, we considered that even small increases in IPSC decay time constants (as seen in W170S and R414H) may directly elicit hyperekplexia, perhaps by a presynaptic effect on motor neurons on an upstream

effect on an excitatory or inhibitory input onto motor neurons. We also rule out this possibility given that the clinically-important drug, tropisetron, increases glycinergic IPSC decay times without causing motor side effects. Third, we considered whether a neurodevelopmental defect may result in fewer glycinergic synapses in adult motor neurons. This idea stemmed from a recent study that concluded that an elevated intracellular chloride concentration late during development ablates α1β glycinergic synapses but spares GABAergic synapses (Schwale et al., 2016). As this mechanism satisfies all our considerations, we propose it is primarily responsible for the gain-of-function hyperekplexia phenotype. To test our hypothesis, overexpression of *GLRA1* gain-of-function mutations in neuronal cultures followed by imaging experiments to quantitate changes in GlyR synapse numbers could provide further insights into the morphological correlates of these functional alterations in glycinergic synapses.

5. Autism-causing $\alpha2^{R350L}$ mutation increases IPSC time courses.

We have characterized the functional properties of a newly identified autism-causing mutation, R350L, which located in the intracellular loop of GlyR α2 subunit. Using artificial synapses, the R350L mutation was found to slow rise and decay times of glycinergic IPSCs. The increased IPSC decay time is mainly due to the prolonged intrinsic channel closing rate. As mutation of Arg-350 to Ala, Lys or Ile did not affect the IPSC decay time, we propose the Leu mutation specifically affects a molecular interaction responsible for the prolonged IPSC time courses. Thus, it would be of interest to identify this molecular interaction.

The importance of α2 GlyR activation in neuronal migration and cortical network formation has already been established. Thus, mutations that affect a2 glyR activation might lead to aberrant neurodevelopment, and hence could conceivably lead to autism. Further experiments are required to establish whether the aberrant glycinergic signaling caused by the R350L mutation may lead to cortical neuronal migration and maturation defects that account for the etiology of autism.

6. Probing the Zn^{2+} concentration in glycinergic synaptic cleft.

It is generally accepted that free Zn^{2+} is concentrated into presynaptic vesicles at many brain glutamatergic synapses and is co-released with neurotransmitter into the synaptic cleft by nerve terminal stimulation. However, phasically released Zn^{2+} at glycinergic synapses is more questionable and the peak Zn^{2+} concentration in the synaptic cleft is more debatable. We generated 'artificial' synapses expressing α1β, $\alpha1^{H107N}\beta$ and $\alpha1^{W170S}\beta$ GlyRs with different Zn^{2+} sensitivities. By comparing the effects of Zn^{2+} chelator, tricine, on IPSCs to the effects of co-applied glycine plus free Zn^{2+} to macropatches, we inferred that synaptic Zn^{2+} rises to at least 1 μM following a single

presynaptic stimulation. Moreover, using the fast high-affinity chelator, ZX1, we found no evidence for tonic Zn^{2+} bound constitutively to high affinity GlyR sites, indicating diffusible Zn^{2+} is likely to be phasically released at glycinergic synapses.

Our experiments provide a preliminary estimation of free Zn^{2+} concentration in the glycinergic synaptic cleft, and a most likely mechanism for Zn^{2+} modulation of glycinergic neurotransmission. Clearly, more detailed investigations are needed. Most importantly, where does the Zn^{2+} come from at glycinergic synapses? Whether the Zn^{2+} and glycine are co-released from presynaptic terminals, or through spillover of Zn^{2+} from neighbouring glutamatergic synapses in the mammalian spinal cord remains unsolved. Whether extrasynaptic GlyRs are also subject to Zn^{2+} modulation is unclear. In addition, the time course of Zn^{2+} in the synapse still needs to be determined and this could help us better evaluate the Zn^{2+} effects on neuronal physiology.

REFERENCES:

Chen X, Webb TI, Lynch JW (2009) The M4 transmembrane segment contributes to agonist efficacy differences between alpha1 and alpha3 glycine receptors. Molecular membrane biology 26:321-332.

Ehrensperger MV, Hanus C, Vannier C, Triller A, Dahan M (2007) Multiple association states between glycine receptors and gephyrin identified by SPT analysis. Biophysical Journal 92:3706-3718.

Fritschy JM, Harvey RJ, Schwarz G (2008) Gephyrin: where do we stand, where do we go? Trends in Neurosciences 31:257-264.

Fuchs C, Abitbol K, Burden JJ, Mercer A, Brown L, Iball J, Anne Stephenson F, Thomson AM, Jovanovic JN (2013) GABA(A) receptors can initiate the formation of functional inhibitory GABAergic synapses. Eur J Neurosci 38:3146-3158.

Graham BA, Schofield PR, Sah P, Margrie TW, Callister RJ (2006) Distinct physiological mechanisms underlie altered glycinergic synaptic transmission in the murine mutants spastic, spasmodic, and oscillator. J Neurosci 26:4880-4890.

Han L, Talwar S, Wang Q, Shan Q, Lynch JW (2013) Phosphorylation of alpha3 glycine receptors induces a conformational change in the glycine-binding site. ACS chemical neuroscience 4:1361-1370.

Harvey RJ, Depner UB, Wassle H, Ahmadi S, Heindl C, Reinold H, Smart TG, Harvey K, Schutz B, Abo-Salem OM, Zimmer A, Poisbeau P, Welzl H, Wolfer DP, Betz H, Zeilhofer HU, Muller U (2004) GlyR alpha3: an essential target for spinal PGE2-mediated inflammatory pain sensitization. Science 304:884-887.

Hirzel K, Muller U, Latal AT, Hulsmann S, Grudzinska J, Seeliger MW, Betz H, Laube B (2006) Hyperekplexia phenotype of glycine receptor alpha1 subunit mutant mice identifies Zn(2+) as an essential endogenous modulator of glycinergic neurotransmission. Neuron 52:679-690.

Manley S, Gillette JM, Lippincott-Schwartz J (2010) Single-particle tracking photoactivated localization microscopy for mapping single-molecule dynamics. Methods Enzymol 475:109-120.

Schwale C, Schumacher S, Bruehl C, Titz S, Schlicksupp A, Kokocinska M, Kirsch J, Draguhn A, Kuhse J (2016) KCC2 knockdown impairs glycinergic synapse maturation in cultured spinal cord neurons. Histochem Cell Biol 145:637-646.

Appendices

Methods

Generation of functional inhibitory synapses incorporating defined combinations of GABA(A) or glycine receptor subunits

Christine L. Dixon[1,3], Yan Zhang[1], & Joseph W. Lynch[1,2]

[1]Queensland Brain Institute and [2]School of Biomedical Sciences, University of Queensland, Brisbane QLD Australia 4072.

[3]Current address: Institute of Neurology, University College London, London, UK.

Running title: *Generation of recombinant inhibitory synapses*

Correspondence to: Professor Joseph Lynch, Queensland Brain Institute, University of Queensland, Brisbane, QLD 4072, Australia. Phone: +617 33466375, Email: j.lynch@uq.edu.au

Keywords: Inhibitory postsynaptic current, IPSC, GABAergic, glycinergic, neuropharmacology, synaptogenesis, electrophysiology.

Abstract: Fast inhibitory neurotransmission in the brain is mediated by wide range of $GABA_A$ receptor ($GABA_AR$) and glycine receptor (GlyR) isoforms, each with different physiological and pharmacological properties. Because multiple isoforms are expressed simultaneously in most neurons, it is difficult to define the properties of inhibitory postsynaptic currents mediated by individual isoforms in vivo. Although recombinant expression systems permit the expression of individual isoforms in isolation, they require exogenous agonist application which cannot mimic the dynamic neurotransmitter profile characteristic of native synapses. We describe a neuron-HEK293 cell co-culture technique for generating inhibitory synapses incorporating defined combinations of $GABA_AR$ or GlyR subunits. Primary neuronal cultures, prepared from embryonic rat cerebral cortex or spinal cord, are used to provide presynaptic GABAergic and glycinergic terminals, respectively. When the cultures are mature, HEK293 cells expressing the subunits of interest plus neuroligin 2A are plated onto the neurons, which rapidly form synapses onto HEK293 cells. Patch clamp electrophysiology is then used to analyze the physiological and pharmacological properties of the inhibitory postsynaptic currents mediated by the recombinant receptors. The method is suitable for investigating the kinetic properties or the effects of drugs on inhibitory postsynaptic currents mediated by defined $GABA_AR$ or GlyR isoforms of interest, the effects of hereditary disease mutations on the formation and function of both types of synapses, and synaptogenesis and synaptic clustering mechanisms. The entire cell preparation procedure takes 2 – 5 weeks.

INTRODUCTION

The central nervous system is comprised of circuits of interconnected neurons that serve to process specific types of information. These circuits regulate their own output by feedback and feedforward connections. Knowledge of the physiological properties of the inhibitory and excitatory synapses that mediate these connections is crucial for understanding the electrical behavior of circuits and ultimately of brain function. Fast inhibitory neurotransmission in these circuits is mediated by GABA type-A receptor ($GABA_AR$) and glycine receptor (GlyR) chloride channels.

$GABA_ARs$ exhibit a particularly broad range of heterogeneity. As members of the pentameric ligand-gated ion channel (pLGIC) family, five subunits are required to form a single functional oligomer. There are 19 $GABA_AR$ genes ($\alpha1 - 6$, $\beta1 - 3$, $\gamma1 - 3$, δ, ε, θ, π and $\rho1 - 3$) with the most common synaptic isoform comprising $\alpha1$, $\beta2$ and $\gamma2$ subunits in a 2:2:1 stoichiometry. Although many hundreds of other subunit combinations are theoretically possible, it is thought that around one hundred exist naturally in the brain (Olsen and Sieghart, 2009). GlyRs exhibit far less diversity with only four genes ($\alpha1 - 3$, β) in humans (Lynch, 2009). They also belong to the pLGIC family and synaptic GlyR isoforms comprise heteromeric assemblies of α and β subunits in a 2:3 or 3:2 stoichiometry (Durisic et al., 2012; Yang et al., 2012).

Each $GABA_AR$ or GlyR isoform has a unique physiological and pharmacological profile and it is the unique properties of a particular isoform that are important for the appropriate functioning of a particular network. Disruptions to these properties can result in neurological disorders. For example, hereditary mutations that affect the function of $GABA_ARs$ or GlyRs can lead to epilepsy (Macdonald et al., 2010) or human hyperekplexia (Bode and Lynch, 2014), respectively. Other disruptive mechanisms are also possible. For example, a post-transcriptional RNA editing mechanism that is upregulated in temporal lobe epilepsy increases the prevalence of $\alpha3$ GlyRs incorporating the P185L mutation (Meier et al., 2005; Eichler et al., 2008; Eichler et al., 2009). Finally, a range of neurological disorders is known to result from aberrant changes to pLGIC phosphorylation status (Talwar and Lynch, 2014). For example, chronic pain sensitization is caused by prostaglandin-induced phosphorylation of $\alpha3$ GlyRs (Harvey et al., 2004; Zeilhofer, 2005; Lynch and Callister, 2006) and ethanol-induced phosphorylation of the $\gamma2$ $GABA_AR$ subunit contributes to alcoholism (Qi et al., 2007).

Thus, characterising the physiological and pharmacological properties of defined $GABA_AR$ and GlyR isoforms under synaptic activation conditions is essential for understanding how neuronal circuits function in health and disease. However, it is difficult to study individual isoforms in their native neuronal environment due to the multitude of other isoforms present, and the difficulty in

pharmacologically or genetically isolating the receptor isoform of interest. The neuron-HEK293 cell co-culture protocols we describe here solve this problem by providing a simple, efficient means of generating functional recombinant inhibitory synapses that selectively incorporate the recombinant $GABA_AR$ or GlyR isoform of interest. A key step is to express neuroligin 2A in the HEK293 cells in order to promote synaptogenesis (Bemben et al., 2015). To generate glycinergic synapses, we also expressed gephyrin, a postsynaptic microtubular-binding protein essential for anchoring GlyRs to synapses (Meyer et al., 1995; Meier et al., 2000).

Co-culture approaches have previously been developed to understand the roles of synaptic adhesion molecules (including neurexin and neuroligin) in the formation of glutamatergic or GABAergic synapses (Scheiffele et al., 2000; Biederer et al., 2002; Dean et al., 2003; Graf et al., 2004; Sara et al., 2005; Kim et al., 2006; Dong et al., 2007; Fuchs et al., 2013) or to investigate the impact of disease-causing neuroligin mutations on GABAergic synaptogenesis (Chubykin et al., 2005; Sun et al., 2011). They have also been employed to characterise the functional properties of inhibitory post-synaptic currents (IPSCs), and have revealed kinetic differences among different $GABA_AR$ isoforms (Wu et al., 2012; Dixon et al., 2014) and GlyR isoforms (Zhang et al., 2014).

The original co-culture protocol, involving postnatal hippocampal neurons and transfected HEK293 cells, was optimized for the immunohistochemical analysis of glutamatergic and GABAergic synapse development (Biederer and Scheiffele, 2007). A more recent protocol outlined an improved procedure for generating recombinant GABAergic synapses between striatal medium spiny GABAergic neurons and transfected HEK293 cells (Brown et al., 2014). However, this was also optimized for monitoring synapse development rather than for recording IPSCs in mature synapses. We have extended the co-culture approach in three ways. First, we describe the first spinal neuron-HEK293 cell co-culture preparation suitable for the efficient generation of recombinant glycinergic synapses. Second, we have simplified the technique for creating GABAergic synapses by using embryonic cortical neurons grown in serum-free media that does not promote the growth of glia (Brewer et al., 1993; Brewer, 1995). We have also have optimized the technique to facilitate the electrophysiological analysis of GABAergic and glycinergic IPSCs.

MATERIALS AND METHODS

Overview

Protocols for all procedures described in this study are detailed in the supplementary information. Lists of reagents and equipment are also provided. An overview of the co-culture procedure is presented in Figure 1. The cerebral cortex contains large populations of GABAergic interneurons that were used to provide presynaptic GABAergic terminals onto HEK293 cells that

recombinantly express the $GABA_AR$ subunits of interest. Similarly, spinal neurons contain large populations of glycinergic interneurons that were used to provide glycinergic presynaptic terminals onto HEK293 cells expressing GlyR subunits of interest. The main steps in preparing the neuronal cultures are summarized in Figure 1 (blue box). The steps involved in HEK293 cell transfection are also described in Figure 1 (green box).

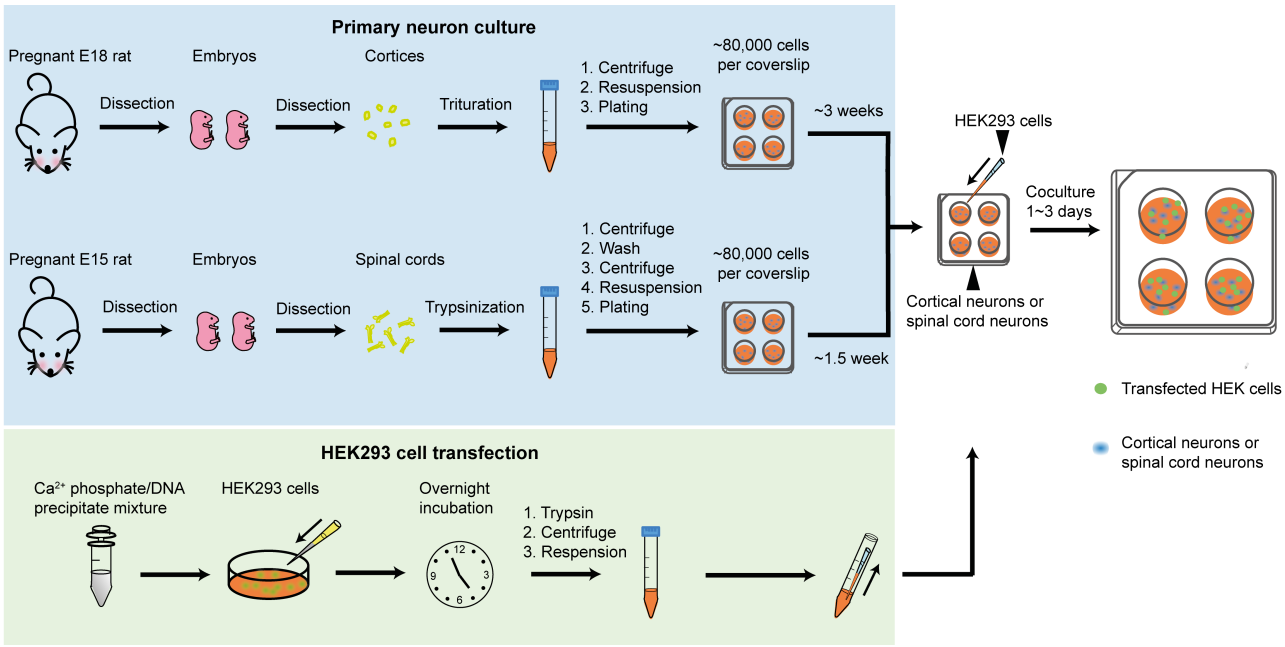

Figure 1. Overview of the co-culture method. The blue box describes the steps involved in preparing neuronal cultures (GABAergic in upper row, glycinergic in lower row). The green box describes the steps involved in transfecting HEK293 cells. The unshaded section (right) illustrates the final step involving HEK293 cells being plated onto the cultured neurons.

Preparation of neuron cultures

Euthanasia of timed-pregnant rats was performed via CO_2 inhalation, in accordance with procedures approved by the University of Queensland Animal Ethics Committee. To produce GABAergic interneuron cultures, E18 rat embryos were surgically removed from timed-pregnant rats and placed into chilled Ca-Mg-free Hank's Balanced Salt Solution (CMF-HBSS) under sterile conditions. The cortical neuronal tissue was then pinched off using fine forceps, taking care to peel away the meninges to keep glial cell numbers down. The dissected neurons were then triturated, centrifuged and resuspended in Dulbecco's Modified Eagles Medium supplemented with 10 % fetal bovine serum (DMEM-FBS). To produce glycinergic interneuron cultures, E15 rat embryos were surgically removed and placed into ice cold CMF-HBSS under sterile conditions. The spinal cords were then removed and pinned at the wider proximal end while meninges were carefully detached. The dissected neurons were then triturated, centrifuged and resuspended in DMEM-FBS.

In both cases, the cells were then counted and between 40,000 – 80,000 neurons were plated

onto each 12 mm poly-D-lysine-coated coverslip in 4-well plates. As previously noted, neuronal density is a key consideration: if it is too low it impairs neuronal survival and if it is too high it encourages neuron clumping (Fuchs et al., 2013). Neuronal cultures were always maintained in a 5 % CO_2 incubator at 37 ^{o}C. After 24 h the entire DMEM-FBS medium was replaced with Neurobasal medium including 2 % B27 and 1 % GlutaMAX supplements. A second (and final) feed 1 wk later replaced half of this medium. In contrast to a previous protocol (Fuchs et al., 2013), we found that antibiotics were unnecessary. Neurons were used in co-culture experiments between 3 – 6 wk later (for GABAergic co-cultures) or 1 – 4 wk later (for glycinergic co-cultures).

Culture and transfection of HEK293 cells

HEK293 cells were cultured in T75 flasks in DMEM-FBS and maintained in a 5 % CO_2 incubator at 37 ^{o}C. The cells were passaged weekly. Prior to transfection, they were trypsinized and plated onto 35 mm culture dishes at a density of 5000 cells/dish. Following overnight incubation, the cells were transfected via a calcium phosphate co-precipitation protocol, using a total of 0.5 – 2.5 μg DNA per dish. Then, following incubation for 5 – 20 hr in a 3% CO_2 incubator, the transfection was terminated by washing twice with divalent cation-free phosphate buffered saline. The cells were then trypsinized, centrifuged and resuspended in Neurobasal medium (including 2% B27 and 1% GlutaMAX supplements) then seeded onto the neurons. One 35 mm dish of HEK293 cells was sufficient to seed 4 coverslips of neurons. Once seeded with HEK293 cells, the co-cultures were returned to the incubator overnight to allow synapses to form. Cultures were used for patch clamp recording over the following 2 – 3 days.

Plasmid DNA

A total of 0.5 – 2.5 μg plasmid DNA should be added to each 35 mm dish of HEK293 cells. This amount may vary according to the individual plasmid expression efficiency, the number and ratios of plasmids to be transfected and the transfection method. When using a calcium phosphate co-precipitation protocol, our recommendations are as follows. When expressing synaptic GlyRs, the total plasmid DNA should comprise: 0.2 μg neuroligin 2A, 0.2 μg gephyrin, 0.1 μg EGFP, with the remainder comprising GlyR subunit DNA that varies according to the number of subunits and the ratio of subunit DNA required. For example, when transfecting GlyR α subunits as homomers, add 0.5 μg DNA. When transfecting α and β GlyR subunits in 1:10 or 1:50 ratios add a total of 2 μg DNA. We recommend transfecting α1:β, α2:β and α3:β subunits in 1:50, 1:50 and 1:10 ratios, respectively (Zhang et al., 2014). When expressing α1β2γ2 $GABA_A$Rs, the α1, β2, γ2, EGFP and

neuroligin 2A plasmid DNAs should be transfected in a 1:1:4:1:1 ratio with a combined total of 0.5 μg DNA.

In experiments described in Figures 2 and 3, we employed plasmid DNAs encoding the human α1 (pCIS), rat α3L (pcDNA3.1) and human β (pcDNA3.1) GlyR subunits, plus mouse neuroligin 2A (pNice) and rat gephyrin P1 (pCIS). In experiments described in Figure 4, we employed human α2 (pcDNA3.1), human α4 (pCIS), β2 (pcDNA3.1) and γ2L (pcDNA3.1) $GABA_AR$ subunits, plus mouse neuroligin 2A (pNice). Site-directed mutagenesis was performed using the QuikChange mutagenesis kit (Agilent Technologies) according to manufacturers' instructions and the successful incorporation of mutations was confirmed by DNA sequencing.

Patch clamp electrophysiology and data analysis

Standard patch-clamp electrophysiology equipment can be used, with the only specific requirement being a fluorescence microscope for identifying GFP fluorescent cells. Coverslips containing the co-cultured cells were placed gently into the recording chamber on the microscope stage and perfused continuously with an extracellular solution comprising (in mM): 140 NaCl, 5 KCl, 2 $CaCl_2$, 1 $MgCl_2$, 10 HEPES, and 10 D-glucose, adjusted to pH 7.4 with NaOH. Patch pipettes were filled with an intracellular solution containing (in mM): 145 CsCl, 2 $CaCl_2$, 2 $MgCl_2$, 10 HEPES, 10 EGTA and 2 MgATP, adjusted to pH 7.4 with NaOH. HEK293 cell selection is largely a matter of trial and error. A good starting point is to select large, strongly fluorescent green cells that are closely surrounded by many neurons, especially small clumps of neurons. Cells with a textured (rather than smooth) appearance often yield abundant IPSCs.

The electrophysiological techniques may vary according to the experimental requirements. For example, if precise quantitation of rise times is required, it is extremely important that the filtering and digitisation rates are high and that pipette series resistance is low to avoid artefactually slowing down the event. In contrast, testing the effect of a drug on IPSC decay rate is less sensitive to filtering, and it may be necessary to use higher resistance pipettes to obtain a membrane seal that is stable enough to permit recordings that are long enough to apply and wash out the drug.

In all experiments described below, series resistance was compensated to 60 % of maximum and was monitored throughout the recording. Spontaneous and action potential-evoked IPSCs in HEK293 cells were recorded at a holding potential −60 mV and currents were filtered at 4 kHz and sampled at 10 kHz. Only cells with a stable series resistance of <25 MΩ throughout the recording period were included in the analysis. Patch pipettes (4 – 8 MΩ resistance) were made from borosilicate glass (GC150F-7.5, Harvard Apparatus). Analyses of IPSC amplitude, 10 – 90% rise time, and decay time constant (single-exponential) were performed using Axograph X (Axograph Scientific). Single peak IPSCs with amplitudes of at least three times above the background noise

were detected using a semi-automated sliding template. Each detected event was visually inspected and only well-separated IPSCs with no inflections in the rising or decay phases (suggestive of superimposed events) were included. The respective parameters from all selected events from a single cell were averaged and are presented as a single data point in Figures 2 – 4. The averages from multiple cells were then pooled to obtain group data. Statistical analysis and plotting were performed on group data with Prism 5 (GraphPad Software). All data are presented as mean ± SEM. One-way and two-way ANOVA were employed for multiple comparisons. For all tests, the number of asterisks corresponds to level of significance: $*p < 0.05$, $**p < 0.01$, $***p < 0.001$ and $****p < 0.0001$.

RESULTS

Glycinergic IPSCs

While we found that some co-cultures exhibited spontaneous activity in almost all green fluorescent HEK293 cells, it was more typical to observe spontaneous glycinergic IPSCs in around 20 % of cells. This success rate is adequate for most experiments.

It is important to establish that the spontaneous IPSCs produced by the co-culture synapses exhibit similar characteristics to those mediated by native synapses incorporating the same subunits. Figure 2a shows sample IPSC recordings from HEK293 cells expressing α1β GlyRs. An IPSC averaged from >200 events recorded from multiple cells is shown in Figure 2b. Mean amplitudes, 10 – 90 % rise times and decay time constants are presented in Figure 2c. Frequency distributions of IPSC amplitudes, 10 – 90% rise times and decay time constants all exhibit monotonic distributions suggesting a single functional population of synapses (Figure 2c). In adult hypoglossal motor neurons, where the α1β GlyR isoform predominates (Lynch, 2009), the 10 – 90 % rise times and decay time constants range between 0.6 – 1.8 and 4.9 – 7.7 ms, respectively (Singer et al., 1998; Graham et al., 2006; Hirzel et al., 2006; Muller et al., 2006). The mean decay time constant (9.3 ms) and the 10 – 90 % rise time (1.9 ms) recorded in our co-culture synapses correspond well with these results.

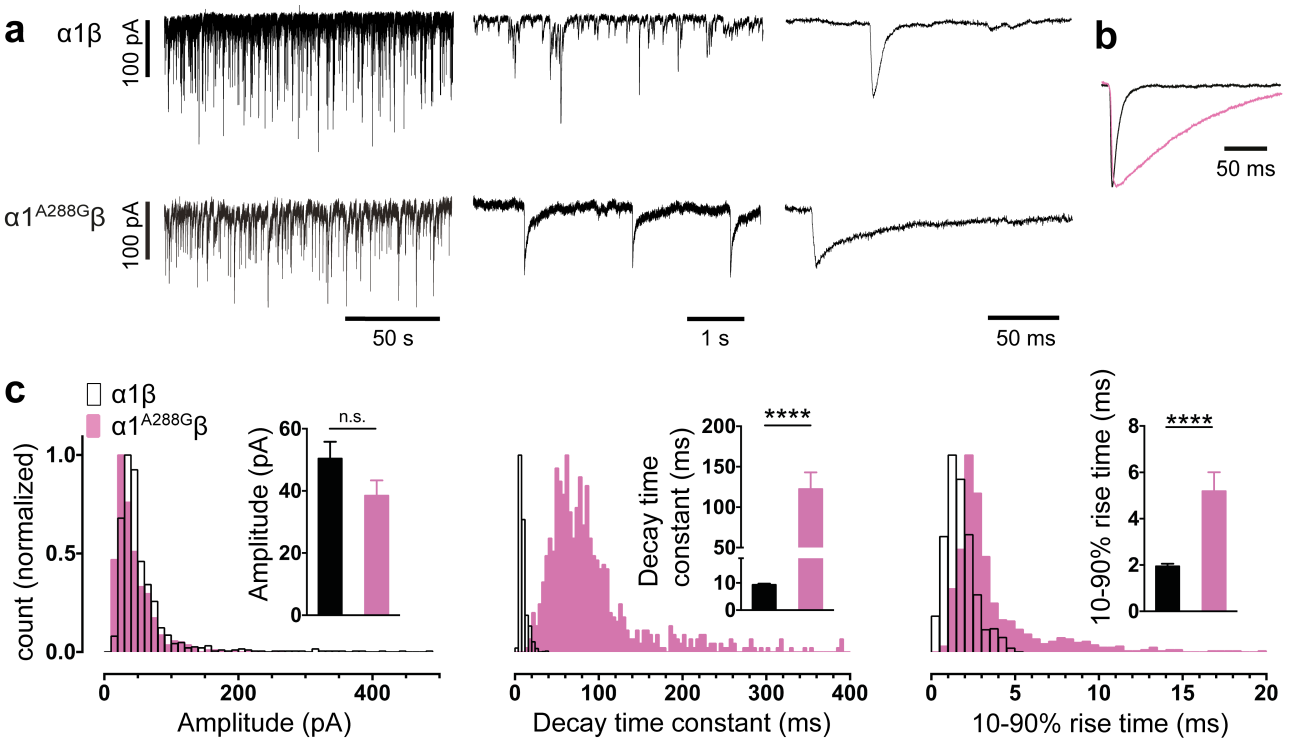

Figure 2. Comparison of the properties of spontaneous glycinergic IPSCs mediated by α1β GlyRs (in black) and $\alpha1^{A288G}\beta$ GlyRs (in pink). (**a**) Sample voltage-clamp recordings at three different time scales for both isoforms. (**b**) Mean IPSC waveforms, each averaged from >200 events from a single cell. (**c**) Mean values and distribution histograms for the peak amplitudes, 10 – 90% rise times and decay time constants of IPSCs recorded from α1β and $\alpha1^{A288G}\beta$ GlyRs. Each data point represents the mean of all IPSCs recorded from a single cell. *$p < 0.05$, ****$p <$ 0.0001 relative to α1β GlyRs.

We performed a similar analysis on α3β co-culture synapses and found the mean IPSC rise and decay times to be remarkably similar to those mediated by α1β GlyRs (Figure 3a – c). These parameters were also distributed monotonically, again suggesting a single population of synapses (Figure 3c). Although α3β-mediated IPSCs have yet to be recorded in isolation in native neurons, evidence to date suggests their rise and decay times are indistinguishable from those mediated by α1β GlyRs (Harvey et al., 2004). This fits well with the results from our engineered synapses.

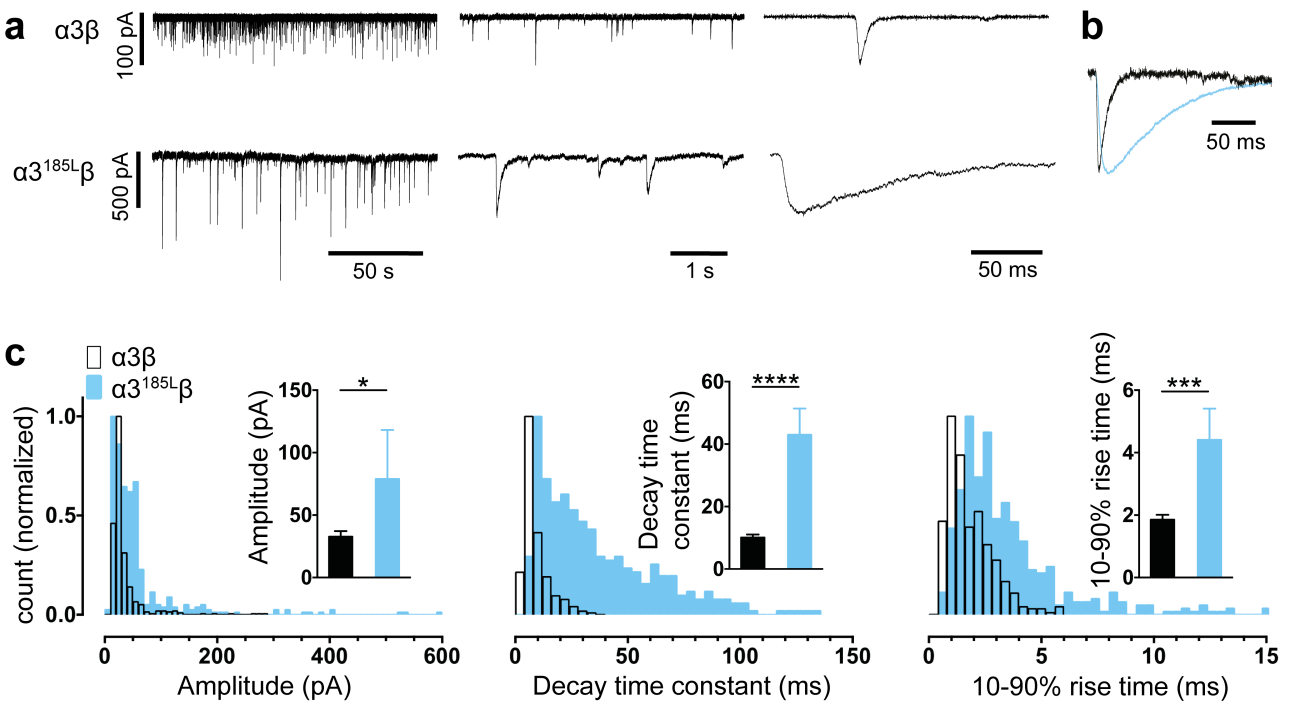

Figure 3. Comparison of the properties of spontaneous glycinergic IPSCs mediated by α3β GlyRs (in black) and $\alpha3^{185L}\beta$ GlyRs (in blue). (**a**) Sample voltage-clamp recordings at three different time scales for both isoforms. (**b**) Mean IPSC waveforms, each averaged from >200 events from a single cell. (**c**) Mean values and distribution histograms for the peak amplitudes, 10 – 90% rise times and decay time constants of IPSCs recorded from α1β and $\alpha3^{185L}\beta$ GlyRs. Each data point represents the mean of all IPSCs recorded from a single cell. *$p < 0.05$, ****$p < 0.0001$ relative to α3β GlyRs.

The α1 GlyR subunit D80A and A52S mutations result in startle disease phenotypes in mice (Graham et al., 2006; Hirzel et al., 2006). We previously demonstrated that engineered synapses incorporating $\alpha1^{D80A}\beta$ and $\alpha1^{A52S}\beta$ GlyRs exhibited accelerated IPSC decay rates closely resembling those recorded in native synapses from mutant mice homozygous for these mutations (Zhang et al., 2014). This provides an important validation of our technique. In this study we sought to determine whether GlyRs may be located both synaptically and peri-synaptically in HEK293 cells by introducing mutations that dramatically enhanced the glycine sensitivity. We reasoned that if GlyRs are located peri-synaptically then enhancing their glycine sensitivity may render them susceptible to activation by synaptically released glycine, and if so this should be detectable as an additional slow rise time component (Wu et al., 2012). As noted above, $\alpha3^{185L}$ results from a post-transcriptional RNA editing mechanism that is upregulated in (and is causative of) human temporal lobe epilepsy (Eichler et al., 2009; Winkelmann et al., 2014). This mutation reduces the glycine EC_{50} from 70.9 to 7.4 μM (Legendre et al., 2009). We also investigated the $\alpha1^{A288G}$ mutation (which is not associated with a disease) because it reduces the glycine EC_{50} from 30.9 to 6.0 μM (Lynagh and Lynch, 2010).

As shown in Figure 2a – c, IPSCs mediated by $\alpha1^{A288G}\beta$ GlyRs exhibited significantly slower rise times and decay time constants, although additional slow components suggestive of peri-synaptic receptors were never observed on the rising phase of IPSCs. As with unmutated α1β GlyRs, the rise and decay times were monotonically distributed (Figure 2c) suggesting a single postsynaptic receptor population. Similarly, Figure 3a – c shows that IPSCs mediated by $\alpha3^{185L}\beta$ GlyRs also exhibited significantly slower rise times and decay time constants that were distributed monotonically. We were not able to unequivocally distinguish a putative peri-synaptic GlyR population in either case.

GABAergic IPSCs

As with glycinergic IPSCs, we typically observed GABAergic IPSCs in around 20 % of HEK293 cells. The rise times and decay time constants of IPSCs recorded from the dominant (α1β2γ2) synaptic subtype (1.2 and 4.0 ms, respectively) are in close accordance with those recorded from neurons known to predominantly express this subtype (Dixon et al., 2014). The co-culture system has revealed that other $GABA_AR$ subunit combinations can yield IPSCs with dramatically different rise and decay times (Wu et al., 2012; Dixon et al., 2014), although it is as yet unclear how these properties relate to those of the same isoforms when expressed in native neuronal synapses.

We have previously demonstrated that the effects of some clinically important drugs on co-culture GABAergic synaptic IPSCs are similar to those recorded at corresponding neuronal synapses. For example, 1 μM diazepam or 0.1 μM flunitrazepam significantly increased the decay time constants of IPSCs mediated by α2-containing $GABA_ARs$ (Dixon et al., 2014) and 1 μM zolpidem or 1 μM eszopiclone increased IPSC magnitudes and decay time constants of IPSCs mediated by α1-containing $GABA_ARs$ (Dixon et al., 2015). Here we extended this characterisation by performing a 'reciprocal' pharmacological comparison of α2β2γ2 and α4β2γ2 $GABA_ARs$, based on the knowledge that α4-containing $GABA_ARs$ are highly sensitive to ethanol and insensitive to benzodiazepines, whereas α2-containing $GABA_ARs$ have the opposite profile (Knoflach et al., 1996; Wallner et al., 2006). As shown in Figure 4a and b, IPSCs mediated by recombinant α2β2γ2 and α4β2γ2 $GABA_ARs$ exhibit identical amplitudes, 10 – 90 % rise times and decay time constants. A physiologically relevant (10 mM) ethanol concentration significantly increased the IPSC decay time constant in α4β2γ2 $GABA_ARs$ whereas 1 μM diazepam had no effect (Figure 4c, d). On the other hand, 1 μM diazepam significantly prolonged the IPSC decay time constant in α2β2γ2 $GABA_ARs$ (Dixon et al., 2014), whereas even a very high (30 mM) ethanol concentration had no effect (Figure 4d).

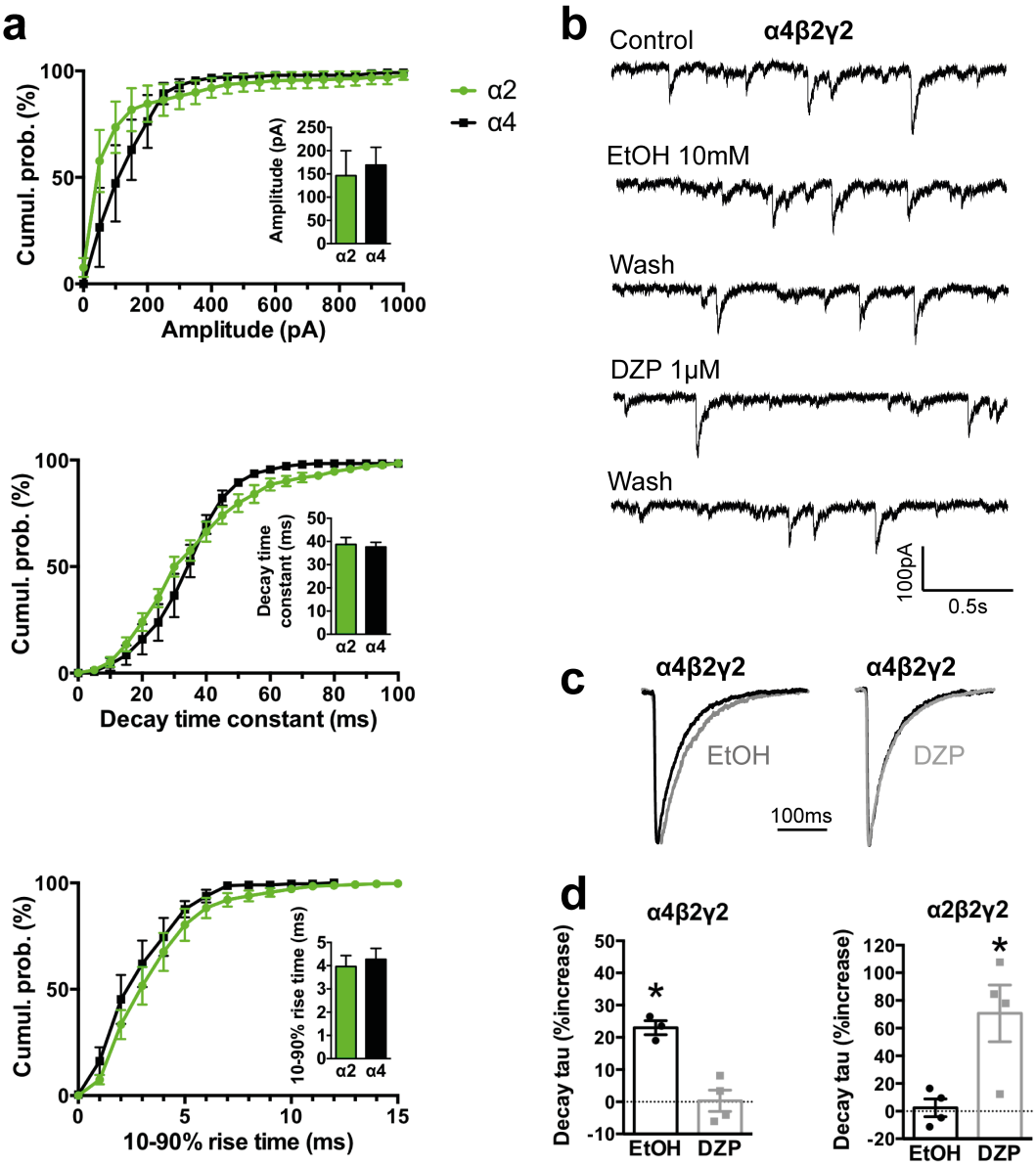

Figure 4. Comparison of kinetics and pharmacological properties of IPSCs mediated by α2β2γ2 and α4β2γ2 $GABA_A$Rs. (**a**) Cumulative probability data averaged from 4 cells expressing α4β2γ2 $GABA_A$Rs were compared to previously published data for α2β2γ2 $GABA_A$Rs (n = 7) (Dixon et al., 2014). We found no significant differences in IPSC amplitudes, 10 – 90 % rise times or decay time constants. (**b**) Sample recordings of spontaneous IPSCs mediated by α4β2γ2 $GABA_A$Rs before and after the application of 10 mM ethanol and 1 μM diazepam. (**c**) Examples of mean IPSC waveforms mediated by α4β2γ2 $GABA_A$Rs, each averaged from >100 events from a single cell, before and after the application of 10 mM ethanol or 1 μM diazepam. (**d**) The decay time constants of IPSCs mediated by α4β2γ2 $GABA_A$Rs were significantly prolonged by 10 mM ethanol but not by 1 μM diazepam (left panel). In contrast, IPSCs mediated by α2β2γ2 $GABA_A$Rs were significantly prolonged by 1 μM diazepam but not by 30 mM ethanol (right panel). Diazepam data for α2β2γ2 $GABA_A$Rs were reproduced from (Dixon et al., 2014). *$p < 0.05$ relative to drug-free control in same cell.

DISCUSSION

Applications of the protocol

We have described protocols for reliably generating recombinant inhibitory synapses that incorporate defined GlyR or $GABA_AR$ isoforms of interest. These are suitable for investigating (1) the kinetics of IPSCs mediated by defined $GABA_AR$ or GlyR isoforms, (2) the effects of drugs on IPSCs mediated by defined $GABA_AR$ or GlyR isoforms, (3) the effect of posttranslational modifications (e.g., phosphorylation) and hereditary disease mutations on the formation and function of both types of synapses, and (4) synaptogenesis and synaptic clustering mechanisms in both types of synapses. We now expand on each of these points.

IPSC kinetics

IPSCs mediated by different synaptic $GABA_AR$ or GlyR isoforms exhibit unique physiological and pharmacological profiles. It is useful to quantitate these properties because they may help in identifying the presence, or even the role, of a particular isoform in a particular neuron and also because accurate parameters provide key inputs into computational models of neuron or network function. Although studying recombinant receptors in standard heterologous expression systems such as HEK293 cells or *Xenopus* oocytes allows the electrophysiological properties of a single isoform to be studied in isolation, this approach is limited because the neurotransmitter must be applied artificially and it cannot mimic the fast (μs) dynamic neurotransmitter concentration profile that exists in the synaptic cleft.

Investigating drug efficacy and selectivity

The $GABA_AR$ is an established therapeutic target for clinical indications including epilepsy, anxiolysis, muscle spasms, sedation and anaesthesia. $GABA_AR$-targeted drugs currently in clinical use are not strongly subtype-selective and this can lead to dose-limiting side effects. For example, diazepam produces effective anxiolysis by positively modulating α2-containing $GABA_ARs$, although it also elicits the side effect of sedation by modulating α1-containing $GABA_ARs$ (Trincavelli et al., 2012). Drugs specific for other isoforms are also being sought. For example, selective modulators of α5-containing $GABA_ARs$ are being developed for a range of indications including stroke, cognitive impairment and schizophrenia (Soh and Lynch, 2015). Although GlyRs are not currently targeted by clinically useful drugs, molecules that selectively enhance α3-containing GlyRs are considered promising as new generation treatments for chronic pain (Zeilhofer, 2005; Lynch and Callister, 2006). When evaluating new molecules as potential therapeutic lead compounds for synaptically-localised receptors, it is important to test their potency, efficacy and subtype-selectivity under realistic synaptic activation

conditions. The system we describe provides the most definitive means available of evaluating drug efficacy and selectivity at IPSCs mediated by defined receptor isoforms.

Investigating disease mutations

Engineered synapses have yet to be used to study disease-causing $GABA_AR$ mutations or modifications, and hence, the method has not realised its full potential as a model system for understanding the molecular pathology of neurological disorders. Mutations in $GABA_AR$ α1 and γ2 subunits have long been associated with genetic epilepsy syndromes (Macdonald et al., 2010). Thus far, the function and pharmacology of epilepsy-causing mutant $GABA_ARs$ have only been investigated using whole-cell recordings of steady-state GABA-activated currents in heterologous expression systems. The differing approaches that have been used to analyze the effects of these mutations have led to controversy, particularly in the case of the $\gamma2^{R43Q}$ mutation (Petrou and Reid, 2012). Moreover, of all the identified epilepsy-causing mutant $GABA_ARs$ that exhibit partial or full expression at the cell membrane, there is an animal knock-in model of only one (Petrou and Reid, 2012). Transgenic animal models are afflicted by compensatory mechanisms that can obfuscate data, especially those involving ion channel genetic manipulations that affect GABAergic transmission (Harris et al., 2011). Because engineered α1β2γ2 $GABA_AR$ synapses successfully recapitulate the kinetics of neuronal IPSCs (Dixon et al., 2014), they may provide a promising means of investigating the synaptic signaling defects induced by hereditary epilepsy mutations to α1 and γ2 subunits.

Glycinergic co-culture synapses incorporating $\alpha1^{D80A}\beta$ and $\alpha1^{A52S}\beta$ GlyRs have been shown to exhibit accelerated IPSC decay rates that strongly resemble those recorded in native synapses from mutant mice homozygous for the same mutations (Zhang et al., 2014). This suggests that the co-culture system should be useful for modelling the effects of hyperekplexia mutations to α1 and β subunits (Bode and Lynch, 2014) and autism mutations to α2 subunits (Pilorge et al., 2015).

Here we investigated the disease-relevant $\alpha3^{185L}$ GlyR under synaptic activation conditions. The P185L substitution results from an RNA-editing mechanism and the incidence of the edited receptors in the hippocampus is increased in patients with temporal lobe epilepsy (Meier et al., 2005; Eichler et al., 2008; Eichler et al., 2009). Although glycinergic synapses are absent in the hippocampus, α3L GlyRs are located presynaptically at glutamatergic synapses (Eichler et al., 2009; Kubota et al., 2010; Winkelmann et al., 2014). As these GlyRs are excitatory due to the collapsed transmembrane chloride gradient, upregulation of RNA-edited $\alpha3^{185L}$ GlyRs would increase the depolarisation of presynaptic terminals (and thus increase glutamate release) due to longer channel

open times (Winkelmann et al., 2014). The resulting alteration in network activity not only leads to recurrent epileptiform discharge but also to cognitive dysfunction and memory deficits (Meier et al., 2014; Winkelmann et al., 2014). Our results demonstrate that the synaptically-localised RNA-edited GlyRs remain open for longer during each synaptic event.

Synaptogenesis and synaptic clustering mechanisms

Co-culture synapses have been used extensively to probe the roles of synaptic adhesion molecules in the formation of glutamatergic or GABAergic synapses (Scheiffele et al., 2000; Biederer et al., 2002; Dean et al., 2003; Graf et al., 2004; Sara et al., 2005; Kim et al., 2006; Dong et al., 2007; Fuchs et al., 2013) or to investigate the impact of disease-causing neuroligin mutations on GABAergic synaptogenesis (Chubykin et al., 2005; Sun et al., 2011). The strengths and weaknesses of co-cultures in this respect have recently been reviewed (Fuchs et al., 2013).

Conclusions

As the presynaptic terminals of our engineered synapses are provided by neurons, their function is likely to resemble those of synapses *in vivo*. Indeed, serial electron microscopic reconstructions of GABAergic terminals onto HEK293 cells have confirmed that their ultrastructures are similar to those of native neurons (Fuchs et al., 2013). However, the postsynaptic specializations of our engineered synapses may not resemble those of neurons given that HEK293 cells do not express all necessary postsynaptic clustering proteins at appropriate levels for synaptogenesis. Moreover, some proteins that they do express may lack neuron-specific post-translational modifications required for correct synaptic function. These factors could ultimately alter the geometry of the synaptic cleft and the postsynaptic receptor clustering density, leading to non-physiological changes in the neurotransmitter concentration profile that could affect IPSC kinetics. This uncertainty is the main limitation of the technique. To address this, we have ascertained using as many subunit combinations as possible that the physiological properties of our engineered synapses resemble those of real synapses. On the other hand, the non-physiological nature of our engineered synapses could also offer opportunities to investigate new clustering or synaptogenesis mechanisms. If, for example, substitution of a particular pLGIC subunit results in a drastic, unexpected slowing of the IPSC rise time, it is possible that synaptic receptors have been de-clustered in a manner that does not occur in neurons. This could in turn lead to the identification of novel clustering molecules and mechanisms. HEK293 cells are ideal for investigating such questions: they do not express all proteins necessary for synaptogenesis, but they do provide a high efficiency of transfection, faithful protein translation and a small, electronically-compact shape appropriate for accurate quantitation of IPSC rise and decay times (Thomas and Smart, 2005).

Supplementary information: Yes.

Acknowledgements: This research was supported by project grants from the Australian Research Council (DP120104373) and the National Health and Medical Research Council (APP1062183). JWL is supported by a Principal Research Fellowship from the National Health and Medical Research Council (APP1058542). We thank Dr. Nela Durisic for critical review of the manuscript. We thank Prof. Jochen Meier and Dr. Aline Winkelmann for kindly supplying the rat GlyR $\alpha 3L^{185L}$ plasmid DNA and Prof. Rob Harvey for the rat gephyrin P1 plasmid DNA.

Author contributions: C.L.D., Y.Z and J.W.L. conceived the project and developed the protocols; C.L.D. and Y.Z. performed experiments and analysed the data; and C.L.D., Y.Z and J.W.L. wrote the manuscript.

Competing financial interests: The authors declare no competing financial interests.

REFERENCES

Bemben, M. A., Shipman, S. L., Nicoll, R. A., and Roche, K. W. (2015). The cellular and molecular landscape of neuroligins. *Trends Neurosci* 38, 496-505.

Biederer, T., Sara, Y., Mozhayeva, M., Atasoy, D., Liu, X., Kavalali, E. T., and Sudhof, T. C. (2002). SynCAM, a synaptic adhesion molecule that drives synapse assembly. *Science* 297, 1525-31.

Biederer, T., and Scheiffele, P. (2007). Mixed-culture assays for analyzing neuronal synapse formation. *Nat Protoc* 2, 670-6.

Bode, A., and Lynch, J. W. (2014). The impact of human hyperekplexia mutations on glycine receptor structure and function. *Mol Brain* 7, 2.

Brewer, G. J. (1995). Serum-free B27/neurobasal medium supports differentiated growth of neurons from the striatum, substantia nigra, septum, cerebral cortex, cerebellum, and dentate gyrus. *J Neurosci Res* 42, 674-83.

Brewer, G. J., Torricelli, J. R., Evege, E. K., and Price, P. J. (1993). Optimized survival of hippocampal neurons in B27-supplemented Neurobasal, a new serum-free medium combination. *J Neurosci Res* 35, 567-76.

Brown, L. E., Fuchs, C., Nicholson, M. W., Stephenson, F. A., Thomson, A. M., and Jovanovic, J. N. (2014). Inhibitory synapse formation in a co-culture model incorporating GABAergic medium spiny neurons and HEK293 cells stably expressing GABAA receptors. *J Vis Exp* e52115.

Chubykin, A. A., Liu, X., Comoletti, D., Tsigelny, I., Taylor, P., and Sudhof, T. C. (2005). Dissection of synapse induction by neuroligins: effect of a neuroligin mutation associated with autism. *J Biol Chem* 280, 22365-74.

Dean, C., Scholl, F. G., Choih, J., DeMaria, S., Berger, J., Isacoff, E., and Scheiffele, P. (2003). Neurexin mediates the assembly of presynaptic terminals. *Nat Neurosci* 6, 708-16.

Dixon, C., Sah, P., Lynch, J. W., and Keramidas, A. (2014). GABAA receptor alpha and gamma subunits shape synaptic currents via different mechanisms. *J Biol Chem* 289, 5399-411.

Dixon, C. L., Harrison, N. L., Lynch, J. W., and Keramidas, A. (2015). Zolpidem and eszopiclone prime alpha1beta2gamma2 GABAA receptors for longer duration of activity. *Br J Pharmacol* 172, 3522-36.

Dong, N., Qi, J., and Chen, G. (2007). Molecular reconstitution of functional GABAergic synapses with expression of neuroligin-2 and GABAA receptors. *Mol Cell Neurosci* 35, 14-23.

Durisic, N., Godin, A. G., Wever, C. M., Heyes, C. D., Lakadamyali, M., and Dent, J. A. (2012). Stoichiometry of the Human Glycine Receptor Revealed by Direct Subunit Counting. *J Neurosci* 32, 12915-12920.

Eichler, S. A., Forstera, B., Smolinsky, B., Juttner, R., Lehmann, T. N., Fahling, M., Schwarz, G., Legendre, P., and Meier, J. C. (2009). Splice-specific roles of glycine receptor alpha3 in the hippocampus. *Eur J Neurosci* 30, 1077-91.

Eichler, S. A., Kirischuk, S., Juttner, R., Schaefermeier, P. K., Legendre, P., Lehmann, T. N., Gloveli, T., Grantyn, R., and Meier, J. C. (2008). Glycinergic tonic inhibition of hippocampal neurons with depolarizing GABAergic transmission elicits histopathological signs of temporal lobe epilepsy. *J Cell Mol Med* 12, 2848-66.

Fuchs, C., Abitbol, K., Burden, J. J., Mercer, A., Brown, L., Iball, J., Anne Stephenson, F., Thomson, A. M., and Jovanovic, J. N. (2013). GABA(A) receptors can initiate the formation of functional inhibitory GABAergic synapses. *Eur J Neurosci* 38, 3146-58.

Graf, E. R., Zhang, X., Jin, S. X., Linhoff, M. W., and Craig, A. M. (2004). Neurexins induce differentiation of GABA and glutamate postsynaptic specializations via neuroligins. *Cell* 119, 1013-26.

Graham, B. A., Schofield, P. R., Sah, P., Margrie, T. W., and Callister, R. J. (2006). Distinct physiological mechanisms underlie altered glycinergic synaptic transmission in the murine mutants spastic, spasmodic, and oscillator. *J Neurosci* 26, 4880-90.

Harris, R. A., Osterndorff-Kahanek, E., Ponomarev, I., Homanics, G. E., and Blednov, Y. A. (2011). Testing the silence of mutations: Transcriptomic and behavioral studies of GABA(A) receptor alpha1 and alpha2 subunit knock-in mice. *Neurosci Lett* 488, 31-5.

Harvey, R. J., Depner, U. B., Wassle, H., Ahmadi, S., Heindl, C., Reinold, H., Smart, T. G., Harvey, K., Schutz, B., Abo-Salem, O. M., Zimmer, A., Poisbeau, P., Welzl, H., Wolfer, D. P., Betz, H., Zeilhofer, H. U., and Muller, U. (2004). GlyR alpha3: an essential target for spinal PGE2-mediated inflammatory pain sensitization. *Science* 304, 884-7.

Hirzel, K., Muller, U., Latal, A. T., Hulsmann, S., Grudzinska, J., Seeliger, M. W., Betz, H., and Laube, B. (2006). Hyperekplexia phenotype of glycine receptor alpha1 subunit mutant mice identifies Zn(2+) as an essential endogenous modulator of glycinergic neurotransmission. *Neuron* 52, 679-90.

Kim, S., Burette, A., Chung, H. S., Kwon, S. K., Woo, J., Lee, H. W., Kim, K., Kim, H., Weinberg, R. J., and Kim, E. (2006). NGL family PSD-95-interacting adhesion molecules regulate excitatory synapse formation. *Nat Neurosci* 9, 1294-301.

Knoflach, F., Benke, D., Wang, Y., Scheurer, L., Luddens, H., Hamilton, B. J., Carter, D. B., Mohler, H., and Benson, J. A. (1996). Pharmacological modulation of the diazepam-insensitive recombinant gamma-aminobutyric acidA receptors alpha 4 beta 2 gamma 2 and alpha 6 beta 2 gamma 2. *Mol Pharmacol* 50, 1253-61.

Kubota, H., Alle, H., Betz, H., and Geiger, J. R. (2010). Presynaptic glycine receptors on hippocampal mossy fibers. *Biochem Biophys Res Commun* 393, 587-91.

Legendre, P., Forstera, B., Juttner, R., and Meier, J. C. (2009). Glycine Receptors Caught between Genome and Proteome - Functional Implications of RNA Editing and Splicing. *Front Mol Neurosci* 2, 23.

Lynagh, T., and Lynch, J. W. (2010). A glycine residue essential for high ivermectin sensitivity in Cys-loop ion channel receptors. *Int J Parasitol* 40, 1477-81.

Lynch, J. W. (2009). Native glycine receptor subtypes and their physiological roles. *Neuropharmacology* 56, 303-9.
Lynch, J. W., and Callister, R. J. (2006). Glycine receptors: a new therapeutic target in pain pathways. *Curr Op Investig Drugs* 7, 48-53.
Macdonald, R. L., Kang, J. Q., and Gallagher, M. J. (2010). Mutations in GABAA receptor subunits associated with genetic epilepsies. *J Physiol* 588, 1861-9.
Meier, J., Meunier-Durmort, C., Forest, C., Triller, A., and Vannier, C. (2000). Formation of glycine receptor clusters and their accumulation at synapses. *J Cell Sci* 113, 2783-95.
Meier, J. C., Henneberger, C., Melnick, I., Racca, C., Harvey, R. J., Heinemann, U., Schmieden, V., and Grantyn, R. (2005). RNA editing produces glycine receptor alpha3(P185L), resulting in high agonist potency. *Nat Neurosci* 8, 736-44.
Meier, J. C., Semtner, M., Winkelmann, A., and Wolfart, J. (2014). Presynaptic mechanisms of neuronal plasticity and their role in epilepsy. *Front Cell Neurosci* 8, 164.
Meyer, G., Kirsch, J., Betz, H., and Langosch, D. (1995). Identification of a gephyrin binding motif on the glycine receptor beta subunit. *Neuron* 15, 563-72.
Muller, E., Le Corronc, H., Triller, A., and Legendre, P. (2006). Developmental dissociation of presynaptic inhibitory neurotransmitter and postsynaptic receptor clustering in the hypoglossal nucleus. *Mol Cell Neurosci* 32, 254-73.
Olsen, R. W., and Sieghart, W. (2009). GABA A receptors: subtypes provide diversity of function and pharmacology. *Neuropharmacology* 56, 141-8.
Petrou, S., and Reid, C. A. (2012). The GABAAgamma2(R43Q) mouse model of human genetic epilepsy. in: Noebels, J.L., Avoli, M., Rogawski, M.A., Olsen, R.W., Delgado-Escueta, A.V., editors. Jasper's Basic Mechanisms of the Epilepsies [Internet]. 4th edition. Bethesda (MD): National Center for Biotechnology Information (US).
Pilorge, M., Fassier, C., Le Corronc, H., Potey, A., Bai, J., De Gois, S., Delaby, E., Assouline, B., Guinchat, V., Devillard, F., Delorme, R., Nygren, G., Rastam, M., Meier, J. C., Otani, S., Cheval, H., James, V. M., Topf, M., Dear, T. N., Gillberg, C., Leboyer, M., Giros, B., Gautron, S., Hazan, J., Harvey, R. J., Legendre, P., and Betancur, C. (2015). Genetic and functional analyses demonstrate a role for abnormal glycinergic signaling in autism. *Mol Psychiatry*.
Qi, Z.-H., Song, M., Wallace, M. J., Wang, D., Newton, P. M., McMahon, T., Chou, W.-H., Zhang, C., Shokat, K. M., and Messing, R. O. (2007). Protein Kinase Cϵ Regulates γ-Aminobutyrate Type A Receptor Sensitivity to Ethanol and Benzodiazepines through Phosphorylation of γ2 Subunits. *J Biol Chem* 282, 33052-33063.
Sara, Y., Biederer, T., Atasoy, D., Chubykin, A., Mozhayeva, M. G., Sudhof, T. C., and Kavalali, E. T. (2005). Selective capability of SynCAM and neuroligin for functional synapse assembly. *J Neurosci* 260-70.
Scheiffele, P., Fan, J., Choih, J., Fetter, R., and Serafini, T. (2000). Neuroligin expressed in nonneuronal cells triggers presynaptic development in contacting axons. *Cell* 101, 657-69.
Singer, J. H., Talley, E. M., Bayliss, D. A., and Berger, A. J. (1998). Development of glycinergic synaptic transmission to rat brain stem motoneurons. *J Neurophysiol* 80, 2608-20.
Soh, M. S., and Lynch, J. W. (2015). Selective Modulators of alpha5-Containing GABAA Receptors and their Therapeutic Significance. *Curr Drug Targets* 16, 735-46.
Sun, C., Cheng, M. C., Qin, R., Liao, D. L., Chen, T. T., Koong, F. J., Chen, G., and Chen, C. H. (2011). Identification and functional characterization of rare mutations of the neuroligin-2 gene (NLGN2) associated with schizophrenia. *Hum Mol Genet* 20, 3042-51.
Talwar, S., and Lynch, J. W. (2014). Phosphorylation mediated structural and functional changes in pentameric ligand-gated ion channels: implications for drug discovery. *Int J Biochem Cell Biol* 53, 218-23.
Thomas, P., and Smart, T. G. (2005). HEK293 cell line: a vehicle for the expression of recombinant proteins. *J Pharmacol Toxicol Methods* 51, 187-200.

Trincavelli, M. L., Da Pozzo, E., Daniele, S., and Martini, C. (2012). The GABAA-BZR complex as target for the development of anxiolytic drugs. *Curr Top Med Chem* 12, 254-69.

Wallner, M., Hanchar, H. J., and Olsen, R. W. (2006). Low dose acute alcohol effects on GABA A receptor subtypes. *Pharmacol Ther* 112, 513-28.

Winkelmann, A., Maggio, N., Eller, J., Caliskan, G., Semtner, M., Haussler, U., Juttner, R., Dugladze, T., Smolinsky, B., Kowalczyk, S., Chronowska, E., Schwarz, G., Rathjen, F. G., Rechavi, G., Haas, C. A., Kulik, A., Gloveli, T., Heinemann, U., and Meier, J. C. (2014). Changes in neural network homeostasis trigger neuropsychiatric symptoms. *J Clin Invest* 124, 696-711.

Wu, X., Wu, Z., Ning, G., Guo, Y., Ali, R., Macdonald, R. L., De Blas, A. L., Luscher, B., and Chen, G. (2012). gamma-Aminobutyric acid type A (GABAA) receptor alpha subunits play a direct role in synaptic versus extrasynaptic targeting. *J Biol Chem* 287, 27417-30.

Yang, Z., Taran, E., Webb, T. I., and Lynch, J. W. (2012). Stoichiometry and subunit arrangement of alpha1beta glycine receptors as determined by atomic force microscopy. *Biochemistry* 51, 5229-31.

Zeilhofer, H. U. (2005). The glycinergic control of spinal pain processing. *Cell Mol Life Sci* 62, 2027-35.

Zhang, Y., Dixon, C. L., Keramidas, A., and Lynch, J. W. (2014). Functional reconstitution of glycinergic synapses incorporating defined glycine receptor subunit combinations. *Neuropharmacology* 89C, 391-397.

Supplementary Information

Protocol for generating functional inhibitory synapses between neurons and HEK293 cells expressing defined combinations of GABA(A) or glycine receptor subunits

REAGENTS

- Timed-pregnant rats at E15 (for spinal cord) or E18 (for cerebral cortex).
- Trypsin 0.05 % in EDTA with phenol red (Gibco 25300-054, Life Technologies)
- Divalent cation free Phosphate-buffered saline solution (PBS)
- Poly-D-lysine (P6407-5MG, Sigma-Aldrich)
- Fetal Bovine Serum (FBS, sterile filtered, Batch number 28301107, Moregate Biotech)
- Dulbecco's modified Eagle's medium (DMEM; Gibco 11995-065, Life Technologies)
- Neurobasal media (Gibco 21103-049, Life Technologies)
- B27 (Gibco 17504-44, Life Technologies)
- Glutamax (Gibco 35050-61, Life Technologies)
- HEK293 cells. We usually use the HEK293 variant AD-293 (240085, Agilent), but have also successfully used Cos9 cells and HEK293T cells.
- Plasmids for: Neuroligin 2A (plasmid 15259, Addgene), green fluorescent protein (GFP), and receptor subunits of interest.
- Hank's Balanced Salt Solution (HBSS; Gibco 14025, Life Technologies)
- Calcium-magnesium free HBSS (CMF-HBSS; H9394, Sigma-Aldrich)
- Trypan blue 0.4 % solution (Fluka 93595 Sigma-Aldrich)
- DNase I (10104159001, Roche Applied Science)
- $CaCl_2$, 250 mM in milliQ water, sterile filtered
- N,N-bis(2-hydroxyethyl)-2-aminoethane- sulfonic acid (BES) buffered saline (BBS; 14280, Sigma-Aldrich)

EQUIPMENT

- 4-well plates (e.g. 176740, Nunclon). We find that multi-well plates are less vulnerable to infection than 35 mm dishes.
- Circular glass coverslips (12 mm diameter, Menzel #1.5, Thermo Fisher Scientific)
- Fine forceps, curved forceps and dissection scissors for embryonic dissection.

- Dissection tools for adult rat
- CO_2 supply and chamber for euthanasia
- 70 % ethanol in spray bottle
- Lab wipes
- Tube rack
- Ice bed
- 100 mm petri dishes
- 50 ml tubes
- 15 ml tubes
- 1.5 ml microcentrifuge tubes
- Pipettes and tips
- Glass pasteur pipettes
- Cigarette lighter
- Rubber bulb for pasteur pipette
- Haemocytometer
- 35 mm dishes for HEK293 cells
- T75 flasks
- Dissecting microscope with light
- Cell culture cabinet (Class II biological safety cabinet or laminar flow hood)
- Centrifuge with rotor for 15 ml tubes
- Bottle/tube roller
- Humidified cell culture incubator at 37 °C, with 5 % CO_2
- Humidified cell culture incubator at 37 °C, with 3 % CO_2 (If unavailable, transfection will still be partly effective at 5 % CO_2)
- A standard patch-clamp electrophysiology rig incorporating either an upright or an inverted fluorescence microscope.

EQUIPMENT SETUP

- Clean glass coverslips: Clean coverslips in bulk by rinsing for 10 min in concentrated hydrochloric or nitric acid.

  CAUTION: When handling acid wear gloves, safety glasses and a lab gown and work in a fume hood. Remove the acid and wash coverslips in running distilled water until the pH returns to neutral (usually 1 – 2 h). Pour off water and store coverslips in a sealed glass container under 100 % ethanol.

REAGENT SETUP

All reagent setup steps should be performed in a cell culture cabinet.

- DMEM-FBS media: DMEM plus 10 % FBS.
- Aliquot B27 in 1 ml tubes and freeze for up to 4 months. Once thawed use aliquots within 1 week.
- Neuron media: In a 50 ml tube combine 1 ml B27, 0.5 ml Glutamax supplement and top up to 50 ml with Neurobasal medium. Loosen the lid and equilibrate to 37 °C and 5 % CO_2 in the cell incubator before use.
- Dilute DNAse I to 10 mg/mL in CMF-HBSS, and stored frozen 1 mL aliquots for up to 6 months.
- Coated coverslips: Make poly-D-lysine stock solution by adding 5 ml cell-culture water to 5 mg of poly-D-lysine, and freeze as 0.5 ml aliquots for up to 6 months. Remove ~40 cleaned coverslips from the ethanol (see equipment setup) and, in a 50 mL tube, rinse with cell culture water. Dilute 1 aliquot of poly-D-lysine stock to 5 ml, and incubate the coverslips on a tube roller for at least 1 h at room temperature. Pour off poly-D-lysine solution and use forceps to spread coverslips out to dry on sterile lab tissue in the cell culture cabinet. **PAUSE POINT:** Poly-D-lysine solution can be refrigerated and re-used within 1 wk. Coated coverslips are best used within 1 wk, but can be stored in a dry sterile tube at room temperature for 1 month.

PROCEDURE

Primary culture

1. Coat coverslips and place one coverslip in each well of 16 x 4-well plates.
2. Outside of the biological safety cabinet, euthanize the pregnant rat with CO_2, open the abdomen and quickly recover the embryos into tubes of chilled CMF-HBSS. If necessary, the embryos can remain on ice for 2-3 h prior to the rest of the procedure.

   CAUTION: Euthanasia of animals must be carried out in accordance with national and institutional guidelines.
3. Steps 3–16 below are carried out within a cell culture cabinet using sterile techniques. Begin with option A for cortical cultures or option B for spinal cord cultures.

A) Isolating cortical neurons (for GABAergic synapses)

i) Remove the heads from 3 embryos and rinse in a 100 mm petri dish containing chilled CMF-HBSS. Fixing each head with straight forceps, use curved forceps to

peel back the skin and skull. Pinch off the top 1 mm of cortical tissue, and place in a fresh dish of CMF-HBSS.

ii) Use fine forceps to peel off the meninges, by grasping blood vessels at the edge of the tissue and teasing them away.

CRITICAL STEP: Failure to remove the meninges will increase glia cell numbers in the culture, decreasing the health and lifespan of the neurons.

iii) Use the flame from a cigarette lighter to lightly polish the tip of a sterile glass Pasteur pipette. Suck up a little fresh CMF-HBSS and gently rinse the cortices, then suck them up and place in a sterile 15 ml tube.

B) Isolating spinal cord neurons (for glycinergic synapses)

i) Remove the head and tail of each E15 embryo using forceps, and transfer it to a 100 mm petri dish filled with ice-cold CMF-HBSS under a dissecting microscope.

CRITICAL STEP: The dissection procedure should be performed on ice.

ii) Place the embryo in the prone position and stabilize the embryo with straight forceps. Slide the other pair of forceps to cut the skin and meninges along midline to open the spinal cord.

iii) Poke the tissue closed to the dorsal lip of the spinal cord with closed forceps. Open the forceps to tear dorsal tissue away. Repeat this operation to detach surrounding tissue from both sides of the spinal cord.

iv) Pin the wider, proximal end of spinal cord with forceps and peel off meninges from the spinal cord.

CRITICAL STEP: Slowly and evenly peel off the meninges and avoid breakage of the spinal cord or the meninges. Failure to remove the meninges will increase the numbers of glial cells in the culture.

v) Use fire-polished glass Pasteur pipette to transfer the isolated dorsal strips to a fresh petri dish containing ice-cold CMF-HBSS.

vi) Collect 7 intact dorsal strips into a 15 ml tube containing 4 ml of 0.05 % trypsin and 1 ml DNase I.

vii) Incubate at 37 ^{o}C in the water bath for 20 min with intermittent agitation.

viii) Stop the digestion by adding 5 ml of trypsin inhibitor (or DMEM/FBS media), and centrifuge at 100 g for 3 min at room temperature.

ix) Discard the supernatant. Wash the tissue pellet by adding 2 ml CMF-HBSS.

4. Use a fire-polished glass pipette to triturate the tissue, gently pipetting up and down 5 to 10 times, taking care to avoid bubbles. Small chunks of tissue should still remain, but the media will become cloudy as cells are released.

   CRITICAL STEP: Pipetting speed needs to be low and the inside diameter of the glass pipette tip is critical. If it is too large it will not dissociate the cells effectively, and if it is too small it will increase cell damage. The optimal size depends on the size of tissue chunks. One solution is to sequentially triturate with three pipettes with decreasing diameters.
5. Allow tissue pieces to settle for 1 min. Then aspirate the supernatant into a fresh 15 ml tube and centrifuge for 3 min at 100 g at room temperature.

   CRITICAL STEP: Be careful not to aspirate the settled debris.
6. Remove supernatant. Gently resuspend pellet in 1 ml of DMEM-FBS.
7. In a 1.5 ml tube, mix 10 µl trypan blue with 10 µl of cell suspension. Load 10 µl into the haemocytometer and count the viable (non-blue) cells, remembering to multiply the final count by 2 to account for the trypan blue dilution. Typically, cortices from 3 embryos or spinal cords from 7 embryos will result in 200-500 cells per 0.1 µl.
8. Dilute cells in DMEM-FBS so that 80 – 100 µl can be plated on each coverslip of 8 dishes, resulting in 80,000 cells per coverslip. Dilute the remaining cells 2-fold, and plate the remaining 8 dishes at 40,000 cells per coverslip.
9. Incubate overnight, and then change media by aspirating the DMEM-FBS and replacing with 500 µl neuron media. Return dishes to the incubator
10. After 1 week in vitro, perform a half media change by removing 250 µl media and topping up with a further 500 µl of fresh neuron media. This is the final feed and will allow the cells to remain healthy for up to 6 weeks.

Preparation of HEK293 cells

11. Trypsinize HEK293 cells in a T75 flask and plate in DMEM-FBS onto 35 mm culture dishes (suggested starting density: 5000 cells per dish). Incubate overnight at 5 % CO_2.
12. To transfect, combine 0.5 – 3 µg total plasmid DNA, with 100 µl of 250 mM $CaCl_2$, then add 100 µl BBS. Vortex and incubate for 10 min at room temperature, then add dropwise to one 35 mm dish of HEK293 cells. When expressing GlyRs, the total plasmid DNA should comprise: 200 ng neuroligin 2A, 200 ng gephyrin, 100 ng GFP, with the remainder comprising GlyR subunit DNA that varies according to the number of subunits and the ratio of subunit DNA required. For example, when transfecting GlyR α subunits as homomers, add 0.5 µg DNA. When transfecting α and β GlyR subunits in 1:10 or 1:50 ratios add a total

of 2 μg DNA. When expressing α1β2γ2 $GABA_A$Rs, the α1, β2, γ2, GFP and neuroligin 2A DNAs should be transfected in a 1:1:4:1: ratio with a combined total of 0.5 μg DNA.

13. Incubate for 5 to 20 h in a 3% CO_2 incubator.
14. Thoroughly rinse each plate with PBS, then incubate in 0.5 ml trypsin until most cells detach (typically 3 min). Quench with 2 ml DMEM-FBS, and remove cell suspension into 15 ml tube. Centrifuge at 100 g for 3 min at room temperature.
    Discard supernatant.
15. Take mature neuron cultures from the incubator and remove around 50 μl from each dish to combine with the HEK293 cell pellet. One 35 mm dish of HEK293 cells can be used to seed about 4 coverslips of neurons.
    CRITICAL STEP Thoroughly resuspend the HEK293 cell pellet in neuron media so that all cells are completely isolated. Well isolated cells are essential for allowing the efficient formation of synaptic contacts and to facilitate electrophysiological recording from identified cells.
16. Return the co-cultures to the incubator overnight to allow synapses to form. Cultures can then be used for 2 – 3 d.

Electrophysiological analysis of spontaneous activity

17. Using fine forceps, place a coverslip gently into an electrophysiological recording bath on the stage of the fluorescence microscope that forms part of the patch-clamp electrophysiology rig. The cells should be perfused continuously with an extracellular solution comprising (in mM): 140 NaCl, 5 KCl, 2 $CaCl_2$, 1 $MgCl_2$, 10 HEPES, and 10 D-glucose, adjusted to pH 7.4 with NaOH. Depending on the experiment, pharmacological agents may be added or the ionic composition may be varied. Because drugs that affect IPSCs may also change the rate of spontaneous activity in the neurons, it is advisable to apply drugs directly to the patch-clamped cell, and expose the rest of the coverslip to control saline as much as possible. We achieve this using a small array of plastic tubes glued together, with control solution flowing through all but the central tube.
18. Patch pipettes (4−8 MΩ resistance), made from borosilicate glass (GC150F-7.5, Harvard apparatus), should be filled with an intracellular solution containing (in mM): 145 CsCl, 2 $CaCl_2$, 2 $MgCl_2$, 10 HEPES, 10 EGTA and 2 MgATP, adjusted to pH 7.4 with NaOH. The ionic composition can be varied according to experimental requirements. Heat polishing the pipette tips can help with seal formation, but be aware of the effect of increased series resistance on rapid events (see next step).

CRITICAL STEP: As IPSCs exhibit rise times in the microsecond range, it is important to filter and digitise currents at a high rate (at least 4 and 10 kHz, respectively) and to apply the maximum possible series resistance compensation.

19. Choosing a cell for electrophysiological recording is a matter of trial and error. A good starting point is to select large, strongly-fluorescent green cells that are closely surrounded by many neurons, especially clumps of neurons. HEK293 cells with a textured (rather than smooth) appearance often yield abundant IPSCs. A good rule of thumb is to target cells that look similar to those that have previously yielded successful recordings.
20. Voltage clamp cells at -70 mV to -50 mV to record spontaneous events for several minutes, or until more than 100 putative events have been collected.
21. The coverslip should be viable for 1 − 2 h. Discard it sooner if cell viability starts to appear degraded. Unused coverslips in 4-well plates should be returned to the incubator as soon as possible to maintain the pH of the medium.
22. Analyses of IPSC amplitudes, 10 − 90% rise times, and decay time constants can performed using a range of analysis software packages including Axograph X (Axograph Scientific), Minianalysis (Synaptosoft) and pClamp10 (Axon Instruments, Molecular Devices).

TIMING

See Figure 1 for an overview of the procedure. Set-up and culturing of primary neurons takes 2 to 3 h (the dissection for spinal cord cultures is longer). Then the neurons must be cultured until maturity, at least 3 wk for cortical neurons and 1 – 1.5 wk for spinal cord neurons. Preparing the HEK293 cells and adding them to the neurons takes about 2 h spread across 3 d. Once HEK293 cells have been added to the neurons, the synapses form within 24 h and at this point the electrophysiological experiments can be commenced.

TROUBLESHOOTING

- Not enough neurons for plating: If there are not enough cells to fill the intended plates, trituration may have been too vigorous (more then 50 % of cells trypan positive) or too gentle (few trypan positive cells and few negative) Experiment with trituration of different strengths. As noted above, the tip size of the flame-polished glass pipette is crucial: a very small opening will damage more cells, but a large opening will not dissociate the cells effectively.
- Massive cell death after seeding: Check the incubator CO_2 level, temperature, and water levels; check the temperature of the trypsin incubation; make fresh neuron media or coverslip coating solution.

- Difficulty forming seals on HEK293 cells: Co-cultured cells are often more difficult to record from than HEK293 cells that have been cultured in isolation. Fire polishing the patch pipette tip can help to form high resistance seals, but be aware of increasing the series resistance.
- Unhealthy neuron cultures leading to little spontaneous activity: Too many glia present in the final cultures (take more care to remove the meninges), or plating density too high or too low.
- Non-transfected HEK293 cells: Adjust DNA ratios, or try fresh BBS. Alternately, other methods of transfecting HEK293 cells could also be applied.
- No detectable spontaneous IPSCs in the HEK293 cells: Check that the cells are expressing functional receptors by directly applying the appropriate neurotransmitter agonist. If there is no current, trouble-shoot the transfection. If agonist-evoked currents are present, check that the neurons exhibit spontaneous spiking activity by recording from a few. If they are not active, the neuronal cultures may be too young or too old, the neuron density may be too high or too low (leading to cell death) or excess glial growth may be impairing neuronal activity. Check that neuroligin is being successfully expressed using immunofluorescent labelling for the HA tag (as shown in Figure 1, inset). If all of these things seem normal but brightly fluorescent HEK293 cells still do not have currents, consider patching cells with different appearances, including those with low fluorescence. We find that large or brightly fluorescent HEK293 cells next to clumps of neurons have the highest probability of showing synaptic activity.